JR-10,003-US PATENT

IN THE UNITED STATES PATENT AND TRADEMARK OFFICE

In re Application of: Ryan

Serial No.: 10/608,463 Group Art Unit: 1652

Filed: June 27, 2003 Examiner: T. Saidha

FOR: ISOLATED GENOMIC POLYNUCLEOTIDE FRAGMENTS FROM CHROMOSOME 12 THAT ENCODE HUMAN CARBOXYPEPTIDASE M AND THE HUMAN MOUSE DOUBLE MINUTE 2 HOMOLOG

Confirmation No.: 6428

APPEAL BRIEF

Mail Stop Appeal
Commissioner for Patents
P.O. Box 1450
Alexandria, VA 22313-1450

Sir:

This Appeal Brief is being submitted in support of the appeal from the rejections set forth in the Office Action mailed on January 2, 2009.

TABLE OF CONTENTS

I. REAL PARTY IN INTEREST

The real party in interest of the present application is Ryogen LLC. Ryogen LLC is the owner of the present application by way of an assignment from the inventor, James W. Ryan of all rights, title, and interest.

II. RELATED APPEALS AND INTERFERENCES

There are no appeals or interferences related to the present application.

III. STATUS OF CLAIMS

Claims 7, 10, 15-18, 20, 24, 25, 30 and 31 stand finally rejected by the Examiner as noted in the Office Action mailed on January 2, 2009 and in the Advisory Action mailed June 24, 2009. Claims 1-6, 8-9, 11, 13, 19, 21 and 26-29 have been canceled. Claims 12, 14, 22, 23 and 32-38 have been withdrawn. The rejection of claims 7, 10, 15-18, 20, 24, 25, 30 and 31 is appealed.

IV. STATUS OF AMENDMENTS

Amendments to claims 7 and 24 subsequent to the Examiner's Final Rejection mailed January 2, 2009 were submitted but were not entered.

V. SUMMARY OF THE CLAIMED SUBJECT MATTER

A. Independent Claim 1

Claim Elements	Support in specification
An isolated nucleic acid molecule 20-51039 contiguous nucleotides in length consisting of a reverse or forward strand of a region of SEQ ID NO:4	Page 9, line 34; page 10, lines 22-26
wherein said region is selected from the group consisting of a 5'-non coding region depicted in nucleotides 51039-41739 of SEQ ID NO:4, a 3'-non-coding region depicted in nucleotides 9503-1 of SEQ ID NO:4, a contiguous intron-exon region between nucleotides 41738-9502 of SEQ ID NO:4, wherein a sequence segment comprising 41738-9502 of SEQ ID NO:4 encodes human mouse double minute 2 homolog depicted in SEQ ID NO:2, a	Page 10: Table 2

contiguous exon-intron region between nucleotide 41738-9502 of SEQ ID NO:4, wherein a sequence segment comprising 41738-9502 of SEQ ID NO:4 encodes human mouse double minute 2 homolog depicted in SEQ ID NO:2, an intron depicted in nucleotides 36385-40645, 36309-33127, 32994-29616, 29564-25577, 25507-25384, 25287-21169, 21006-14110, 13953-13267, and/or 13188-10665, a region comprising a dinucleotide of the following group: 41739-41738, 40645-40646, 36309-36310, 36384-36385, 32994-32995, 33126-33127, 29564-29565, 29615-29616, 25507-25508, 25287-25288, 25383-25384, 25576-25577, 21006-21007, 21168-21169, 14109-14110, 13953-13954, 13266-13267, 13188-13189, 10664-10665 and/or 9504-9503	
a transcription binding site selected from the group consisting of BINDING SITES huMDM2, location in SEQ ID NO:4 AP1_C: 36-46, 2876-2886; AP4_Q5: 7944-7980; AP4_Q6: 7943-59, 8924-8940, 9294-9310; ARNT_01: 1682-1706, 2193-2217, 9201-9225; BRN2_01: 1040-1058, 7803-7821; CAAT_01: 3292-3306; CDPCR3HD_01: 6522-6540; CEBPB_01: 1424-1438, 3917-3931, 4178-4192, 4787-4801, 6855-6869; CREL_01: 5630-5642; DELTAEF1_01: 83-95, 6328-6340; FREAC7_01: 2757-2773, 5154-5170, 5823-5839; GATA1_04: 4846-4858, 7017-7029; GATA1_05: 8464-8476; GATA2_02: 6045-6057, 6073-6085, 6142-6154; GATA2_03: 2489-2501, 3323-3335, 3384-3396,	Page 9, line 29 to page 10, line 2; Table 3 on pages 10-12

7393-7405; GATA3_02: 3264-3276, 6870-6882; GATA3_03: 40-52, 5729-5741, 6529-6541, 6874-6886, 7041-7053, 7589-7601; GATA_C: 7 349-7361, 8188-8200; HFH2_01: 1743-1759, 7995-8011; HFH3_01: 502-518, 1739-1755, 4160-4176, 9402-9418, 9418-9434; HFH8_01: 8184-8200; IK2_01: 951-963, 3588-3600; MZF1_01: 1202-1210, 1447-1455, 4997-4005, 5424-5432; NF1_Q6: 1480-1500, 8166-8182; NFAT_Q6: 4190-4208, 6009-6027; NKX25_01: 741-755, 1648-1662, 1885-1899, 1984-1998, 3609-3623, 4928-4942, 5060-5074, 5889-5903, 8850-8864, 9190-9204; NKX25_02: 2584-2599, 2970-2984, 4644-4658, 5179-5193, 6482-6496; NMYC_01: 2560-2572; RORA1_01: 220-238, 2638-2656; S8_01: 4644-4656, 4842-4854, 4845-4857, 5200-5212, 5371-5383, 5735-5747, 6482-6494, 6541-6553, 6544-6556, 6772-6784, 7270-7292, 7273-7285; SOX5_01: 1355-1371, 1430-1446, 3094-3110, 3155-3171, 4669-4685, 4692-4708, 4789-4805; SRY_02: 4164-4180, 5665-5681; TATA_01: 1261-1277, 2574-2590, 2723-2739, 2733-	

2749, 2770-2786, 4199-4215, 4206-4222;

TATA_C: 5900-5916, 7456-7472, 7702-7718, 7917-7933; and

XFD2_01: 7702-7218, 7917-7933;

a transcription binding site selected from the group consisting of

BINDING SITES huMDM2, location in SEQ ID NO:4
AP1_C: 12109-12119, 12695-12705, 22600-22610, 24166-24176, 31311-31321, 35234-35244, 39184-39194;

AP1_Q2: 11952-11962, 12068-12078, 14798-14808, 21748-21758, 22613-22623, 23676-23686, 26562-26572, 30046-30056;

AP1_Q4: 12695-12705, 31311-31321, 35234-35244, 36295-36305, 38784-38794, 39188-39198;

AP4_Q6: 31635-31651;

BRN2_01: 13448-13466, 14764-14782, 28094-28112, 40027-40045;

CAAT_01: 11288-11302, 15054-15068;

CDPCR3HD_01: 11286-11304, 13284-13302, 20846-20864, 29344-29362;

CEBPB_01: 29241-29255;

CREL_01: 36091-36103, 38873-38885;

DELTAEF1_01: 18083-18095, 20385-20397, 26955-26967;

FREAC7_01: 11982-11998, 15187-15202, 16523-16539, 16529-16545, 16587-16603, 16604-16620, 16676-16642, 16633-16649, 16644-16660, 16650-16666, 16657-16673, 16673-16689, 16762-16778, 21332-21348, 25689-25700, 26529-26545, 27767-27783, 29495-29511;

GATA1_02: 10916-10928, 15775-15789, 18162-18174, 26088-26100, 32518-32530;

GATA1_03: 28012-28024;

GATA1_04: 11153-11165, 11630-11642, 13778-13790, 17439-17451, 19300-19312, 21606-21618, 22743-22755, 23747-23759, 25806-25818, 26529-26541, 29424-29436, 30455-30467, 32761-32778, 33352-33364, 33960-33972, 36101-36113, 40007-40019; GATA1_05: 11590-11602, 26550-26562, 36737-36749; GATA1_06: 18772-18784, 23054-23066, 35568-35580, 37855-37867; GATA2_02: 20755-20767, 30830-30842, 34755-34767, 36285-36297, 39143-39155, 39641-39653, 40586-40598; GATA2_03: 13535-13547, 22711-22723, 23161-23173, 25028-25040, 27237-27249, 36277-36289; GATA3_02: 11558-11570, 16470-16482, 17225-17237, 19619- 19631, 22156-22168, 22443-22455, 24713-24725, 27619-27631, 32716-32728, 34124-34136, 34163-34175, 36832-36844, 38403-38415; GATA3_03: 10869-10881, 11515-11527, 13845-13857, 17221-17233, 18952-18964, 20050-20062, 40171-40183; GATA_C: 15848-15860, 18899-18911, 23640-23652, 29072-29084, 30881-30893, 33198-33210, 37472-37484, 38621-38633; GFI1_01: 35469-35481, 35492-35504; HFH2_01: 15939-15955, 24636-24652, 25866-25882, 32171-32187, 35372-35388, 39457-35473; HFH3_01: 13340-13356, 19218-19234, 21328-21344, 21336-21352, 21344-21360, 28062-28078, 32125-32141; HFH8_01: 14133-14149, 22578-22584; HNF3B_01: 13150-13166, 16505-16521, 25264-25280, 29443-29459, 37654-37670; IK2_01: 11547-11559, 17144-17156, 18961-18973, 23883-23895, 27617-27629, 28908-28920, 29241-29253, 30752-30764, 34768-34780;	

LYF1_01: 12319-12331, 19191-19203, 37226-37238, 39430-39442; MAX_01: 22974-22986, 33339-33351; MZF1_01: 26105-26113, 35187-35195; NF1_Q6: 12048-12064, 33334-33354; NFAT_Q6: 13295-13313, 14157-14175, 14311-14329, 14414-14432, 18269-18287. 19326-19344, 20801-20819, 21177-21195, 22537-22555, 23861-23879, 25392-25410, 25879-25897, 27524-27542, 30636-30654, 30718-30736, 31525-31543, 33655-33673, 34726-34744, 34917-34535, 34990-35008, 35979-35997, 36479-36493, 36577-36595, 37154-37172, 40224-40242, 40365-40383; NKX25_01: 12041-12055, 12340-12354, 12471-12485, 12742-12756, 12877-12891, 13849-13863, 18995-19009, 21440-21454, 21883-21897, 28426-28440, 30964-30978, 32033-32047, 32265-32279; NKX25_02: 10998-11012, 12711-12725, 14131-14145, 14726-14740, 16024-16038; NMYC_01: 18753-18765, 18754-18766, 23076-23088, 30534-30546, 34400-34412; RORA1_01: 13134-13152, 22966-22984, 24934-24952, 33341-33359, 34760-34778; S8_01: 11000-11012, 11977-11989, 12048-12060, 12051-12063, 13747-13759, 13923-13935, 13926-13938, 14676-14688, 14679-14691, 16026-16038, 16313-16325, 16316-16328, 17515-17527, 20756-20768, 20759-20771, 23154-23166, 23157-23169, 25198-25210, 25201-25213, 26651-26663, 27508-27520, 27511-27523, 29450-29462, 29478-28490, 29775-29787, 29778-29790, 29813-29825, 29816-29828, 31329-31341, 31677-31689, 31680-31692, 31732-31744, 31735-31747, 36137-36149, 36140-36152, 36812-36824, 36815-36827, 37413-37425, 38679-38691, 39474-39486, 39477-39489; SOX5_01: 27397-27413, 27572-27588, 28100-28116, 29230-29246, 29439-29455, 30690-30706, 31595-31611, 33871-33887, 34113-34129, 34624-34640, 37668-37684, 38582-38598, 39124-	

39140, 40410-40426;

SRY_02: 20016-20032, 22410-22426, 27329-27345, 29162-29178, 29499-29515, 30646-30662, 31503-31519, 35928-35944, 37324-37340;

TATA_01: 32722-32738, 32729-32745, 32807-32823, 33825-33841, 34120-34136, 35433-35449, 36593-36609;

TATA_C: 11015-11031, 11817-11833, 13635-13651, 14930-14946;

TCF11_01: 18543-18549, 22574-22580, 31281-31297, 31489-31505, 38754-38770;

USF_01: 23075-23087, 32577-32589;

VMYB_02: 11526-11538, 17384-17396, 18400-18412, 19549-19561, 22188-22200, 40486-40508 and

XFD2_01: 16620-16636, 18153-18169, 22102-22118, 23141-23157.

And a transcription binding site selected from the group consisting of

BINDING SITES huMDM2 location in SEQ ID NO:4

AP1_C: 44584-44594, 49069-49079:

AP1_Q2: 42174-42184, 45217-45227, 48422-48422, 50447-50457;

AP1_Q4: 42702-42712, 50806-50816;

AP4_Q6: 42117-42133, 42118-42134, 42244-42260, 45432-45448; 45433-45449, 46609-46625;

BRN2_01: 42310-42328, 44022-44040, 47514-47532, 48900-48918, 48967-48985;

CAAT_01: 44866-44880;

CDPCR3HD_01: 45671-45689, 49219-49237;

CREL_01: 42437-42449, 49797-49809;

FREAC7_01: 47026-47042, 47292-47308, 47658-47674;

GATA1_02: 43482-43494, 48926-48938, 49284-49296;

GATA1_03: 47371-47383;

GATA1_04: 43054-43066, 43162-43162, 43967-43979, 45464-45476, 45916-45928, 47763-47775;

GATA1_05: 49319-49331, 49459-49471;

GATA1_06: 47590-47602;

GATA2_02: 42660-42672, 43475-43487;

GATA2_03: 43714-43726, 50948-50960;

GATA3_02: 49155-49167, 49844-49856;

GATA3_03: 42202-42214, 44810-44822, 48438-48450, 49136-49148, 49337-49349, 49869-49881;

GATA_C: 44011-44023, 45256-45268, 45823-45835, 47915-47927, 49201-49213, 49573-49585;

GFI1_01: 46606-46618, 47063-47075;

HFH3_01: 47030-47046, 47284-47300, 47288-47304;

IK2_01: 45275-45287;

LYF1_01: 44564-44576, 46991-47003, 49567-49579;

MAX_01: 43234-43246, 48726-48738;

MZF1_01: 41772-41780, 42290-42298, 42295-42303, 44507-44515, 45105-45113, 45203-45211, 49948-49956, 50774-50782;

NF1_Q6: 50209-50229;

NFAT_Q6: 42061-42079, 44418-44436, 46399-46417,

47974-47992, 49267-49285, 49964-49982, 50392-50410; NKX25_01: 42394-42408, 43507-43521, 46115-46129; RORA1_01: 45073-45091, 48718-48736; S8_01: 43552-43564, 45214-45226, 47160-47172, 48419-48431, 49295-49307, 50379-50391; SOX5_01: 43716-43732, 46351-46367, 47156-47172, 47774-47790, 47868-47884, 47974-47990, 48915-48931, 50323-50339; TATA_01: 45588-45604, 47625-47641, 48026-48042, 48659-48675, 49056-49072, 49079-49095, 49152-49168; TCF11_01: 49115-49131; VMYB_02: 42010-42022, 42279-42291, 44651-44663; XFD2_01: 42870-42886, 42910-42926.	

B. Independent Claim 24

Claim Element	Support in Specification
An isolated nucleic acid molecule 20-5000 contiguous nucleotides in length	Page 9, line 35 to page 10, line 2
consisting of a reverse or forward strand of a contiguous exon intron region between nucleotides 41738-9502 of SEQ ID NO:4 or contiguous intron-exon region between nucleotides 41738-9502 of SEQ ID NO:4,	Page 10, Table 2 and page 14, lines 29-32
wherein a sequence segment comprising 41738-9502 of SEQ ID NO:4 encodes human mouse double minute 2 homolog depicted in SEQ ID NO:2	Page 2, lines 7-13; page 10, Table 2

VI. GROUNDS OF REJECTION TO BE REVIEWED ON APPEAL

A. Whether claims 7, 10, 15-18, 20, 24, 25, 30 and 31 comply with the written description requirement under 35 USC §112, first paragraph

B. Whether claim 7, 10, 15-18, 20, 24, 25, 30 and 31 are unpatentable over Muzny et al. , Genbank Accession No. AC025423 ("Muzny") in view of Vogelstein et al., US Patent No. 5,411,860 ("Vogelstein").

VII. ARGUMENT

A. Claims 7, 10, 15-18, 20, 24, 25, 30 and 31 Comply With the Written Description Requirement

In the final rejection dated January 2, 2009, it was asserted that claim 7, with dependent claims 10, 15-18, 20, 30 and 31, as amended on March 3, 2005 and August 29, 2005 and claim 24, with dependent claim 25, added on March 3, 2005 and amended on August 29, 2005 to recite "wherein a sequence segment comprising 41738-9502 of SEQ ID NO: 4 encodes human mouse double minute 2 homolog depicted in SEQ ID NO:2, ... a region comprising a dinucleotide of the following group: 41739-41738, ... and/or 9504-9503" (lines 12-15 of claim 7) constitutes new matter and lacks support. Appellant had traversed and pointed out that there is more than adequate support in the specification for claims 7, 10, 15-18, 20, 30 and 31 and in particular, for the sequence segment 41738-9502, the **nucleotide ranges** for the various sites for huMDM2 location in SEQ ID NO:4, specific ranges that relate to the specific dinucleotide ranges or specific 'exon/intron' organization in terms of the

specific nucleotide range(s) and in particular, the region comprising a dinucleotide i.e., nucleotides '41739-41738'.

In response, the Advisory Action on page 3 states

> Applicant does not indicate and the examiner is unable to locate adequate support in the specification for such positions/ranges in SEQ 10 NO: 4. It is also noted that claim 7, starting from line 17, indicate ***nucleotide ranges*** for various binding sites for huMDM2, location in SEQ 10 NO:4 (claims filed 9/14/2008), pages 2-8. However, there is no basis for these nucleotide ranges (For Example: AP1_C: 36-46, 2876-2886; AP4_Q5: 7944-7980 .....
>
> Thus there is no indication that the specific segments or ranges were within the scope of the invention as conceived by Applicants at the time the application was filed.

The Advisory Action on page 5 further states

> Applicants arguments are considered but not found to be persuasive because the specification as originally filed does not teach the specific ranges that related to the specific dinucleotide ranges or the specific *'exon/intron'* organization in term of the specific nucleotide range(s).
>
> Based upon the teachings of Table 2, on page 10, wherein Exon 1 begins at nucleotide 40726 of SEQ **ID** NO:4 and the stop codon terminates at nucleotide 10091 of SEQ ID NO:4. However is it not clear that nucleotides 41738-9502 of SEQ ID NO: 4 would constitute a sequence segment that encodes human mouse double minute 2 homolog protein. Similarly, the region comprising a dinucleotide i.e., nucleotides '41739-41738', does not have no basis in the instant specification.

In response, and as stated in previous responses, there is more than adequate support in the specification for the positions/ranges in SEQ ID NO:4 recited in claims 7, 24 and 25. On page 4, lines 25-30 of the specification, it is stated:

> The invention is directed to isolated genomic polynucleotide fragments that encode ...human mouse double minute 2 homolog, which in a specific embodiment are...human mouse double minute 2 homolog genes, as well as vectors and hosts containing these fragments and polynucleotide fragments hybridizing to noncoding regions, as well as antisense oligonucleotides to these fragments.

Further, the specification on page 14, lines 29-33 states:

> The present invention also relates to nucleic acid constructs comprising a polynucleotide sequence containing the exon/intron segments of the ….human mouse double minute 2 homolog gene (nucleotides 1-51039 of SEQ ID NO:4).

Table 2 on page 10 of the specification shows "exon/intron organization of the human mouse double minute 2 homolog gene… in SEQ ID NO:4, 51039 base pairs; nucleotides 99541-150579 in the genomic clone of accession no. AC025423 (reverse strand cloning)". Exon 1 according to Table 2 begins at nucleotide 40726 of SEQ ID NO:4 and the stop codon terminates at nucleotide 10091 of SEQ ID NO:4. However, there are further nucleotide sequences set forth in SEQ ID NO:4, nucleotides 51039-40727 at the 5' end and nucleotides 1-10090 at the 3' end. It is merely implicit in Table 2 that the minimum genomic DNA sequence encoding human mouse double minute 2 homolog ("MDM2") protein ranges from nucleotides 40726-10091. Certainly a larger sequence can encode human MDM2 protein, such as the recited nucleotides 41738-9502 of SEQ ID NO:4. As noted above, the human MDM2 gene is actually encompassed by nucleotides 1-51039 of SEQ ID NO:4). Thus, there is support for the recitation in claims 7 for the phrase "wherein a sequence segment comprising 41738-9502 of SEQ ID NO: 4 encodes human MDM2 depicted in SEQ ID NO:2, ... a region comprising a dinucleotide of the following group: 41739-41738, ... and/or 9504-9503" (lines 12-15 of claim 7).

Further, there is support for the recitation "a region comprising a dinucleotide of the following group: 41739-41738" in claims 7 and 25. In particular, Applicant notes that page 9, lines 29-32 states:

> The invention is further directed to polynucleotide fragments containing or hybridizing to noncoding regions of the …human mouse double minute 2 homolog genes. These include but are not limited to an expression control element, an intron, a 5'non-coding region, a 3'-non-coding region and splice junctions (see tables 1-2, as well as transcription factor binding sites (see Table 3).

A region encompassing the dinucleotide 41739-41738 would be within the 3'-noncoding region and would thus constitute a fragment containing a 3'non-coding region.

Similarly, it is Appellant's position that the dinucleotide ranges of the specific exon/intron organization would be taught as well. This is because the various exon/intron (splice) junctions are disclosed in Table 2 and it is clearly indicated that fragments containing

these exon/intron junction would be encompassed as well. Specifically it is stated on page 9, line 33 to page 10, line 44:

> The polynucleotide fragments may be a short polynucleotide fragment that is between about 20 nucleotides to about 50 nucleotides in length. Such shorter fragments may be useful for diagnostic purposes. Such short polynucleotide fragments are also preferred with respect to polynucleotides containing or hybridizing to polynucleotides containing splice junctions. Alternatively larger fragments, e.g., of about 50, 150, 500, 600, 2000 or about 5000 nucleotides in length may be used.

Finally, with respect to lack of support of transcription binding sites recited in claim 7, it is Appellant's position that Table 2 lists various transcription factor binding sites. Each site is readily found in SEQ ID NO:4. Appellant notes that fragments 20 nucleotides in length are disclosed in the specification as well (see p. 10, lines 13-18). It is stated in the specification:

> ...These include but are not limited to an intron, a 5'-non-coding region, a 3'-noncoding region and splice junctions (see table 1), as well as transcription factor binding sites (see table 2). The polynucleotide fragments may be a short polynucleotide fragment which is at least 15, 16, 17, 18 or 19 nucleotides in length but may be between about 20 nucleotides to about 50 nucleotides in length. Such shorter fragments may be useful for diagnostic purposes.

One of ordinary skill in the art would given the information provided in Table 2 and tools known to one of ordinary skill in the art as of the priority date been able to identify the transcription sites recited in claim 7 such as the program Matinspector and is commercially available from Geomatix Gmbh (www.geomatix.de). Such programs were available as of the priority date of the instant application. Furthermore, as noted in MPEP 2163,

> While there is no *in haec verba* requirement, newly added claim limitations must be supported in the specification through express, implicit, or inherent disclosure.

Given that there is information in Table 2 indicating the presence of all of the recited transcription factor binding sites, given that the sequences of these transcription factor binding sites are well known in the art, given that one of ordinary skill in the art could have identified the transcription binding sites recited and given that SEQ ID NO:4 is known, there is sufficient support in the specification to meet the criteria set forth in the MPEP. Thus, no new matter has been added with respect to claim 7.

In conclusion, there is adequate support for the phrase in claim 7 "wherein a sequence segment comprising 41738-9502 of SEQ ID NO:4 encodes human mouse double minute 2 homolog depicted in SEQ ID NO:2, ... a region comprising a dinucleotide of the following group: 41739-41738, ... " as well as claim 24 directed to an isolated nucleic acid molecule 20-5000 nucleotides in length consisting of a reverse or forward strand of a contiguous exon-intron region or intron-exon region between nucleotides 41738-9502 of SEQ ID NO:4 and claim 25 directed to an isolated nucleic acid molecule 20-5000 nucleotides in length comprising nucleotides 41739-41738,...". Further, claims 10, 15-18, 20, 24, 25, 30 and 31 ultimately depend from claim 7. Thus, arguments made with respect to claim 7 would apply to these claims as well.

B. Claims 7, 10, 15-18, 20, 24, 25, 30 and 31 are not Obvious over Muzny et al. in view of Vogelstein

In the final rejection dated January 2, 2009, the Office Action stated:

> It would have been obvious to one of ordinary skill in the art at the time the invention was made to use said cDNA to identify the genomic DNA that encodes the human MDM2 homolog of SEQ ID NO:2. The motivation is provided by Vogelstein et al. who teach that it binds to oncogene p53 and is diagnostic of tumorigenesis (citation omitted). The state of the art provides various techniques for obtaining genomic DNA using cDNA probes that are usually labeled. The comparison of genomic and cDNA would result in the identification of regions comprising exon-intron and intron-exon junctions within coding and noncoding regions. One of ordinary skill in the art would have been motivated to use said non-coding regions or fragments thereof of at least 20 nucleotides and up to 5000 or 51039 nucleotides (the entire length of SEQ ID NO:4) nucleotides for detecting splice variants of the genomic DNA encoding human MDM2 homolog in genomic nucleotide samples from an individual, for example. As a matter of convenience a non-coding region such as an exon-intron or intron-exon region or fragments thereof can be present in a kit or on a solid support. Further, said support can be a microarray according to a customary use of nucleic acid molecules in the art.

Appellant had traversed the rejection. In the response dated May 30, 2009, Appellant had asserted that it would not have been obvious to combine the disclosure of Muzny and

Vogelstein given that there was no suggestion to do so and further to assert that undue experimentation would have been required not only to locate the MDM2 gene but also identify exon-intron junctions.

In response, in the Advisory Action dated June 24, 2009, the following assertions are made:

> With regard to the 103(a) rejection, Applicant's arguments can be summarized as follows: 1) Muzny contains a small portion of chromosome 12, where the location of the MDM2 gene was indicated by Vogelstein as 12q12-14 while Applicant found it on 12q and 2) the MDM cDNA constitutes only 1.6% of the clone disclosed by Muzny, therefore it would be undue experimentation to locate the MDM2 gene and identify its exon-intron junctions.
>
> Applicant further argues Second, Appellant asserts that there would not be a reasonable expectation of success of obtaining the claimed non-coding sequences of SEQ ID NO: 4 in view of the cited references. Vogelstein placed the human MDM2 homologue gene at 12q12-14. As noted above, there was actually a previous disclosure stating that the MDM2 was located between 12q14.3-15 (see, for example, Andersen et al., 1996, Mammalian Genome 7: 780-783 and Bureau, 1995, Genomics 28: 109-112, submitted and disclosed in previous response attached hereto as Exhibit 1). However, given the conflicting locations published as of the priority, one of ordinary skill in the art would not have known which location was actually correct" (Brief, page 14).
>
> This is not agreed with because the actual location does not matter as long as it is a part of the Muzny sequence, which it is. Applicant did not need to separate the Muzny sequence into the fragments containing different arms of chromosome 12. In fact, Applicant did not isolate the fragment 12q12-14 or 12q14.3-15. He run cDNA against the genomic DNA disclosed by Muzny and found the location of the gene where it was. This experiment was performed according to the knowledge and the state of the art as evidenced by Watson et al. Watson et al. teach that "once the first genes were cloned, introns were identified by comparing the cloned genomic DNA with the corresponding cloned cDNA" ("Recombinant DNA", page 137, 2nd column, form PTO892 mailed 4/16/07). Applicant's argument would be convincing if the exact location would need to be known before the comparison of the genomic and the cDNA is made. This is not the case because the work is done on the genomic DNA that is known without fragmentation thereof. Applicants further

> argues that "Watson would not apply in this case since in Watson, the genes themselves were actually cloned" (ibid, page 18, last sentence). This is not persuasive because Muzny provided the piece of the genomic DNA containing the requisite gene. Having the cDNA, it does not require undue experimentation to identify the fragment of the genomic DNA corresponding to the gene and exon-intron locations within said gene.
>
> The second type of Applicant's arguments concerns with the fact that the cDNA constitutes only 1.6% of the genomic DNA. While a large quantity of the experimentation may be involved, it is not undue because sufficient guidance and knowledge are provided by the art.

Appellant maintains that the claimed invention is not obvious over the cited references for several reasons. (1) One of ordinary skill in the art could not have predicted where the human MDM2 gene was located; (2) The conflicting teachings in the art with respect to the possible location of the human MDM2 gene is of particular significance; (3) At best, this would still be an "obvious to try" situation; (4) There was a long felt need and it is likely that others had tried but failed before the priority date of the instant application. Each of these reasons will be discussed in further detail below:

(1) One of ordinary skill in the art could not have predicted where the MDM2 gene was located

Muzny merely discloses the sequence of a genomic clone containing chromosome 12 sequences, not isolated SEQ ID NO:4 (see Evidence Appendix). No indication is provided is provided in the Muzny disclosure as to which portion of chromosome 12 has actually been sequenced. Vogelstein (see Evidence Appendix) merely discloses the human MDM2 cDNA. Appellant was the first to identify SEQ ID NO:4 and determine that it did indeed encode human MDM2 and in particular determine the claimed noncoding sequences.

Muzny only disclosed the sequence of the clone AC025423. There was no indication at the time of the filing date of the instant application that AC025423 actually contained SEQ ID NO:4, more specifically a sequence encoding human MDM2. Muzny only sequenced a small portion of chromosome 12, the chromosome 12 BAC clone AC025423 which contains less than 0.12% of the chromosome (about 157 kB vs. about 132,000 Kb). The clone's sub-

site on chromosome 12 apparently was not then known. Muzny did not even suggest, must less state whether the clone AC025423 did or did not contain any gene. The determination of a sequence of genomic DNA does not necessarily imply the presence of a gene. This is because it is well known in the art and was certainly well known when the instant invention was made and as of the filing date of the instant application that most genomic DNA contains "junk" DNA, not genes (see, e.g., Wong et al., 2000, "Is Junk DNA Mostly Intron DNA?" Genome Research 10: 1672-1678 in Evidence Appendix that discuss "junk" DNA in further detail). As is evident from this review article, junk DNA was well known as of the priority date of the above-referenced application. When obtaining genomic clone sequences, one of skill in the art would not have any way of knowing whether or not it actually contains a gene(s) or just junk DNA. Even noting that a clone has a high GC content is a poor guide to a sequence's likely gene content, especially given the presence of pseudogenes. Therefore, *contra* to assertions made in the Advisory Action, disclosure of this particular sequence would not indicate to the skilled artisan that this clone would necessarily contain a gene.

The clone AC025423 is 150,579 nucleotides in length. The cDNA sequence only contains 2372 nucleotides (1.6% of AC025423). However, one of ordinary skill in the art would not know where or how these 2372 nucleotides are interspersed within the AC025423 clone or if indeed it is even present. No teachings are provided as to the structure of the MDM2 gene itself: number and size of exons, number and size of introns, locations of exons and introns and number and size of 5' and 3' untranslated regions. The possibilities are close to infinite. Thus there would not be a reasonable expectation of success of obtaining the claimed sequences given that the isolation and identification of the claimed sequences constitutes undue experimentation.

Appellant wishes to further emphasize that the size of the cDNA relative to the isolated genomic clone is of particular significance. If, for example, the cDNA constituted 50% of a particular genomic clone, considerable less experimentation would be involved in determining the sequence of a particular gene than when it is merely 1.6% of the genomic clone.

Watson has been mentioned during prosecution to support the premise that it would be simple to locate intron/exon junctions in the Muzny sequence. Appellant asserts that the teachings of Watson would be of little significance. Watson et al. provides a general

description as to how introns may be located by comparing cloned cDNA to cloned genomic DNA. However, it would not be feasible to compare cDNA to the entire Muzny sequence. Smaller fragments would be necessary. As will be discussed in further detail below, trying to find the MDM2 gene given the teachings of Muzny, Vogelstein and even Watson would metaphorically be like "throwing darts".

(2) The conflicting teachings in the art with respect to the possible location of the MDM2 gene is of particular significance

Appellants disagree with the assertion that the "actual location does not matter as long as it is a part of the Muzny sequence, which it is". As noted in previous responses, Vogelstein placed the human MDM2 homologue gene at 12q12-14. Actually, this finding is incorrect. After the publication of Vogelstein, the gene was found not to be located at 12q12-14. The gene is actually several millions of base pairs away at 12q15 (see, for example, Andersen et al., 1996, Mammalian Genome 7:780-783, Bureau, 1995, Genomics 28: 109-112 and Genecard and set forth in the Evidence Appendix, attached hereto as Exhibit 1 and previously made of record). Thus, even if these two references were indeed combined, the ordinary skilled artisan would have looked for the MDM2 gene in the wrong location and thus would not have obtained the claimed sequences. Once one of ordinary skill in the art was unable to find the human MDM2 gene at 12q12-14, one of ordinary skill would have had no clear direction as to where the MDM2 gene was located on that particular sequence or if indeed it would be located on that sequence at all. The human MDM2 gene is interspersed among the recited Muzny sequence. Thus the possible location of the MDM2 gene is of particular significance since it would be less likely that one of ordinary skill in the art would have a reasonable expectation of success.

(3) At best, this would still be an "obvious to try" situation

It is Appellant's view that the combination of the two references would still constitute "obvious to try" even under KSR v Teleflex. *KSR v Teleflex*, 82 USPQ2d 1385; 127 S.Ct. 1727 (2007) and *In re Kubin*, 561 F.3d 1351 (Fed. Cir. 2009). Appellant notes that the "Examination Guidelines for Determining Obviousness Under 35 U.S.C. 103 in View of the Supreme Court Decision in *KSR International Co. v. Teleflex*", 72 FR 57526 (October 10,

2007) (hereinafter "Examination Guidelines") stated with respect to "obvious to try" the following:

> To reject a claim based on this rationale, Office personnel must resolve the *Graham* factual inquiries. Office personnel must then articulate the following:
>
> (1) a finding that at the time of the invention, there had been a recognized problem or need in the art, which may include a design need or market pressure to solve a problem;
>
> (2) a finding that there had been a finite number of identified, predictable potential solutions to the recognized need or problem;
>
> (3) a finding that one of ordinary skill in the art could have pursued the known potential solutions with a reasonable expectation of success; and
>
> (4) whatever additional findings based on the *Graham* factual inquiries may be necessary, in view of the facts of the case under consideration, to explain a conclusion of obviousness.

Ex parte Kubin, 83 USPQ2d 1410, 2007 WL 2070495 (Bd. App. & Int. 2007) was cited as an example in the Examination Guidelines of a situation where a finite number of identified, predictable solutions are provided with a reasonable expectation of success. However, in the Federal Circuit decision affirming *Ex parte Kubin*, *In re Kubin* 561 F.3d 1351 (Fed. Cir. 2009), the Court stated:

> To differentiate between proper and improper applications of "obvious to try," this court outlined two classes of situations where "obvious to try" is erroneously equated with obviousness under § 103. In the first class of cases, what would have been "obvious to try" would have been to vary all parameters or try each of numerous possible choices until one possibly arrived at a successful result, where the prior art gave either no indication of which parameters were critical or no direction as to which of many possible choices is likely to be successful (citing *In re O'Farrell*, 853 F.2d 894, 903 (Fed. Cir. 1988)). In such circumstances, where a defendant merely throws metaphorical darts at a board filled with combinatorial prior art possibilities, courts should not succumb to hindsight claims of obviousness. The inverse of this proposition is succinctly encapsulated by the Supreme Court's statement in *KSR* that where a skilled artisan merely pursues "known options" from a "finite number of

> identified, predictable solutions," obviousness under § 103 arises. 550 U.S. at 421.
>
> The second class of *O'Farrell's* impermissible "obvious to try" situations occurs where what was "obvious to try" was to explore a new technology or general approach that seemed to be a promising field of experimentation, where the prior art gave only general guidance as to the particular form of the claimed invention or how to achieve it.

As stated above, the teaching of the prior art would constitute metaphorically throwing the darts. Muzny et al. merely discloses a chromosome 12 genomic sequence. No direction is provided in Muzny regarding the location of the MDM2 gene. Further, The clone AC025423 is 150,579 nucleotides in length. No indication is even given as to where the MDM2 gene is contained within this clone. The cDNA sequence only contains 2372 nucleotides (1.6% of AC025423). However, one of ordinary skill in the art would not know where or how these 2372 nucleotides are interspersed within the AC025423 clone or if indeed it is even present. No teachings are provided as to the structure of the MDM2 gene itself: number and size of exons, number and size of introns, locations of exons and introns and number and size of 5' and 3' untranslated regions. Additionally, the situation is further complicated by the two disclosures in the art regarding the possible location of the Muzny sequence, Vogelstein and Andersen. Specifically as noted above, Appellant notes that Vogelstein placed the human MDM2 homolog gene at 12q12-14. After publication of Vogelstein, the MDM2 homolog gene was found to be located several kilobases away at 12q15. One of skill in the art would not have known where to look.

The second "obvious to try" situation would apply as well. This is because only general guidance is provided in the art with respect to detecting intron/exon junctions. Specifically, Watson et al. on pages 137-138, states

> Once the first genes were cloned, introns were identified by comparing the cloned genomic DNA with the corresponding cloned cDNA. For small genes, such as the beta-globin gene, the sizes of the introns and the locations of intron-exon boundaries were precisely determined by sequencing cloned genomic DNA and comparing the sequence with the cDNA sequence and with the protein sequence. Introns exist in genes from all eukaryotic animals, in plant genes, and, surprisingly, in genes of the *E coli* phage T4. Often the introns of a gene contain many more nucleotides than do its coding exons, thus

> accounting for the previously unexplained large sizes of many primary RNA transcripts. The number and size of introns vary widely from one gene to another.

There is no specific methodology provided regarding how to locate the human MDM2 gene itself or even its size. Further, even Watson admits to variability of size and location of introns.

Further, the claimed invention can be distinguished from the facts in *Kubin*. Specifically, in *Kubin*, the claimed invention was directed to

> An isolated nucleic acid molecule comprising a polynucleotide encoding a polypeptide at least 80% identical to amino acids 22-221 of SEQ ID NO:2, wherein the polypeptide binds CD48.

Id.

In the rejection affirmed by the Board, the Examiner asserted that

> The skilled artisan would have been motivated to isolate the nucleic acid sequence corresponding to NAIL, based on Valiante's disclosure of p38 (which is the same protein as NAIL) and Valiante's express teachings how to isolate p38 cDNA by using conventional techniques, such as taught in Sambrook, including using mAbC1.7, a probe specific for p38.

Id.

This finding of obviousness in *Kubin* appeared to be predicated on the obviousness of isolating NAIL cDNA, not any other nucleic acid sequences encoding the NAIL protein. *In re Kubin* specifically states

> Moreover, the record strongly reinforces …the board's factual finding that one of ordinary skill would have been motivated to isolate NAIL cDNA, given Valiante's teaching that p38 is "Expressed by virtually all human NK cells and thus plays a role in the immune response"….The record shows that the prior art teaches a protein of interest, a motivation to isolate the gene coding for that protein, and illustrative instructions to use a monoclonal antibody specific to the protein for cloning this gene.

Id.

In contrast, the claimed invention is directed to a nucleic acid molecule 20-51039 contiguous nucleotides in length consisting of a reverse or forward strand of a region of SEQ ID NO:4. SEQ ID NO:4 is a genomic sequence, not cDNA encoding MDM2. This is very different from *Kubin* which involves deducing the NAIL cDNA sequence from NAIL

polypeptide sequence and subsequently isolating this sequence. The art cited in the instant application was a cDNA sequence and a genomic clone containing chromosome 12 sequence. Considerably more and undue experimentation would be involved in identifying and isolating the genomic sequence and consequently the claimed regions comprising the recited noncoding regions of the MDM2 gene than in identifying cDNA in view of a disclosure of a polypeptide sequence. The claimed sequence is between 20-51039 nucleotides in length. The Muzny sequence is 150,579 nucleotides in length. No direction or frame of reference is provided as to where the MDM2 sequence could be located. Furthermore, although Vogelstein, disclosed the MDM2 cDNA, no direction is provided as to the location of exons, introns, 5' untranslated and/or 3' untranslated regions.

It is Appellant's view that the claimed invention is more analogous to *Ex Parte Koide*, Appeal 2009-1912, 2009 WL 1719400 (Bd. Pat. App. & Intfer. 2009) decided subsequent to *In re Kubin*. In *Koide*, it was held that claims to a fibronectin molecule containing a stabilizing mutation of at least one of Asp7, Asp23 or Glu9 were not obvious over a prior art disclosure of randomly screening Fibronectin type III polypeptides at a variety of positions and the disclosure of a Fibronectin type III subunit binding domain since "there is no predictable expectation that performing the random screening methods of the cited prior art would predictably result in the polypeptides containing the recited mutations. Here, there is no indication that performing the recombinant DNA methods would necessarily result in the claimed nucleic acid molecules.

(4) There was a long felt need and it is likely that others had tried but failed before the priority date of the instant application.

There has been a great deal of interest in the scientific community in human MDM2 given its potential use as a diagnostic and therapeutic agent. This interest is summarized in Vogelstein. Additionally, Appellant submitted during prosecution an IDS listing four references relating to MDM2 (a copy of the 1449 Form previously submitted and made of record and included in Evidence Appendix). However, there was absolutely no disclosure or suggestion of the genomic organization of MDM2 genomic DNA until the instant application was filed. An independent disclosure of the genomic organization of the human MDM2 gene was not available until July 21, 2004, more than one year after the filing date of the instant

application (see Liang et al., 2004, Gene 338:217-223, previously made of record in the Supplemental Appeal Brief submitted March 2, 2008). The dearth of knowledge regarding the human MDM2 gene was actually admitted to by Liang et al. on the first page of his article where it was stated "Although the human MDM2 cDNA sequence has been reported, the genomic organization of the human gene has not been documented". Further, Liang et al. discussed the usefulness of determining the genomic structure and organization of the human MDM2 gene on page 218:

> One of the distinctive properties of MDM2 is the possession of an extremely complex expression pattern. Its multiple-sized transcripts and proteins have been found in tumour samples and cell lines by a number of groups (citations omitted). In our previous studies, five alternatively sized transcripts of the human MDM2 were found in human ovarian tumour, bladder tumour and leukaemic cell samples (citation omitted)....Here we present data demonstrating two further MDM2 transcript forms with internal sequence deletions in human tumour tissue. We Hypothesised that these transcripts are generated by alternative splicing. To test this hypothesis and to explore the associated mechanisms, we have investigated the genomic structure and organization of the human MDM2 gene...

It is well established case law that secondary considerations such as commercial success, long felt need, unexpected results must be considered before making an obviousness determinations (see, for example, *Shackelton v J Kaufman Iron Works, Inc.*, 689 F.2d 334, (Fed Cir 1982) and *Ortloff v Gulsby Engineering*, 884 F2d 1399, 2 USPQ2d 1335 (Fed. Cir. 1989), reh'g denied Sept. 1989).

Respectfully submitted,

/Cheryl H Agris/

Date: October 2, 2009

Cheryl H. Agris, Reg. No. 34,086
P.O. Box 8459
Pelham, N.Y. 10803
(914) 712-0093

CLAIMS APPENDIX

7. An isolated nucleic acid molecule 20-51039 contiguous nucleotides in length consisting of a reverse or forward strand of a region of SEQ ID NO:4, wherein said region is selected from the group consisting of a 5'-non coding region depicted in nucleotides 51039-41739 of SEQ ID NO:4, a 3'-non-coding region depicted in nucleotides 9503-1 of SEQ ID NO:4, a contiguous intron-exon region between nucleotides 41738-9502 of SEQ ID NO:4, wherein a sequence segment comprising 41738-9502 of SEQ ID NO:4 encodes human mouse double minute 2 homolog depicted in SEQ ID NO:2, a contiguous exon-intron region between nucleotide 41738-9502 of SEQ ID NO:4, wherein a sequence segment comprising 41738-9502 of SEQ ID NO:4 encodes human mouse double minute 2 homolog depicted in SEQ ID NO:2, an intron depicted in nucleotides 36385-40645, 36309-33127, 32994-29616, 29564-25577, 25507-25384, 25287-21169, 21006-14110, 13953-13267, and/or 13188-10665, a region comprising a dinucleotide of the following group: 41739-41738, 40645-40646, 36309-36310, 36384-36385, 32994-32995, 33126-33127, 29564-29565, 29615-29616, 25507-25508, 25287-25288, 25383-25384, 25576-25577, 21006-21007, 21168-21169, 14109-14110, 13953-13954, 13266-13267, 13188-13189, 10664-10665 and/or 9504-9503; a transcription binding site selected from the group consisting of

BINDING SITES	huMDM2, location in SEQ ID NO:4
AP1_C:	36-46, 2876-2886;
AP4_Q5:	7944-7980;

AP4_Q6:	7943-59, 8924-8940, 9294-9310;
ARNT_01:	1682-1706, 2193-2217, 9201-9225;
BRN2_01:	1040-1058, 7803-7821;
CAAT_01:	3292-3306;
CDPCR3HD_01:	6522-6540;
CEBPB_01:	1424-1438, 3917-3931, 4178-4192, 4787-4801, 6855-6869;
CREL_01:	5630-5642;
DELTAEF1_01:	83-95, 6328-6340;
FREAC7_01:	2757-2773, 5154-5170, 5823-5839;
GATA1_04:	4846-4858, 7017-7029;
GATA1_05:	8464-8476;
GATA2_02:	6045-6057, 6073-6085, 6142-6154;
GATA2_03:	2489-2501, 3323-3335, 3384-3396, 7393-7405;

GATA3_02: 3264-3276, 6870-6882:

GATA3_03: 40-52, 5729-5741, 6529-6541, 6874-6886, 7041-7053, 7589-7601;

GATA_C: 7 349-7361, 8188-8200;

HFH2_01: 1743-1759, 7995-8011;

HFH3_01: 502-518, 1739-1755, 4160-4176, 9402-9418, 9418-9434;

HFH8_01: 8184-8200;

IK2_01: 951-963, 3588-3600;

MZF1_01: 1202-1210, 1447-1455, 4997-4005, 5424-5432;

NF1_Q6: 1480-1500, 8166-8182;

NFAT_Q6: 4190-4208, 6009-6027;

NKX25_01: 741-755, 1648-1662, 1885-1899, 1984-1998, 3609-3623, 4928-4942, 5060-5074, 5889-5903, 8850-8864, 9190-9204;

NKX25_02: 2584-2599, 2970-2984, 4644-4658, 5179-5193, 6482-6496;

NMYC_01: 2560-2572;

RORA1_01: 220-238, 2638-2656;

S8_01: 4644-4656, 4842-4854, 4845-4857, 5200-5212, 5371-5383, 5735-5747, 6482-6494, 6541-6553, 6544-6556, 6772-6784, 7270-7292, 7273-7285;

SOX5_01: 1355-1371, 1430-1446, 3094-3110, 3155-3171, 4669-4685, 4692-4708, 4789-4805;

SRY_02: 4164-4180, 5665-5681;

TATA_01: 1261-1277, 2574-2590, 2723-2739, 2733-2749, 2770-2786, 4199-4215, 4206-4222;

TATA_C: 5900-5916, 7456-7472, 7702-7718, 7917-7933; and

XFD2_01: 7702-7218, 7917-7933; .

a transcription binding site selected from the group consisting of

BINDING SITES huMDM2, location in SEQ ID NO:4

AP1_C: 12109-12119, 12695-12705, 22600-22610, 24166-24176, 31311-31321, 35234-35244, 39184-39194;

AP1_Q2: 11952-11962, 12068-12078, 14798-14808, 21748-21758, 22613-22623, 23676-23686, 26562-26572, 30046-30056;

AP1_Q4: 12695-12705, 31311-31321, 35234-35244, 36295-36305, 38784-38794, 39188-39198;

AP4_Q6: 31635-31651;

BRN2_01: 13448-13466, 14764-14782, 28094-28112, 40027-40045;

CAAT_01: 11288-11302, 15054-15068;

CDPCR3HD_01: 11286-11304, 13284-13302, 20846-20864, 29344-29362;

CEBPB_01: 29241-29255;

CREL_01: 36091-36103, 38873-38885;

DELTAEF1_01: 18083-18095, 20385-20397, 26955-26967;

FREAC7_01: 11982-11998, 15187-15202, 16523-16539, 16529-16545, 16587-16603, 16604-16620, 16676-16642, 16633-16649, 16644-16660, 16650-16666, 16657-16673, 16673-16689, 16762-16778, 21332-21348, 25689-25700, 26529-26545, 27767-27783, 29495-29511;

GATA1_02: 10916-10928, 15775-15789, 18162-18174, 26088-26100, 32518-32530;

GATA1_03: 28012-28024;

GATA1_04: 11153-11165, 11630-11642, 13778-13790, 17439-17451, 19300-19312, 21606-21618, 22743-22755, 23747-23759, 25806-25818, 26529-26541, 29424-29436, 30455-30467, 32761-32778, 33352-33364, 33960-33972, 36101-36113, 40007-40019;

GATA1_05: 11590-11602, 26550-26562, 36737-36749;

GATA1_06: 18772-18784, 23054-23066, 35568-35580, 37855-37867;

GATA2_02: 20755-20767, 30830-30842, 34755-34767, 36285-36297, 39143-39155, 39641-39653, 40586-40598;

GATA2_03: 13535-13547, 22711-22723, 23161-23173, 25028-25040, 27237-27249, 36277-36289;

GATA3_02: 11558-11570, 16470-16482, 17225-17237, 19619- 19631, 22156-22168, 22443-22455, 24713-24725, 27619-27631, 32716-32728, 34124-34136, 34163-34175, 36832-36844, 38403-38415;

GATA3_03: 10869-10881, 11515-11527, 13845-13857, 17221-17233, 18952-18964, 20050-20062, 40171-40183;

GATA_C: 15848-15860, 18899-18911, 23640-23652, 29072-29084, 30881-30893, 33198-33210, 37472-37484, 38621-38633;

GFI1_01: 35469-35481, 35492-35504;

HFH2_01: 15939-15955, 24636-24652, 25866-25882, 32171-32187, 35372-35388, 39457-35473;

HFH3_01: 13340-13356, 19218-19234, 21328-21344, 21336-21352, 21344-21360, 28062-28078, 32125-32141;

HFH8_01: 14133-14149, 22578-22584;

HNF3B_01: 13150-13166, 16505-16521, 25264-25280, 29443-29459, 37654-37670;

IK2_01: 11547-11559, 17144-17156, 18961-18973, 23883-23895, 27617-27629, 28908-28920, 29241-29253, 30752-30764, 34768-34780;

LYF1_01: 12319-12331, 19191-19203, 37226-37238, 39430-39442;

MAX_01: 22974-22986, 33339-33351;

MZF1_01: 26105-26113, 35187-35195;

NF1_Q6: 12048-12064, 33334-33354;

NFAT_Q6: 13295-13313, 14157-14175, 14311-14329, 14414-14432, 18269-18287. 19326-19344, 20801-20819, 21177-21195, 22537-22555, 23861-23879, 25392-25410, 25879-25897, 27524-

27542, 30636-30654, 30718-30736, 31525-31543, 33655-33673, 34726-34744, 34917-34535, 34990-35008, 35979-35997, 36479-36493, 36577-36595, 37154-37172, 40224-40242, 40365-40383;

NKX25_01: 12041-12055, 12340-12354, 12471-12485, 12742-12756, 12877-12891, 13849-13863, 18995-19009, 21440-21454, 21883-21897, 28426-28440, 30964-30978, 32033-32047, 32265-32279;

NKX25_02: 10998-11012, 12711-12725, 14131-14145, 14726-14740, 16024-16038;

NMYC_01: 18753-18765, 18754-18766, 23076-23088, 30534-30546, 34400-34412;

RORA1_01: 13134-13152, 22966-22984, 24934-24952, 33341-33359, 34760-34778;

S8_01: 11000-11012, 11977-11989, 12048-12060, 12051-12063, 13747-13759, 13923-13935, 13926-13938, 14676-14688, 14679-14691, 16026-16038, 16313-16325, 16316-16328, 17515-17527, 20756-20768, 20759-20771, 23154-23166, 23157-23169, 25198-25210, 25201-25213, 26651-26663, 27508-27520, 27511-27523, 29450-29462, 29478-28490, 29775-29787, 29778-29790, 29813-29825, 29816-29828, 31329-31341, 31677-31689, 31680-31692, 31732-31744, 31735-31747, 36137-36149, 36140-36152, 36812-36824, 36815-36827, 37413-37425, 38679-38691, 39474-39486, 39477-39489;

SOX5_01: 27397-27413, 27572-27588, 28100-28116, 29230-29246, 29439-29455, 30690-30706, 31595-31611, 33871-33887, 34113-34129, 34624-34640, 37668-37684, 38582-38598, 39124-39140, 40410-40426;

SRY_02: 20016-20032, 22410-22426, 27329-27345, 29162-29178, 29499-29515, 30646-

30662, 31503-31519, 35928-35944, 37324-37340;

TATA_01: 32722-32738, 32729-32745, 32807-32823, 33825-33841, 34120-34136, 35433-35449, 36593-36609;

TATA_C: 11015-11031, 11817-11833, 13635-13651, 14930-14946;

TCF11_01: 18543-18549, 22574-22580, 31281-31297, 31489-31505, 38754-38770;

USF_01: 23075-23087, 32577-32589;

VMYB_02: 11526-11538, 17384-17396, 18400-18412, 19549-19561, 22188-22200, 40486-40508 and

XFD2_01: 16620-16636, 18153-18169, 22102-22118, 23141-23157,

And a transcription binding site selected from the group consisting of

BINDING SITES

huMDM2, 1 location in SEQ ID NO:4

AP1_C: 44584-44594, 49069-49079;

AP1_Q2: 42174-42184, 45217-45227, 48422-48422, 50447-50457;

AP1_Q4: 42702-42712, 50806-50816;

AP4_Q6: 42117-42133, 42118-42134, 42244-42260, 45432-45448; 45433-45449, 46609-46625;

BRN2_01: 42310-42328, 44022-44040, 47514-47532, 48900-48918, 48967-48985;

CAAT_01: 44866-44880;

CDPCR3HD_01: 45671-45689, 49219-49237;

CREL_01: 42437-42449, 49797-49809;

FREAC7_01: 47026-47042, 47292-47308, 47658-47674;

GATA1_02: 43482-43494, 48926-48938, 49284-49296;

GATA1_03: 47371-47383;

GATA1_04: 43054-43066, 43162-43162, 43967-43979, 45464-45476, 45916-45928, 47763-47775;

GATA1_05: 49319-49331, 49459-49471;

GATA1_06: 47590-47602;

GATA2_02: 42660-42672, 43475-43487;

GATA2_03: 43714-43726, 50948-50960;

GATA3_02: 49155-49167, 49844-49856;

GATA3_03: 42202-42214, 44810-44822, 48438-48450, 49136-49148, 49337-49349, 49869-49881;

GATA_C: 44011-44023, 45256-45268, 45823-45835, 47915-47927, 49201-49213, 49573-49585;

GFI1_01: 46606-46618, 47063-47075;

HFH3_01: 47030-47046, 47284-47300, 47288-47304;

IK2_01: 45275-45287;

LYF1_01: 44564-44576, 46991-47003, 49567-49579;

MAX_01: 43234-43246, 48726-48738;

MZF1_01: 41772-41780, 42290-42298, 42295-42303, 44507-44515, 45105-45113, 45203-45211, 49948-49956, 50774-50782;

NF1_Q6: 50209-50229;

NFAT_Q6: 42061-42079, 44418-44436, 46399-46417, 47974-47992, 49267-49285, 49964-49982, 50392-50410;

NKX25_01: 42394-42408, 43507-43521, 46115-46129;

RORA1_01: 45073-45091, 48718-48736;

S8_01: 43552-43564, 45214-45226, 47160-47172, 48419-48431, 49295-49307, 50379-50391;

SOX5_01: 43716-43732, 46351-46367, 47156-47172, 47774-47790, 47868-47884, 47974-47990, 48915-48931, 50323-50339;

TATA_01: 45588-45604, 47625-47641, 48026-48042, 48659-48675, 49056-49072, 49079-49095, 49152-49168;

TCF11_01: 49115-49131;

VMYB_02: 42010-42022, 42279-42291, 44651-44663; and

XFD2_01: 42870-42886, 42910-42926.

10. A composition comprising the nucleic acid molecule of claim 7 and a carrier.

15. A kit comprising the nucleic acid molecule of claim 7.

16. The kit according to claim 15, in which the nucleic acid molecule is labeled with a detectable substance.

17. A solid support comprising the nucleic acid molecule of claim 7.

18. The solid support of claim 17 wherein said support is a microarray.

20. The solid support of claim 18, which further comprises a nucleic acid molecule encoding human mouse double minute 2 homolog, complementary sequence thereof or a portion of said nucleic acid molecule containing at least 20 contiguous nucleotides.

22. A method of identifying variants of SEQ ID NO:4, or its complementary sequence, comprising

isolating genomic DNA from a subject and determining the presence or absence of a variant in said genomic DNA using the nucleic acid molecule of claim 7.

23. A method for detecting the presence or absence of SEQ ID NO:4 or its complementary sequence in a sample, said method comprising (a) contacting the sample with the nucleic acid molecule of claim 7 and (b) determining whether the nucleic acid molecule binds to said

nucleic acid sequence in the sample.

24. An isolated nucleic acid molecule 20-5000 contiguous nucleotides in length consisting of a reverse or forward strand of a contiguous exon-intron region between nucleotides 41738-9502 of SEQ ID NO:4, or contiguous intron-exon region between nucleotides 41738-9502 of SEQ ID NO:4, wherein a sequence segment comprising 41738-9502 of SEQ ID NO:4 encodes human mouse double minute 2 homolog depicted in SEQ ID NO:2.

25. The isolated nucleic acid molecule of claim 24, wherein said nucleic acid molecule is 20-5000 contiguous nucleotides in length and comprises nucleotides 41739-41738, 40645-40646, 36309-36310, 36384-36385, 32994-32995, 33126-33127, 29564-29565, 29615-29616, 25507-25508, 25287-25288, 25383-25384, 25576-25577, 21006-21007, 21168-21169, 13953-13954, 14109-14110, 13188-13189, 13266-13267, 10664-10665 and/or 9504-9503 of SEQ ID NO:4 or their reverse strands.

30. A microarray comprising a plurality of the nucleic acid molecules of claim 7.

31. The microarray of claim 30 wherein said microarray further comprises a nucleic acid molecule encoding human mouse double minute 2 homolog, complementary sequence thereof or a portion of said nucleic acid molecule containing at least 20 contiguous nucleotides.

32. A method for detecting the presence of a nucleic acid sequence of SEQ ID NO:4 or its complementary sequence in a sample, said method comprising contacting the sample with the

nucleic acid molecule of claim 7 and determining whether the nucleic acid molecule binds to said nucleic acid sequence in the sample.

EVIDENCE APPENDIX

1. Muzny et al. (description of sequence of AC025423 made of record by Examiner)

2. Vogelstein et al., US Patent No. 5,411,860 and NM_002392 (made of record by examiner)

3. Watson, Recombinant DNA

4. Genecard profile of human MDM2 submitted with amendment dated August 25, 2005

5. Anderson et al., 1996, Mammalian Genome 7:780-783 submitted with amendment dated August 25, 2005

6. Bureau, 1995, Genomics 28: 109-112 submitted with amendment dated August 25, 2005

7. Information Disclosure Statement submitted March 1, 2005 (and references submitted)

8. Liang et al. submitted with Appeal Brief dated March 2, 2008

9. Wong et al., 2000, Genome Research 10: 1672-1678

1: AC025423 Reports Homo sapiens 12 B...[gi:14578057]

LOCUS AC025423 150579 bp DNA linear PRI 23-JAN-2003
DEFINITION Homo sapiens 12 BAC RP11-61I02 (Roswell Park Cancer Institute Human BAC Library) complete sequence.
ACCESSION AC025423
VERSION AC025423.32 GI:14578057
KEYWORDS HTG.
SOURCE Homo sapiens (human)
ORGANISM Homo sapiens
Eukaryota; Metazoa; Chordata; Craniata; Vertebrata; Euteleostomi; Mammalia; Eutheria; Primates; Catarrhini; Hominidae; Homo.
REFERENCE 1 (bases 1 to 150579)
AUTHORS Muzny,D.M., Adams,C., Adio-Oduola,B., Ali-osman,F.R., Allen,C., Alsbrooks,S.L., Amaratunge,H.C., Are,J.R., Banks,T., Barbaria,J., Benton,J., Bimage,K., Blankenburg,K., Bonnin,D., Bouck,J., Bowie,S., Brieva,M., Brown,E., Brown,M., Bryant,N.P., Buhay,C., Burch,P., Burkett,C., Burrell,K.L., Byrd,N.C., Carron,T.F., Carter,M., Cavazos,S.R., Chacko,J., Chavez,D., Chen,G., Chen,R., Chen,Z., Chiu,D., Chowdhry,I., Christopoulos,C., Cleveland,C.D., Cox,C., Coyle,M.D., Dathorne,S.R., David,R., Davila,M.L., Davis,C., Davy-Carroll,L., Dederich,D.A., Delaney,K.R., Delgado,O., Denn,A.L., Ding,Y., Dinh,H.H., Douthwaite,K.J., Draper,H., Dugan-Rocha,S., Durbin,K.J., Earnhart,C., Edgar,D., Edwards,C.C., Elhaj,C., Emerling,S., Escotto,M., Falls,T., Ferraguto,D., Flagg,N., Ford,J., Foster,P., Frantz,P., Gabisi,A., Gao,J., Garcia,A., Garner,T., Garza,N., Gill,R., Gorrell,J.H., Guevara,W., Gunaratne,P., Hale,S., Hamilton,K., Han,J., Harris,C., Harris,K., Hart,M., Havlak,P., Hawes,A., Hernandez,J., Hernandez,O., Hodgson,A., Hogues,M., Holloway,C., Hollins,B., Homsi,F., Howard,S., Huber,J., Hulyk,S., Hume,J., Ioshikhes,I., Jackson,L.E., Jacobson,B., Jia,Y., Johnson,R., Jolivet,S., Joudah,S., Karlsson,E., Kelly,S., Khan,U., King,L., Korvah,J., Kovar,C., Kratovic,J., Kureshi,A., Landry,N., Leal,B., Lee,E., Lewis,L.C., Lewis,L., Li,J., Li,Z., Lichtarge,O., Lieu,C., Liu,J., Liu,W., Loulseged,H., Lozado,R.J., Lu,X., Lucier,A., Lucier,R., Luna,R., Ma,J., Maheshwari,M., Mapua,P., Marondel,I., Martin,R., Martindale,A., Martinez,E., Massey,E., Mawhiney,E., McLeod,M.P., Meador,M., Mei,G., Merscher,S., Metzker,M., Miller,A., Miner,G., Miner,Z., Mitchell,T., Mohabbat,K., Montgomery,K.T., Morgan,M., Morris,S., Moser,M., Neal,D., Nelson,D., Newtson,J., Newtson,N., Nguyen,A., Nguyen,N., Nguyen,N., Nickerson,E., Nwokenkwo,S., Oguh,M., Okwuonu,G., Oragunye,N., Oviedo,R., Pace,A., Payton,B., Peery,J., Perez,L., Peters,L., Pickens,R., Primus,E., Pu,L.L., Quiles,M., Ren,Y., Rives,M., Rojas,A., Rojubokan,I., Rolfe,M., Ruiz,S., Savery,G., Scherer,S., Scott,G., Shen,H., Shim,C., Shooshtari,N., Sisson,I., Sodergren,E., Sonaike,T., Sparks,A., Stanley,H., Stone,H., Sutton,A., Svatek,A., Tabor,P., Tamerisa,A., Tamerisa,K., Tang,H., Tansey,J., Taylor,C., Taylor,T., Telfrod,B., Thomas,N., Thomas,S., Usmani,K., Vasquez,L., Vera,V., Villalon,D., Vinson,R., Wall,R., Wang,S., Ward-Moore,S., Warren,R.,

h cb h g e e e e fcg

Washington,C., Watlington,S., Williams,G., Williamson,A., Wieczyk,R., Wooden,S., Worley,K., Wu,C., Wu,Y., Wu,Y.F., Zhou,J., Zorrilla,S., Kucherlapati,R., Weinstock,G. and Gibbs,R.

TITLE Direct Submission
JOURNAL Unpublished

REFERENCE 2 (bases 1 to 150579)
AUTHORS Worley,K.C.
TITLE Direct Submission
JOURNAL Submitted (09-MAR-2000) Human Genome Sequencing Center, Department of Molecular and Human Genetics, Baylor College of Medicine, One Baylor Plaza, Houston, TX 77030, USA

REFERENCE 3 (bases 1 to 150579)
AUTHORS Worley,K.C.
TITLE Direct Submission
JOURNAL Submitted (30-JUN-2001) Human Genome Sequencing Center, Department of Molecular and Human Genetics, Baylor College of Medicine, One Baylor Plaza, Houston, TX 77030, USA

REFERENCE 4 (bases 1 to 150579)
AUTHORS Worley,K.C.
TITLE Direct Submission
JOURNAL Submitted (30-SEP-2002) Human Genome Sequencing Center, Department of Molecular and Human Genetics, Baylor College of Medicine, One Baylor Plaza, Houston, TX 77030, USA

REFERENCE 5 (bases 1 to 150579)
AUTHORS Worley,K.C.
TITLE Direct Submission
JOURNAL Submitted (23-JAN-2003) Human Genome Sequencing Center, Department of Molecular and Human Genetics, Baylor College of Medicine, One Baylor Plaza, Houston, TX 77030, USA

COMMENT On Jun 30, 2001 this sequence version replaced gi:14575757.
INFORMATION: http://www.hgsc.bcm.tmc.edu/ or email gc-help@bcm.tmc.edu

CLONE LENGTH: This sequence does not necessarily represent the entire insert of this clone. Overlapping regions of clones are only sequenced and submitted once, so the sequence for the remainder of the insert may be found in the record for the adjacent clones. Overlapping clones are noted at the beginning and end of the Features listing.

ANNOTATION OF FEATURES:
STSs are identified using ePCR (Genome Res. 7:541-550) searches of a local database that includes entries from dbSTS, GDB, and local mapping efforts.
Repeats are identified using RepeatMasker (A. Smit and P. Green, unpublished.) for Human and Mouse sequences.
Genes and Region of sequence similarity are identified by BLAST (Nuc. Acids Res. 25:3389-3402) similarity (expect < 1e-34) to the EST and cDNA sequences. Genes demonstrate at least two exons flanked by consensus splice sites that maintained sequence continuity across the splice junctions. Sequences that are not identical matches are annotated as similar.

SEQUENCING READ COVERAGE:Sequencing is completed to a minimum standard of double strand coverage with a minimum of 2 clones and 2 reads with no ambiguities or 2 chemistries with a minimum of 2 clones and 3 reads with no ambiguities. If the sequence quality for a region does not meet this standard, it will be indicated in the annotation as Low Coverage.

```
            QUALITY OF INDIVIDUAL BASES:This sequence meets stringent quality
            standards - estimated error rate less than 1 per 10,000 bases.
            Reports of lowest quality individual bases and measures of base
            quality are listed below. Description of the metrics can be found
            at URL:
            http://qc.bcm.tmc.edu:8088/quality.info/genbank.annotation.html.

            QUALSTAT-REPORT.
FEATURES             Location/Qualifiers
     source          1..150579
                     /organism="Homo sapiens"
                     /mol_type="genomic DNA"
                     /db_xref="taxon:9606"
                     /chromosome="12"
                     /clone="RP11-61102"
     misc_feature    1..1998
                     /note="overlaps bases 96763..98760 of clone AC133749"
                     /function="clone overlap"
     repeat_region   complement(84..376)
                     /rpt_family="AluJb"
     STS             112..380
                     /standard_name="163887"
     repeat_region   complement(395..526)
                     /rpt_family="L2"
     repeat_region   1610..1838
                     /rpt_family="AluJb"
     repeat_region   complement(1857..2163)
                     /rpt_family="AluSx"
     repeat_region   2353..3314
                     /rpt_family="MER4-internal"
     repeat_region   3319..3635
                     /rpt_family="AluJo"
     repeat_region   4067..4746
                     /rpt_family="LTR8A"
     repeat_region   4779..5068
                     /rpt_family="AluJo"
     repeat_region   5150..5291
                     /rpt_family="L2"
     repeat_region   complement(6105..6362)
                     /rpt_family="MIR"
     repeat_region   6808..6930
                     /rpt_family="L2"
     repeat_region   7845..8088
                     /rpt_family="AluJb"
     repeat_region   8089..8114
                     /rpt_family="(CAAA)n"
     repeat_region   8274..8307
                     /rpt_family="(CA)n"
     repeat_region   8371..8654
                     /rpt_family="L1MB2"
     repeat_region   9026..9335
                     /rpt_family="L1MC2"
     repeat_region   9346..9439
                     /rpt_family="A-rich"
     repeat_region   9443..9666
                     /rpt_family="L1M1"
     repeat_region   9973..10073
                     /rpt_family="LTR37B"
     repeat_region   10074..10257
                     /rpt_family="(TA)n"
```

repeat_region	10289..10653
	/rpt_family="(TA)n"
repeat_region	10666..10821
	/rpt_family="LTR37B"
repeat_region	complement(11068..11199)
	/rpt_family="AluJo/FRAM"
repeat_region	11364..11538
	/rpt_family="L2"
repeat_region	complement(11956..12173)
	/rpt_family="MER20"
repeat_region	complement(12540..12607)
	/rpt_family="L1"
repeat_region	12797..13099
	/rpt_family="AluSx"
repeat_region	complement(13269..13362)
	/rpt_family="MER5A"
repeat_region	13888..14200
	/rpt_family="AluY"
repeat_region	14201..14242
	/rpt_family="(CAAA)n"
repeat_region	14243..14265
	/rpt_family="AluY"
repeat_region	14269..14580
	/rpt_family="AluSq"
repeat_region	complement(14680..14784)
	/rpt_family="MIR"
repeat_region	complement(14816..14853)
	/rpt_family="L1PA6"
repeat_region	14851..14973
	/rpt_family="L1PA6"
repeat_region	complement(15100..15219)
	/rpt_family="MER5B"
repeat_region	15328..15385
	/rpt_family="GA-rich"
repeat_region	16238..16266
	/rpt_family="GC_rich"
repeat_region	16285..16309
	/rpt_family="GC_rich"
repeat_region	complement(17545..17644)
	/rpt_family="MIR"
repeat_region	complement(17704..18015)
	/rpt_family="AluSg"
repeat_region	18513..18537
	/rpt_family="AT_rich"
repeat_region	19097..19398
	/rpt_family="AluSq"
repeat_region	19419..19438
	/rpt_family="(TTTA)n"
repeat_region	20108..20173
	/rpt_family="L2"
repeat_region	20324..20346
	/rpt_family="AT_rich"
repeat_region	20471..20735
	/rpt_family="AluJb"
repeat_region	complement(20866..21040)
	/rpt_family="MIR"
repeat_region	complement(21081..21763)
	/rpt_family="L1PA3"
repeat_region	21763..22907
	/rpt_family="L1PA3"

NCBI

Sequence Revision History

Revision history for AC025423

GI	Version	Update Date	Status	I	II
14578057	32	Jan 23 2003 4:22 AM	Live	◉	○
14578057	32	Sep 30 2002 11:59 AM	Dead	○	◉
14578057	32	Jun 30 2001 4:17 AM	Dead	○	○
14575757	31	Jun 29 2001 4:09 AM	Dead	○	○
14547368	30	Jun 26 2001 4:45 AM	Dead	○	○
14547368	30	Jun 25 2001 4:47 AM	Dead	○	○
14532332	29	Jun 24 2001 4:19 AM	Dead	○	○
14333711	28	Jun 10 2001 4:08 AM	Dead	○	○
14333711	28	Jun 9 2001 4:15 AM	Dead	○	○
14328936	27	Jun 8 2001 4:13 AM	Dead	○	○
14327716	26	Jun 7 2001 4:09 AM	Dead	○	○
14318341	25	Jun 6 2001 4:13 AM	Dead	○	○
14149585	24	May 19 2001 4:26 AM	Dead	○	○
14030796	23	May 14 2001 4:10 AM	Dead	○	○
14029854	22	May 13 2001 4:16 AM	Dead	○	○
14028873	21	May 12 2001 4:13 AM	Dead	○	○
13959114	20	May 7 2001 4:13 AM	Dead	○	○
13957550	19	May 6 2001 9:19 AM	Dead	○	○
13957550	19	May 5 2001 4:12 AM	Dead	○	○
13940523	18	May 4 2001 4:21 AM	Dead	○	○
13928603	17	May 2 2001 4:09 AM	Dead	○	○
13661843	16	Apr 21 2001 4:14 AM	Dead	○	○
13661843	16	Apr 20 2001 4:20 AM	Dead	○	○
13661843	16	Apr 19 2001 4:18 AM	Dead	○	○
13661843	16	Apr 18 2001 2:03 PM	Dead	○	○

13605934	15	Apr 14 2001 4:22 AM	Dead	○	○
13605934	15	Apr 13 2001 4:14 AM	Dead	○	○
13605934	15	Apr 12 2001 4:10 AM	Dead	○	○
12831256	14	Feb 18 2001 4:14 AM	Dead	○	○
12831256	14	Feb 17 2001 4:26 AM	Dead	○	○
12831256	14	Feb 15 2001 4:27 AM	Dead	○	○
12829983	13	Feb 14 2001 4:34 PM	Dead	○	○
12280685	12	Jan 18 2001 4:16 AM	Dead	○	○
12248203	11	Jan 17 2001 4:16 AM	Dead	○	○
12225259	10	Jan 15 2001 4:13 AM	Dead	○	○
12225259	10	Jan 14 2001 4:13 AM	Dead	○	○
12083926	9	Jan 12 2001 4:16 AM	Dead	○	○
9966558	8	Sep 6 2000 5:30 AM	Dead	○	○
9966558	8	Sep 5 2000 5:22 AM	Dead	○	○
8699775	7	Jun 26 2000 5:15 AM	Dead	○	○
8699775	7	Jun 25 2000 7:09 AM	Dead	○	○
8164471	6	Jun 15 2000 12:10 PM	Dead	○	○
8164471	6	Jun 2 2000 7:54 AM	Dead	○	○
7985973	5	May 22 2000 7:11 AM	Dead	○	○
7407868	4	Apr 5 2000 5:11 AM	Dead	○	○
7407868	4	Apr 4 2000 7:42 AM	Dead	○	○
7264143	3	Mar 19 2000 5:35 PM	Dead	○	○
7229044	2	Mar 12 2000 5:21 AM	Dead	○	○
7229044	2	Mar 11 2000 10:40 PM	Dead	○	○
7211834	1	Mar 9 2000 5:29 AM	Dead	○	○

Accession AC025423.32 was first seen at NCBI on Mar 9 2000 5:29 AM

US005411860A

United States Patent [19]

Vogelstein et al.

[11] Patent Number: 5,411,860

[45] Date of Patent: May 2, 1995

[54] **AMPLIFICATION OF HUMAN MDM2 GENE IN HUMAN TUMORS**

[75] Inventors: **Bert Vogelstein; Kenneth W. Kinzler,** both of Baltimore, Md.

[73] Assignee: **The Johns Hopkins University,** Baltimore, Md.

[21] Appl. No.: **903,103**

[22] Filed: **Jun. 23, 1992**

Related U.S. Application Data

[63] Continuation-in-part of Ser. No. 867,840, Apr. 7, 1992, abandoned.

[51] **Int. Cl.**[5] **C12Q 1/68;** C12P 19/34

[52] **U.S. Cl.** **435/6;** 435/91.2; 436/813

[58] **Field of Search** 435/6, 91.2; 935/77; 436/813

[56] **References Cited**

PUBLICATIONS

Romkes et al. Biochemistry 30:3247–3255 (1991) "Cloning & Expression of CDNA for . . . ".

Fakharzadeh, et al., "Tumorigenic Potential Associated with Enhanced Expression of a Gene That is Amplified in a Mouse Tumor Cell Line", *The EMBO Journal,* 10(6):1565–1569 (1991).

Hinds, et al., "Mutant p53 DNA Clones From Human Colon Carcinomas Cooperate With Ras in Transforming Primary Rat Cells: A Comparison of the Hot Spot Mutant Phenotypes", *Cell Growth & Differentiation,* 1:561–580 (1990).

Oliner, et al., "Amplification of a Gene Encoding a p53–Associated Protein in Human Sarcomas, " *Nature,* 358:80–83 (1992).

Oliner, et al., "Oncoprotein MDM2 Conceals the Activation Domain of Tumour Suppressor p53", *Nature,* 362(6423):857–860 (1993), abstract.

Leach et al., "p53 Mutation and MDM2 Amplification in Human Soft Tissue Sarcomas," *Cancer Research,* 53:2231–2234 (1993).

Momand, et al., "The mdm-2 Oncogene Product Forms a Complex With the p53 Protein and Inhibits p53–Mediated Transactivation," *Cell,* 69:1237–1245 (1992).

Primary Examiner—Margaret Parr
Assistant Examiner—Eggerton Campbell
Attorney, Agent, or Firm—Banner, Birch, McKie & Beckett

[57] **ABSTRACT**

A human gene has been discovered which is genetically altered in human tumor cells. The genetic alteration is gene amplification and leads to a corresponding increase in gene products. Detecting that the gene, designated hMDM2, has become amplified or detecting increased expression of gene products is diagnostic of tumorigenesis. Human MDM2 protein binds to human p53 and appears to allow the cell to escape from p53-regulated growth.

12 Claims, 12 Drawing Sheets

FIG. 1A(1)

```
   1   GCACCGCGCGAGCTTGGCTGCTTCTGGGGC

                                      * AG
  84   GGCCGCGACCCCTCTGACCGAGATCCTGCTG

       CGT  GC  GG CTCCGCGCTCCCCG GAAG
 168   GTGCCCTGGCCCGGAGAGTGGAATGATCCCC

       ACC GACACCCCTGGGGGACC   TCG AT
 252   GGAGTCTTGAGGGACCCCCGACTCCAAGCGC
   1

       T    C  G        C  G
 336   CCTACTGATGGTGCTGTAACCACCTCACAGA
   9    P  T  D  G  A  V  T  T  S  Q
        S     E        A  S

         G         C     A  G     C
 420   TTATTAAAGTCTGTTGGTGCACAAAAAGACA
  37    L  L  K  S  V  G  A  Q  K  D
                                  N

       A G         C         G  G  C
 504   CGATTATATGATGAGAAGCAACAACATATTG
  65    R  L  Y  D  E  K  Q  Q  H  I

          G                      G A
 588   GTGAAAGAGCACAGGAAAATATATACCATGA
  93    V  K  E  H  R  K  I  Y  T  M
                                  A

        GC          G   AC    G C
 672   TCTGTGAGTGAGAACAGGTGTCACCTTGAAG
 121    S  V  S  E  N  R  C  H  L  E
           L        S     R  Q  P
```

FIG. 1A(2)

```
CTGTGTGGCCCTGTGTGTCGGAAAGATGGAGCAAGA

AGCCGC GC TTCTC TCG TCGAGCT TG ACGAC
CTTTCGCAGCCAGGAGCACCGTCCCTCCCCGGATTA

 GTCGGAA ATGCGC G AAGTAG   CC   T CT
GAGGCCCAGGGCGTCGTGCTTCCGCAGTAGTCAGTC

ACCGCG TTCTCCT C GCCTC     C
GAAAACCCCGGATGGTGAGGAGCAGGCAAATGTGCA
                                M  C


                          T
TTCCAGCTTCGGAACAAGAGACCCTGGTTAGACCAA
I  P  A  S  E  Q  E  T  L  V  R  P

    C              A  A A       A
CTTATACTATGAAAGAGGTTCTTTTTTATCTTGGCC
T  Y  T  M  K  E  V  L  F  Y  L  G
                  I  I        I

 G                    C          G
TATATTGTTCAAATGATCTTCTAGGAGATTTGTTTG
V  Y  C  S  N  D  L  L  G  D  L  F
                                  V

       A  T  A  G CT  A G       A----
TCTACAGGAACTTGGTAGTAGTCAATCAGCAGGAAT
I  Y  R  N  L  V  V  V  N  Q  Q  E
                  A     S        -

            TG     T C T G     C  CA
GTGGGAGTGATCAAAAGGACCTTGTACAAGAGCTTC
G  G  S  D  Q  K  D  L  V  Q  E  L
            L        P  L     A  P
```

FIG. 1A(3)

AGCCGAGCCCGAGGGGC	83	Human nt
CATG CGCTCA G C		Mouse nt
GTGCGTACGAGCGCCCA	167	Human nt
GGGCGAGC GAGACC		Mouse nt
CCCGTGAAGGAAACTGG	251	Human nt
G		Mouse nt
ATACCAACATGTCTGTA	335	Human nt
N T N M S V	8	Human a.a.
		Mouse a.a.
A		Mouse nt
AGCCATTGCTTTTGAAG	419	Human nt
K P L L L K	36	Human a.a.
		Mouse a.a.
G		Mouse nt
AGTATATTATGACTAAA	503	Human nt
Q Y I M T K	64	Human a.a.
		Mouse a.a.
A C G T		Mouse nt
GCGTGCCAAGCTTCTCT	587	Human nt
G V P S F S	92	Human a.a.
		Mouse a.a.
----- T C		Mouse nt
CATCGGACTCAGGTACA	671	Human nt
S S D S G T	120	Human a.a.
- -		Mouse a.a.
CA		Mouse nt
AGGAAGAGAAACCTTCA	755	Human nt
Q E E K P S	148	Human a.a.
P		Mouse a.a.

FIG. 1B(1)

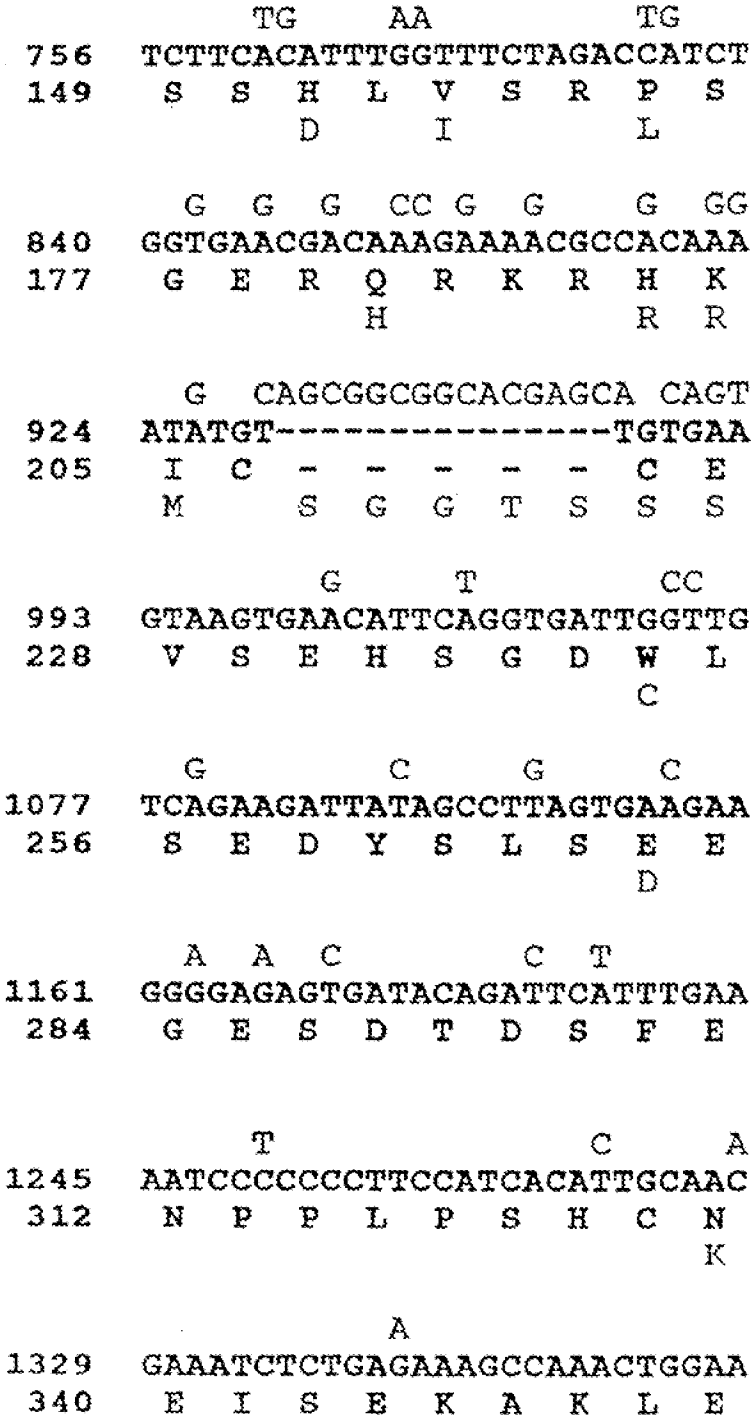
TG AA TG
756 TCTTCACATTTGGTTTCTAGACCATCT
149 S S H L V S R P S
D I L
G G G CC G G G GG
840 GGTGAACGACAAAGAAAACGCCACAAA
177 G E R Q R K R H K
H R R
G CAGCGGCGGCACGAGCA CAGT
924 ATATGT----------TGTGAA
205 I C - - - - - C E
M S G G T S S S
G T CC
993 GTAAGTGAACATTCAGGTGATTGGTTG
228 V S E H S G D W L
C
G C G C
1077 TCAGAAGATTATAGCCTTAGTGAAGAA
256 S E D Y S L S E E
D
A A C C T
1161 GGGGAGAGTGATACAGATTCATTTGAA
284 G E S D T D S F E
T C A
1245 AATCCCCCCCTTCCATCACATTGCAAC
312 N P P L P S H C N
K
A
1329 GAAATCTCTGAGAAAGCCAAACTGGAA
340 E I S E K A K L E

FIG. 1B(2)

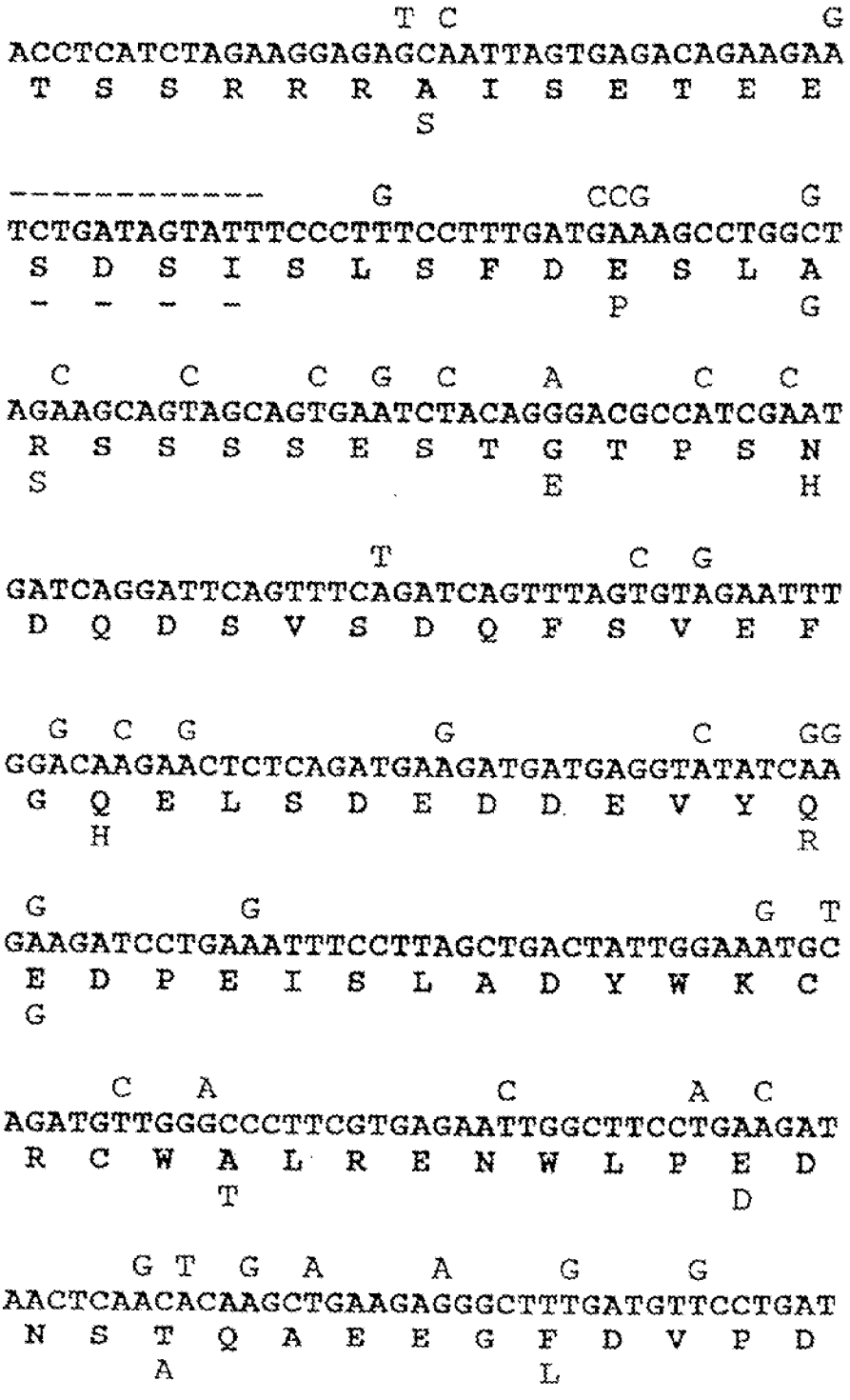
T C G
ACCTCATCTAGAAGGAGAGCAATTAGTGAGACAGAAGAA
T S S R R R A I S E T E E
S
G CCG G
TCTGATAGTATTTCCCTTTCCTTTGATGAAAGCCTGGCT
S D S I S L S F D E S L A
P G
C C C G C A C C
AGAAGCAGTAGCAGTGAATCTACAGGGACGCCATCGAAT
R S S S S E S T G T P S N
S E H
T C G
GATCAGGATTCAGTTTCAGATCAGTTTAGTGTAGAATTT
D Q D S V S D Q F S V E F
G C G G C GG
GGACAAGAACTCTCAGATGAAGATGATGAGGTATATCAA
G Q E L S D E D D E V Y Q
H R
G G G T
GAAGATCCTGAAATTTCCTTAGCTGACTATTGGAAATGC
E D P E I S L A D Y W K C
G
C A C A C
AGATGTTGGGCCCTTCGTGAGAATTGGCTTCCTGAAGAT
R C W A L R E N W L P E D
T D
G T G A A G G
AACTCAACACAAGCTGAAGAGGGCTTTGATGTTCCTGAT
N S T Q A E E G F D V P D
A L

FIG. 1B(3)

```
  CA        GC  C                      Mouse nt
AATTCAGATGAATTATCT      839   Human nt
 N  S  D  E  L  S       176   Human a.a.
    T           P               Mouse a.a.

      AGC G                        Mouse nt
CTGTGTGTAATAAGGGAG      923   Human nt
 L  C  V  I  R  E       204   Human a.a.
       E  L                    Mouse a.a.

 A          C A  C               Mouse nt
CCGGATCTTGATGCTGGT      992   Human nt
 P  D  L  D  A  G       227   Human a.a.
 Q           D                  Mouse a.a.

       G     G                    Mouse nt
GAAGTTGAATCTCTCGAC     1076   Human nt
 E  V  E  S  L  D       255   Human a.a.
                                Mouse a.a.

  C  A  C     A                  Mouse nt
GTTACTGTGTATCAGGCA     1160   Human nt
 V  T  V  Y  Q  A       283   Human a.a.
                T               Mouse a.a.

  C                             Mouse nt
ACTTCATGCAATGAAATG     1244   Human nt
 T  S  C  N  E  M       311   Human a.a.
                                Mouse a.a.

  G              T              Mouse nt
AAAGGGAAAGATAAAGGG     1228   Human nt
 K  G  K  D  K  G       339   Human a.a.
                V               Mouse a.a.

G C     GCTG C  A               Mouse nt
TGTAAAAAAACTATAGTG     1412   Human nt
 C  K  K  T  I  V       367   Human a.a.
 G        L  T  E               Mouse a.a.
```

FIG. 1C(1)

```
                G T A     C         C         G
1413  AATGATTCCAGAGAGTCATGTGTTGAGGAA
 368   N  D  S  R  E  S  C  V  E  E
          A  K     P     A

        C  A     G     C  C        G
1494  TCTCAGCCATCAACTTCTAGTAGCATTATT
 395   S  Q  P  S  T  S  S  S  I  I
                                   V

        C                       C  CT     G
1578  GAAGAGAGTGTGGAATCTAGTTTGCCCCTT
 423   E  E  S  V  E  S  S  L  P  L
        D                       F  S

          T  C     G  T     C  C  T A
1662  GTCCATGGCAAAACAGGACATCTTATGGCC
 451   V  H  G  K  T  G  H  L  M  A
                                   S

             G     C                 G
1746  AGACAACCAATTCAAATGATTGTGCTAACT
 479   R  Q  P  I  Q  M  I  V  L  T
                                   S

1830  TAACCCTAGGAATTTAGACAACCTGAAATT
1914  TTAGTATAATTGACCTACTTTGGTAGTGGA
1998  ACTCCTAATTTTAAATAATTTCTACTCTGT
2082  ATGTAACTTATTATTTTTTTTGAGACCGAG
2166  CTCTGCCCTCCCCGGGTTCGCACCATTCTC
2250  TAATTTTTTGTACTTTTAGTAGAGACAGGG
2334  CTCGGCCTCCCAAAGTGCTGGGATTACAGG
```

FIG. 1C(2)

```
G CAGC  G  G  GGCCGA   GA GC C TG  C
AAT---GATGATAAAATTACACAAGCTTCACAATCAC
 N  -  D  D  K  I  T  Q  A  S  Q  S
 D  S  E  E     A  E     T  P  L

                  AGC            G--- A
TATAGCAGCCAAGAAGATGTGAAAGAGTTTGAAAGGG
 Y  S  S  Q  E  D  V  K  E  F  E  R
                  S              L  -  K

         C     A         C  C  G  G  G
AATGCCATTGAACCTTGTGTGATTTGTCAAGGTCGAC
 N  A  I  E  P  C  V  I  C  Q  G  R

  T  C  G                    A     A  C
TGCTTTACATGTGCAAAGAAGCTAAAGAAAAGGAATA
 C  F  T  C  A  K  K  L  K  K  R  N

  C   AA    C        CTCA A A  T
TATTTCCCCTAGTTGACCTG---TCTATAAGAGAATT
 Y  F  P
       N

TATTCACATATATCAAAGTGAGAAAATGCCTCAATTC
ATAGTGAATACTTACTATAATTTGACTTGAATATGTA
CTTAAATGAGAAGTACTTGGTTTTTTTTTTCTTAAAT
TCTTGCTCTGTTACCCAGGCTGGAGTGCAGTGGGTGA
CTGCCTCAGCCTCCCAATTAGCTTGGCCTACAGTCAT
TTTCACCGTGTTAGCCAGGATGGTCTCGATCTCCTGA
CATGAGCCACCG
```

FIG. 1C(3)

G G C		Mouse nt
AAGAAAGTGAAGACTAT	1493	Human nt
Q E S E D Y	394	Human a.a.
D		Mouse a.a.
G G GC		Mouse nt
AAGAAACCCAAGACAAA	1577	Human nt
E E T Q D K	422	Human a.a.
H		Mouse a.a.
C		Mouse nt
CTAAAAATGGTTGCATT	1661	Human nt
P K N G C I	450	Human a.a.
		Mouse a.a.
G C		Mouse nt
AGCCCTGCCCAGTATGT	1745	Human nt
K P C P V C	478	Human a.a.
		Mouse a.a.
T *		Mouse nt
ATATATTTCTAACTATA	1829	Human nt
	491	Human a.a.
		Mouse a.a.
ACATAGATTTCTTCTCT	1913	Human nt
GCTCATCCTTTACACCA	1997	Human nt
ATGTATATGACATTTAA	2081	Human nt
TCTTGGCTCACTGCAAG	2165	Human nt
CTGCCACCACACCTGGC	2249	Human nt
CCTCGTGATCCGCCCAC	2333	Human nt
	2372	Human nt

FIG. 2

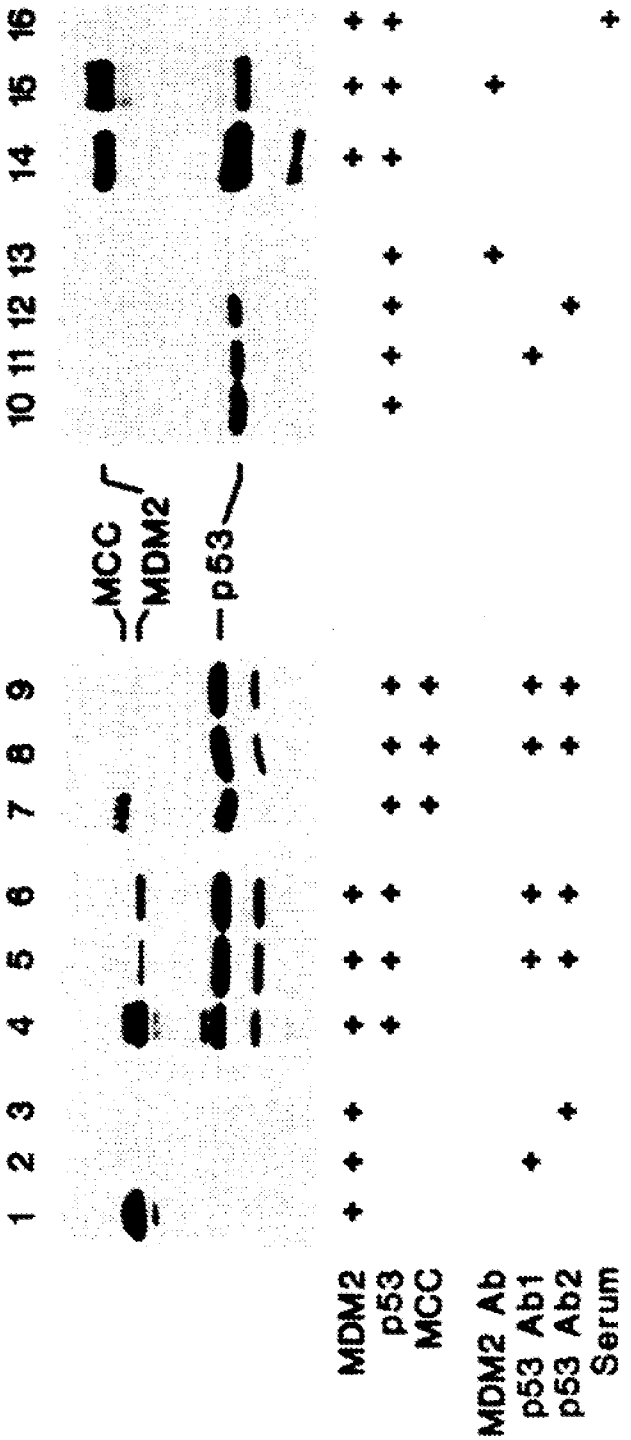
16
15
14
13
12
11
10
9
8
7
6
5
4
3
2
1
MCC
MDM2
p53
MDM2
p53
MCC
MDM2 Ab
p53 Ab1
p53 Ab2
Serum

FIG. 3

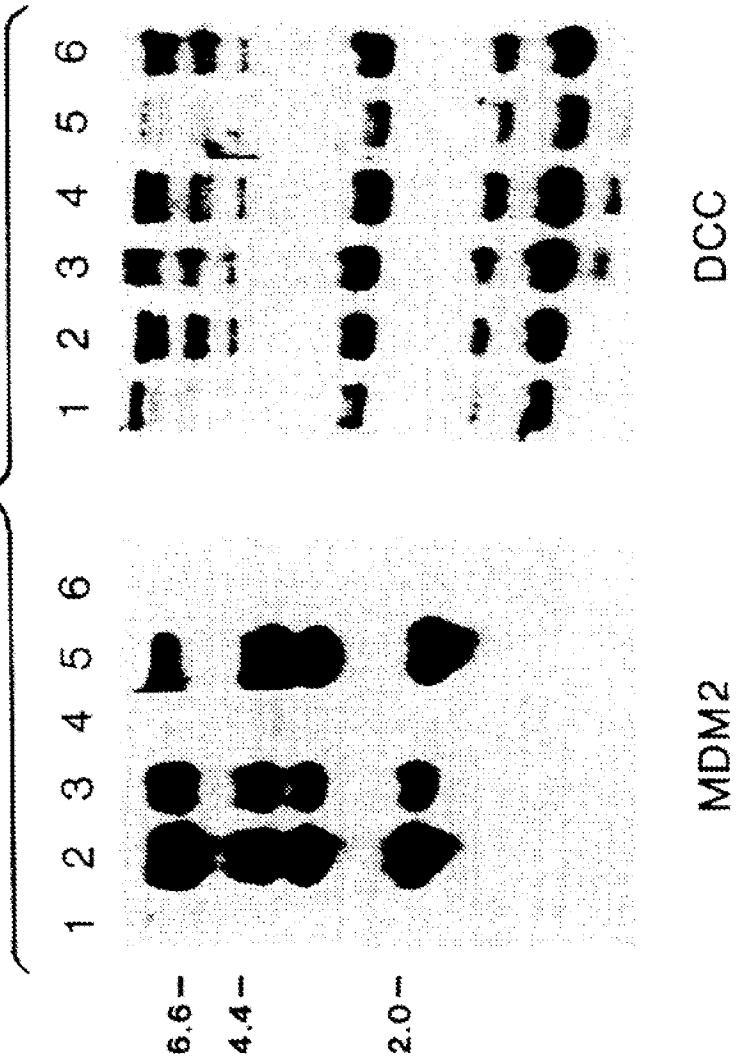

FIG. 4A

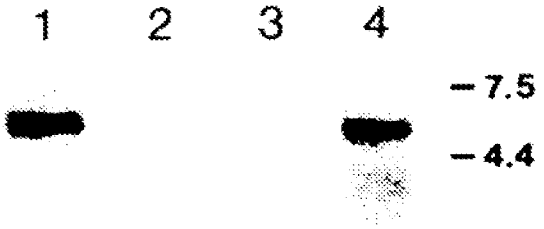

FIG. 4B

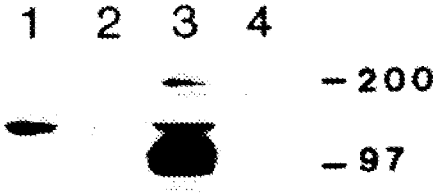

FIG. 4C

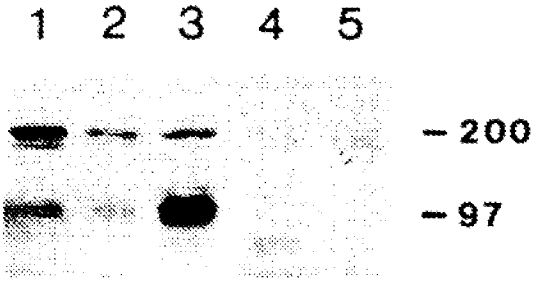

AMPLIFICATION OF HUMAN MDM2 GENE IN HUMAN TUMORS

This application is a continuation-in-part of U.S. application Ser. No. 07/867,840, filed on Apr. 7, 1992, which is now abandoned.

FIELD OF THE INVENTION

The invention relates to the area of cancer diagnostics and therapeutics. More particularly, the invention relates to the detection of a gene which is amplified in certain human tumors.

BACKGROUND OF THE INVENTION

According to the Knudson model for tumorigenesis (Cancer Research, 1985, vol. 45, p. 1482), there are tumor suppressor genes in all normal cells which, when they become non-functional due to mutation, cause neoplastic development. Evidence for this model has been found in cases of retinoblastoma and colorectal tumors. The implicated suppressor genes in these tumors, RB and p53 respectively, were found to be deleted or altered in many of the tumors studied.

The p53 gene product, therefore, appears to be a member of a group of proteins which regulate normal cellular proliferation and suppression of cellular transformation. Mutations in the p53 gene have been linked to tumorigenesis, suggesting that alterations in p53 protein function are involved in cellular transformation. The inactivation of the p53 gene has been implicated in the genesis or progression of a wide variety of carcinomas (Nigro et al., 1989, Nature 342:705–708), including human coWrectal carcinoma (Baker et al., 1989, Science 244:217–221), human lung cancer (Takahashi et al., 1989, Science 246:491–494; Iggo et al., 1990, Lancet 335:675–679), chronic myelogenous leukemia (Kelman et al, 1989, Proc. Natl. Acad. Sci. USA 86:6783–6787) and osteogenic sarcomas (Masuda et al., 1987, Proc. Natl. Acad. Sci. USA 84:7716–7719).

While there exists an enormous body of evidence linking p53 gene mutations to human tumorigenesis (Hollstein et al., 1991, Science 253:49–53) little is known about cellular regulators and mediators of p53 function.

Hinds et al. (Cell Growth & Differentiation, 1990, 1:571–580), found that p53 cDNA clones, containing a point mutation at amino acid residue 143, 175, 273 or 281, cooperated with the activated ras oncogene to transform primary rat embryo fibroblasts in culture. These mutant p53 genes are representative of the majority of mutations found in human cancer. Hollstein et al., 1991, Science 253:49–53. The transformed fibroblasts were found to produce elevated levels of human p53 protein having extended half-lives (1.5 to 7 hours) as compared to the normal (wild-type) p53 protein (20 to 30 minutes).

Mutant p53 proteins with mutations at residue 143 or 175 form an oligomeric protein complex with the cellular heat shock protein hsc70. While residue 273 or 281 routants do not detectably bind hsc70, and are poorer at producing transformed foci than the 175 mutant, complex formation between mutant p53 and hsc70 is not required for p53-mediated transformation. Complex formation does, however, appear to facilitate this function. All cell lines transformed with the mutant p53 genes are tumorigenic in athymic (nude) mice. In contrast, the wild-type human p53 gene does not possess transforming activity in cooperation with ras. Tuck and Crawford, 1989, Oncogene Res. 4:81–96.

Hinds et al. supra also expressed human p53 protein in transformed rat cells. When the expressed human p53 was immunoprecipitated with two p53 specific antibodies directed against distinct epitopes of p53, an unidentified M_r 90,000 protein was coimmunoprecipitated. This suggested that the rat M_r 90,000 protein is in a complex with the human p53 protein in the transformed rat cell line.

As mentioned above, levels of p53 protein are often higher in transformed cells than normal cells. This is due to mutations which increase its metabolic stability (Oven et al., 1981, Mol. Cell. Biol. 1:101–110; Reich et al., (1983), Mol. Cell. Biol. 3:2143–2150). The stabilization of p53 has been associated with complex formation between p53 and viral or cellular proteins. (Linzer and Levine, 1979, Cell 17:43–52; Crawford et al., 1981, Proc. Natl. Acad. Sci. USA 78:41–45; Dippold et al., 1981, Proc. Natl. Acad. Sci. USA 78:1695–1699; Lane and Crawford, 1979, Nature (Lond.) 278:261–263; Hinds et al., 1987, Mol. Cell. Biol. 7:2863–2869; Finlay et al., 1988, Mol. Cell. Biol. 8:531–539; Sarnow et al., 1982, Cell. 28:387–394; Gronostajski et al., 1984, Mol. Cell. Biol. 4:442–448; Pinhasi-Kimhi et al., 1986, Nature (Lond.) 320:182–185; Ruscetti and Scolnick, 1983, J. Virol. 46:1022–1026; Pinhasi and Oren, 1984, Mol. Cell. Biol. 4:2180–2186; and Sturzbecher et al., 1987, Oncogene 1:201–211.) For example, p53 protein has been observed to form oligomeric protein complexes with the SV40 large T antigen, the adenovirus type 5 E1B-M_r 55,000 protein, and the human papilloma virus type 16 or 18 E6 product. Linzer and Levine, 1979, Cell 17:43–52; Lane and Crawford, 1979, Nature, 278:261–263; Sarnow et al., 1982, Cell 28:387–394; Werness et al., 1990, Science, 248:76–79. Similarly, complexes have been observed of $p105^{RB}$ (the product of the retinoblastoma susceptibility gene) with T antigen (DeCaprio et al., 1988, Cell 54:275–283), the adenovirus E1A protein (Whyte et al., 1988, Nature 334:124–129) and the E7 protein of human papilloma virus 16 or 18 (Münger et al., 1989, EMBO J. 8:4099–4105). It has been suggested that interactions between these viral proteins and $p105^{RB}$ inactivate a growth-suppressive function of $p105^{RB}$, mimicking deletions and mutations commonly found in the RB gene in tumor cells. In a similar fashion, oligomeric protein complex formation between these viral proteins and p53 may eliminate or alter the function of p53. Finlay et al., 1989, Cell 57:1083–1093.

Fakharzadeh et al. (EMBO J. 1991, 10:1565–1569) analyzed amplified DNA sequences present in a tumorigenic mouse cell line (i.e., 3T3DM, a spontaneously transformed derivative of mouse Balb/c cells). Studies were conducted to determine whether any of the amplified genes induced tumorigenicity following introduction of the amplified genes into a nontransformed recipient cell (e.g., mouse NIH3T3 or Rat2 cells). The resulting cell lines were tested for tumorigenicity in nude mice. A gene, designated MDM2, which is amplified more than 50-fold in 3T3DM cells, induced tumorigenicity when overexpressed in NIH3T3 and Rat 2 cells. From the nucleotide and predicted amino acid sequence of mouse MDM2 (mMDM2), Fakharzadeh speculated that this gene encodes a potential DNA binding protein that functions in the modulation of expression of other genes and, when present in excess, interferes with normal constraints on cell growth.

SUMMARY OF THE INVENTION

It is an object of the invention to provide a method for diagnosing a neoplastic tissue, such as sarcoma, in a human.

It is another object of the invention to provide a cDNA molecule encoding the sequence of human MDM2.

Yet another object of the invention is to provide a preparation of human MDM2 protein which is substantially free of other human cellular proteins.

Still another object of the invention is to provide DNA probes capable of hybridizing with human MDM2 genes or mRNA molecules.

Another object of the invention is to provide antibodies immunoreactive with human MDM2 protein.

Still another object of the invention is to provide kits for detecting amplification or elevated expression of human MDM2.

Yet another object of the invention is to provide methods for identifying compounds which interfere with the binding of human MDM2 to human p53.

A further object of the invention is to provide a method of treating a neoplastic human cell.

It has now been discovered that hMDM2, a heretofore unknown human gene, plays a role in human cancer. The hMDM2 gene has been cloned and the recombinant derived hMDM2 protein shown to bind to human p53 in vitro. hMDM2 has been found to be amplified in some neoplastic cells and the expression of hMDM2-encoded products has been found to be correspondingly elevated in tumors with amplification of this gene. The elevated levels of MDM2 appear to sequester p53 and allow the cell to escape from p53-regulated growth.

BRIEF DESCRIPTION OF THE DRAWINGS

FIG. 1A–C shows the cDNA sequence of human MDM2. In this figure, human and mouse nucleotide and amino acid sequences are compared, the mouse sequence being shown only where it differs from the corresponding human sequence.

FIG. 2 shows that hMDM2 binds to p53.

FIG. 3 illustrates the amplification of the hMDM2 gene in sarcomas.

FIG. 4A–C illustrates hMDM2 expression.

DETAILED DESCRIPTION OF THE INVENTION

It is a discovery of the present invention that a gene exists which is amplified in some human tumors. The amplification of this gene, designated MDM2, is diagnostic of neoplasia or the potential therefor. Detecting the elevated expression of human MDM2-encoded products is also diagnostic of neoplasia or the potential for neoplastic transformation. Over a third of the sarcomas surveyed, including the most common bone and soft tissue forms, were found to have amplified hMDM2 sequences. Expression of hMDM2 was found to be correspondingly elevated in tumors with the gene amplification.

Other genetic alterations leading to elevated hMDM2 expression may be involved in tumorigenesis also, such as mutations in regulatory regions of the gene. Elevated expression of hMDM2 may also be involved in tumors other than sarcomas including but not limited to those in which p53 inactivation has been implicated. These include c,l,rectal carcinoma, lung cancer and chronic myelogenous leukemia.

According to one embodiment of the invention, a method of diagnosing a neoplastic tissue in a human is provided. Tissue or body fluid is isolated from a human, and the copy number of human MDM2 genes is determined. Alternatively, expression levels of human MDM2 gene products can be determined. These include protein and mRNA.

Body fluids which may be tested include urine, serum, blood, feces, saliva, and the like. Tissues suspected of being neoplastic are desirably separated from normal appearing tissue for analysis. This can be done by paraffin or cry, star sectioning or flow cytometry, as is known in the art. Failure to separate neoplastic from non-neoplastic cells can confound the analysis. Adjacent non-neoplastic tissue or any normal tissue can be used to determine a base-line level of expression or copy number, against which the amount of hMDM2 gene or gene products can be compared.

The human MDM2 gene is considered to be amplified if the cell contains more than the normal copy number (2) of this gene per genome. The various techniques for detecting gene amplification are well known in the art. Gene amplification can be determined, for example, by Southern blot analysis, as described in Example 4, wherein cellular DNA from a human tissue is digested, separated, and transferred to a filter where it is hybridized with a probe containing complementary nucleic acids. Alternatively, quantitative polymerase chain reaction (PCR) employing primers can be used to determine gene amplification. Appropriate primers will bind to sequences that bracket human MDM2 coding sequences. Other techniques for determining gene copy number as are known in the art can be used without limitation.

The gene product which is measured may be either mRNA or protein. The term elevated expression means an increase in mRNA production or protein production over that which is normally produced by non-cancerous cells. Although amplification has been observed in human sarcomas, other genetic alterations leading to elevated expression of MDM2 may be present in these or other tumors. Other tumors include those of lung, breast, brain, colorectal, bladder, prostate, liver, skin, and stomach. These, too, are contemplated by the present invention. Non-cancerous cells for use in determining base-line expression levels can be obtained from cells surrounding a tumor, from other humans or from human cell lines. Any increase can have diagnostic value, but generally the mRNA or protein expression will be elevated at least about 3-fold, 5-fold, and in some cases up to about 100-fold over that found in non-cancerous cells. The particular technique employed the detecting mRNA or protein is not critical to the practice of the invention. Increased production of mRNA or protein may be detected, for example, using the techniques of Northern blot analysis or Western blot analysis, respectively, as described in Example 4 or other known techniques such as ELISA, immunoprecipitation, RIA and the like. These techniques are also well known to the skilled artisan.

According to another embodiment of the invention, nucleic acid probes or primers for the determining of human MDM2 gene amplification or elevated expression of mRNA are provided. The probe may comprise ribo- or deoxyribonucleic acids and may contain the entire human MDM2 coding sequence, a sequence com-

plementary thereto, or fragments thereof. A probe may contain, for example, nucleotides 1-949, or 1-2372 as shown in FIG. 1. Generally, probes or primers will contain at least about 14 contiguous nucleotides of the human sequence but may desirably contain about 40, 50 or 100 nucleotides. Probes are typically labelled with a fluorescent tag, a radioisotope, or the like to render them easily detectable. Preferably the probes will hybridize under stringent hybridization conditions. Under such conditions they will not hybridize to mouse MDM2. The probes of the invention are complementary to the human MDM2 gene. This means that they share 100% identity with the human sequence.

hMDM2 protein can be produced, according to the invention, substantially free of other human proteins. Provided with the DNA sequence, those of skill in the art can express the cDNA in a non-human cell. Lysates of such cells provide proteins substantially free of other human proteins. The lysates can be further purified, for example, by immunoprecipitation, coprecipitation with p53, or by affinity chromatography.

The antibodies of the invention are specifically reactive with hMDM2 protein. Preferably, they do not cross-react with MDM2 from other species. They can be polyclonal or monoclonal, and can be raised against native hMDM2 or a hMDM2 fusion protein or synthetic peptide. The antibodies are specifically immunoreactive with hMDM2 epitopes which are not present on other human proteins. Some antibodies are reactive with epitopes unique to human MDM2 and not present on the mouse homolog. The antibodies are useful in conventional analyses, such as Western blot analysis, ELISA and other immunological assays for the detection of proteins. Techniques for raising and purifying polyclonal antibodies are well known in the art, as are techniques for preparing monoclonal antibodies. Antibody binding can be determined by methods known in the art, such as use of an enzyme-labelled secondary antibody, staphylococcal protein A, and the like.

According to another embodiment of the invention, interference with the expression of MDM2 provides a therapeutic modality. The method can be applied in vivo, in vitro, or ex vivo. For example, expression may be downregulated by administering triple-strand forming or antisense oligonucleotides which bind to the hMDM2 gene or mRNA, respectively, and prevent transcription or translation. The oligonucleotides may interact with unprocessed pre-mRNA or processed mRNA. Small molecules and peptides which specifically inhibit MDM2 expression can also be used. Similarly, such molecules which inhibit the binding of MDM2 to p53 would be therapeutic by alleviating the sequestration of p53.

Such inhibitory molecules can be identified by screening for interference of the hMDM2/p53 interaction where one of the binding partners is bound to a solid support and the other partner is labeled. Antibodies specific for epitopes on hMDM2 or p53 which are involved in the binding interaction will interfere with such binding. Solid supports which may be used include any polymers which are known to bind proteins. The support may be in the form of a filter, column packing matrix, beads, and the like. Labeling of proteins can be accomplished according to any technique known in the art. Radiolabels, enzymatic labels, and fluorescent labels can be used advantageously. Alternatively, both hMDM2 and p53 may be in solution and bound molecules separated from unbound subsequently. Any separation technique known in the art may be employed, including immunoprecipitation or immunoaffinity separation with an antibody specific for the unlabeled binding partner.

A cDNA molecule containing the coding sequence of hMDM2 can be used to produce probes and primers. In addition, it can be expressed in cultured cells, such as *E. coli*, to yield preparations of hMDM2 protein substantially free of other human proteins. The proteins produced can be purified, for example, with immunoaffinity techniques using the antibodies described above.

Kits are provided which contain the necessary reagents for determining gene copy number, such as probes or primers specific for the hMDM2 gene, as well as written instructions. The instructions can provide calibration curves to compare with the determined values. Kits are also provided to determine elevated expression of mRNA (i.e., containing probes) or hMDM2 protein (i.e., containing antibodies). Instructions will allow the tester to determine whether the expression levels are elevated. Reaction vessels and auxiliary reagents such as chromogens, buffers, enzymes, etc. may also be included in the kits.

The human MDM2 gene has now been identified and cloned. Recombinant derived hMDM2 has been shown to bind to human p53. Moreover, it has been found that hMDM2 is amplified in some satcomas. The amplification leads to a corresponding increase in MDM2 gene products. Such amplification is associated with the process of tumorigenesis. This discovery allows specific assays to be performed to assess the neoplastic or potential neoplastic status of a particular tissue.

The following examples are provided to exemplify various aspects of the invention and are not intended to limit the scope of the invention.

EXAMPLE 1

To obtain human cDNA clones, a cDNA library was screened with a murine MDM2 (mMDM2) cDNA probe. A cDNA library was prepared by using polyadenylated RNA isolated from the human colonic carcinoma cell line CaCo-2 as a template for the production of random hexamer primed double stranded cDNA. Gubler and Hoffmann, 1983, Gene 25:263-268. The cDNA was ligated to adaptors and then to the lambda YES phage vector, packaged, and plated as described by Elledge et al. (Proc. Natl. Acad. Sci. USA, 1991, 88:1731-1735). The library was screened initially with a ^{32}P-labelled (Feinberg and Vogelstein, 1983, Anal. Biochem. 132:6-13) mMDM2 cDNA probe (nucleotides 259 to 1508 (Fakharzadeh et al., 1991, EMBO J. 10:1565-1569)) and then rescreened with an hMDM2 cDNA clone containing nucleotides 40 to 702.

Twelve clones were obtained, and one of the clones was used to obtain thirteen additional clones by rescreening the same library. In total., twenty-five clones were obtained, partially or totally sequenced, and mapped. Sequence analysis of the twenty-five clones revealed several cDNA forms indicative of alternative splicing. The sequence shown in FIG. 1 is representative of the most abundant class and was assembled from three clones: c14-2 (nucleotides 1-949), c89 (nucleotides 467-1737), and c33 (nucleotides 390-2372). The 3' end of the untranslated region has not yet been cloned in mouse or human. The 5' end is likely to be at or near nucleotide 1. There was an open reading frame extending from the 5' end of the human cDNA sequence to nucleotide 1784. Although the signal for translation

initiation could not be unambiguously defined, the ATG at nucleotide 312 was considered the most likely position for several reasons. First, the sequence similarity between hMDM2 and mMDM2 fell off dramatically upstream of nucleotide 312. This lack of conservation in an otherwise highly conserved protein suggested that the sequences upstream of the divergence may not code for protein. Second, an anchored polymerase chain reaction (PCR) approach was employed in an effort to acquire additional upstream cDNA sequence. Ochman et al., 1985, In: PCR Technology: Principles and Applications for DNA Amplification (Erlich, ed.) pp. 105–111 (Stockton, New York). The 5' ends of the PCR derived clones were very similar (within 3 bp) to the 5' ends of clones obtained from the cDNA library, suggesting that the 5' end of the hMDM2 sequence shown in FIG. **1** may represent the 5' end of the transcript. Third, in vitro translation of the sequence shown in FIG. **1**, beginning with the methionine encoded by the nucleotide 312 ATG, generated a protein similar in size to that observed in human cells.

In FIG. **1**, hMDM2 and mMDM2 nucleotide and amino acid sequences are compared. The mouse sequence is only shown where it differs from the corresponding human sequence. Asterisks mark the 5' and 3' boundaries of the previously published mMDM2 cDNA. Fakharzadeh et al., 1991, EMBO J. 10:1565–1569. Dashes indicate insertions. The mouse and human amino acid sequences are compared from the putative translation start site at nucleotide 312 through the conserved stop codon at nucleotide 1784.

Comparison of the human and mouse MDM2 coding regions revealed significant conservation at the nucleotide (80.3%) and amino acid (80.4%) levels. Although hMDM2 and mMDM2 bore little similarity to other genes recorded in current databases, the two proteins shared several motifs. These included a basic nuclear localization signal (Tanaka, 1990, FEBS Letters 271:4146) at codons 181 to 185, several casein kinase II serine phosphorylation sites (Pinna, 1990, Biochem. et. Biophys. Acta. 1054:267–284) at codons 166 to 169, 192 to 195, 269 to 272, and 290 to 293, an acidic activation domain (Ptashne, 1988, Nature 355:683–689) at codons 223 to 274, and two metal binding sites (Harrison, 1991, Nature 353:715) at codons 305 to 322 and 461 to 478, neither of which is highly related to known DNA binding domains. The protein kinase A domain noted in mMDM2 (Fakharzadeh et al., 1991, EMBO J. 10:1565–1569) was not conserved in hMDM2.

EXAMPLE 2

To determine whether the hMDM2 protein could bind to human p53 protein in vitro, an hMDM2 expression vector was constructed from the cDNA clones. The hMDM2 expression vector was constructed in pBluescript SK+ (Stratagene) from overlapping cDNA clones. The construct contained the sequence shown in FIG. **1** from nucleotide 312 to 2176. A 42 bp black beetle virus ribosome entry sequence (Dasmahapatra et al., 1987, Nucleic Acid Research 15:3933) was placed immediately upstream of this hMDM2 sequence in order to obtain a high level of expression. This construct, as well as p53 (E1-Deriy et al., 1992, Nature Genetics, in press) and MCC (Kinzler et al., 1991, Science 251:1366–1370)constructs in pBluescript SK+, were transcribed with T7 RNA polymerase and translated in a rabbit reticulocyte lysate (Promega) according to the manufacturer's instructions.

Although the predicted size of the protein generated from the construct was only 55.2 kd (extending from the methionine at nucleotide 312 to nucleotide 1784), in vitro translated protein migrated at approximately 95 kilodaltons.

Ten μl of lysate containing the three proteins (hMDM2, p53 and MCC), alone or mixed in pairs, were incubated at 37° C. for 15 minutes. One microgram (10 μl) of p53 Ab1 (monoclonal antibody specific for the C-terminus of p53) or Ab2 (monoclonal antibody specific for the N-terminus of p53) (Oncogene Science), or 5 μl of rabbit serum containing MDM2 Ab (polyclonal rabbit anti-hMDM2 antibodies) or preimmune rabbit serum (obtained from the rabbit which produced the hMDM2 Ab), were added as indicated. The polyclonal rabbit antibodies were raised against an *E. coli*-produced hMDM2 -glutathione S-transferase fusion protein containing nucleotides 390 to 816 of the hMDM2 cDNA. Ninety μl of RIPA buffer (10 mM tris [pH 7.5], 1% sodium deoxycholate, 1% NP40, 150 mM NaCl, 0.1% SDS), SNNTE buffer (Levin and George, 1992, submitted for publication), or Binding Buffer (E1-Defiy et al., 1992, Nature Genetics, in press) were then added and the mixtures allowed to incubate at 4° C. for 2 hours.

Two milligrams of protein A sepharose were added to each tube, and the tubes were rotated end-over-end at 4° C. for 1 hour. After pelleting and washing, the immunoprecipitates were subjected to SDS-polyacrylamide gel electrophoresis and the dried gels autoradiographed for 10 to 60 minutes in the presence of Enhance (New England Nuclear).

FIG. **2** shows the co-precipitation of hMDM2 and p53. The three buffers produced similar results, although the co-precipitation was less efficient in SNNTE buffer containing 0.5M NaCl (FIG. **2**, lanes **5** and **8**) than in Binding Buffer containing 0.1M NaCl (FIG. **2** lanes **6** and **9**).

In vitro translated hMDM2, p53 and MCC proteins were mixed as indicated above and incubated with p53 Ab1, p53 Ab2, hMDM2 Ab, or preimmune serum. Lanes **1**, **4**, **7**, **10** and **14** contain aliquots of the protein mixtures used for immunoprecipitation. The bands running slightly faster than p53 are polypeptides produced from internal translation initiation sites.

The hMDM2 protein was not immunoprecipitated with monoclonal antibodies to either the C-terminal or N-terminal regions of p53 (FIG. **2**, lanes **2** and **3**). However, when in vitro translated human p53 was mixed with the hMDM2 translation product, the anti-p53 antibodies precipitated hMDM2 protein along with p53, demonstrating an association in vitro (FIG. **2**, lanes **5** and **6**). As a control, a protein of similar electrophoretic mobility from another gene (MCC (Kinzler et al., 1991, Science 251:1366–1370)) was mixed with p53. No co-precipitation of the MCC protein was observed (FIG. **2**, lanes **8** and **9**). When an in vitro translated mutant form of p53 (175^{his}) was mixed with hMDM2 protein, a similar co-precipitation of hMDM2 and p53 proteins was also observed.

In the converse of the experiments described above, the anti-hMDM2 antibodies immunoprecipitated p53 when mixed with hMDM2 protein (FIG. **2**, lane **15**) but failed to precipitate p53 alone (FIG. **5**, lane **13**). Preimmune rabbit serum failed to precipitate either hMDM2 or p53 (FIG. **2**, lane **16**).

EXAMPLE 3

In order to ascertain the chromosomal localization of hMDM2, somatic cell hybrids were screened with an hMDM2 cDNA probe. A human-hamster hybrid containing only human chromosome 12 was found to hybridize to the probe. Screening of hybrids containing portions of chromosome 12 (Turc-Carel et al., 1986, Cancer Genet. Cytogenet. 23:291–299) with the same probe narrowed the localization to chromosome 12q12–14.

EXAMPLE 4

Previous studies have shown that this region of chromosome 12 is often aberrant in human sarcomas. Mandahl et al., 1987, Genes Chromosomes & Cancer 1:9–14; Turc-Carel et al., 1986, Cancer Genet. Cytogenet. 23:291–299; Meltzer et al., 1991, Cell Growth & Differentiation 2:495–501. To evaluate the possibility that hMDM2 was genetically altered in such cancers, Southern blot analysis was performed.

FIG. 3 shows examples of the amplification of the hMDM2 gene in sarcomas. Cellular DNA (5 μg) was digested with EcoRI, separated by agarose gel electrophoresis, and transferred to nylon as described by Reed and Mann (Nucl. Acids Res., 1985, 13:7207–7215). The cellular DNA was derived from five primary sarcomas (lanes **1-4, 6**) and one sarcoma cell line (OsA-CL, lane **5**). The filters were then hybridized with an hMDM2 cDNA fragment probe nucleotide 1-949 (see FIG. 1), or to a control probe which identifies fragments of similar size (DCC gene, 1.65 cDNA fragment). Fearon, 1989, Science 247:49–56. Hybridization was performed as described by Vogelstein et al. (Cancer Research, 1987, 47:4806–4813). A striking amplification of hMDM2 sequences was observed in several of these tumors. (See FIG. 3, lanes **2, 3** and **5**). Of 47 sarcomas analyzed, 17 exhibited hMDM2 amplification ranging from 5 to 50 fold. These tumors included 7 to 13 liposarcomas, 7 of 22 malignant fibrous histiocytomas (MFH), 3 of 11 osteosarcomas, and 0 and 1 rhabdomyosarcomas. Five benign soft tissue tumors (lipomas) and twenty-seven carcinomas (colorectal or gastric) were also tested by Southern blot analysis and no amplification was observed.

EXAMPLE 5

This example illustrates that gene amplification is associated with increased expression.

FIG. 4A illustrates hMDM2 expression as demonstrated by Northern blot analysis. Because of RNA degradation in the primary sarcomas, only the cell lines could be productively analyzed by Northern blot. RNA was separated by electrophoresis in a MOPS-formaldehyde gel and electrophoretically transferred to nylon filters. Transfer and hybridization were performed as described by Kinzler et al. (Nature, 1988, 332:371–374). The RNA was hybridized to the hMDM2 fragment described in FIG. 3. Ten μg of total RNA derived, respectively, from two sarcoma cell lines (OsA-CL, lane **1** and RC13, lane **2**) and the colorectal cancer cell line (CaCo-2) used to make the cDNA library (lane **3**). Lane **4** contains 10 μg of polyadenylated CaCo-2 RNA. RNA sizes are shown in kb. In the one available sarcoma cell line with hMDM2 amplification, a single transcript of approximately 5.5 kb was observed (FIG. **4A**, lane **1**). The amount of this transcript was much higher than in a sarcoma cell line without amplification (FIG. **4A**, lane **2**) or in a carcinoma cell line (FIG. **4A**, lane **3**). When purified mRNA (rather than total RNA) from the carcinoma cell line was used for analysis, an hMDM2 transcript of 5.5 kb could also be observed (FIG. **4A**, lane **4**).

FIG. 4B illustrates hMDM2 expression as demonstrated by Western blot analysis of the sarcoma cell lines RC13 (lane **1**), OsA-CL (lane **3**), HOS (lane **4**), and the carcinoma cell line CaCo-2 (lane **2**).

FIG. 4C illustrates hMDM2 expression as demonstrated by Western blot analysis of primary sarcomas. Lanes **1** to **3** contain protein from sarcomas with hMDM2 amplifications, and lanes **4** and **5** contain protein from sarcomas without hMDM2 amplification.

Western blots using affinity purified MDM2 Ab were performed with 50 μg protein per lane as described by Kinzler et al. (Mol. Cell. Biol., 1990, 10:634–642), except that the membranes were blocked in 10% nonfat dried milk and 10% goat serum, and secondary antibodies were coupled to horseradish peroxidase, permitting chemiluminescent detection (Amersham ECL). MDM2 Ab was affinity purified with a pATH-hMDM2 fusion protein using methods described in Kinzler et al. (Mol. Cell. Biol., 1990, 10:634–642). Nonspecifically reactive proteins of 85, 120 and 200 kd were observed in all lanes, irrespective of hMDM2 amplification status. hMDM2 proteins, of 97 kd, were observed only in the hMDM2-amplified tumors. Protein marker sizes are shown in kd.

A protein of approximately 97 kilodaltons was expressed at high levels in the sarcoma cell line with hMDM2 amplification (FIG. **4B**, lane **3**), whereas no expression was evident in two sarcoma cell lines without amplification or in the carcinoma cell line (FIG. **4B**, lanes **1, 2** and **4**). Five primary sarcomas were also examined by Western blot analysis. Three primary sarcomas with amplification expressed the same size protein as that observed in the sarcoma cell line (FIG. **4C**, lanes **1–3**), while no protein was observed in the two sarcomas without amplification (FIG. **4C**, lanes **4** and **5**).

Expression of the hMDM2 RNA in the sarcoma with amplification was estimated to be at least 30 fold higher than that in the other lines examined. This was consistent with the results of Western blot analysis.

The above examples demonstrate that hMDM2 binds to p53 in vitro and is genetically altered (i.e., amplified) in a significant fraction of sarcomas, including MFH, liposarcomas, and osteosarcomas. These are the most common sarcomas of soft tissue and bone. Weiss and Enzinger, 1978, Cancer 41:2250–2266; Malawer et al., 1985, In: *Cancer: Principles and Practice of Oncology*, DeVita et al., Eds., pp. 1293–1342 (Lippincott, Pa.).

Human MDM2 amplification is useful for understanding the pathogenesis of these often lethal cancers.

MDM2 may functionally inactivate p53 in ways similar to those employed by virally encoded oncoproteins such as SV40 T-antigen, adenovirus E1B, and HPV E6. Lane and Bechimol, 1990, Genes and Development 4:1–8; Werness et al., 1990, Science 248:76. Consistent with this hypothesis, no sarcomas with hMDM2 amplification had any of the p53 gene mutations that occur commonly in other tumors. hMDM2 amplification provides a parallel between viral carcinogenesis and the naturally occurring genetic alterations underlying sporadic human cancer. The finding that expression of hMDM2 is correspondingly elevated in tumors with amplification of the gene are consistent with the finding that MDM2 binds to p53, and with the hypothesis that

overexpression of MDM2 in sarcomas allows escape from p53 regulated growth control. This mechanism of tumorigenesis has striking parallels to that previously observed for virally induced tumors (Lane and Benchimol, 1990, Genes and Development 4:1–8; Werness et al., 1990, Science 248:76), in which vital oncogene products bind to and functionally inactivate p53.

SEQUENCE LISTING

(1) GENERAL INFORMATION:

(i i i) NUMBER OF SEQUENCES: 4

(2) INFORMATION FOR SEQ ID NO:1:

(i) SEQUENCE CHARACTERISTICS:
(A) LENGTH: 2372 base pairs
(B) TYPE: nucleic acid
(C) STRANDEDNESS: double
(D) TOPOLOGY: linear

(i i) MOLECULE TYPE: cDNA

(i i i) HYPOTHETICAL: NO

(i v) ANTI-SENSE: NO

(v i) ORIGINAL SOURCE:
(A) ORGANISM: Homo sapiens
(B) CELL LINE: CaCo-2

(v i i i) POSITION IN GENOME:
(B) MAP POSITION: 12q13-14

(i x) FEATURE:
(A) NAME/KEY: CDS
(B) LOCATION: 512..1784

(x i) SEQUENCE DESCRIPTION: SEQ ID NO:1:

```
GCACCGCGCG AGCTTGGCTG CTTCTGGGGC CTGTGTGGCC CTGTGTGTCG GAAAGATGGA      60

GCAAGAAGCC GAGCCCGAGG GGCGGCCGCG ACCCCTCTGA CCGAGATCCT GCTGCTTTCG     120

CAGCCAGGAG CACCGTCCCT CCCCGGATTA GTGCGTACGA GCGCCCAGTG CCCTGGCCCG     180

GAGAGTGGAA TGATCCCCGA GGCCCAGGGC GTCGTGCTTC CGCAGTAGTC AGTCCCCGTG     240

AAGGAAACTG GGGAGTCTTG AGGGACCCCC GACTCCAAGC GCGAAAACCC CGGATGGTGA     300

GGAGCAGGCA A ATG TGC AAT ACC AAC ATG TCT GTA CCT ACT GAT GGT GCT       350
                Met Cys Asn Thr Asn Met Ser Val Pro Thr Asp Gly Ala
                  1               5                  10

GTA ACC ACC TCA CAG ATT CCA GCT TCG GAA CAA GAG ACC CTG GTT AGA       398
Val Thr Thr Ser Gln Ile Pro Ala Ser Glu Gln Glu Thr Leu Val Arg
      15                  20                  25

CCA AAG CCA TTG CTT TTG AAG TTA TTA AAG TCT GTT GGT GCA CAA AAA       446
Pro Lys Pro Leu Leu Leu Lys Leu Leu Lys Ser Val Gly Ala Gln Lys
  30                  35                  40                  45

GAC ACT TAT ACT ATG AAA GAG GTT CTT TTT TAT CTT GGC CAG TAT ATT       494
Asp Thr Tyr Thr Met Lys Glu Val Leu Phe Tyr Leu Gly Gln Tyr Ile
                  50                  55                  60

ATG ACT AAA CGA TTA TAT GAT GAG AAG CAA CAA CAT ATT GTA TAT TGT       542
Met Thr Lys Arg Leu Tyr Asp Glu Lys Gln Gln His Ile Val Tyr Cys
              65                  70                  75

TCA AAT GAT CTT CTA GGA GAT TTG TTT GGC GTG CCA AGC TTC TCT GTG       590
Ser Asn Asp Leu Leu Gly Asp Leu Phe Gly Val Pro Ser Phe Ser Val
          80                  85                  90

AAA GAG CAC AGG AAA ATA TAT ACC ATG ATC TAC AGG AAC TTG GTA GTA       638
Lys Glu His Arg Lys Ile Tyr Thr Met Ile Tyr Arg Asn Leu Val Val
      95                  100                 105

GTC AAT CAG CAG GAA TCA TCG GAC TCA GGT ACA TCT GTG AGT GAG AAC       686
Val Asn Gln Gln Glu Ser Ser Asp Ser Gly Thr Ser Val Ser Glu Asn
  110                 115                 120                 125
```

-continued

```
AGG TGT CAC CTT GAA GGT GGG AGT GAT CAA AAG GAC CTT GTA CAA GAG          714
Arg Cys His Leu Glu Gly Gly Ser Asp Gln Lys Asp Leu Val Gln Glu
                130                 135                 140

CTT CAG GAA GAG AAA CCT TCA TCT TCA CAT TTG GTT TCT AGA CCA TCT          762
Leu Gln Glu Glu Lys Pro Ser Ser Ser His Leu Val Ser Arg Pro Ser
            145                 150                 155

ACC TCA TCT AGA AGG AGA GCA ATT AGT GAG ACA GAA GAA AAT TCA GAT          810
Thr Ser Ser Arg Arg Arg Ala Ile Ser Glu Thr Glu Glu Asn Ser Asp
        160                 165                 170

GAA TTA TCT GGT GAA CGA CAA AGA AAA CGC CAC AAA TCT GAT AGT ATT          858
Glu Leu Ser Gly Glu Arg Gln Arg Lys Arg His Lys Ser Asp Ser Ile
    175                 180                 185

TCC CTT TCC TTT GAT GAA AGC CTG GCT CTG TGT GTA ATA AGG GAG ATA          906
Ser Leu Ser Phe Asp Glu Ser Leu Ala Leu Cys Val Ile Arg Glu Ile
190                 195                 200                 205

TGT TGT GAA AGA AGC AGT AGC AGT GAA TCT ACA GGG ACG CCA TCG AAT          954
Cys Cys Glu Arg Ser Ser Ser Ser Glu Ser Thr Gly Thr Pro Ser Asn
                210                 215                 220

CCG GAT CTT GAT GCT GGT GTA AGT GAA CAT TCA GGT GAT TGG TTG GAT         1002
Pro Asp Leu Asp Ala Gly Val Ser Glu His Ser Gly Asp Trp Leu Asp
            225                 230                 235

CAG GAT TCA GTT TCA GAT CAG TTT AGT GTA GAA TTT GAA GTT GAA TCT         1050
Gln Asp Ser Val Ser Asp Gln Phe Ser Val Glu Phe Glu Val Glu Ser
        240                 245                 250

CTC GAC TCA GAA GAT TAT AGC CTT AGT GAA GAA GGA CAA GAA CTC TCA         1118
Leu Asp Ser Glu Asp Tyr Ser Leu Ser Glu Glu Gly Gln Glu Leu Ser
    255                 260                 265

GAT GAA GAT GAT GAG GTA TAT CAA GTT ACT GTG TAT CAG GCA GGG GAG         1166
Asp Glu Asp Asp Glu Val Tyr Gln Val Thr Val Tyr Gln Ala Gly Glu
270                 275                 280                 285

AGT GAT ACA GAT TCA TTT GAA GAA GAT CCT GAA ATT TCC TTA GCT GAC         1214
Ser Asp Thr Asp Ser Phe Glu Glu Asp Pro Glu Ile Ser Leu Ala Asp
                290                 295                 300

TAT TGG AAA TGC ACT TCA TGC AAT GAA ATG AAT CCC CCC CTT CCA TCA         1262
Tyr Trp Lys Cys Thr Ser Cys Asn Glu Met Asn Pro Pro Leu Pro Ser
            305                 310                 315

CAT TGC AAC AGA TGT TGG GCC CTT CGT GAG AAT TGG CTT CCT GAA GAT         1310
His Cys Asn Arg Cys Trp Ala Leu Arg Glu Asn Trp Leu Pro Glu Asp
        320                 325                 330

AAA GGG AAA GAT AAA AGG GAA ATC TCT GAG AAA GCC AAA CTG GAA AAC         1358
Lys Gly Lys Asp Lys Gly Glu Ile Ser Glu Lys Ala Lys Leu Glu Asn
    335                 340                 345

TCA ACA CAA GCT GAA GAG GGC TTT GAT GTT CCT GAT TGT AAA AAA ACT         1406
Ser Thr Gln Ala Glu Glu Gly Phe Asp Val Pro Asp Cys Lys Lys Thr
350                 355                 360                 365

ATA GTG AAT GAT TCC AGA GAG TCA TGT GTT GAG GAA AAT GAT GAT AAA         1454
Ile Val Asn Asp Ser Arg Glu Ser Cys Val Glu Glu Asn Asp Asp Lys
                370                 375                 380

ATT ACA CAA GCT TCA CAA TCA CAA GAA AGT GAA GAC TAT TCT CAG CCA         1502
Ile Thr Gln Ala Ser Gln Ser Gln Glu Ser Glu Asp Tyr Ser Gln Pro
            385                 390                 395

TCA ACT TCT AGT AGC ATT ATT TAT AGC AGC CAA GAA GAT GTG AAA GAG         1550
Ser Thr Ser Ser Ser Ile Ile Tyr Ser Ser Gln Glu Asp Val Lys Glu
        400                 405                 410

TTT GAA AGG GAA GAA ACC CAA GAC AAA GAA GAG AGT GTG GAA TCT AGT         1598
Phe Glu Arg Glu Glu Thr Gln Asp Lys Glu Glu Ser Val Glu Ser Ser
    415                 420                 425

TTG CCC CTT AAT GCC ATT GAA CCT TGT GTG ATT TGT CAA GGT CGA CCT         1646
Leu Pro Leu Asn Ala Ile Glu Pro Cys Val Ile Cys Gln Gly Arg Pro
430                 435                 440                 445

AAA AAT GGT TGC ATT GTC CAT GGC AAA ACA GGA CAT CTT ATG GCC TGC         1694
Lys Asn Gly Cys Ile Val His Gly Lys Thr Gly His Leu Met Ala Cys
```

-continued

```
                    450                 455                 460

TTT ACA TGT GCA AAG AAG CTA AAG AAA AGG AAT AAG CCC TGC CCA GTA      1742
Phe Thr Cys Ala Lys Lys Leu Lys Lys Arg Asn Lys Pro Cys Pro Val
                465                 470                 475

TGT AGA CAA CCA ATT CAA ATG ATT GTG CTA ACT TAT TTC CCC              1784
Cys Arg Gln Pro Ile Gln Met Ile Val Leu Thr Tyr Phe Pro
            480                 485                 490

TAGTTGACCT GTCTATAAGA GAATTATATA TTTCTAACTA TATAACCCTA GGAATTTAGA    1844

CAACCTGAAA TTTATTCACA TATATCAAAG TGAGAAAATG CCTCAATTCA CATAGATTTC    1904

TTCTCTTTAG TATAATTGAC CTACTTTGGT AGTGGAATAG TGAATACTTA CTATAATTTG    1964

ACTTGAATAT GTAGCTCATC CTTTACACCA ACTCCTAATT TTAAATAATT TCTACTCTGT    2024

CTTAAATGAG AAGTACTTGG TTTTTTTTTT CTTAAATATG TATATGACAT TTAAATGTAA    2084

CTTATTATTT TTTTTGAGAC CGAGTCTTGC TCTGTTACCC AGGCTGGAGT GCAGTGGGTG    2144

ATCTTGGCTC ACTGCAAGCT CTGCCCTCCC CGGGTTCGCA CCATTCTCCT GCCTCAGCCT    2204

CCCAATTAGC TTGGCCTACA GTCATCTGCC ACCACACCTG GCTAATTTTT TGTACTTTTA    2264

GTAGAGACAG GGTTTCACCG TGTTAGCCAG GATGGTCTCG ATCTCCTGAC CTCGTGATCC    2324

GCCCACCTCG GCCTCCCAAA GTGCTGGGAT TACAGGCATG AGCCACCG                  2372
```

(2) INFORMATION FOR SEQ ID NO:2:

(i) SEQUENCE CHARACTERISTICS:
(A) LENGTH: 491 amino acids
(B) TYPE: amino acid
(D) TOPOLOGY: linear

(i i) MOLECULE TYPE: protein

(x i) SEQUENCE DESCRIPTION: SEQ ID NO:2:

```
Met Cys Asn Thr Asn Met Ser Val Pro Thr Asp Gly Ala Val Thr Thr
  1               5                  10                  15

Ser Gln Ile Pro Ala Ser Glu Gln Glu Thr Leu Val Arg Pro Lys Pro
            20                  25                  30

Leu Leu Leu Lys Leu Leu Lys Ser Val Gly Ala Gln Lys Asp Thr Tyr
        35                  40                  45

Thr Met Lys Glu Val Leu Phe Tyr Leu Gly Gln Tyr Ile Met Thr Lys
    50                  55                  60

Arg Leu Tyr Asp Glu Lys Gln Gln His Ile Val Tyr Cys Ser Asn Asp
65                  70                  75                  80

Leu Leu Gly Asp Leu Phe Gly Val Pro Ser Phe Ser Val Lys Glu His
                85                  90                  95

Arg Lys Ile Tyr Thr Met Ile Tyr Arg Asn Leu Val Val Val Asn Gln
            100                 105                 110

Glu Glu Ser Ser Asp Ser Gly Thr Ser Val Ser Glu Asn Arg Cys His
        115                 120                 125

Leu Glu Gly Gly Ser Asp Gln Lys Asp Leu Val Gln Glu Leu Gln Glu
    130                 135                 140

Glu Lys Pro Ser Ser Ser His Leu Val Ser Arg Pro Ser Thr Ser Ser
145                 150                 155                 160

Arg Arg Arg Ala Ile Ser Glu Thr Glu Glu Asn Ser Asp Glu Leu Ser
                165                 170                 175

Gly Glu Arg Gln Arg Lys Arg His Lys Ser Asp Ser Ile Ser Leu Ser
            180                 185                 190

Phe Asp Glu Ser Leu Ala Leu Cys Val Ile Arg Glu Ile Cys Cys Glu
        195                 200                 205

Arg Ser Ser Ser Ser Glu Ser Thr Gly Thr Pro Ser Asn Pro Asp Leu
```

-continued

```
     210                 215                 220

Asp Ala Gly Val Ser Glu His Ser Gly Asp Trp Leu Asp Gln Asp Ser
225                 230                 235                 240

Val Ser Asp Glu Phe Ser Val Glu Phe Glu Val Glu Ser Leu Asp Ser
                245                 250                 255

Glu Asp Tyr Ser Leu Ser Glu Glu Gly Gln Glu Leu Ser Asp Glu Asp
            260                 265                 270

Asp Glu Val Tyr Gln Val Thr Val Tyr Glu Ala Gly Glu Ser Asp Thr
        275                 280                 285

Asp Ser Phe Glu Glu Asp Pro Glu Ile Ser Leu Ala Asp Tyr Trp Lys
    290                 295                 300

Cys Thr Ser Cys Asn Glu Met Asn Pro Pro Leu Pro Ser His Cys Asn
305                 310                 315                 320

Arg Cys Trp Ala Leu Arg Glu Asn Trp Leu Pro Glu Asp Lys Gly Lys
                325                 330                 335

Asp Lys Gly Glu Ile Ser Glu Lys Ala Lys Leu Glu Asn Ser Thr Glu
            340                 345                 350

Ala Glu Glu Gly Phe Asp Val Pro Asp Cys Lys Lys Thr Ile Val Asn
        355                 360                 365

Asp Ser Arg Glu Ser Cys Val Glu Glu Asn Asp Asp Lys Ile Thr Glu
    370                 375                 380

Ala Ser Glu Ser Glu Glu Ser Glu Asp Tyr Ser Glu Pro Ser Thr Ser
385                 390                 395                 400

Ser Ser Ile Ile Tyr Ser Ser Glu Glu Asp Val Lys Glu Phe Glu Arg
                405                 410                 415

Glu Glu Thr Gln Asp Lys Glu Glu Ser Val Glu Ser Ser Leu Pro Leu
            420                 425                 430

Asn Ala Ile Glu Pro Cys Val Ile Cys Gln Gly Arg Pro Lys Asn Gly
        435                 440                 445

Cys Ile Val His Gly Lys Thr Gly His Leu Met Ala Cys Phe Thr Cys
    450                 455                 460

Ala Lys Lys Leu Lys Lys Arg Asn Lys Pro Cys Pro Val Cys Arg Gln
465                 470                 475                 480

Pro Ile Glu Met Ile Val Leu Thr Tyr Phe Pro
                485                 490
```

(2) INFORMATION FOR SEQ ID NO:3:

(i) SEQUENCE CHARACTERISTICS:
(A) LENGTH: 1710 base pairs
(B) TYPE: nucleic acid
(C) STRANDEDNESS: double
(D) TOPOLOGY: linear

(i i) MOLECULE TYPE: cDNA

(i i i) HYPOTHETICAL: NO

(i v) ANTI-SENSE: NO

(v i) ORIGINAL SOURCE:
(A) ORGANISM: Mus musculus

(i x) FEATURE:
(A) NAME/KEY: CDS
(B) LOCATION: 202..1668

(x i) SEQUENCE DESCRIPTION: SEQ ID NO:3:

```
GAGGAGCCGC CGCCTTCTCG TCGCTCGAGC TCTGGACGAC CATGGTCGCT CAGGCCCCGT      60

CCGCGGGGCC TCCGCGCTCC CCGTGAAGGG TCGGAAGATG CGCGGGAAGT AGCAGCCGTC     120

TGCTGGGCGA GCGGGAGACC GACCGGACAC CCCTGGGGGA CCCTCTCGGA TCACCGCGCT     180
```

-continued

```
TCTCCTGCGG CCTCCAGGCC A ATG TGC AAT ACC AAC ATG TCT GTG TCT ACC          231
                        Met Cys Asn Thr Asn Met Ser Val Ser Thr
                         1               5                  10

GAG GGT GCT GCA AGC ACC TCA CAG ATT CCA GCT TCG GAA CAA GAG ACT          279
Glu Gly Ala Ala Ser Thr Ser Gln Ile Pro Ala Ser Glu Glu Glu Thr
                    15                  20                  25

CTG GTT AGA CCA AAA CCA TTG CTT TTG AAG TTG TTA AAG TCC GTT GGA          327
Leu Val Arg Pro Lys Pro Leu Leu Leu Lys Leu Leu Lys Ser Val Gly
                30                  35                  40

GCG CAA AAC GAC ACT TAC ACT ATG AAA GAG ATT ATA TTT TAT ATT GGC          375
Ala Gln Asn Asp Thr Tyr Thr Met Lys Glu Ile Ile Phe Tyr Ile Gly
            45                  50                  55

CAG TAT ATT ATG ACT AAG AGG TTA TAT GAC GAG AAG CAG CAG CAC ATT          423
Gln Tyr Ile Met Thr Lys Arg Leu Tyr Asp Glu Lys Gln Gln His Ile
        60                  65                  70

GTG TAT TGT TCA AAT GAT CTC CTA GGA GAT GTG TTT GGA GTC CCG AGT          471
Val Tyr Cys Ser Asn Asp Leu Leu Gly Asp Val Phe Gly Val Pro Ser
    75                  80                  85                  90

TTC TCT GTG AAG GAG CAC AGG AAA ATA TAT GCA ATG ATC TAC AGA AAT          519
Phe Ser Val Lys Glu His Arg Lys Ile Tyr Ala Met Ile Tyr Arg Asn
                95                 100                 105

TTA GTG GCT GTA AGT CAG CAA GAC TCT GGC ACA TCG CTG AGT GAG AGC          567
Leu Val Ala Val Ser Gln Gln Asp Ser Gly Thr Ser Leu Ser Glu Ser
            110                 115                 120

AGA CGT CAG CCT GAA GGT GGG AGT GAT CTG AAG GAT CCT TTG CAA GCG          615
Arg Arg Gln Pro Glu Gly Gly Ser Asp Leu Lys Asp Pro Leu Gln Ala
        125                 130                 135

CCA CCA GAA GAG AAA CCT TCA TCT TCT GAT TTA ATT TCT AGA CTG TCT          663
Pro Pro Glu Glu Lys Pro Ser Ser Ser Asp Leu Ile Ser Arg Leu Ser
    140                 145                 150

ACC TCA TCT AGA AGG AGA TCC ATT AGT GAG ACA GAA GAG AAC ACA GAT          711
Thr Ser Ser Arg Arg Arg Ser Ile Ser Glu Thr Glu Glu Asn Thr Asp
155                 160                 165                 170

GAG CTA CCT GGG GAG CGG CAC CGG AAG CGC CGC AGG TCC CTG TCC TTT          759
Glu Leu Pro Gly Glu Arg His Arg Lys Arg Arg Arg Ser Leu Ser Phe
                175                 180                 185

GAT CCG AGC CTG GGT CTG TGT GAG CTG AGG GAG ATG TGC AGC GGC GGC          807
Asp Pro Ser Leu Gly Leu Cys Glu Leu Arg Glu Met Cys Ser Gly Gly
            190                 195                 200

ACG AGC AGC AGT AGC AGC AGC AGC AGC AGC GAG TCC ACA GAG ACG CCC TCG      855
Thr Ser Ser Ser Ser Ser Ser Ser Ser Ser Glu Ser Thr Glu Thr Pro Ser
        205                 210                 215

CAT CAG GAT CTT GAC GAT GGC GTA AGT GAG CAT TCT GGT GAT TGC CTG          903
His Gln Asp Leu Asp Asp Gly Val Ser Glu His Ser Gly Asp Cys Leu
    220                 225                 230

GAT CAG GAT TCA GTT TCT GAT CAG TTT AGC GTG GAA TTT GAA GTT GAG          951
Asp Gln Asp Ser Val Ser Asp Gln Phe Ser Val Glu Phe Glu Val Glu
235                 240                 245                 250

TCT CTG GAC TCG GAA GAT TAC AGC CTG AGT GAC GAA GGG CAC GAG CTC          999
Ser Leu Asp Ser Glu Asp Tyr Ser Leu Ser Asp Glu Gly His Glu Leu
                255                 260                 265

TCA GAT GAG GAT GAT GAG GTC TAT CGG GTC ACA GTC TAT CAG ACA GGA      1047
Ser Asp Glu Asp Asp Glu Val Tyr Arg Val Thr Val Tyr Gln Thr Gly
            270                 275                 280

GAA AGC GAT ACA GAC TCT TTT GAA GGA GAT CCT GAG ATT TCC TTA GCT      1095
Glu Ser Asp Thr Asp Ser Phe Glu Gly Asp Pro Glu Ile Ser Leu Ala
        285                 290                 295

GAC TAT TGG AAG TGT ACC TCA TGC AAT GAA ATG AAT CCT CCC CTT CCA      1143
Asp Tyr Trp Lys Cys Thr Ser Cys Asn Glu Met Asn Pro Pro Leu Pro
    300                 305                 310
```

-continued

```
TCA CAC TGC AAA AGA TGC TGG ACC CTT CGT GAG AAC TGG CTT CCA GAC      1191
Ser His Cys Lys Arg Cys Trp Thr Leu Arg Glu Asn Trp Leu Pro Asp
315                 320                 325                 330

GAT AAG GGG AAA GAT AAA GTG GAA ATC TCT GAA AAA GCC AAA CTG GAA      1239
Asp Lys Gly Lys Asp Lys Val Glu Ile Ser Glu Lys Ala Lys Leu Glu
                335                 340                 345

AAC TCA GCT CAG GCA GAA GAA GGC TTG GAT GTG CCT GAT GGC AAA AAG      1287
Asn Ser Ala Gln Ala Glu Glu Gly Leu Asp Val Pro Asp Gly Lys Lys
            350                 355                 360

CTG ACA GAG AAT GAT GCT AAA GAG CCA TGT GCT GAG GAG GAC AGC GAG      1335
Leu Thr Glu Asn Asp Ala Lys Glu Pro Cys Ala Glu Glu Asp Ser Glu
        365                 370                 375

GAG AAG GCC GAA CAG ACG CCC CTG TCC CAG GAG AGT GAC GAC TAT TCC      1383
Glu Lys Ala Glu Gln Thr Pro Leu Ser Gln Glu Ser Asp Asp Tyr Ser
    380                 385                 390

CAA CCA TCG ACT TCC AGC AGC ATT GTT TAT AGC AGC CAA GAA AGC GTG      1431
Gln Pro Ser Thr Ser Ser Ser Ile Val Tyr Ser Ser Gln Glu Ser Val
395                 400                 405                 410

AAA GAG TTG AAG CAG GAA ACG CAG CAC AAA GAC GAG AGT GTG GAA TCT      1479
Lys Glu Leu Lys Gln Glu Thr Gln His Lys Asp Glu Ser Val Glu Ser
                415                 420                 425

AGC TTC TCC CTG AAT GCC ATC GAA CCA TGT GTG ATC TGC CAG GGG CGG      1527
Ser Phe Ser Leu Asn Ala Ile Glu Pro Cys Val Ile Cys Gln Gly Arg
            430                 435                 440

CCT AAA AAT GGC TGC ATT GTT CAC GGC AAG ACT GGA CAC CTC ATG TCA      1575
Pro Lys Asn Gly Cys Ile Val His Gly Lys Thr Gly His Leu Met Ser
        445                 450                 455

TGT TTC ACG TGT GCA AAG AAG CTA AAA AAA AGA AAC AAG CCC TGC CCA      1623
Cys Phe Thr Cys Ala Lys Lys Leu Lys Lys Arg Asn Lys Pro Cys Pro
    460                 465                 470

GTG TGC AGA CAG CCA ATC CAA ATG ATT GTG CTA AGT TAC TTC AAC          1668
Val Cys Arg Gln Pro Ile Gln Met Ile Val Leu Ser Tyr Phe Asn
475                 480                 485

TAGCTGACCT GCTCACAAAA ATAGAATTTT ATATTTCTAA CT                       1710
```

(2) INFORMATION FOR SEQ ID NO:4:

(i) SEQUENCE CHARACTERISTICS:
(A) LENGTH: 489 amino acids
(B) TYPE: amino acid
(D) TOPOLOGY: linear

(ii) MOLECULE TYPE: protein

(xi) SEQUENCE DESCRIPTION: SEQ ID NO:4:

```
Met Cys Asn Thr Asn Met Ser Val Ser Thr Glu Gly Ala Ala Ser Thr
 1               5                  10                  15

Ser Glu Ile Pro Ala Ser Glu Gln Glu Thr Leu Val Arg Pro Lys Pro
            20                  25                  30

Leu Leu Leu Lys Leu Leu Lys Ser Val Gly Ala Gln Asn Asp Thr Tyr
        35                  40                  45

Thr Met Lys Glu Ile Ile Phe Tyr Ile Gly Gln Tyr Ile Met Thr Lys
    50                  55                  60

Arg Leu Tyr Asp Glu Lys Gln Gln His Ile Val Tyr Cys Ser Asn Asp
65                  70                  75                  80

Leu Leu Gly Asp Val Phe Gly Val Pro Ser Phe Ser Val Lys Glu His
                85                  90                  95

Arg Lys Ile Tyr Ala Met Ile Tyr Arg Asn Leu Val Val Val Asn Gln
            100                 105                 110

Gln Asp Ser Gly Thr Ser Leu Ser Glu Ser Arg Arg Gln Pro Glu Gly
        115                 120                 125
```

-continued

```
Gly Ser Asp Leu Lys Asp Pro Leu Gln Ala Pro Pro Glu Glu Lys Pro
    130                 135                 140

Ser Ser Ser Asp Leu Ile Ser Arg Leu Ser Thr Ser Ser Arg Arg Arg
145                 150                 155                 160

Ser Ile Ser Glu Thr Glu Glu Asn Thr Asp Glu Leu Pro Gly Glu Arg
                165                 170                 175

His Arg Lys Arg Arg Arg Ser Leu Ser Phe Asp Pro Ser Leu Gly Leu
            180                 185                 190

Cys Glu Leu Arg Glu Met Cys Ser Gly Gly Thr Ser Ser Ser Ser Ser
        195                 200                 205

Ser Ser Ser Glu Ser Thr Glu Thr Pro Ser His Gln Asp Leu Asp Asp
    210                 215                 220

Gly Val Ser Glu His Ser Gly Asp Cys Leu Asp Gln Asp Ser Val Ser
225                 230                 235                 240

Asp Gln Phe Ser Val Glu Phe Glu Val Glu Ser Leu Asp Ser Glu Asp
                245                 250                 255

Tyr Ser Leu Ser Asp Glu Gly His Glu Leu Ser Asp Glu Asp Asp Glu
            260                 265                 270

Val Tyr Arg Val Thr Val Tyr Gln Thr Gly Glu Ser Asp Thr Asp Ser
        275                 280                 285

Phe Glu Gly Asp Pro Glu Ile Ser Leu Ala Asp Tyr Trp Lys Cys Thr
    290                 295                 300

Ser Cys Asn Glu Met Asn Pro Pro Leu Pro Ser His Cys Lys Arg Cys
305                 310                 315                 320

Trp Thr Leu Arg Glu Asn Trp Leu Pro Asp Asp Lys Gly Lys Asp Lys
                325                 330                 335

Val Glu Ile Ser Glu Lys Ala Lys Leu Glu Asn Ser Ala Gln Ala Glu
            340                 345                 350

Glu Gly Leu Asp Val Pro Asp Gly Lys Lys Leu Thr Glu Asn Asp Ala
        355                 360                 365

Lys Glu Pro Cys Ala Glu Glu Asp Ser Glu Glu Lys Ala Glu Gln Thr
    370                 375                 380

Pro Leu Ser Gln Glu Ser Asp Asp Tyr Ser Glu Pro Ser Thr Ser Ser
385                 390                 395                 400

Ser Ile Val Tyr Ser Ser Glu Glu Ser Val Lys Glu Leu Lys Glu Glu
                405                 410                 415

Thr Gln His Lys Asp Glu Ser Val Glu Ser Ser Phe Ser Leu Asn Ala
            420                 425                 430

Ile Glu Pro Cys Val Ile Cys Glu Gly Arg Pro Lys Asn Gly Cys Ile
        435                 440                 445

Val His Gly Lys Thr Gly His Leu Met Ser Cys Phe Thr Cys Ala Lys
    450                 455                 460

Lys Leu Lys Lys Arg Asn Lys Pro Cys Pro Val Cys Arg Gln Pro Ile
465                 470                 475                 480

Gln Met Ile Val Leu Ser Tyr Phe Asn
                485
```

We claim:

1. A method of screening for a neoplastic tissue in a human comprising:

detecting amplification of a human MDM2 gene or elevated expression of a human MDM2 gene by detecting human MOM2 mRNA in a tissue or body fluid isolated from a human, wherein amplification of the human MDM2 gene or elevated expression of the human MDM2 gene provides a method of screening for neoplasia or the potential for neoplastic development.

2. The method of claim 1 wherein gene amplification is detected.

3. The method of claim 1 wherein said mRNA is detected by Northern blot analysis by hybridizing mRNA from said tissue to a human MDM2 nucleotide probe.

4. The method of claim 3 wherein the human MDM2 nucleotide probe comprises nucleotides 1-2372 of

human MDM2, as shown in FIG. 1, or fragments thereof consisting of at least 14 contiguous nucleotides.

5. The method of claim 2 wherein the gene amplification is detected using polymerase chain reaction.

6. The method of claim 2 wherein amplification of the human MDM2 gene is detected by Southern blot analysis wherein the human MDM2 gene is hybridized with a nucleotide probe which is complementary to hMDM2 DNA.

7. The method of claim 2 wherein gene amplification is determined by comparing the copy number of hMDM2 in the tissue to the copy number of hMDM2 in a normal tissue of the human.

8. The method of claim 1 wherein elevated expression of a human MDM2 gene is determined by comparing the amount of hMDM2 mRNA in the tissue to the amount of hMDM2 mRNA in a normal tissue of the human.

9. The method of claim 2 wherein gene amplification is detected when at least 3-fold more hMDM-2 DNA is observed in the tissue relative to a control sample comprising a normal tissue.

10. The method of claim 1 wherein elevated expression is detected when at least 3-fold more hMDM-2 mRNA is observed in the tissue relative to a control sample comprising a normal tissue.

11. The method of claim 1 wherein the neoplasia is a sarcoma.

12. The method of claim 11 wherein the sarcoma is a liposarcoma, malignant fibrous histiocytoma, or osteosarcoma.

* * * * *

UNITED STATES PATENT AND TRADEMARK OFFICE

CERTIFICATE OF CORRECTION

PATENT NO. : 5,411,860
DATED : May 2, 1995
INVENTOR(S) : Bert Vogelstein and Kenneth Kinzler

It is certified that error appears in the above-indentified patent and that said Letters Patent is hereby corrected as shown below:

At column 1, line 3 insert the following:

"This invention was made with government support under Grant CA43460, CA35494 and CA41183 awarded by the National Institutes of Health. The government has certain rights in this invention."

Signed and Sealed this
Fifth Day of August, 1997

Bruce Lehman

Attest:

Attesting Officer

BRUCE LEHMAN

Commissioner of Patents and Trademarks

SECOND EDITION

Recombinant DNA

James D. Watson
Michael Gilman
Jan Witkowski
Mark Zoller

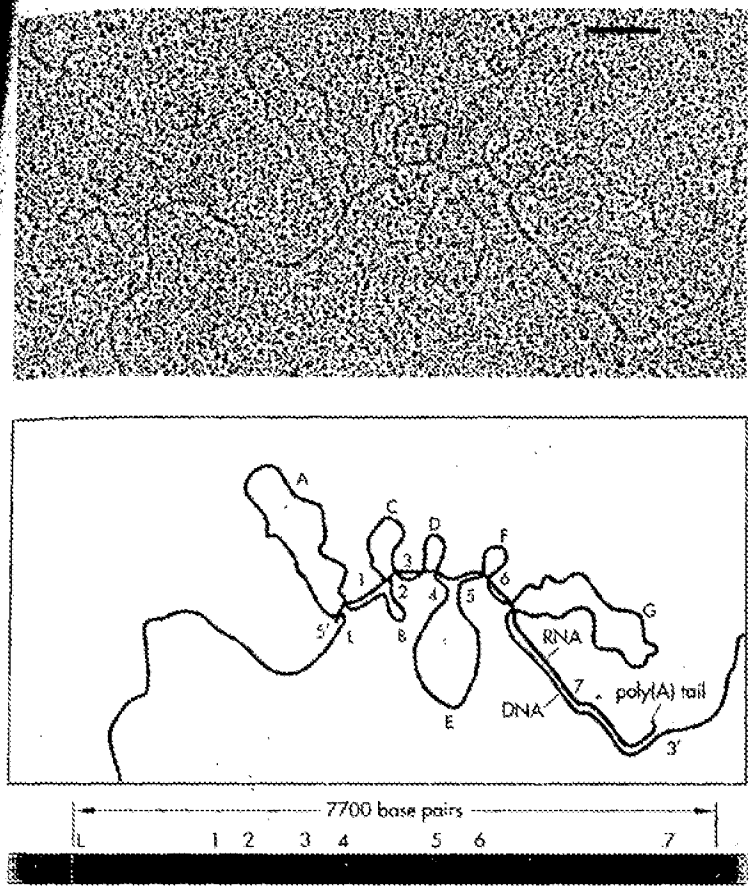

FIGURE 8-2
Examination of gene structure by electron microscopy of DNA–mRNA hybrids. DNA containing the gene for ovalbumin was hybridized with ovalbumin mRNA. The regions of the gene that hybridize to the mRNA are eight exons (L, 1-7). Genomic DNA that encodes introns does not hybridize to the mRNA but forms seven loops (A-G). The upper portion of the figure shows the actual electron micrograph. Regions where genomic DNA hybridized to mRNA form a thicker line than do the single-stranded genomic DNA loops. The locations and lengths of the introns were estimated simply by plotting the position of each loop along the mRNA molecule. Because the length of the mRNA (in nucleotides) was known, the approximate positions of the introns could be calculated. The middle portion of the figure shows the interpretation of the electron micrograph. The 5′ and 3′ ends of the mRNA are indicated. The bottom portion shows a scheme of the structure of the ovalbumin gene determined subsequently by DNA sequence analysis of the exon-intron boundaries in genomic DNA and comparison with the cDNA sequence. The exons are shown in green and the introns are shown in red (modified from Chambon, 1981).

Introns Are Discovered in Eukaryotic Genes

Excited by these results, people working on the structure of eukaryotic genes searched for splicing of cellular RNAs. Within a very short time after the discovery of adenovirus splicing, the coding sequences of β-globin, ovalbumin, and immunoglobulin genes were also found to be interrupted by noncoding DNA. Proof that chromosomal genes were spliced came initially by electron microscopy. The sizes and locations of these introns were then estimated by a technique called *S1 nuclease mapping* (Figure 8-3). The regions of the chromosomal DNA not present in the mature mRNA were given the name *introns*. The coding sequences were called *exons*, because the processed mRNAs, without the introns, "exit" from the nucleus to the cytoplasm. It should be noted that at the time that the electron microscopy experiments on adenovirus were done, no one had cloned a cellular gene yet. Once the first genes were cloned, introns were identified by comparing the cloned genomic DNA with the corresponding cloned cDNA. For small genes, such as the β-globin gene, the sizes of the introns and the locations of intron-exon boundaries were precisely determined by sequencing cloned genomic DNA and

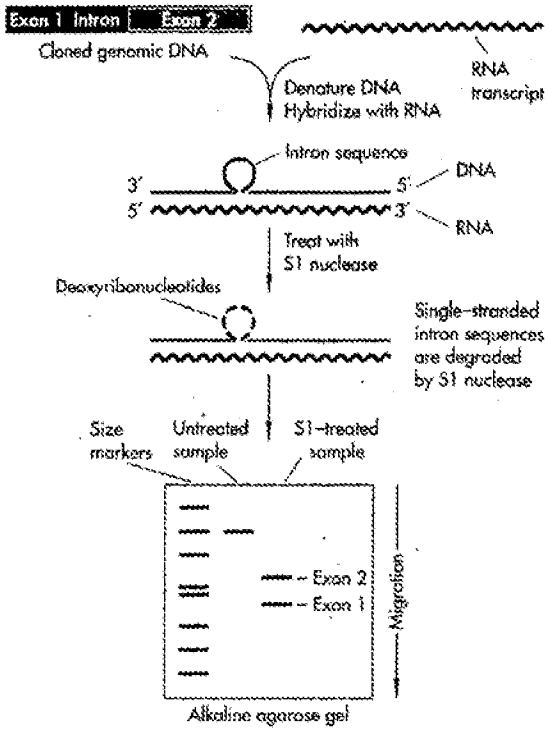

FIGURE 8-3
S1 nuclease mapping finds introns in a gene. Total cellular RNA is hybridized to a cloned genomic DNA fragment that contains a single intron. An RNA–DNA heteroduplex is formed between the gene DNA and its corresponding mRNA by base-pairing of complementary sequences. Intron sequences in the gene do not hybridize with the mRNA, so these DNA sequences form single-stranded loops. The RNA–DNA hybrid is treated with S1 nuclease, an enzyme that digests single-stranded DNA into mononucleotides. The unpaired intron sequences thus are digested, a process that splits the genomic DNA into two fragments. The sizes of these two DNA fragments are determined by gel electrophoresis. From this information, the length and location of the intron in the gene are deduced.

comparing the sequence with the cDNA sequence and with the protein sequence.

Introns exist in genes from all eukaryotic animals, in plant genes, and, surprisingly, in genes of the *E. coli* phage T4. Often the introns of a gene contain many more nucleotides than do its coding exons, thus accounting for the previously unexplained large sizes of many primary RNA transcripts. The number and size of introns vary widely from one gene to another. Two introns are present in all genes of the β-globin family (Figure 8-4). The sizes of introns in the β-globin genes from different species differ slightly, but their positions are always the same relative to the coding sequence. The ovalbumin gene is more complicated than the β-globin gene and contains seven introns. The length of introns can vary from 31 nucleotides in an SV40 gene to over 210,000 nucleotides in the human dystrophin gene. A few genes, such as the genes coding for the α and β forms of interferon and most of the genes from the yeast *Saccharomyces cerevisiae* do not contain introns. Intronless mammalian genes can also be generated through recombinant DNA tricks and tested to see how they function in vivo. For certain genes, the complete removal of introns has no consequence. Such genes produce fully active mRNA transcripts. However, for other genes, the removal of their natural introns somehow blocks the exit of functional mRNA products to the cytoplasm. Perhaps in these latter cases the newly made transcripts adopt configurations incompatible with exit from the nucleus.

Specific Base Sequences Are Found at Exon-Intron Boundaries

By the summer of 1978, just a year after the first split genes were discovered, the sequences of many exon-intron boundaries from cellular genes had been determined. It was hoped that such sequence data would be useful in predicting the location of an intron in a gene and would also explain how splicing was accomplished. People expected to find that the sequence at the upstream (5′) and downstream (3′) ends of an intron would be complementary. These sequences would therefore be expected to hybridize and form a stretch of double-stranded RNA, which would be recognized and precisely excised by specific splicing enzymes. However, this idea was soon discounted, since the sequences at the ends of the introns were not complementary. The upstream and downstream splice sites therefore could not be brought together by self-

GeneCard for gene *MDM2* GC12P067488

Approved UCL/HGNC/HUGO Human Gene Nomenclature database symbol
MDM2 (Mdm2, transformed 3T3 cell double minute 2, p53 binding protein (mous

Aliases and Descriptions
(According to GDB, OMIM, HUGO, LocusLink, SWISS-PROT/TrEMBL and/or GeneLoc)

- hdm2 (ω)
- Mdm2, transformed 3T3 cell double minute 2, p53 binding protein (mouse) (GDB, ω)
- mouse double minute 2, human homolog of; p53-binding protein (GDB)
- p53-binding protein MDM2 (ω)
- Ubiquitin-protein ligase E3 Mdm2 (EC 6.3.2.-) (p53-binding protein Mdm2) (Oncop

Previous GC identifiers: GC12M068977 GC12P069030 GC12P068918

Chromosomal Location
(According to GeneLoc and/or HUGO and/or LocusLink (NCBI build 34), Genomic Views According to UCSC and Ensembl)

Chromosome: **12** GeneLoc gene densities
LocusLink cytogenetic band: **12q14.3-q15** *Ensembl cytogenetic band:* **12q15**

Gene in genomic location: bands according to Ensembl, locations according to Gene

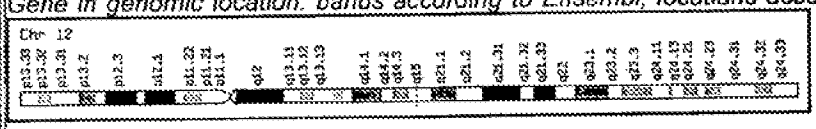

GeneLoc location for GC12P067488: (about GC identifiers)
Start: **67,488,238** bp from pter
End: **67,520,481** bp from pter
Size: **32,243** bases
Orientation: **plus** strand

Genomic View:
UCSC Golden Path with GeneCards custom track

Proteins
(According to SWISS-PROT/TrEMBL and/or MIPS PDB rendering according to OCA)

Swiss-Prot: MDM2_HUMAN

- **Size**: 491 amino acids; 55232 Da
- **Cofactor**: ZINC IS REQUIRED FOR UBIQUITIN LIGASE E3 ACTIVITY.
- **Subunit**: BINDS P53, P73, ARF(P14), RIBOSOMAL PROTEIN L5 AND SPECIFIC WITH RETINOBLASTOMA PROTEIN (RB), E1A-ASSOCIATED PROTEIN P300 A
- **Subcellular location**: NUCLEAR AND CYTOPLASMIC. EXPRESSED PREDOMI INTERACTION WITH ARF(P14) RESULTS IN THE LOCALIZATION OF BOTH PR NUCLEOLAR LOCALIZATION SIGNALS IN BOTH ARF(P14) AND MDM2 MAY BE NUCLEOLAR LOCALIZATION OF BOTH PROTEINS.
- **Alternative products**: Alternative splicing.
- **Post-translational modifications**: PHOSPHORYLATED IN RESPONSE TO IONI
- **Miscellaneous**: MDM2 RING FINGER MUTATIONS THAT FAILED TO UBIQUITI P53 FOR DEGRADATION WHEN EXPRESSED IN CELLS.
- **3D structure:** PDB id 1YCR (3D)

MIPS Pedant Viewer: 74112 74106 74107 74108 74109

REFSEQ proteins (5 alternative transcripts): NP_002383.1 NP_006869.1 NP_006870.1 NP_006871.

Protein Domains/ Families
(According to InterPro, ProtoNet, SWISS-PROT/TrEMBL)

InterPro Domains and Families:
IPR001876 Znf_RanGDP
IPR003121 SWIB
IPR001841 Znf_ring

Mammalian Genome 7, 780–783 (1996).

Mammalian Genome

YAC clones that extend the human Chromosome 12cen-12q15 region contig map

S.E. Andersen, N.J. Lench, A.F. Markham

Molecular Medicine Unit, University of Leeds, Clinical Sciences Building, St James's University Hospital, Leeds LS9 7TF, UK

Received: 4 March 1996 / 5 June 1996

Human Chromosome (Chr) 12q13 is a region of clinical interest in that a variety of disease phenotypes have been localized to the area. A number of relatively detailed genetic maps of the region around human Chr 12q13 are now available. A second-generation YAC contig map of human Chr 12, which extensively covers this area, has also been produced. This has resolved a number of discrepancies in the previous genetic maps. The current YAC contig map contains only five small gaps in the approximately 45 cM region between the polymorphic microsatellite markers *D12S333* and *D12S106*. A number of expressed sequences have also been localized with varying degrees of precision to the region around 12q13.

In an attempt to generate YAC resources with low levels of chimerism and to facilitate disease and EST mapping in this genomic area, we now describe the isolation of 130 YACs from the ICI library (Anand et al. 1990). We have used 36 genetic markers and 11 ESTs from five previous Chr 12 maps (Guyer and Cann, 1992; Weissenbach et al. 1992; Schoenmakers et al. 1994; Kucherlapati et al. 1994; Gyapay et al. 1994). Our data can be integrated with the most recent second-generation YAC contig map of Chr 12 (Krauter et al. 1995). We have mapped the WNT-1 gene (Nusse et al. 1991) at 62–66 cM (based on the 200 cM overall Chr 12 map of Krauter et al. 1995) in close proximity to *D12S339* (in the contig gap between *D12S85* and *D12S361*) and the GPD1 gene. This is an area under-represented in the latest Chr 12 contig map. We have also observed close linkage between GADD153 and GLI at 77 cM in the interval between *D12S312* and *D12S90* (Krauter et al. 1995). The markers *D12S17* and *D12S96* also co-localize at 71 cM in the area between *D12S390* and *D12S398*, which has enabled us to position several first-generation genetic markers with respect to these points. We have isolated YACs for LRP/A2MR, which is known to be physically linked to GLI (Forus and Myklebost 1992). These may be of value in closing a gap at 76 cM in the current map immediately centromeric of GADD153/GLI. The YAC 11GH7 containing *D12S312* may also be useful in this respect as it is the closest known marker proximal to the same contig gap. Similarly, YACs containing MDM2 and *D12S43* may help to close the gap between RAP1B and *D12S80* at 85 cM. As well as YACs containing COL2A1 and LALBA, which are included in the latest contig map, we have isolated YACs for PMCA, CD63, and PAB1, which are as yet not accurately positioned on the map. *D12S59* or IGF-1 containing YACs described herein are now known to map distal to our region of interest at 113 cM and 118 cM respectively (Krauter et al. 1995). Vectorette YAC end sequencing (Riley et al. 1990) has enabled us to generate other novel STSs and corresponding YACs from the region.

Novel YACs identified with 36 genetic markers from the 12q13 region and from 11 expressed sequences in the region are presented in Table 1. Where known, a corresponding YAC from the second-generation YAC contig map of human Chr 12 is included in Table 1 for ease of cross-reference (Krauter et al. 1995). The 47 loci screened all produced at least one positive YAC and, in most cases, multiple YACs, consistent with a ×3.5-fold genomic representation of this library (Anand et al. 1990). In a number of cases, the same YAC was identified with more than one genetic marker, implying that these markers lie in close physical proximity (the average insert size of the YACs in this library is 350 kb). *D12S339* and the WNT-1 oncogene both gave positive signals with YACs 26BB4, 28AD4, and 32BC2 in the region of the 64 cM contig gap (Fig. 1). *D12S368* and *D12S174* at around 68 cM both identified YAC 30AD11. *D12S17* and *D12S96* both identified the YACs 20BB4 and 20BF12. This places *D12S17* at the 71 cM locus in the middle of the KRT gene family and centromeric of *D12S398*, *D12S359*, *D12S19*, *D12S325*, HOXC5, and *D12S103* respectively. GADD153 and GLI1 at 76 cM identify the YAC 26EG10, confirming the close physical linkage of these two genes. This locus is immediately telomeric of a gap at 76 cM in the current second-generation YAC contig map, and end sequencing of 26EG10 may assist in contig closure. The markers *D12S305* and *D12S104* at 77 cM both identify the YAC 10ED1 concordant with the second-generation map. End sequencing of 10ED1 and rescreening of the YAC library identified 15BE5. This YAC also contains *D12S90*, confirming marker order *D12S90*, *D12S305*, *D12S104*. *D12S83* and *D12S334* both identify the YAC 34CA7, confirming their physical proximity at 77 cM also (Krauter et al. 1995).

YACs for which sequencing of human DNA insert termini has been performed are shown in Table 1. Following confirmation of localization to Chr 12 with the Coriell Mapping Panel, additional YACs were isolated as shown (Table 1). These increase the YAC coverage at *D12S96/17* (71 cM, 20BF12), *D12S90/305/104* (77 cM, 10ED1, 15BE5), and *D12S43* around the 86 cM region (34HH10). A number of YACs proved to be chimeric during analysis; the right-hand end of 40AA12 (a YAC identified using primers from the MDM2 gene) maps to human Chr 1. The MDM2 YAC 6FD11 is also highly chimeric by FISH analysis (data not shown). The MDM2 YAC 40CB5 was not chimeric by FISH analysis and was used to confirm its localization to the 12q14 region (Fig. 2; Heighway et al. 1994). The other YAC termini sequences in Table 1 all map to Chr 12 by PCR analysis of somatic cell hybrids.

In the last four years, six separate Chr 12 maps have been presented which include markers in and around the 12q13 region. The NIH/CEPH collaborative mapping group comprehensive genetic linkage map of the human genome (Guyer and Cann 1992), in conjunction with data of Schoenmakers and associates (1994), provided an approximate marker order cen–COL2A1–ELA1–*D12S29–D12S15–D12S25–D12S14–D12S4–D12S18–D12S16–D12S17–D12S6–D12S28–D12S22–D12S28–D12S19–D12S43–D12S8–D12S64–D12S7*–tel, with the latter probably located distally in 12q15. In complementary studies in 1992, Weissenbach and colleagues described another set of markers across the same

Correspondence to: A.F. Markham

Table 1. YACs identified with known genetic markers and ESTs. YACs in bold are detected by more than one marker. CEPH YACs are included for ease of cross reference. YACs identified by rescreening the library with Vectorette-generated end sequences are also included (Riley et al. 1990) as are the novel STSs generated in this process. The NIGMS monochromosomal human/rodent somatic cell-hybrid mapping panels #1 and #2 (NIGMS, Coriell Repository, Camden, N.J., USA) were screened by PCR amplification with newly generated oligonucleotides from YAC insert termini as primers. PCR conditions were as described for the YAC library screening. The panel was screened to confirm localization to human Chr12 and thus to ensure, to a first approximation, that the identified YACs were not chimeric. These sequences have been assigned Genbank accession numbers U51106–U51111.

Markers	Tm (°C)	$MgCl_2$ (mM)	Identified ICI YACs	CEPH YACs
D12S87	58.5	1.5	**20BB4; 20BF12**	—
D12S43	55.0	1.8	9GC9; 34HH10	—
D12S58	53.0	2.0	27ID4; 27ID8; 29GE6	—
D12S59	53.0	1.5	18H2; 13GD4	707f6
D12S80	53.0	2.0	5FF10; 18EG1; 19DH6; 32HE12; 34DD7; 37FC5; 38GG8	749a7
D12S83	50.0	1.5	**34CA7**	799a11
D12S85	53.5	2.0	5IA12; 12HC4; 12IE9; 18CH4; 21GB5; 37EH10; 39DB1	690k1; 767g5
D12S87	52.0	2.0	1HG9; 10IG5; 10IG6; 23BA10; 37AE2; 37FA3	759b2
D12S90	53.0	1.5	4DD8; 9EG8; **15BE5**; 23ID1; 34HA8; 36IC2	770a7
D12S96	53.0	2.4	**20BB4; 20BF12**	934b7
D12S103	53.0	1.5	7DF1	790f7
D12S104	52.0	1.0	**10ED1**; 30AA4; 39EH4	907f2
D12S106	53.0	1.5	33FH8; 35HF4; 39III2	763a8
D12S118	49.0	1.5	5HB11; 18DA9	—
D12S131	54.5	1.5	pool 8A	—
D12S137	55.0	1.5	40AP6	396e10
D12S174	59.5	1.5	**30AD11**	717g8
D12S305	51.0	1.5	**10ED1**; 20HH9; 38BC9	907f2
D12S312	55.0	1.5	11GH7	790f7
D12S313	51.0	1.5	21AA8	751a4
D12S325	52.0	1.5	8BB12; 8EC4; 24BF5; 39BB1	928a12
D12S326	54.5	1.5	30FE5	806e12
D12S329	56.5	1.5	11GC11; 16GG9; 24FH7	970d8
D12S331	51.5	1.5	9GD6; 11FD5; 40GB12	690h5
D12S333	53.0	1.5	6HG8; 12GG4; 12GH4; 19DD7; 34DD8	952a6
D12S334	49.0	1.5	**34CA7**; 35ID6	799a11
D12S335	52.5	1.5	pool 15F, 34G, 35G; 39F	755d7
D12S337	55.0	1.5	18AG10; 20EB9; 22EC12; 27BH9	925h12
D12S339	57.5	1.5	5FA12; 9CG7; **26BB4; 28AD4; 32BC2**	—
D12S345	49.0	1.5	19FF10; 29HD4; 29HD11; 33BH12; 37IB1	951h6
D12S347	53.0	1.5	11BD7	951a5
D12S350	57.0	1.5	16BB1; 34CE11; 27EE5; 29CB3; 35CC11; 39HB2; 40CC4	814f12
D12S355	52.5	1.5	39CB8	959a5
D12S361	53.0	1.5	26BG9; 40CD11	951a5
D12S368	53.0	1.5	**30AD11**	717g8
D12S371	55.5	1.5	9CB11; 10IH6; 23CC10; 37IC10	926b3

Genes	Tm (°C)	$MgCl_2$ (mM)	
LALBA	53.5	1.5	38FA5
COL2A1	57.0	3.0	11A5; 35BF10
GADD153	58.0	1.5	**26EG10**
GLI	53.5	1.5	26EG1; **25EG10**
WNT1	55.0	1.5	**26BB4; 28AD4; 32BC2**
MDM2	56.5	1.5	6FD11; 40AA12; 40CB5; 26DC3
LRPA2MR	56.0	1.5	13FE9; 15DD6
FAB	52.5	1.5	11GG9
CD63	58.0	1.5	26AB8; 27GE12; 33AG6
PMCA	65.0	3.0	4AF4
IGF1	61.0	2.5	17DF5; 30EC4; 39CF12

Original YAC	Left side YACs	Right YACs
10ED1	30AA4; 39ED3	**15BE5**; 29IE10
20BF12	18EF6; 19IC6; 32DA10; 36EF3; 37DD1; 37IF5	N/D
34HH10	14BC11	N/D

Table 1. *Continued.*

YAC clone	Right end sequences
10ED1	5'-TGC TCC TTC CGC TTT ACA CTT TGG GTC TTA GAT GAT GGG CAG TAT TTA GCG AAC GTA TTA TGG TTG GAG GGG CCT TTA TTG CAG AAT GAA CAC AAT CAG CAG AGG TAC AAA GAT GAG AAA ACA CCT CGC TAT TTG GGA ATA ATA TAT TTA CAA
Chrom 12 end	GTG AAA ACC TAT GTT ATA ACT AAG AAG ATT ACC TGT T-3'
40AA12	5'-GGA ATT CAC TTA GTA AAA AAT ACA CAT TTA ATA TAC TAC ATA ATC AAG TTG AGG ATC TAC ATA TTC AGC ATA ATA ATT AAA ATT CTC CAA ACA GTG CCC ACG
Chrom 1 end	TTT CAA ATG AAG TTA CAT ATC ACT ATC TTT TAA AGT AAG AAT GCA TCA TTG CAT TGC AGT AGA TCC ACG GAG AGG CAG GGA T-3'
YAC clone	Left end sequences
10ED1	5'-TTC TAT ATC ATT GAG TAA GAT AAA GAG CCA AGA GTC TGT ATT GAT AAA GAA TTG ATC TTT GTA TTT TCC TGA GGT TAC AAA AAT ATT CCA CAT TTT CTC CTA AAA
Chrom 12 end	CCT TTA AAC TTT TAC AAA TTA ATT AAA TCT TCC ATC CAC TTC AAA TTT GTG TTC TGT GTA TAA TAT GAA GTA AAG ATT GAG ATT CAT TGC GTC ATA TGT TAT TCA-3'
20BF12	5'-GAA TTC TTC CAG GAT AAA TGG CTG GGA TAC GTG GCA GGA GAA AGC AAT GCT CAC CCT ATT CCC GGA TGC ACT TCA TCA GAG CAA TTA TAG ACT GGT CTG TAT GTA
Chrom 12 end	GTC TCA CAG AAG AGC TTT GCT CAG AAG TCA TCT TAG TTA TTA ATT AGA CCA ATA AAA TTC TTG ATG GTC AAA TAG GT-3'
34HH10	5'-AAG CAT TTC CAT GAC TCA CAG AGT CCC CAA GGA ATA GAG TAC AAC TAG GAG ATG AGT CGT GGC ATG GAA GGA AAA GTC AA-3'
Chrom 12 end	
40AA12	5'-GTT GGT TTA AGG GGC AAG ACT TTA ATT TAT CAC TAC GGA ATT CAT TTT ATA AGT GAA ATC TGA TCC ACA AAT TTT AAC ACT ATA TTC AGC AAA TGA TAA ACA
Chrom 12 end	TAT TTT GCA GC-3'

region from *D12S87* to D12S106, a region at that stage thought to be of around 35 cM. The reported order of markers was cen–D12S87–D12S85–D12S96–D12S103–D12S90–D12S104–D12S83–D12S102–D12S80–D12S92–D12S106–tel. It was not clear at that time how these two different sets of markers overlapped. This was established to some extent in the report of the 2nd International Workshop on Human Chromosome 12 Mapping (Kucherlapati et al. 1994).

The 1993/94 Genethon human genetic linkage map (Gyapay et al. 1994) described 28 genetic markers over an expanded 45 cM region flanked by *D12S87* and *D12S106*. This map was integrated with that of Weissenbach and coworkers (1992). Most recently, a second-generation YAC contig map of human Chr 12 has been produced (Krauter et al. 1995). This represents an almost complete physical map of the region 12cen–12q15 and resolves many of the conflicts concerning accurate ordering of genetic markers. Indeed, the contig map places *D12S87*, previously viewed as a 12q11 marker, on the short arm with *D12S333* even more distal on 12p11. The marker *D12S331* is now positioned at 55 cM just below the centromere on the q arm. However, this latest map still contains five gaps in the region we have been investigating and does not include many first-generation genetic markers, some of which can now be placed on the map.

While the second-generation YAC contig map of the 12q13 region can now be considered as definitive, comparison of the data therein with previous genetic maps and the results described in this paper allows us to draw some useful additional conclusions. Working from centromere to qter, there is an EST (ATP5B) mapping in the 12q11-12 region (Kucherlapati et al. 1994) that is not included in the YAC contig map. This presumably lies between the centromere (54 cM) and the LALBA/*D12S120*/COL2A1/VDR/*D12S85* locus, which is now well resolved on the physical map but was not clearly discriminated on the genetic map. It is therefore possible that ATP5B maps in the first gap in the current YAC contig at around 59 cM. The marker *D12S339*, which was included between *D12S85* and D12S361 (around the 64 cM mark) in the 1993/94 Genethon map, is not included in the 1995 YAC contig map. We have now shown that *D12S339* is closely linked physically to WNT1. It seems probable that these two markers map in the sec-

ond contig gap around 64 cM on proximal 12q. The 1994 Chromosome 12 Workshop map links WNT1 with *D12S131*, *D12S6*, *D12S17*, and *D12S71* (Kucherlapati et al. 1994). Our data contradict these results in that we have demonstrated tight physical linkage between *D12S17* and *D12S96*, the latter now mapping more distally at 71 cM in the middle of the keratin gene cluster. Nevertheless, it would be worth while to screen YAC libraries with *D12S6*, *D12S71* (*D12S131* is reported herein), because it is conceivable that these may also lie in the 64 cM 12q YAC contig gap. The data of Schoenmakers and associates are also valuable in this regard. They localized a series of first-generation Chr 12 markers to the region between COL2A1 and *D12S17*. Their approximate locus order was cen–ELA1–*D12S29*–*D12S15*–*D12S25*–*D12S14*–*D12S4*–*D12S18*–*D12S16*–*D12S17*–tel. They also mapped *D12S6* distal to *D12S17*, which by our data would also place it distal to *D12S96*. Thus, the two genetic maps are somewhat at variance. However, ELA1, *D12S29*, *D12S15*, *D12S25*, *D12S14*, *D12S4*, *D12S18*, and *D12S16* would be potential markers to use to identify YACs in an attempt to fill the second YAC contig gap at 64 cM.

Our physical linkage of *D12S17* and *D12S96*, plus the 1995 localization of *D12S19* at 71 cM (Krauter et al. 1995), would suggest (by comparison of the 1992 NIH/CEPH map with the data of Schoenmakers et al.), that *D12S6*, *D12S28*, and *D12S22* map between *D12S96* and *D12S19*. This can now be easily confirmed because the YAC contig is complete between these points. Again, the 1992 NIH/CEPH map and Schoenmakers and colleagues (1994) have previously placed the markers *D12S43*, *D12S8*, *D12S64*, and *D12S7* distal to *D12S19*. The 1994 workshop report (Kucherlapati et al. 1994) linked *D12S8*, *D12S43*, and LYZ with *D12S80*, which is now positioned on the YAC contig at 87 cM. This is immediately telomeric of a fourth gap in the YAC contig at 85 cM. *D12S8*, *D12S43*, and LYZ are useful markers to screen YAC libraries in an attempt to bridge the 85 cM contig gap between RAP1B and *D12S80*. Furthermore, the 1994 workshop report (Kucherlapati et al. 1994) links the IFN-γ and RAP1B loci with *D12S56*. Again, *D12S56* may be useful in filling the gap in this region. Moreover, Bureau and coworkers (1995) have mapped the MDM2 gene in close linkage to IFN-γ, but the MDM2 gene is not included on the 1995 contig. It is, therefore, also possible that MDM2 lies in the same contig gap. In support of this, the MDM2 YACs differ from our *D12S313* YAC immediately proximal to IFN-γ. This suggests that MDM2 may be distal to IFN-γ. While two of the YACs described herein for MDM2 are highly chimeric (6FD11 and 40AA12), the YACs 40CB5 (Fig. 2) and 26DC3 (Heighway et al. 1994) have been localized by FISH analysis to 12q14.3-q15 and may be useful in bridging the contig gap. This cytogenetic localization is in agreement with the reported localization of IFN-γ (Bureau et al. 1995) and with the mapping of the slightly distal markers *D12S213* and *D12S115* to 12q14-q15 by Fejzo and associates (1995). It is interesting that the previously noted co-amplification of the GLI, CDK4 and MDM2 genes in human sarcomas (Khatib et al. 1993) is entirely consistent with the genetic map of this region. The YACs for *D12S350* and *D12S326* may prove useful in bridging a fifth gap, which they flank at 91 cM in the current contig map.

D12S64 may be some way distal to the *D12S8*/*D12S43*/*D12S80* locus at 12q14-q15, and in fact *D12S7* maps at 103 cM, considerably distal to the *D12S106* marker at 98 cM which we have taken as the boundary of our area of investigation. Similarly, *D12S58*, for which three YACs are described herein, now maps at 113 cM, beyond the 12q15 region. At the centromeric end of the region, *D12S59* and *D12S345*, both map adjacent to the centromere on the short arm of Chr 12 (Kucherlapati et al. 1994; Krauter et al. 1995). Our *D12S87* YACs also map on the p arm, as do our most distal YACs for *D12S333*(12p11).

Of the ESTs that have been used in this study to generate YAC clones, LALBA, COL2A1, GADD153, and GLI are already positioned on the 1995 YAC contig map at around 60, 61, 77, and 77 cM respectively. The IGF1 gene, for which we have identified a number of YACs, maps distal to *D12S106* at around 118 cM. These YACs are therefore included in Table 1 only for archival purposes. Of the ESTs for which we have isolated YACs that are not yet positioned on the 1995 YAC contig map, the WNT1 clones promise to be of value in that they map with *D12S339* in a current contig gap at 64 cM. Similarly, our MDM2 YAC clones may map in the current YAC contig gap at 85 cM. At present, the precise positions of PMCA, CD63, and PAB1 on the physical map remain to be confirmed. Finally, we have isolated YACs for the LRP/A2MR gene (Paulien et al. 1992), which has been physically mapped 300 kb from GLI (Forus and Myklebost 1992). These may be useful in closing a third YAC contig gap in this region between *D12S312* and GADD153 at 76 cM, as indeed may the *D12S312* and GADD153/GLI YACs described herein. The availability of a wide range of YAC reagents from the 12cen-12q15 region will without question facilitate gene cloning exercises in this area of the genome and should allow us to resolve some of the outstanding

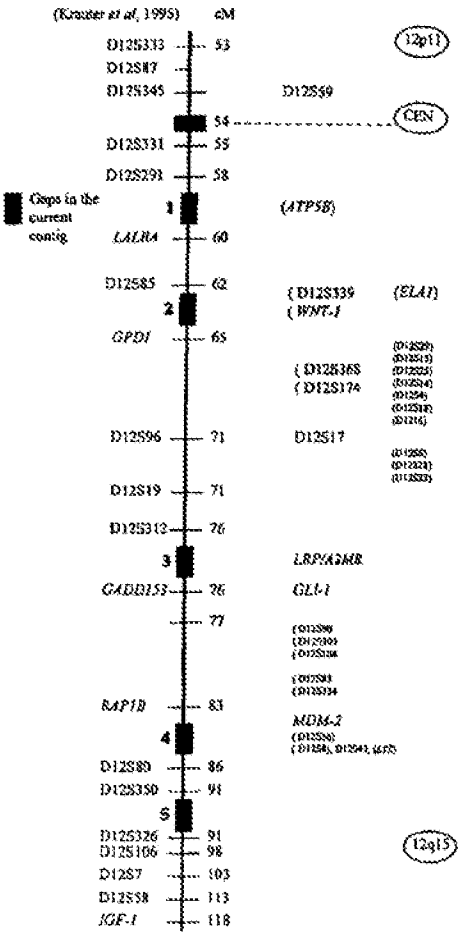

Fig. 1. Schematic 12p11-12q15 genetic map highlighting gaps in the current YAC contig and the positioning of additional markers for some of which new YACs are described herein. The ICI YAC library (Anand et al. 1990) was screened by the polymerase chain reaction (PCR) with available genetic markers from the region. Standard PCRs contained 100 ng pooled YAC DNA solution, 30 pmol of each primer, 1.0 × Taq buffer (Promega), 0.2 mM dNTPs (Promega), 2u *Taq* DNA polymerase (Promega), and 1.5 mM $MgCl_2$ except in specific cases shown in Table 1 where higher $MgCl_2$ concentrations were necessary. All PCRs were carried out with a Techne PHC-3 thermal cycler. The denaturing step was 5 min/95°C for purified DNA; 10 min/95°C for whole yeast cells; followed by 38 cycles of 30 s/95°C, 30 s/primer Tm and 1 min/72°C, with a final elongation step of 10 min/72°C.

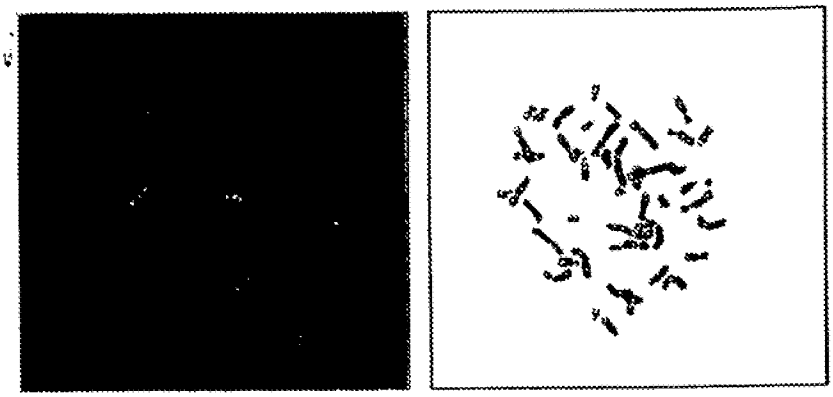

Fig. 2. Fluorescent in situ hybridization analysis of the MDM2 YAC 40CB5 confirming localization of this gene to 12q14-15.

questions concerning the frequent translocations encountered in the region in a variety of malignancies.

Acknowledgments. Research in the authors' laboratories is supported by the Medical Research Council, the Wellcome Trust, the Yorkshire Cancer Research Campaign and the West Riding Medical Research Trust. We thank the Candlelighters for additional provision of specific research support for this project, J.P. Leek for FISH analysis, C.A. Higgins for manuscript preparation and Zeneca plc for library access.

References

Anand, R., Riley, J.H., Butler, R., Smith, J.C., Markham, A.F. (1990). A 3.5 genome equivalent multi-access YAC library: construction, characterisation, screening and storage. Nucleic Acids Res., 18, 1951–1956.

Bureau, J.F., Bibl, F., Brahic, M., Le Paslier, D. (1995). The gene coding for interferon-γ is linked to the D12S335 and D12S313 microsatellites and to the MDM2 gene. Genomics 28, 109

Fejzo, M.S., Yoon, S.J., Montgomery, K.T., Rein, M.S., Weremowicz, S., Krauter, K.S., Dorman, T.E., Fletcher, J.A., Mao, J., Muir, D.T., Kucherlapati, R.S., Morton, C.C. (1995). Identification of a YAC spanning the translocation breakpoints in uterine leiomyomata, pulmonary chondroid hamartoma, and Lipoma: physical mapping of the 12q14-q15 breakpoint region in uterine leiomyomata. Genomics, 26, 265–271.

Forus, A., Myklebost, O. (1992). A physical map of a 1.3-Mb region on the long arm of chromosome 12, spanning the GLI and LRP loci. Genomics, 14, 117–120.

Guyer, M., Cann, H. (1992). A comprehensive genetic linkage map of the human genome: NIH/CEPH Collaborative Mapping Group. Science (reprint) pp 3–66.

Gyapay, G., Morissette, J., Vignal, A., Dib, C., Fizames, C., Millasseau, P., Marc, S., Bernadi, G., Lathrop, M., Weissenbach, J. (1994). The 1993–94 Genethon human genetic linkage map. Nature Genet. 7, 246–339.

Heighway, J., Mitchell, E.L.D., Jones, D., White, G.R.M., Santibanez Koref, M.F. (1994). A transcribed polymorphism and sub-localisation of MDM2. Hum. Genet., 93, 611–612.

Khatib, Z.A., Matsushime, H., Valentine, M., Shapiro, D.N., Sherr, C.J., Look, A.T. (1993). Coamplification of the *CDK4* gene with *MDM2* and *GLI* in human sarcomas. Cancer Res., 53, 5535–5541.

Krauter, K., Montgomery, K., Yoon, S.J., LeBlanc-Straceski, J., Renault, B., Marondel, I., Herdman, V., Cupelli, L., Banks, A., Lieman, J., Menninger, J., Bray-Ward, P., Nadkarni, P., Weissenbach, J., LePaslier, D., Rigault, P., Chumakov, I., Cohen, D., Miller, P., Ward, D., Kucherlapati, R. (1995). A second-generation YAC contig map of human chromosome 12. Nature, 377, S321–S333.

Kucherlapati, R., Craig, I., Marynen, P. (1994). Report of the second international workshop on human chromosome 12 mapping 1994. Cytogenet. Cell Genet. 67, 245–276.

Nusse, R., Brown, A., Papkoff, J., Scambler, P., Shackleford, G., McMahon, A., Moon, R., Varmus, H. (1991). A new nomenclature for int-1 and related genes: the Wnt gene family. Cell, 64, 231–232.

Paulien, S., Sandberg, A.A., Herz, J., Gemmill, R.M. (1992). Putative apolipoprotein receptor gene (LRP, A2MR) is not rearranged in either myxoid liposarcoma or lipomas with translocations in 12q13-14. Cancer Gent. Cytogenet., 60, 125–130.

Riley, J.H., Butler, R., Ogilvie, D., Finniear, R., Jenner, D.E., Powell, S., Anand, R., Smith, J.C., Markham, A.F. (1990). A novel, rapid method for the isolation of terminal sequences from yeast artificial chromosome (YAC) clones. Nucleic Acids Res., 18, 2887–2890.

Schoenmakers, E.F.P.M., Kools, P.F.J., Mols, R., Kazmierczak, B., Bartnitzke, S., Bullerdiek, J., Dal Cin, P., De Jong, P.J., Van Den Berghe, H., Van De Ven, W.J.M. (1994). Physical mapping of chromosome 12q breakpoints in lipoma, pleomorphic salivary gland adenoma, uterine leiomyoma and myxoid liposarcoma. Genomics, 20, 210–222.

Weissenbach, J., Gyapay, G., Dib, C., Vignal, A., Morissette, J., Millasseau, P., Vaysseix, G., Lathrop, M. (1992). A second-generation linkage map of the human genome. Nature 359, 794–801.

SHORT COMMUNICATION

The Gene Coding for Interferon-γ Is Linked to the D12S335 and D12S313 Microsatellites and to the MDM2 Gene

J. F. BUREAU,* F. BIHL,* M. BRAHIC,*,[1] AND D. LE PASLIER†

*Unité des Virus Lents, Institut Pasteur, URA CNRS 1157, 28 rue du Dr. Roux, 75724 Paris Cedex 15, France; and †Centre d'Etude du Polymorphisme Humain, 27 rue Juliette Dodu, 75010 Paris, France

Received March 13, 1995; accepted April 27, 1995

Interferon-γ is a cytokine with multiple effects. It interferes with the replication of several viruses and plays a key role in the regulation of immune responses. Therefore, the gene coding for interferon-γ could be implicated in the susceptibility of humans to several diseases. We have localized this gene close to the D12S335 and D12S313 microsatellites on both the physical and the genetic maps of the human genome. We also physically mapped this gene close to the MDM2 locus on chromosome band 12q15. Finally, we describe the organization of the *Ifg*, *Myf-6*, *Mdm1*, and *Mdm2* loci on mouse chromosome 10, in a region syntenic to human chromosome band 12q15.

Interferon-γ (IFNG) was discovered because of its antiviral property (12), although it is now studied chiefly because of its central role in the regulation of immune responses. This cytokine is secreted by $CD4^+$ T cells committed to the Th1 pathway, by $CD8^+$ T cells, and by activated macrophages. Because of these multiple functions, the gene coding for IFNG is a good candidate gene for control of susceptibility to various infectious as well as immune-mediated diseases of humans and other mammals. The persistent infection of the mouse central nervous system by Theiler's virus is a case in point. The *Ifg* gene is a good candidate for control of the persistence of the infection for two reasons: (i) Persistence is controlled by a gene that was mapped to the telomeric region of chromosome 10, close to the *Ifg* locus (5). (ii) Resistant 129Sv mice whose gene coding for the IFNG receptor has been inactivated become susceptible (8).

A precise localization of the human IFNG gene was not available until the present work. This gene had been localized to band 12q24 using FISH and by screening a panel of somatic hybrid cell lines (14, 19). Recently, Ruiz-Linares (17) described a microsatellite in the first intron of this gene, and Awata *et al.* (3) reported a difference in the allelic distribution of this marker between a group of patients with insulin-dependent diabetes mellitus and a control group. For future studies using the candidate gene approach, it would be extremely useful to locate precisely the IFNG gene in particular with respect to polymorphic microsatellites markers.

With this goal in mind, we screened the YAC library from CEPH (1) by PCR using two primers (forward 5′-GCTGTTATAATTATAGCTTGT-3′ and reverse 5′-AGGGTATTATTATACGAGCT-3′) derived from those described by Ruiz-Linares (17) for the IFNG microsatellite. PCR was performed using a kit from Amersham. After denaturation at 94°C for 2 min, 200 ng of DNA in 25 μl was submitted to 40 cycles of amplification (94°C, 40 s; 50°C, 40 s; 72°C, 15 s). Using this procedure, we isolated clone 825G7 of the YAC library. We found that clone 825G7 belonged to a contig of 25 other YAC clones, according to inter-*Alu* PCR patterns described in the CEPH–Généthon WWW server (6). All clones in this contig contained either both microsatellites D12S335 and D12S313 or one of the two. Each clone was tested for the presence of the IFNG microsatellite. Eleven clones contained the IFNG microsatellite. Ten also contained both the D12S335 and D12S313 microsatellites (YAC clones 745A10, 743E2, 751A4, 809H4, 823D1, 870H3, 924E4, 926A6, and 983H8), and one, YAC clone 763F1, contained only the D12S313 microsatellite. Therefore, these results demonstrate that the IFNG gene is physically linked to the D12S335 and D12S313 microsatellites.

To confirm the position of the IFNG locus on the genetic map, we analyzed the segregation of alleles of five microsatellite markers in the eight families that have been used to construct the Généthon map (10). Besides markers D12S335 and D12S313, we used two more microsatellites located on either side of the D12S335–D12S313 region. One was taken from a group of six cosegregating markers (D12S104, D12S305, D12S355, D12S334, D12S83, and D12S329) centromeric to the D12S335 marker and the other from a group of three cosegregating markers (D12S344, D12S80, and D12S92) telomeric to the D12S313 marker. For each family, a pair of markers was chosen according to its polymorphism within the family. The parental meiosis were not informative for

[1] To whom correspondence should be addressed. Fax: 33 (1) 40 61 31 67. E-mail: mbrahic@pasteur.fr.

GENOMICS 28, 109–112 (1995)
0888-7543/95 $12.00

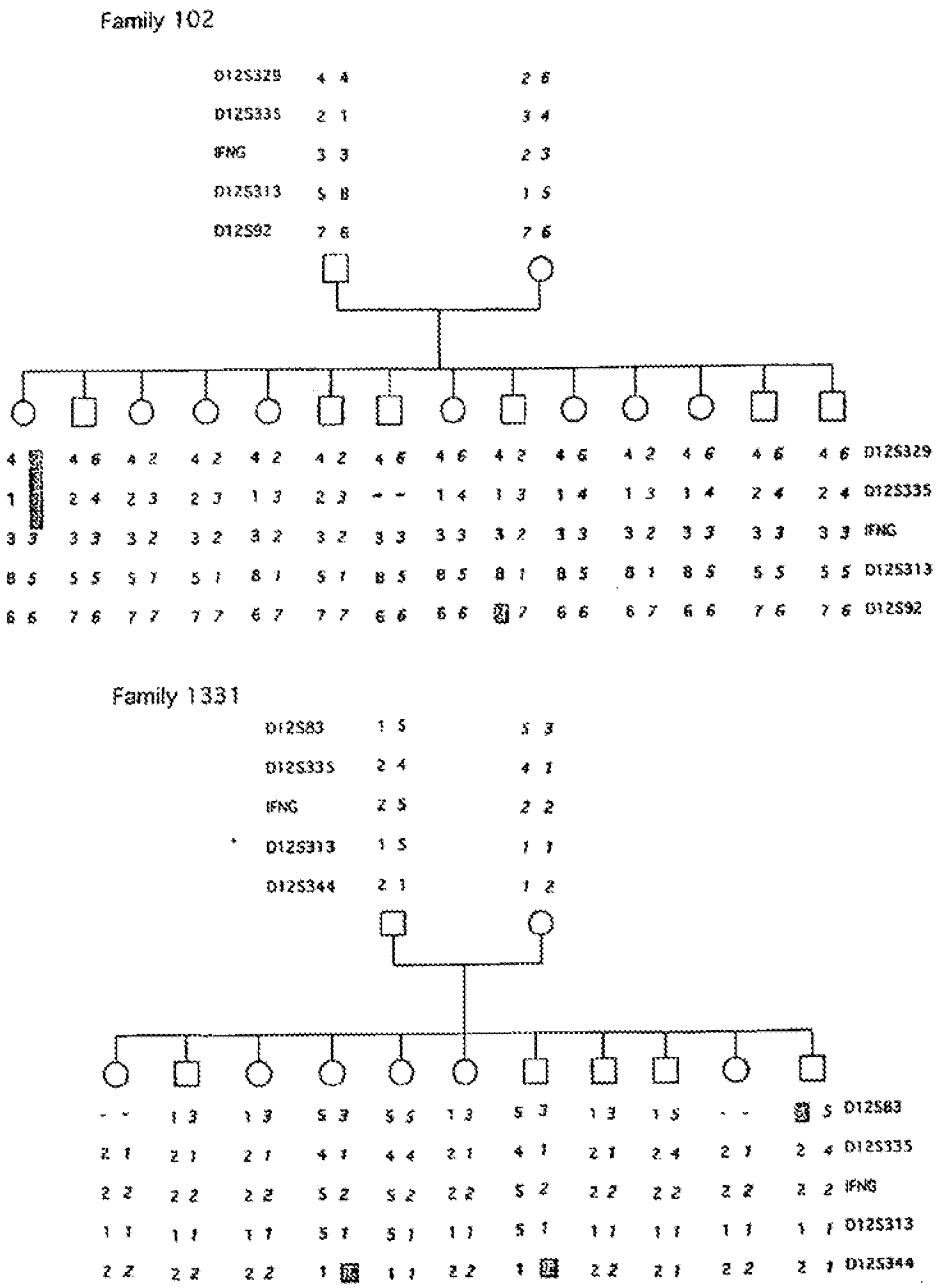

FIG. 1. Segregation of the alleles of IFNG and four microsatellite markers in two families. Maternal alleles are shown italicized. The genotypes of the microsatellites were obtained from the Généthon database. Dashes correspond to cases for which genotypes were not available. Stippled areas indicate a recombination event, and bold face identifies alleles from each parent. The alleles of IFNG are numbered according to the size of the amplified DNA, from the smaller to the larger fragment.

two families. The pedigrees of the other six were analyzed for the markers described above: IFNG, D12S335, D12S313, and the two flanking microsatellites. The results are presented in Fig. 1 for two families and summarized in Table 1. No recombination was observed between the D12S313 and the IFNG markers among 137 informative meioses. Only one recombination was observed between the D12S335 and the IFNG markers among 135 informative meioses. Analysis revealed that the flanking markers were indeed less linked to the IFNG locus than the D12S335 and D12S313 markers.

We next showed, by physical and genetic mapping, that the IFNG locus is linked to the D12S313 and D12S335 loci. Indeed, YAC clone 926A6 was recognized by these three markers. This YAC clone is chimeric and contains regions of both chromosome 12 (band

TABLE 1

Genetic Localization of IFNG

	No. crossing over with IFNG	No. of informative meioses
D12S329/D12S83	5 (3.9 cM)	129
D12S335	1 (0.8 cM)	135
D12S313	0 (0.0 cM)	137
D12S344/D12S92	6 (4.4 cM)	137

12q15) and chromosome 5, as shown by FISH (6, 9). Therefore, our results localize the IFNG locus to band 12q15, which is different from the previously published localization (band 12q24) (19). The region of human chromosome 12 to which we localize the IFNG gene is syntenic to a region of the mouse genome where we and others have previously localized the mouse *Ifg* gene (2, 5, 18). In our work, the positions of loci *Mdm1, Ifg,* and *Myf6* and of three microsatellites D10Mit10, D10Mit14, and D10Mit164 from the Whitehead Institute were determined using the progeny of a F1 (B10.S × SJL/J) × B10.S backcross (Fig. 2) (5). This backcross was typed for more than 100 loci that were distributed among all of the autosomal chromosomes. The results showed that the *Mdm1, Ifg,* and *Myf6* loci were linked to each other in the telomeric region of chromosome 10. Other authors have also reported that the *Mdm1, Mdm2, Mdm3,* and *Ifg* loci are closely linked (2, 18). Interestingly, the MDM2 locus has been localized by FISH to human chromosome 12q14.3–q15 (11). Thus, the analysis of the syntenic region of the mouse genome agrees with our localization of the IFNG locus to human chromosome 12q15.

We confirmed the physical linkage of the MDM2 and IFNG loci by screening, with the MDM2 PCR (11), the contig of YAC clones recognized by at least one of the D12S335, D12S313, and IFNG microsatellites. The MDM2 marker recognized three YAC clones (751A4, 870H3, and 983H8) that were also recognized by the D12S335, D12S313, and IFNG microsatellites. Thus, the MDM2 and IFNG loci are physically linked. The MDM2 gene, which codes for a p53-like protein, is located in a region associated with several cancers (15, 16). New polymorphic markers for this region are of particular interest since the only one available so far is a *Nla*IV polymorphic restriction site (11).

The *Myf6* locus is located in the region of mouse chromosome 10 syntenic to human chromosome band 12q15 (4). Therefore, we decided to localize the MYF-6 locus physically. We screened the CEPH YAC library using MYF-6-specific primers (forward 5′-AGACCTTCTCC-ACGCAGCAG-3′ and reverse 5′-GCGAAATCTGTTG-TGCAGCT-3′) under PCR conditions identical to those described above for the MDM2 marker. Two clones, 921C6 and 982A6, were isolated. We found that both belonged to a contig of nine other YAC clones, according to inter-*Alu* PCR patterns described in the CEPH–Généthon WWW server (6). Three of them, clones 940B8, 937D9, and 949H4, contained the MYF-6 marker. According to the CEPH–Généthon server, clones 940B8 and 937D9 contained the D12S106 microsatellite, a marker 15 cM from the D12S313 microsatellite, toward the telomere (10). Figure 3 shows the position of these various markers on human chromosome 12q15 and mouse chromosome 10. The organization of the syntenic regions is very similar. IFNG/D12S313 and D12S106 are 15 cM apart, whereas Ifg/Mdm1 and Myf6 are 5 cM apart. However, since 1 cM is, on average, equivalent to 1.7 Mb in the mouse and 1.0 Mb in human, the physical distances between the markers in mouse and in human could be of the same order.

In conclusion, we have shown that the IFNG and the MDM2 genes are close to each other and to the D12S335 and D12S313 microsatellites. These markers are most likely localized to chromosome bands 12q14.3–q15, in a region syntenic to the telomeric part

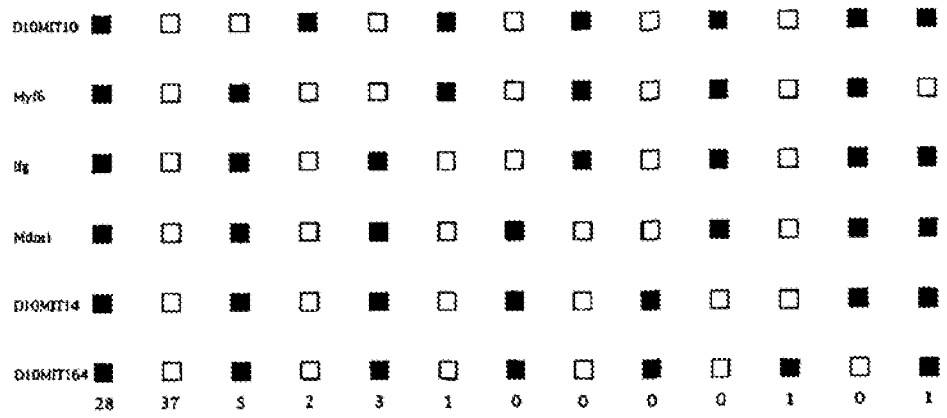

FIG. 2. Segregation of the alleles of *Ifg, Mdm1, Myf6,* and some markers published by the Whitehead Institute (7) in 78 F1 (SJL/J × B10.S) × B10.S mice. The *Ifg* and *Mdm1* markers were described in Bureau *et al.* (5). A microsatellite was found in the second intron of *Myf6* and used to design two PCR primers (forward 5′-GAAAGGGCACTGGGCTGTAC-3′ and reverse 5′-CGCCGGATTTGGCTGTTGCT-3′) (13). Black squares represent homozygous mice; white squares represent heterozygous mice. Numbers under each column represent the number of mice with each genotype.

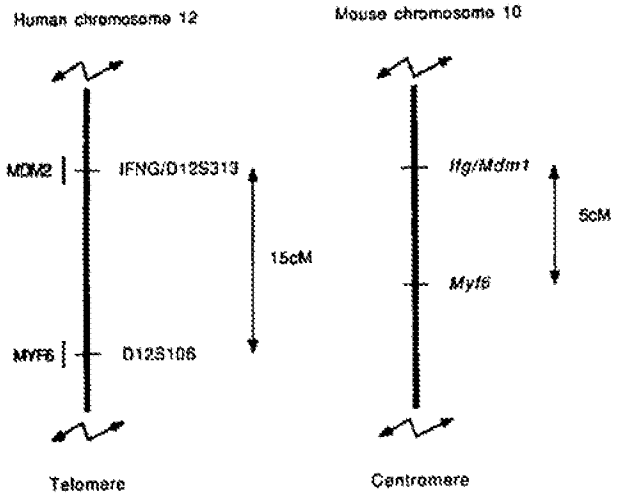

FIG. 3. Genetic maps of the syntenic regions of human chromosome 12q15 and mouse chromosome 10. The MDM2 and MYF6 genes were localized by physical mapping only. The other human genes and markers were localized by both physical and genetic mapping.

of mouse chromosome 10. This information will be extremely useful in human genetic studies in which the IFNG and MDM2 genes will be candidate genes.

ACKNOWLEDGMENTS

We thank C. Dib and J. Weissenbach for their help; C. Petit for helpful discussion; and M. Gau for preparing the manuscript. This work was supported by grants from the Institut Pasteur Fondation, the ARSEP, the CNRS, the GREG, and the NMSS.

REFERENCES

1. Albertsen, H. M., Abderrahim, H., Cann, H. M., Dausset, J., Le Paslier, D., and Cohen, D. (1990). Construction and characterization of a yeast artificial chromosome library containing seven haploid human genome equivalents. *Proc. Natl. Acad. Sci. USA* **87:** 4256–4260.
2. Ashar, H. R., Benson, K. F., Jenkins, N. A., Gilbert, D. J., Copeland, N. G., and Chada, K. K. (1994). Ifg, Gli, Mdm1, Mdm2, and Mdm3: Candidate genes for the mouse pg locus. *Mamm. Genome* **5:** 608–611.
3. Awata, T., Matsumoto, C., Urakami, T., Hagura, R., Amemiya, S., and Kanazawa, Y. (1994). Association of polymorphism in the interferon gamma gene with IDDM. *Diabetologia* **37:** 1159–1162.
4. Braun, T., Bober, E., Winter, B., Rosenthal, N., and Arnold, H. H. (1990). Myf-6, a new member of the human gene family of myogenic determination factors: Evidence for a gene cluster on chromosome 12. *EMBO J.* **9:** 821–831.
5. Bureau, J. F., Montagutelli, X., Bihl, F., Lefebvre, S., Guénet, J. L., and Brahic, M. (1993). Mapping loci influencing the persistence of Theiler's virus in the murine central nervous system. *Nature Genet.* **5:** 87–91.
6. Cohen, D., Chumakov, I., and Weissenbach, J. (1993). A first-generation physical map of the human genome. *Nature* **366:** 698–701.
7. Dietrich, W. F., Miller, J. C., Steen, R. G., Merchant, M., Damron, D., Nahf, R., Gross, A., Joyce, D. C., Wessel, M., Dredge, R. D., Marquis, A., Stein, L. D., Goodman, N., Page, D. C., and Lander, E. S. (1994). A genetic map of the mouse with 4006 simple sequence length polymorphisms. *Nature Genet.* **7:** 220–225.
8. Fiette, L., Aubert, C., Müller, U., Huang, S., Aguet, M., and Brahic, M. (1995). Theiler's virus infection of 129Sv mice that lack the interferon alpha/beta or interferon gamma receptors. *J. Exp. Med.* **181.**
9. Francke, U. (1994). Digitized and differentially shaded human chromosome ideograms for genomic applications. *Cytogenet. Cell Genet.* **65:** 206–219.
10. Gyapay, G., Morissette, J., Vignal, A., Dib, C., Fizames, C., Millasseau, P., Marc, S., Bernardi, G., Lathrop, M., and Weissenbach, J. (1994). The 1993–94 Généthon human genetic linkage map. *Nature Genet.* **7:** 246–339.
11. Heighway, J., Mitchell, E. L. D., Jones, D., White, G. R. M., and Santibanez Koref, M. F. (1994). A transcribed polymorphism and sub-localisation of MDM2. *Hum. Genet.* **93:** 611–612.
12. Isaacs, A., Lindenmann, J., and Valentine, R. C. (1957). Virus interference. II. Some properties of interferon. *Proc. R. Soc. London B* **147:** 268–273.
13. Miner, J. H., and Wold, B. (1990). Herculin, a fourth member of the myoD family of muscle regulatory genes. *Proc. Natl. Acad. Sci. USA* **87:** 1089–1093.
14. Naylor, S. L., Sakaguchi, A. Y., Shows, T. B., Law, M. L., Goeddel, D. V., and Gray, P. W. (1983). Human immune interferon gene is located on chromosome 12. *J. Exp. Med.* **57:** 1020–1027.
15. Oliner, J. D., Kinzler, K. W., Meltzer, P. S., George, D. L., and Vogelstein, B. (1992). Amplification of a gene encoding a p53-associated protein in human sarcomas. *Nature* **358:** 80–83.
16. Reifenberger, G., Lui, L., Ichimura, K., Schmidt, E. E., and Collins, V. P. (1993). Amplification and overexpression of the MDM2 gene in a subset of human malignant gliomas without p53 mutations. *Cancer Res.* **533:** 2736–2739.
17. Ruiz-Linares, A. (1993). Dinucleotide repeat polymorphism in the interferon-gamma (IFNG) gene. *Hum. Mol. Genet.* **2:** 1508.
18. Taylor, B. A., Rowe, L., and Grieco, D. (1992). Close linkage of Mdm-1, a gene amplified and overexpressed in a transformed 3T3 cell line, with gamma interferon (Ifg) on Chromosome 10 of the mouse. *Mamm. Genome* **3:** 700–704.
19. Trent, J. M., Olson, S., and Lawn, R. M. (1982). Chromosomal localization of human leukocyte, fibroblast, and immune interferon genes by means of *in situ* hybridization. *Proc. Natl. Acad. Sci. USA* **79:** 7809–7813.

JR-10,003-US PATENT

IN THE UNITED STATES PATENT AND TRADEMARK OFFICE

In re Application of: Ryan

Serial No.: 10/608,463 Group Art Unit: 1652

Filed: June 27, 2003 Examiner: E. Slobodyansky

FOR: ISOLATED GENOMIC POLYNUCLEOTIDE FRAGMENTS FROM CHROMOSOME 12 THAT ENCODE HUMAN CARBOXYPEPTIDASE M AND THE HUMAN MOUSE DOUBLE MINUTE 2 HOMOLOG

Confirmation No.: 6428

INFORMATION DISCLOSURE STATEMENT

Commissioner for Patents
P.O. Box 1450
Alexandria, VA 22313-1450

Sir:

In accordance with 37 C.F.R. 1.56, 1.97 and 1.98, Applicants submit herewith references which they believe may be material to the patentability of this application and with respect to which there may be a duty to disclose in accordance with 37 C.F.R. 1.56.

While the references may be "material" under 37 C.F.R. 1.56, it is not intended to constitute an admission that the references are "prior art" unless specifically designated as such.

The filing of this Information Disclosure Statement shall not be construed as a representation that no other material references than those listed exist or that a search has been conducted.

The references are listed in PTO form 1449 which is in accordance with the requirements of M.P.E.P. 609. A copy of the references is also enclosed.

The references are as follows:

U.S. Patent Documents

Foreign Patent Documents

Other Documents

1. RIES et al., 2000, Cell 103:321-330
2. REHLI et al., 1995, J. Biol. Chem. 270:15644-9
3. OLINER et al., 1992, Nature 358: 80-3
4. TAN et al., 1989, J. Biol. Chem. 264: 13165-70

It is respectfully requested that these references be considered by the Patent and Trademark Office in its examination of the above-identified application and be made of record therein. The Examiner is also invited to contact the Undersigned if there are any questions concerning this paper or the attached references.

The Information Disclosure Statement submitted herewith is being filed

[] before the mailing date of a first Office Action on the merits

[x] after the mailing date of a first Office Action on the merits. Please charge the fee of $180 to credit card. Form PTO-2038 is attached.

[] An International Search Report is enclosed. References cited in the International Search report are asterisked.

Respectfully submitted,

Date: 3/1/05

Cheryl M. Agris, Reg. No. 34,086
P.O. Box 806
Pelham, N.Y. 10803
(914) 712-0093

PTO/SB/08A (04-03)
Approved for use through 04/30/2003. OMB 0651-0031
U.S. Patent and Trademark Office: U.S. DEPARTMENT OF COMMERCE

Substitute for form 1449/PTO

INFORMATION DISCLOSURE STATEMENT BY APPLICANT

(Use as many sheets as necessary)

Sheet 1 of 2

Complete if Known	
Application Number	10/608,463
Filing Date	June 27, 2003
First Named Inventor	Ryan
Art Unit	1652
Examiner Name	E. Slobodyansky
Attorney Docket Number	JR10003

U. S. PATENT DOCUMENTS

Examiner Initials*	Cite No.[1]	Document Number Number-Kind Code[2] (if known)	Publication Date MM-DD-YYYY	Name of Patentee or Applicant of Cited Document	Pages, Columns, Lines, Where Relevant Passages or Relevant Figures Appear
		US-			
		US-			
		US-			
		US-			
		US-			
		US-			
		US-			
		US-			
		US-			
		US-			
		US-			
		US-			
		US-			
		US-			
		US-			
		US-			
		US-			
		US-			
		US-			
		US-			

FOREIGN PATENT DOCUMENTS

Examiner Initials*	Cite No.[1]	Foreign Patent Document Country Code[3] Number[4] Kind Code[5] (if known)	Publication Date MM-DD-YYYY	Name of Patentee or Applicant of Cited Document	Pages, Columns, Lines, Where Relevant Passages Or Relevant Figures Appear	T[6]

Examiner Signature		Date Considered	

*EXAMINER: Initial if reference considered, whether or not citation is in conformance with MPEP 609. Draw line through citation if not in conformance and not considered. Include copy of this form with next communication to applicant. [1] Applicant's unique citation designation number (optional). [2] See Kinds Codes of USPTO Patent Documents at www.uspto.gov or MPEP 901.04. [3] Enter Office that issued the document, by the two-letter code (WIPO Standard ST.3). [4] For Japanese patent documents, the indication of the year of the reign of the Emperor must precede the serial number of the patent document. [5] Kind of document by the appropriate symbols as indicated on the document under WIPO Standard ST. 16 if possible. [6] Applicant is to place a check mark here if English language Translation is attached.

PTO/SB/08B (04-03)
Approved for use through 04/30/2003. OMB 0651-0031
U.S. Patent and Trademark Office; U.S. DEPARTMENT OF COMMERCE

Substitute for form 1449/PTO

INFORMATION DISCLOSURE STATEMENT BY APPLICANT

(Use as many sheets as necessary)

Sheet 2 of 2

	Complete if Known
Application Number	10/608,463
Filing Date	June 27, 2003
First Named Inventor	Ryan
Art Unit	1652
Examiner Name	E. Slobodyansky
Attorney Docket Number	JR10003

NON PATENT LITERATURE DOCUMENTS			
Examiner Initials*	Cite No.[1]	Include name of the author (in CAPITAL LETTERS), title of the article (when appropriate), title of the item (book, magazine, journal, serial, symposium, catalog, etc.), date, page(s), volume-issue number(s), publisher, city and/or country where published.	T[2]
		RIES et al., 2000, Cell 103: 321-330.	
		REHLI et al., 1995, J. Biol. Chem. 270: 15644-15649.	
		OLINER et al., 1992, Nature 358:80-83.	
		TAN et al., 1989, J. Biol. Chem. 264: 13165-13170.	

Examiner Signature		Date Considered	

*EXAMINER: Initial if reference considered, whether or not citation is in conformance with MPEP 609. Draw line through citation if not in conformance and not considered. Include copy of this form with next communication to applicant.

1 Applicant's unique citation designation number (optional). 2 Applicant is to place a check mark here if English language Translation is attached.

Amplification of a gene encoding a p53-associated protein in human sarcomas

J. D. Oliner*, K. W. Kinzler*†, P. S. Meltzer‡, D. L. George§ & B. Vogelstein*

* The Johns Hopkins Oncology Center, 424 North Bond Street, Baltimore, Maryland 21231, USA
‡ Departments of Pediatrics and Radiation Oncology, University of Michigan Cancer Center, MSRB 11 C5608, 1150 West Medical Center Drive, Ann Arbor, Michigan 48109, USA
§ Department of Human Genetics, University of Pennsylvania, Clinical Research Building, Philadelphia, Pennsylvania 19104, USA

DESPITE extensive data linking mutations in the p53 gene to human tumorigenesis[1], little is known about the cellular regulators and mediators of p53 function. MDM2 is a strong candidate for one such cellular protein; the *MDM2* gene was originally identified by virtue of its amplification in a spontaneously transformed derivative of mouse BALB/c cells[2] and the MDM2 protein subsequently shown to bind to p53 in rat cells transfected with p53 genes[3,4]. To determine whether MDM2 plays a role in human cancer, we have cloned the human *MDM2* gene. Here we show that recombinant-derived human MDM2 protein binds human p53 *in vitro*, and we use *MDM2* clones to localize the human *MDM2* gene to chromosome 12q13–14. Because this chromosomal position appears to be altered in many sarcomas[5–7], we looked for changes in human *MDM2* in such cancers. The gene was amplified in over a third of 47 sarcomas, including common bone and soft tissue forms. These results are consistent with the hypothesis that MDM2 binds to p53, and that amplification of *MDM2* in sarcomas leads to escape from p53-regulated growth control. This mechanism of tumorigenesis parallels that for virally-induced tumours[8,9], in which viral oncogene products bind to and functionally inactivate p53.

To obtain human complementary DNA clones, a murine *MDM2* cDNA probe was used to initiate cDNA walking in a human library (see legend to Fig. 1). Sequence analysis of 25 clones revealed several cDNA forms indicative of alternative splicing. The predominant human form is compared with its murine counterpart in Fig. 1. There was an open reading frame extending from the 5' end of the human cDNA sequence to nucleotide 1,784. Although this signal for translation initiation could not be unambiguously defined, the ATG at nucleotide 312 was considered the most likely position for several reasons. First, the sequence similarity between human and mouse *MDM2* declined dramatically upstream of nucleotide 312. Second, an inverse polymerase chain reaction (PCR) was used in an attempt to acquire additional upstream cDNA sequence[10]. The 5' ends of the PCR-derived clones were very similar (within 12 base pairs) to the 5' ends of clones obtained from the cDNA library, indicating that the 5' end of the human *MDM2* sequence shown in Fig. 1 may represent the 5' end of the transcript. Third, *in vitro* translation of the sequence shown in Fig. 1, beginning with the methionine encoded by the ATG at position 312, generated a protein similar in size to that observed in human cells (see below).

Comparison of the human and mouse *MDM2* coding regions showed that they were 80.3% identical and shared a basic nuclear localization signal at codons 181 to 185 (ref. 11), several casein kinase II serine-phosphorylation sites[12], an acidic activation domain at codons 223 to 274 (ref. 13), and two metal-binding sites at codons 305 to 322 and 461 to 478, neither of which is highly related to known DNA-binding domains[14].

To determine whether the human MDM2 protein could bind to human p53 protein *in vitro*, a human *MDM2* expression vector was constructed from the cDNA clones (see legend to Fig. 2). RNA transcribed from this vector using T7 RNA polymerase was used to program a rabbit reticulocyte lysate. Although the predicted size of the protein generated from the construct was only 55.2K (M_r 55,200, extending from the methionine at nucleotide 312 to nucleotide 1,784), protein translated *in vitro* migrated at ~90 K. The MDM2 protein was not immunoprecipitated with antibodies against either the C-terminal or N-terminal regions of p53 (Fig. 2, lanes 2 and 3). But when *in vitro*-translated human p53 was mixed with the human *MDM2* translation product, the anti-p53 antibodies precipitated MDM2 protein with p53 (Fig. 2, lanes 5 and 6). As a control, a protein of similar electrophoretic mobility (MCC[15]) was mixed with p53 and there was no coprecipitation (Fig. 2, lanes 8 and 9). When an *in vitro*-translated His-175 mutant form of p53 was mixed with human MDM2 protein, a similar coprecipitation of MDM2 and p53 proteins was also observed (data not shown).

Polyclonal rabbit antibodies were raised against an *Escherichia coli*-produced human MDM2-glutathione S-transferase fusion protein. The anti-MDM2 antibodies immunoprecipitated p53 when mixed with MDM2 protein (Fig. 2, lane 15) but failed to precipitate p53 alone (Fig. 2, lane 13).

To establish the chromosomal localization of human *MDM2*, somatic cell hybrids were screened, and a human–hamster hybrid containing only human chromosome 12 hybridized to the human *MDM2* probe. Screening of hybrids containing portions of chromosome 12 (ref. 16) with the same probe narrowed the localization to chromosome 12q13–14. Because this region of chromosome 12 is often aberrant in human sarcomas[5–7], southern blot analysis to evaluate whether *MDM2* was genetically altered in such cancers. We found a striking amplification of *MDM2* sequences in several of these tumours (see examples in Fig. 3, lanes 2, 3 and 5). Of 47 sarcomas analysed, 17 showed a 5–50-fold *MDM2* amplification. These tumours included 7 of 13 liposarcomas, 7 of 22 malignant fibrous histiocytomas, 3 of 11 osteosarcomas, and 0 of 1 rhabdomyosarcoma. Five benign soft tissue tumours (lipomas) and seventy-four carcinomas (colorectal or gastric) were also analysed by Southern blotting and no amplification was seen.

We next determined whether this gene amplification was associated with increased expression. Because of RNA degradation in primary sarcomas, only the cell lines could be productively analysed by northern blotting. In the one available sarcoma cell line with *MDM2* amplification, a single transcript of ~5.5 kilobases (kb) was observed (Fig. 4*a*, lane 1). The amount of this transcript was much higher than in a sarcoma cell line without amplification (Fig. 4*a*, lane 2) or in a carcinoma cell line (Fig. 4*a*, lane 3). When purified messenger RNA (rather than total RNA) from the carcinoma cell line was used for analysis, a human *MDM2* transcript of 5.5 kb could also be observed (Fig. 4*a*, lane 4). Expression of the *MDM2* RNA in the sarcoma with amplification was estimated to be at least 30-fold higher than that in the other lines examined. This was consistent with results from western blot analysis. A protein of M, ~90K was expressed at high levels in the sarcoma cell line with *MDM2* amplification (Fig. 4*b*, lane 3), whereas no expression was evident in two sarcoma cell lines without amplification or in the carcinoma cell line (Fig. 4*b*, lanes 1, 2 and 4). Five primary sarcomas were also analysed by western blotting. Three primary sarcomas with amplification expressed the same sized protein as that in the sarcoma cell line (Fig. 4*c*, lanes 1–3), but no protein was observed in the two sarcomas without amplification (Fig. 4*c*, lanes 4 and 5).

Our results demonstrate that human MDM2 binds to p53 *in vitro* and is genetically altered in a significant fraction of the most common sarcomas of soft tissue and bone[17,18]. It is important to note, however, that amplifications in human tumours

† To whom correspondence should be addressed.

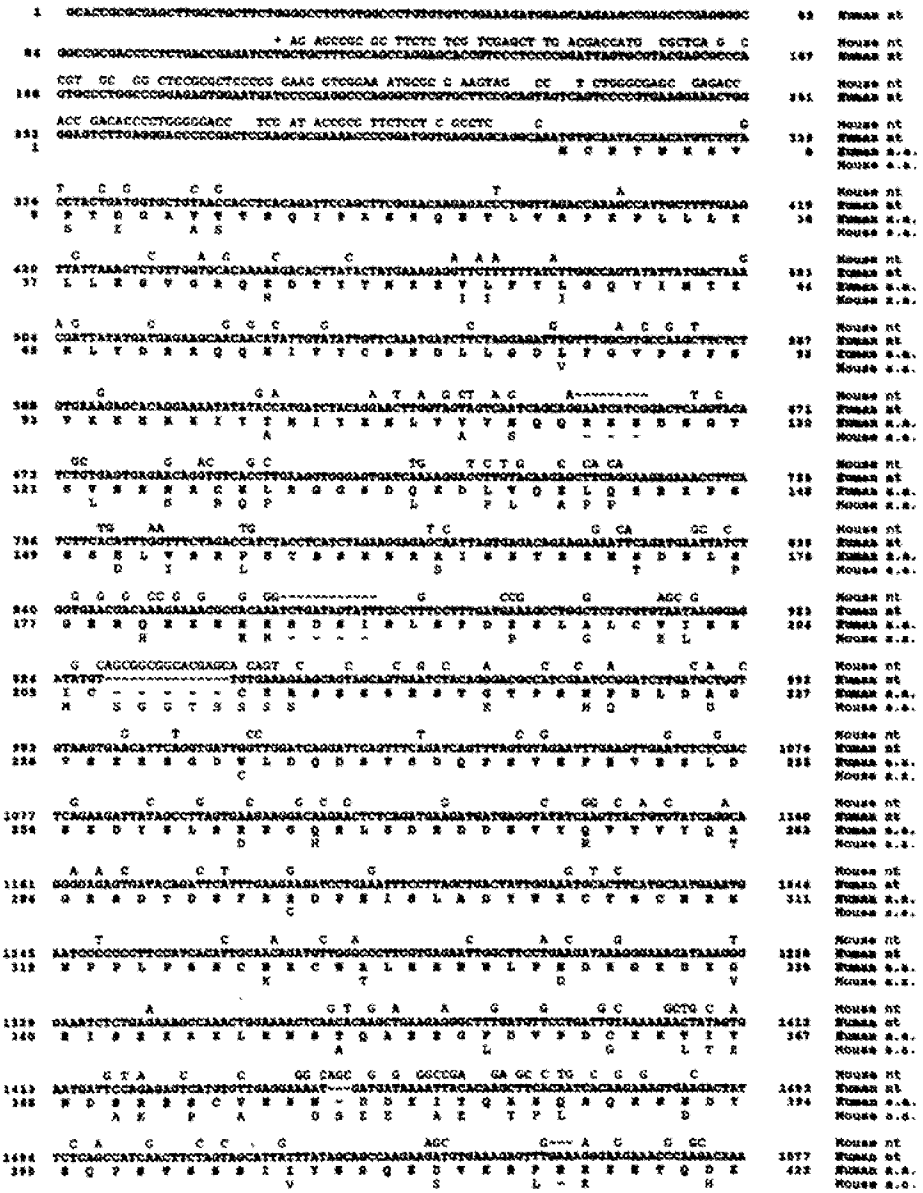

FIG. 1 Human *MDM2* cDNA sequence: human and mouse *MDM2* nucleotide (nt) and amino-acid (a.a.) sequences are compared (single-letter code). The mouse sequence is only shown where it differs from the corresponding human sequence. Asterisks mark the 5′ and 3′ boundaries of the previously published mouse *MDM2* cDNA[2]. Dashes indicate insertions.

METHODS. Polyadenylated RNA isolated from the human colonic carcinoma cell line CaCo-2 was used as a template for the production of random hexamer-primed double-stranded cDNA[22]. The cDNA was ligated to adaptors and then to the lambda YES phage vector, packaged and plated as described[23]. The library was screened initially with a ^{32}P-labelled [24] mouse *MDM2* cDNA probe (nt 259 to 1,508; ref. 2) and then rescreened with a human *MDM2* cDNA clone containing nt 40 to 702. In total, 25 clones were obtained, partially or totally sequenced, and mapped. The sequence shown is representative of the most abundant class and was assembled from three clones: c14~2 (nt 1~949), c89 (nt 467~1,737), and c33 (nt 390~2,372). The 3′ end of the untranslated region has not yet been cloned. The 5′ end is likely to be at or near nt 1 (see text). The mouse and human amino-acid sequences are compared from the putative translation start site at nt 312 to the conserved stop codon at nt 1,784. This nucleotide sequence has been deposited at the EMBL Data Library, accession number Z12020.

often involve large stretches of the genome, encompassing 300 to 1,000 kb[7,19-21]. Other genes in the *MDM2* amplicon could contribute to, or be responsible for, the growth advantage afforded by the amplification event. Nevertheless, MDM2 is a good candidate for the 'target' of amplification for two reasons. First, MDM2 has oncogenic activity after transfection into NIH3T3 cells[2]. Second, it binds to a protein (p53) with known growth suppressive effects on a wide variety of human tumour types. MDM2 may functionally inactivate p53 in ways similar to those employed by virally encoded oncoproteins such as simian virus 40 T antigen, adenovirus E1B and human papilloma virus E6 (refs. 4, 8, 9). Consistent with this hypothesis, no sarcomas with *MDM2* amplification (of five tested) had any of the p53 gene mutations that occur commonly in other tumours

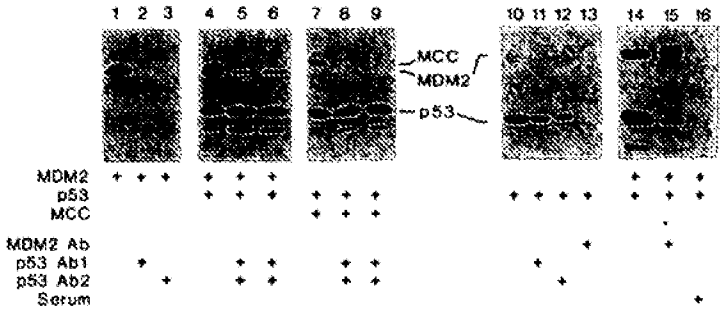

FIG. 2 Coprecipitation of human MDM2 and p53. *In vitro*-translated MDM2, p53 and MCC proteins were mixed as indicated and incubated with p53 Ab1 (monoclonal antibody specific for the C terminus of p53), p53 Ab2 (monoclonal antibody specific for the N terminus of p53), MDM2 Ab (polyclonal rabbit anti-human MDM2 antibodies), or serum (preimmune serum obtained from the rabbit that produced the MDM2 antibody). Lanes 1, 4, 7, 10 and 14 contain aliquots of the protein mixtures used for immunoprecipitation. Bands running slightly faster than p53 are polypeptides produced from internal translation initiation sites.

METHODS. A human *MDM2* expression vector was constructed in pBluescript SK+(Stratagene) from overlapping cDNA clones. The construct contained the sequence shown in Fig. 1 from nt 312 to 2,176. A 42-bp black beetle virus ribosome entry sequence[25] was placed immediately upstream of this *MDM2* sequence in order to obtain high expression. This construct, as well as p53 (ref. 26) and *MCC*[15] constructs in pBluescript SK+, were transcribed with T7 RNA polymerase and translated in a rabbit reticulocyte lysate (Promega) according to the manufacturer's instructions. Lysate (10 μl) containing the three proteins, alone or mixed in pairs, was incubated at 37 °C for 15 min. 1 μg (10 μl) of p53 Ab1 or Ab2 (Oncogene Science) or 5 μl of rabbit serum containing MDM2 antibody or preimmune rabbit serum, were added as indicated. 90 μl RIPA buffer (10 mM Tris, pH 7.5, 1% sodium deoxycholate, 1% NP40, 150 mM NaCl, 0.1% SDS), SNNTE buffer[3], or binding buffer[28] were then added and the mixtures allowed to incubate at 4 °C for 2 h. The three buffers produced similar results, although the coprecipitation was less efficient in SNNTE buffer (containing 0.5 M NaCl; lanes 5 and 8) than in binding buffer (containing 0.1 M NaCl; lanes 6 and 9). Following addition of 2 mg protein A-Sepharose, the tubes were rotated end-over-end at 4 °C for 1 h. After pelleting and washing, immunoprecipitates were electrophoresed on SDS–polyacrylamide gels and the dried gels autoradiographed in the presence of Enhance (New England Nuclear). Rabbits were immunized with a glutathione *S*-transferase (Pharmacia)–MDM2 fusion protein containing human MDM2 from the region corresponding to nt 390–816.

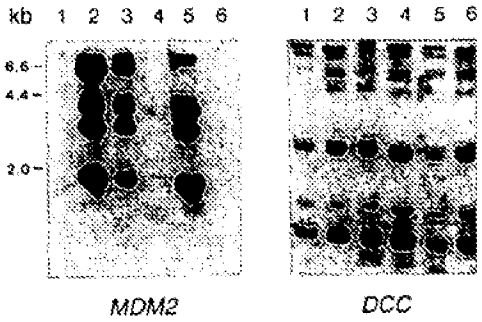

FIG. 3 Amplification of the human *MDM2* gene in sarcomas. DNA (5 μg) was digested with *EcoRI*, separated by agarose gel electrophoresis and transferred to nylon as described[27]. Filters were then hybridized with a human *MDM2* cDNA fragment probe (nt 1–949; Fig. 1) or to a control probe that identifies fragments of similar size (pDCC 1.65; ref. 28). Hybridization was as previously described[29]. DNA was derived from 5 primary sarcomas (lanes 1–4, 6) and one sarcoma cell line (OsA-CL, lane 5). On longer exposure, the same sized *MDM2* fragments were observed in lanes 1, 4 and 6. DNA fragment sizes are shown on the left in kb.

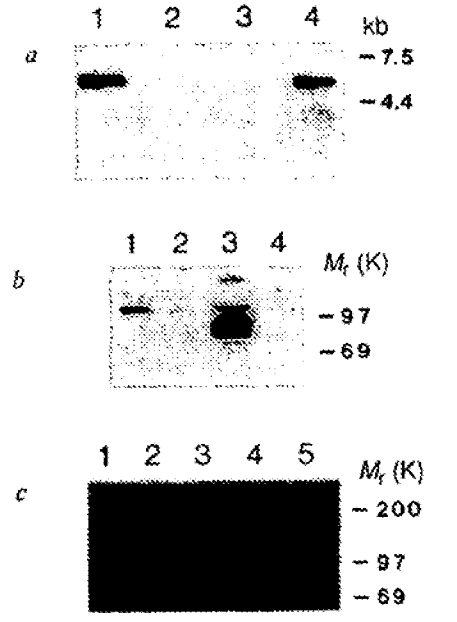

FIG. 4 *MDM2* expression. *a*, Northern blot analysis. RNA was separated by electrophoresis in a MOPS–formaldehyde gel and electrophoretically transferred to nylon filters. Transfer and hybridization were as described[30]. RNA was hybridized to the *MDM2* fragment described in Fig. 3 legend. Total RNA (10 μg) was derived, respectively, from two sarcoma cell lines (OsA-CL, lane 1 and RC13, lane 2) and the colorectal cancer cell line (CaCo-2) used to make the cDNA library (lane 3). Lane 4 contains 10 μg polyadenylated CaCo-2 RNA. RNA sizes are shown on the right in kb. *b*, Western blot analysis of the sarcoma cell lines RC13 (lane 1), OsA-CL (lane 3), HOS (lane 4), and the carcinoma cell line CaCo-2 (lane 2). *c*, Western blot analysis of primary sarcomas. Lanes 1 to 3 contain protein from sarcomas with *MDM2* amplifications, and lanes 4 and 5 contain protein from sarcomas without *MDM2* amplification. Western blots using affinity-purified MDM2 antibody were performed with 50 μg protein per lane as described [31], except that the membranes were blocked in 10% non-fat dried milk and 10% goat serum, and secondary antibodies were coupled to horseradish peroxidase to allow chemiluminescent detection (Amersham ECL). MDM2 antibody was affinity-purified with a pATH-MDM2 fusion protein using methods described in ref. 31. Nonspecific reactive proteins of 75, 105 and 170K are seen in all lanes, irrespective of *MDM2* amplification. MDM2 proteins, of M_r 90K, were observed only in the MDM2-amplified tumours. Protein marker sizes are shown on the right.

(unpublished results with T. Tokino and D. Sidransky). The amplification of *MDM2* provides another provocative parallel between viral carcinogenesis and the naturally occurring genetic alterations underlying sporadic human cancer. □

Received 28 March; accepted 5 May 1992.

1. Hollstein, M., Sidransky, D., Vogelstein, B. & Harris, C. C. *Science* **253**, 49–53 (1991).
2. Fakharzadeh, S., Trusko, R. S. & George, D. *EMBO J* **10**, 1565–1569 (1991).
3. Hinds, P. W. *et al. Cell Growth Differ.* **1**, 571–580 (1990).
4. Momand, J., Zambetti, G. P., Olson, D. C., George, D. L. & Levine, A. J. *Cell* (in the press).
5. Mandahl, N. *et al. Genes Chrom. Cancer* **1**, 9–14 (1989).
6. Turc-Carel, C. *et al. Cancer genet. Cytogenet.* **23**, 291–299 (1986).
7. Meltzer, P. S. *et al. Cell Growth Differ.* **2**, 495–501 (1991).
8. Lane, D. P. & Benchimol, S. *Genes Dev.* **4**, 1–8 (1990).
9. Werness, B. A., Levine, A. J. & Howley, P. M. *Science* **248**, 76–79 (1990).
10. Ochman, H., Ajioka, J., Garza, D. & Hartl, D. in *PCR Technology: Principles and Applications for DNA Amplification* (ed. Erlich, H. A.) 105–111 (Stockton, New York, 1989).
11. Tanaka, K. *et al. FEBS Lett.* **271**, 41–46 (1990).
12. Pinna, L. A. *Biochim. biophys. Acta* **1054**, 267–284 (1990).
13. Ptashne, M. *Nature* **335**, 683–689 (1988).
14. Harrison, S. C. *Nature* **353**, 715–719 (1991).
15. Kinzler, K. W. *et al. Science* **251**, 1366–1370 (1991).
16. Law, M. L. *et al. Am. hum. Genet.* **50**, 131–137 (1986).
17. Weiss, S. W. & Enzinger, F. M. *Cancer* **41**, 2250–2266 (1978).
18. Malawer, M.M., Abelson, H. T. & Suit, H. D. in *Cancer: Principles and Practice of Oncology* (ed. DeVita, V. T., Hellman, S. & Rosenberg, S. A.) 1293–1342 (Lippincott, Philadelphia, 1985).
19. Kinzler, K. W. *et al. Science* **236**, 70–73 (1987).
20. Kinzler, K. W. *et al. Proc. natn. Acad. Sci. U.S.A.* **83**, 1031–1035 (1986).
21. Brodeur, G.M. & Seeger, R.C. *Cancer genet. Cytogenet.* **15**, 101–111 (1986).
22. Gubler, U. & Hoffmann, B. J. *Gene* **25**, 263–268 (1983).
23. Elledge, S. J., Mulligan, J. T., Ramer, S. W., Spottswood, M. & Davis, R. W. *Proc. natn. Acad. Sci. U.S.A.* **88**, 1731–1735 (1991).
24. Feinberg, A. & Vogelstein, B. *Analyt. Biochem.* **132**, 6–13 (1983).
25. Dasmahapatra, B., Rozhon, E. J. & Schwartz, J. *Nucleic Acids Res.* **16**, 3933 (1987).
26. El-Deiry, W. S., Kern, S. E., Pietenpol, J. A., Kinzler, K. W. & Vogelstein, B. *Nature Genet.* **1**, 45–49 (1992).
27. Reed, K. C. & Mann, D. A. *Nucleic Acids Res.* **13**, 7207–7215 (1985).
28. Fearon, E. R. *et al. Science* **247**, 49–56 (1989).
29. Vogelstein, B. *et al. Cancer Res.* **47**, 4806–4813 (1987).
30. Kinzler, K. W., Ruppert, J. M., Bigner, S. H. & Vogelstein B. *Nature* **332**, 371–374 (1988).
31. Kinzler, K. W. & Vogelstein, B. *Molec. cell. Biol.* **10**, 634–642 (1990).

ACKNOWLEDGEMENTS. We thank A. J. Levine for the information about MDM2–p53 interaction that stimulated this work, M. L. Law for somatic cell hybrids, S. Elledge for the lambda YES vector, and T. Gwiazda for preparation of the manuscript. This work was supported by the Preuss Foundation, the Clayton Fund, and grants from the National Institutes of Health.

Wild-type p53 activates transcription *in vitro*

George Farmer, Jill Bargonetti, Hua Zhu, Paula Friedman, Ron Prywes & Carol Prives

Department of Biological Sciences, Columbia University, New York 10027, USA

THE p53 protein is an important determinant in human cancer and regulates the growth of cells in culture[1-3]. It is known to be a sequence-specific DNA-binding protein[4,5] with a powerful activation domain[6-8], but it has not been established whether it regulates transcription directly. Here we show that intact purified wild-type human and murine p53 proteins strongly activate transcription *in vitro*. This activation depends on the ability of p53 to bind to a template bearing a p53-binding sequence. By contrast, tumour-derived mutant p53 proteins cannot activate transcription from the template at all, and when complexed to wild-type p53, these mutants block transcriptional activation by the wild-type protein. Moreover, the simian virus 40 large T antigen inhibits wild-type p53 from activating transcription. Our results support a model in which p53 directly activates transcription but this activity can be inhibited by mutant p53 and SV40 large T antigen through interaction with wild-type p53.

A DNA-binding immunoassay has been used to screen human genomic clones and show that p53 binds specifically to a region upstream of the transcription start site for the human ribosomal gene cluster (RGC)[5]. We have confirmed and extended this observation by DNase I footprinting and shown that addition of immunopurified p53 to a DNA fragment containing the RGC

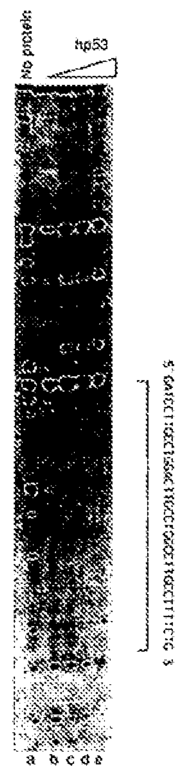

FIG. 1 The p53 protein binds specifically to a site in the human ribosomal gene cluster. DNA binding was assayed in 50-μl volumes containing 40 mM creatine phosphate, pH 7.7, 4 mM ATP, 7 mM $MgCl_2$, bovine serum albumin (0.2 mg ml^{-1}) 0.5 mM dithiothreitol, 10 ng carrier plasmid (pAT153) and 10 fmol of 5′ ^{32}P-labelled DNA fragment containing the ribosomal gene cluster (RGC) p53-binding site[4] and either no protein (lane a) or increasing amounts of wild-type human p53 in increments of 15 ng up to 60 ng (lanes b–e). DNase I treatment of mixtures and processing of samples for electrophoresis on 8% polyacrylamide urea gels has been described[5]. Wild-type p53 was immunopurified from Sf27 cells expressing a recombinant baculovirus, pEV55hwt, using the monoclonal antibody Pab421 crosslinked to Sepharose A[14].

site leads to strong and specific protection of only the RGC region (Fig. 1). All tumour-derived mutant p53 proteins tested failed to protect this sequence (J.B. *et al.*, manuscript in preparation).

To determine whether p53 can activate transcription *in vitro*, we used as templates the plasmids fos1wt and fos1mt, which contain the human RGC p53 DNA-binding fragment or a mutated RGC fragment respectively (Fig. 2*a*). Three partially purified fractions from HeLa cell nuclear extracts were used as a source of transcription factors[9]. RNA products were analysed by S1 nuclease digestion using specific probes for each construct. Increasing amounts of p53 stimulated transcription from fos1wt (compare lanes 1–4 with lanes 5–8). These reaction mixtures also included a construct containing an abridged adenovirus major late promoter (pMLS; ref. 10) whose transcription was not significantly affected by p53.

The p53 protein activated transcription from another promoter as well (Fig. 2*b*). Plasmids containing either one or sixteen copies of the RGC site, or one mutant RGC site, inserted adjacent to the polyoma virus early promoter to create Py1wt, Py16wt and Py1mt, respectively, were used as templates in transcription reactions. We found that p53 activated transcription of constructs containing the wild-type RGC (lanes 1–9) but not the mutant RGC (lanes 10–12). Diagrams of the templates and the test probe used in these experiments are shown in Fig. 2*c* with the expected S1 nuclease products.

The high incidence of p53 gene mutations in cancer patients suggests that alteration of the normal function of p53 is an important part of the oncogenic process. Therefore it was of interest to examine whether tumour-derived mutant p53 proteins activate transcription. The mutant p53 proteins we chose are defective in both nonspecific and specific DNA binding[4,5,11], so providing an opportunity to confirm that p53 must bind DNA to activate transcription. We compared the ability of wild-type and two tumour-derived mutant p53 proteins with mutations at either amino acid 175 (His 175) or at amino acid 273 (His 273)

THE JOURNAL OF BIOLOGICAL CHEMISTRY
Vol. 264, No. 22, Issue of August 5, pp. 13165-13170, 1989
Printed in U.S.A.

Molecular Cloning and Sequencing of the cDNA for Human Membrane-bound Carboxypeptidase M

COMPARISON WITH CARBOXYPEPTIDASES A, B, H, AND N*

(Received for publication, April 21, 1989)

Fulong Tan‡, Shu Jin Chan§, Donald F. Steiner§, James W. Schilling¶, and Randal A. Skidgel‡

From the ‡Laboratory of Peptide Research and Departments of Pharmacology and Anesthesiology, University of Illinois College of Medicine, Chicago, Illinois, 60680, the §Howard Hughes Medical Institute and Department of Biochemistry and Molecular Biology, University of Chicago, Chicago, Illinois 60637, and ¶California Biotechnology, Inc., Mountain View, California 94043

Carboxypeptidase M, a widely distributed membrane-bound carboxypeptidase that can regulate peptide hormone activity, was purified to homogeneity from human placenta (Skidgel, R. A., Davis, R. M., and Tan, F. (1989) *J. Biol. Chem.* 264, 2236–2241). The NH_2-terminal 31 amino acids were sequenced, and two complementary oligonucleotide probes were synthesized and used to isolate a carboxypeptidase M clone from a human placental cDNA library. Sequencing of the cDNA insert (2009 base pairs) revealed an open reading frame of 1317 base pairs coding for a protein of 439 residues. The NH_2-terminal protein sequence matched the deduced amino acid sequence starting with residue 14. Hydropathic analysis revealed hydrophobic regions at the NH_2 and COOH termini. The NH_2-terminal 13 amino acids probably represent part of the signal peptide, and the COOH-terminal hydrophobic region may act either as a transmembrane anchor or as a signal for attachment to a phosphatidylinositol glycan moiety. The carboxypeptidase M sequence contains six potential Asn-linked glycosylation sites, consistent with its glycoprotein nature. The sequence of carboxypeptidase M was 41% identical with that of the active subunit of human plasma carboxypeptidase N, 41% identical with bovine carboxypeptidase H (carboxypeptidase E, enkephalin convertase), and 15% with either bovine pancreatic carboxypeptidase A or B. Many of the active site residues identified in carboxypeptidases A and B, including all of the zinc-binding residues (2 histidines and a glutamic acid), are conserved in carboxypeptidase M. These data indicate that all of the metallocarboxypeptidases are related, but the nondigestive carboxypeptidases with more specialized functions, present in cell membranes, blood plasma, or secretory granules (i.e., carboxypeptidase M, carboxypeptidase N and carboxypeptidase H), are more closely related to each other (41–49% identity) than they are to carboxypeptidase A or B (15–20% identity).

Carboxypeptidases which specifically remove COOH-terminal basic amino acids (Arg or Lys) have important functions in many biological processes, including protein digestion, activation, inactivation or modulation of peptide hormone activity, and alteration of the physical properties of proteins and enzymes (1). The actual role that the various mammalian arginine/lysine carboxypeptidases play *in vivo* is probably related to their localization as well as their physical properties. For example, pancreatic carboxypeptidase B (EC 3.4.17.2) is not normally found outside the pancreas or small intestine, except in cases of acute pancreatitis when low levels can be detected in blood (2). The half-life of carboxypeptidase B injected into the bloodstream is on the order of minutes (3) because of its low molecular weight and lack of glycosylation, consistent with its major function in protein and peptide degradation in the digestive tract. In contrast, human plasma carboxypeptidase N (kininase I, anaphylatoxin inactivator, arginine carboxypeptidase, EC 3.4.17.3) circulates in plasma as a large (M_r = 280,000) tetrameric complex of two active subunits (M_r = 48,000–55,000) and two glycosylated inactive subunits (M_r = 83,000) which stabilize the active subunits and keep them in the circulation (4–6). One of the functions of carboxypeptidase N is to protect the body from potent vasoactive and inflammatory peptides containing COOH-terminal Arg or Lys (*e.g.* kinins, anaphylatoxins) which are released into the circulation (1, 4, 7).

Carboxypeptidase H (also known as enkephalin convertase or carboxypeptidase E, EC 3.4.17.10) is an arginine/lysine carboxypeptidase with an acid pH optimum and is located in secretory granules of pancreatic islets, adrenal gland, pituitary, and brain (8–12). This enzyme probably removes the residual COOH-terminal Arg or Lys remaining after initial endoprotease cleavage during prohormone processing at the intragranular acid pH (1, 12).

Carboxypeptidase M is a membrane-bound arginine/lysine carboxypeptidase found in many tissues and cultured cells (1, 13–15). It was recently purified to homogeneity from human placenta (16). Because of its presence on plasma membranes and optimal activity at neutral pH, it is ideally situated to act on peptide hormones at local tissue sites where it could control their activity before or after interaction with specific plasma membrane receptors (1). Here we report the cloning and sequencing of the cDNA for human carboxypeptidase M. The results show that carboxypeptidase M is a unique enzyme which exhibits similarity to carboxypeptidases A, B, H, and N, and its sequence is consistent with the properties we determined for the purified protein (16).

EXPERIMENTAL PROCEDURES

Materials—Restriction enzymes were purchased from Boehringer Mannheim or New England Biolabs, [γ-^{32}P]ATP and ^{35}S-dATP were

* This study was supported by Grants DK13914 (to D. F. S.), HL36473, and HL36082 from the National Institutes of Health and by the Howard Hughes Medical Institute. The costs of publication of this article were defrayed in part by the payment of page charges. This article must therefore be hereby marked "*advertisement*" in accordance with 18 U.S.C. Section 1734 solely to indicate this fact.

The nucleotide sequence(s) reported in this paper has been submitted to the GenBank™/EMBL Data Bank with accession number(s) J04970.

from Amersham Corp., and nitrocellulose filters were from Schleicher & Schuell. All other solvents and chemicals were of reagent grade or better.

Purification and NH_2-terminal Sequence Analysis of Human Carboxypeptidase M—Carboxypeptidase M was purified to homogeneity from human placental microvilli as described (16) by sequential column chromatography on DEAE-Trisacryl, Q-Sepharose, arginine-Sepharose, and Mono-Q HR in high performance liquid chromatography. Samples (50–60 μg) of native carboxypeptidase M and carboxypeptidase M reduced with dithiothreitol and alkylated with vinyl pyridine (17) were dialyzed against 5% acetic acid and subjected to sequencing on an Applied Biosystems sequenator (model 477).

Oligonucleotide Synthesis and Labeling—Oligonucleotides used for screening cDNA libraries and for sequencing were synthesized on an Applied Biosystems model 380B DNA synthesizer. After complete deprotection, oligonucleotide probes used for screening were further purified by electrophoresis and elution from 20% polyacrylamide-urea gels and then 5′ end-labeled with [γ-^{32}P]ATP using T4 polynucleotide kinase (18).

Screening of cDNA Libraries—Two human placental cDNA libraries, a λgt10 library obtained from Dr. P. Seeburg of Genentech, and a λgt11 library purchased from Clontech, Palo Alto, CA, were screened using standard techniques (18) with two labeled synthetic oligonucleotide probes complementary to two adjacent regions of the NH_2-terminal amino acid sequence. Triplicate filter lifts were made from each plate and hybridized with each probe separately or with a mixture of both probes.

Subcloning and DNA Sequence Analysis—Positive plaques were purified by rescreening at low density, and DNA was prepared by the plate lysis method (18). The DNA was cleaved with *Eco*RI, the 2-kilobase pair (kb)[1] insert was purified by agarose gel electrophoresis and then subcloned into the *Eco*RI site of PGEM4Z or M13mp18. Large-scale preparation of plasmid or phage DNA was performed as described (18). *Hin*dIII restriction fragments (640, 240, and 1170 base pairs (bp)) were purified on agarose gel electrophoresis and subcloned into the *Eco*RI/*Hin*dIII site of M13mp18 (19). Single-stranded DNA was prepared and was sequenced using the dideoxy chain termination method (19) employing ^{35}S-dATP (1000 Ci/mmol, Du Pont-New England Nuclear) and Sequenase (United States Biochemical Corp., Cleveland, OH) according to the manufacturer's instructions. In some regions, specific synthetic oligonucleotides were used to prime the chain termination reaction. The cDNA clone for carboxypeptidase M was completely sequenced on both strands. Nucleotide and amino acid sequences were analyzed with the DNASTAR software package (DNASTAR, Madison, WI).

Northern Analysis—Total RNA was isolated from human placenta, kidney, and liver by the guanidine thiocyanate method (19). The RNA (20 μg) was separated by electrophoresis on a 1.2% agarose gel containing 0.66 M formaldehyde (19), transferred to nitrocellulose, and hybridized using a nick-translated ^{32}P-labeled mixture of the 240- and 640-bp *Hin*dIII restriction fragments of carboxypeptidase M cDNA (19). Human placental poly(A$^+$) mRNA was isolated from total RNA by oligo(dT)-cellulose chromatography (19) and 0.1–1 μg used in the Northern analysis as above.

RESULTS AND DISCUSSION

NH_2-terminal Sequencing and Isolation of a Clone Encoding Human Carboxypeptidase M—Human carboxypeptidase M was purified from placenta, and the following sequence of the first 31 amino acids was obtained on a gas-phase sequenator: Leu-Asp-Phe-Asn-Tyr-His-Arg-Gln-Glu-Gly-Met-Glu-Ala-Phe-Leu-Lys-Thr-Val-Ala-Gln-Xaa-Tyr-Ser-Ser-Val-Thr-His-Leu-His-Ser-Ile. No amino acid was detected at position 21, probably due to the presence of a glycosylated asparagine residue (see below). Two oligonucleotide probes (17-mers, each with 32-fold degeneracy), complementary to adjacent regions of the NH_2-terminal sequence were synthesized: 5′ GA(C/T)TT(C/T)AA(C/T)TA(C/T)CA(C/T)CG 3′, corresponding to Asp^2-Arg^7, and 5′ CA(G/A)GA(G/A)GG(A/G/C/T)ATGGA(G/A)GC 3′, corresponding to Gln^8-Ala^{13}. These probes were labeled with [γ-^{32}P]ATP and used to screen approximately 500,000 plaques from the two human placental cDNA libraries. From the initial screening, two positive clones which hybridized with both probes were obtained: λCPM$_1$ and λCPM$_2$. Both clones contained a 2-kb insert, gave identical restriction maps with *Bam*HI and *Hin*dIII, and were therefore considered to be the same. All further work was carried out using λCPM$_1$.

Sequence Analysis of Human Carboxypeptidase M cDNA—The cDNA was sequenced completely in both strands using the strategy outlined in Fig. 1. Sequence analysis revealed the insert is 2009 bp long with an open reading frame of 1317 bp coding for a protein of 439 amino acids (Fig. 2). The cDNA did not contain the initiator Met, but the amino acid sequence predicted by the cDNA matches exactly the partial NH_2-terminal protein sequence determined for carboxypeptidase M, indicating the clone is authentic and that it codes for the entire mature protein. Hydropathic analysis of the sequence reveals two hydrophobic regions: one at the NH_2 terminus and one at the COOH terminus (Fig. 3). The NH_2-terminal 18 amino acids probably represent a portion of the signal peptide, as the NH_2-terminal sequence of the mature protein does not contain this sequence (Figs. 2 and 4). In addition, as was shown for other signal peptides (20), it is hydrophobic and contains amino acids with small side chains at the −1 and −3 positions relative to the potential signal peptidase cleavage site (Fig. 2). Thus, the mature protein would consist of 426 residues with a calculated molecular weight of 48,709, in good agreement with the value of 47,600 ± 1,000 determined for deglycosylated carboxypeptidase M in sodium dodecyl sulfate-polyacrylamide gel electrophoresis (16).

Potential Membrane Binding Region—Carboxypeptidase M is tightly bound to plasma membranes in various tissues and cells (1, 13–15). As a membrane enzyme, it could be anchored by either a hydrophobic transmembrane segment or by covalent attachment to phosphatidylinositol-glycan (21–23). Because the NH_2-terminal hydrophobic sequence is a cleaved signal peptide, the COOH-terminal hydrophobic region (residues 411–425) is the most likely domain to function as either a membrane anchor or as a signal for phosphatidylinositol glycan attachment (Figs. 2 and 3). This stretch of 15 residues is flanked by charged lysines (Figs. 2 and 4) as is common with membrane-spanning domains, but it is somewhat shorter than the putative sequence of 20 hydrophobic and uncharged amino acids thought to be necessary to span the membrane as an α helix (21). However, at least two other membrane-bound proteins, the β subunit of the T-cell antigen receptor (24) and angiotensin I-converting enzyme (25) contain COOH-terminal membrane-spanning regions of only 17 amino acids, and deletion mutation studies of stomatitis virus glycoprotein (26) and bacteriophage fl gene III protein (27) have shown that a stretch of 12–14 amino acids is sufficient

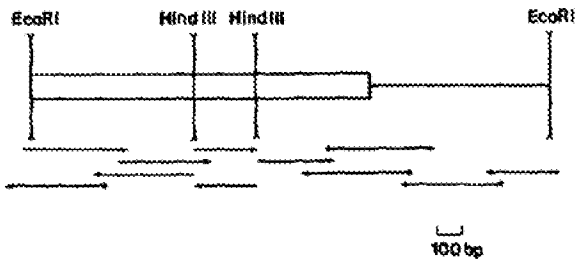

FIG. 1. **Restriction map and sequencing strategy of the carboxypeptidase M cDNA clone.** The 2.0-kb insert is shown with the coding region represented by the *open rectangle*. *Arrows* show the origins and directions of sequencing. *Arrows* with *asterisks* indicate sequencing reactions which were primed with specific oligonucleotide primers.

[1] The abbreviations used are: kb, kilobase pair; bp, base pairs.

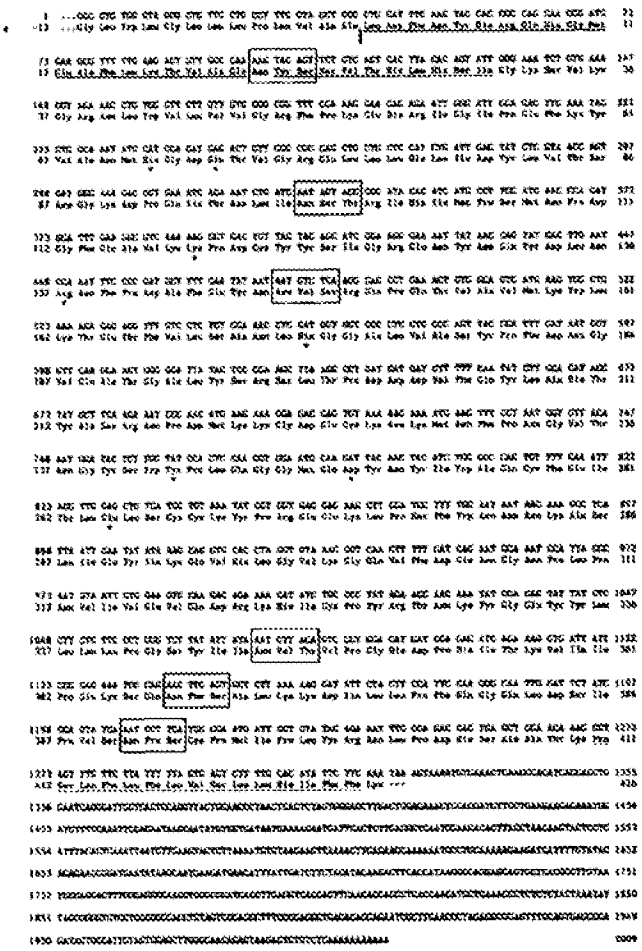

FIG. 2. **The nucleotide sequence encoding human carboxypeptidase M and the deduced amino acid sequence.** The amino acid sequence is numbered from −13 to 426. The *arrow* denotes the site of cleavage of the signal peptide based on the NH_2-terminal sequence determined for the purified protein (*underlined* with a *solid line*). Potential *N*-linked glycosylation sites are boxed. Putative active site residues are marked with asterisks (see text). The COOH-terminal hydrophobic sequence is indicated by the *dashed underline*.

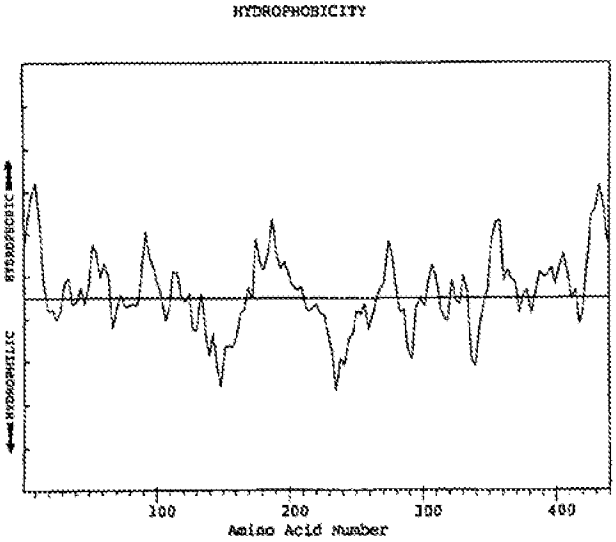

FIG. 3. **Hydropathic analysis of the deduced amino acid sequence of human carboxypeptidase M.** The hydrophobicity of carboxypeptidase M was determined according to the method of Kyte and Doolittle (36) using a window of 15 residues. Tracings above the center line indicate hydrophobic regions and below the line, hydrophilic regions.

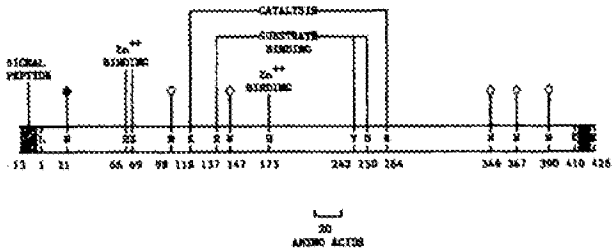

FIG. 4. **Schematic diagram of the sequence of human carboxypeptidase M.** Important amino acid residues are numbered and shown in single letter code. Putative zinc binding, substrate binding, and catalytic residues are labeled. The *hatched areas* denote regions of significant hydrophobicity. Potential asparagine-linked glycosylation sites are indicated by *open diamonds*, and the *solid diamond* marks the Asn determined to be glycosylated by amino acid sequencing.

to span the membrane and anchor the proteins. Three explanations for these observations have been proposed (26, 27): 1) the shorter (less than 20 residues) hydrophobic segments could exist in a conformation more extended than an α helix; 2) the membrane may be locally deformed to accommodate a shorter α helix; 3) charged amino acids are also buried in the lipid bilayer. Alternatively, as has been shown for all phosphatidylinositol-glycan anchored proteins that have been sequenced (22, 23), the COOH-terminal hydrophobic region may serve to temporarily anchor carboxypeptidase M in the membrane of the rough endoplasmic reticulum followed by removal of the hydrophobic tail during attachment to a phosphatidylinositol-glycan anchor.

The amino acid sequence alone cannot distinguish between the two possible modes of membrane attachment. We have preliminary evidence (not shown) which indicates that carboxypeptidase M in the placenta is attached via a phosphatidylinositol-glycan tail, whereas a previous study concluded that carboxypeptidase M in pig or human kidney microvillar membranes was not anchored in this fashion (28). Although this could be due to the presence of a phosphatidylinositol-glycan anchor that is resistant to phospholipase C in the kidney, it is now known that some proteins (*e.g.* acetylcholinesterase, neural cell adhesion molecule) can be bound to the plasma membrane by more than one type of anchor (22, 23). These different forms are presumed to arise via alternative RNA processing which yields mRNAs with different 3′ exons. Consistent with this possibility, in the case of carboxypeptidase M, is the presence of a 5.1-kb mRNA species in human kidney which is not present in the placenta as determined by Northern analysis (see below).

Potential N-glycosylation Sites—Carboxypeptidase M is a glycoprotein as determined by its binding to concanavalin A and reduction in size after chemical deglycosylation (16). Carboxypeptidase M contains about 23% carbohydrate by weight (16). Consistent with these findings is the presence of six potential *N*-glycosylation sites (Asn-Xaa-Ser/Thr) in the predicted protein sequence (Figs. 2 and 4). During NH_2-terminal protein sequencing, no amino acid was found at position 21, one of the predicted glycosylation sites, indicating this asparagine is glycosylated.

Northern Analysis—A Northern blot of RNA isolated from human liver, kidney, and placenta was probed with a ^{32}P-

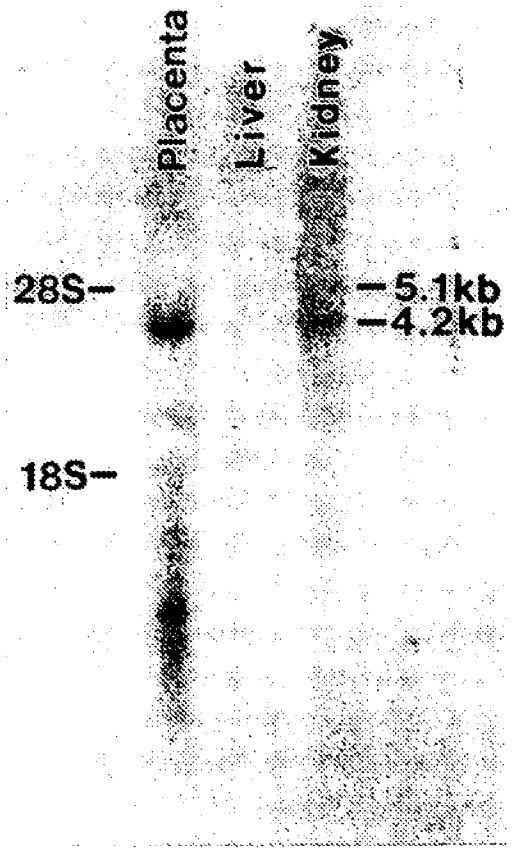

FIG. 5. **Northern analysis of total RNA from human tissues.** Total RNA (20 μg) from human placenta, liver, or kidney was separated on an agarose-formaldehyde gel, blotted onto nitrocellulose, and probed with a ^{32}P-labeled mixture of the 240- and 640-bp *Hin*dIII restriction fragments of carboxypeptidase M cDNA.

labeled mixture of the 240- and 640-bp *Hin*dIII restriction fragments of carboxypeptidase M cDNA (Fig. 5). A 24-h exposure revealed a single mRNA species of 4.2 kb in the placenta and two light bands of 4.2 and 5.1 kb in the kidney (Fig. 5). After long exposure (2 weeks), two light bands were seen in the liver RNA sample which were the same size as those in the kidney (not shown). A repeat of the Northern blot on poly(A$^+$) RNA isolated from the placenta gave the same 4.2-kb band seen in the blot of total RNA (not shown). The relative amounts of mRNA are consistent with the levels of carboxypeptidase M activity we have found in these tissues: it is lowest in the liver,[2] higher in kidney, and highest in the placenta (13). However, the size of the mRNA in the placenta is significantly larger than the 2-kb cloned cDNA we have isolated. Although the 3′ end of the cDNA clone contains a poly(A) tract, it appears not to represent true poly(A) tailing, as a polyadenylation signal was not found (Fig. 2). Moreover, we have recently isolated a genomic clone containing human carboxypeptidase M, and partial sequence analysis revealed the presence of the same poly(A) tract.[3] Thus, the carboxypeptidase M mRNA likely contains a larger 3′-untranslated region than shown in Fig. 2 and also a 5′-untranslated region of undetermined length. The additional 5.1-kb band in the kidney and liver mRNA could arise from alternative splicing,

[2] R. M. Davis, P. A. Deddish, and R. A. Skidgel, unpublished results.

[3] F. Tan and S. Chan, unpublished results.

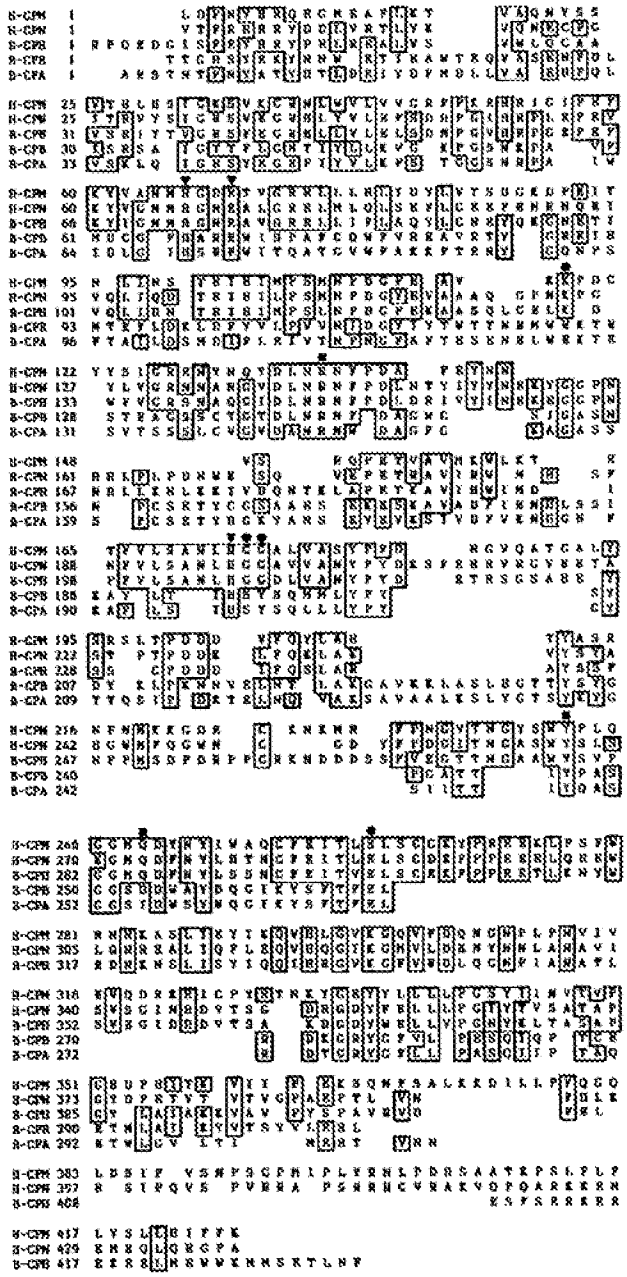

FIG. 6. **Comparison of the sequences of human carboxypeptidases M and N and bovine carboxypeptidases H, B, and A.** For human carboxypeptidase N, the sequence given is for the lower molecular weight active subunit. Residues which are identical in at least three of the five sequences are *boxed*. Gaps were introduced to optimize the alignment. Amino acids thought to be important in the active centers of bovine carboxypeptidases A and B are marked as follows: *solid triangles*, zinc-binding residues; *solid circles*, catalytic residues; *solid squares*, substrate binding residues. Abbreviations: *H*, bovine; *H*, human; *CP*, carboxypeptidase.

the use of multiple transcription start sites or multiple polyadenylation signals.

Comparison with Other Carboxypeptidases—A computer search of the protein data base revealed significant similarity of the sequence of human carboxypeptidase M to those of bovine carboxypeptidases A (29), B (30), and H (31). There was also a high degree of similarity to the partial protein

TABLE I

Amino acid sequence identity of mammalian carboxypeptidases

The values given are percent identity, calculated by dividing the number of identical residues by the number of amino acids in the longer of the two sequences compared. Abbreviations: H, human; B, bovine; CP, carboxypeptidase. H-CPN refers to the sequence of the active subunit of human carboxypeptidase N.

	H-CPM	H-CPN	B-CPH	B-CPB	B-CPA
			%		
H-CPM		41	41	15	15
H-CPN			49	17	19
B-CPH				17	20
B-CPB					48

sequence of the active subunit of human carboxypeptidase N (32) and to the full sequence (deduced from the cDNA) published recently (33). Fig. 6 shows the alignment of the five carboxypeptidases. The overall identity of human carboxypeptidase M was highest (41%) with bovine carboxypeptidase H and the active subunit of human plasma carboxypeptidase N, whereas the identity with bovine pancreatic carboxypeptidase A or B was much less (Table I). Certain regions are highly conserved (69–93% identity) between carboxypeptidases M, N, and H. These are residues 57–75, 100–114, 126–141, 166–184, and 258–276 (numbered according to carboxypeptidase M; Fig. 6). Most of these regions contain residues which correspond to active site residues identified in bovine carboxypeptidases A and B. Thus, the three zinc-binding residues (His^{69}, Glu^{72}, and His^{196} in carboxypeptidase A), two of the substrate-binding residues (Arg^{145} and Tyr^{248}), and the catalytic glutamic acid (Glu^{270}) are strictly conserved in all of the carboxypeptidases (Fig. 6). Other residues presumed to be involved in catalysis, such as Ser^{197} and Tyr^{198} of bovine carboxypeptidase A, are not conserved in carboxypeptidases M, N, and H which all contain glycine residues in these positions (Fig. 6). However, it was proposed for a recent model of carboxypeptidase A (34) that the carbonyl oxygen of Ser^{197} functions to stabilize the tetrahedral intermediate of the substrate and that the side chains of Ser^{197} and Tyr^{198} are not involved in catalysis. Thus, the carbonyl oxygen of Gly may be able to fulfill this role in carboxypeptidases M, N, and H. In carboxypeptidase A, Arg^{127} is thought to polarize the scissile carbonyl group in the substrate (34). Carboxypeptidases M, N, and H contain Lys in this position (Fig. 6) which may have the same function. Because carboxypeptidases B, M, N, and H all specifically cleave COOH-terminal basic amino acids (Arg or Lys), a negatively charged active site residue would be required to bind the positively charged substrate side chain. In carboxypeptidase B, the substrate side-chain-binding residue is Asp^{253}. Although carboxypeptidases M, N, and H have Gln in this position (which could not function in the same way), all three enzymes contain Asp as the next residue, which might serve the same role (Fig. 6).

The regions of sequence identity between carboxypeptidases M, N, and H are spread throughout the proteins with one exception: the COOH-terminal regions have essentially no similarity (Fig. 6). This is probably due to the differences in distribution and functions of the enzymes. As stated above, the COOH-terminal part of carboxypeptidase M probably serves as either a transmembrane anchor or as a signal for attachment to phosphatidylinositol glycan, whereas in carboxypeptidase H the COOH-terminal portion may mediate binding to granule membranes by forming an amphipathic helix (31). In carboxypeptidase N, the COOH-terminal region contains many basic residues which can explain the rapid conversion of the M_r = 55,000 form of the active subunit to an M_r = 48,000 form by various serine proteases (5, 6, 33).

When the sequence identities of all five carboxypeptidases are compared (Table I), they can be divided into two groups: 1) the digestive carboxypeptidases A and B and 2) carboxypeptidases H, M, and N which are present in secretory granules, cell membranes, or blood plasma and thus have different functions. The sequence identity of the enzymes within each group ranges from 41 to 49%, whereas the sequence identity between the two groups is only 15–20% (Table I). Thus, it is possible that an ancestral carboxypeptidase gene duplicated and diverged to evolve into two separate precursor genes, one of which gave rise to carboxypeptidases A and B and the other to carboxypeptidases H, M, and N. A second carboxypeptidase A-type enzyme was recently discovered in rat pancreas which has 63% sequence identity with either rat or bovine carboxypeptidase A, but so far it has not been found in any other species (35). Although carboxypeptidases A and B participate in protein and peptide degradation in the digestive tract, carboxypeptidases H, M, and N have evolved to perform more specialized functions. These include prohormone processing in the acid environment of secretory granules (carboxypeptidase H) or regulation of peptide hormone activity at neutral pH in the blood (carboxypeptidase N) or at the cell surface (carboxypeptidase M) (1, 4, 12).

Acknowledgments—We thank Paul Gardner for synthesizing the oligonucleotides used and Dr. Ervin G. Erdös for encouragement and helpful discussions.

REFERENCES

1. Skidgel, R. A. (1988) *Trends Pharmacol. Sci.* **9**, 299–304
2. Delk, A. S., Durie, P. R., Fletcher, T. S., and Largman, C. (1985) *Clin. Chem.* **31**, 1294–1300
3. Erdös, E. G., Renfrew, A. G., Sloane, E. M., and Wohler, J. R. (1963) *Ann. N. Y. Acad. Sci.* **104**, 222–234
4. Erdös, E. G. (ed) (1979) in *Handbook of Experimental Pharmacology*, Vol. 25, Supplement, pp. 428–487, Springer-Verlag, Heidelberg, Federal Republic of Germany
5. Levin, Y., Skidgel, R. A., and Erdös, E. G. (1982) *Proc. Natl. Acad. Sci. U. S. A.* **79**, 4618–4622
6. Plummer, T. H., Jr., and Hurwitz, M. Y. (1978) *J. Biol. Chem.* **253**, 3907–3912
7. Huey, R., Bloor, C. M., Kawahara, M. S., and Hugli, T. E. (1983) *Am. J. Pathol.* **112**, 48–60
8. Zühlke, H., Steiner, D. F., Lernmark, A., and Lipsey, C. (1975) *Ciba Found. Symp.* **41**, 183–195
9. Davidson, H. W., and Hutton, J. C. (1987) *Biochem. J.* **245**, 575–582
10. Hook, V. Y., and Loh, Y. P. (1984) *Proc. Natl. Acad. Sci. U. S. A.* **81**, 2776–2780
11. Fricker, L. D., and Snyder, S. H. (1983) *J. Biol. Chem.* **258**, 10950–10955
12. Fricker, L. D. (1988) *Annu. Rev. Physiol.* **50**, 309–321
13. Skidgel, R. A., Johnson, A. R., and Erdös, E. G. (1984) *Biochem. Pharmacol.* **33**, 3471–3478
14. Johnson, A. R., Skidgel, R. A., Gafford, J. T., and Erdös, E. G. (1984) *Peptides* **5**, 789–796
15. Deddish, P., Skidgel, R. A., Becker, R. P., and Erdös, E. G. (1989) *FASEB J.* **3**, A1026
16. Skidgel, R. A., Davis, R. M., and Tan, F. (1989) *J. Biol. Chem.* **264**, 2236–2241
17. Tarr, G. E. (1986) in *Methods of Protein Microcharacterization* (Shively, J. E., ed) pp. 155–194, Humana Press, Clifton, NJ
18. Maniatis, T., Fritsch, E. F., and Sambrook, J. (1982) *Molecular Cloning: A Laboratory Manual*, Cold Spring Harbor Laboratory, Cold Spring Harbor, NY
19. Davis, L. G., Dibner, M. D., and Battey, J. F. (1986) *Basic Methods in Molecular Biology*, Elsevier Scientific Publishing Co., Inc., New York
20. von Heijne, G. (1985) *J. Mol. Biol.* **184**, 99–105
21. Wickner, W. T., and Lodish, H. F. (1985) *Science* **230**, 400–407
22. Low, M. G. (1987) *Biochem. J.* **244**, 1–13
23. Low, M. G. (1989) *FASEB J.* **3**, 1600–1608
24. Yanagi, Y., Yoshikai, Y., Leggett, K., Clark, S. P., Aleksander, I.,

and Mak, T. (1984) *Nature* **308**, 145–149
25. Soubrier, F., Alhenc-Gelas, F., Hubert, C., Allegrini, J., John, M., Tregear, G., and Corvol, P. (1988) *Proc. Natl. Acad. Sci. U. S. A.* **85**, 9386–9390
26. Adams, G. A., and Rose, J. K. (1985) *Cell* **41**, 1007–1015
27. Davis, N. G., Boeke, J. D., and Model, P. (1985) *J. Mol. Biol.* **181**, 111–121
28. Hooper, N. M., and Turner, A. J. (1988) *FEBS Lett.* **229**, 340–344
29. Bradshaw, R. A., Ericsson, L. H., Walsh, K. A., and Neurath, H. (1969) *Proc. Natl. Acad. Sci. U. S. A.* **63**, 1389–1394
30. Titani, K., Ericsson, L. H., Walsh, K. A., and Neurath, H. (1975) *Proc. Natl. Acad. Sci. U. S. A.* **72**, 1666–1670
31. Fricker, L. D., Evans, C. J., Esch, F. S., and Herbert, E. (1986) *Nature* **323**, 461–464
32. Skidgel, R. A., Bennett, C. D., Schilling, J. W., Tan, F., Weerasinghe, D. K., and Erdös, E. G. (1988) *Biochem. Biophys. Res. Commun.* **154**, 1323–1329
33. Gebhard, W., Schube, M., and Eulitz, M. (1989) *Eur. J. Biochem.* **178**, 603–607
34. Christianson, D. W., David, P. R., and Lipscomb, W. N. (1987) *Proc. Natl. Acad. Sci. U. S. A.* **84**, 1512–1515
35. Gardell, S. J., Craik, C. S., Clauser, E., Goldsmith, E. J., Stewart, C.-B., Graf, M., and Rutter, W. J. (1988) *J. Biol. Chem.* **263**, 17828–17836
36. Kyte, J., and Doolittle, R. F. (1982) *J. Mol. Biol.* **157**, 105–132

THE JOURNAL OF BIOLOGICAL CHEMISTRY
Vol. 270, No. 26, Issue of June 30, pp. 15644–15649, 1995
Printed in U.S.A.

Carboxypeptidase M Is Identical to the MAX.1 Antigen and Its Expression Is Associated with Monocyte to Macrophage Differentiation*

(Received for publication, March 17, 1995, and in revised form, May 1, 1995)

Michael Rehli, Stefan W. Krause, Marina Kreutz, and Reinhard Andreesen‡

From the Department of Hematology and Oncology, University of Regensburg, 93042 Regensburg, Germany

The two monoclonal antibodies MAX.1 and MAX.11 recognize cell surface antigens that are almost undetectable on monocytes but highly expressed on differentiated macrophages. Biochemical characterization revealed that both antibodies detect the same 58–64-kDa glycoprotein anchored to the plasma membrane by glycosyl-phosphatidylinositol linkage. We purified the MAX.1/11 antigen by immunoaffinity chromatography using monoclonal antibody MAX.11. The NH_2-terminal amino acid sequence was determined and turned out to be identical to the NH_2-terminal sequence of the membrane-bound carboxypeptidase M. By precipitation with antibodies MAX.1 and MAX.11, membrane preparations of macrophages and placental microvilli were almost completely depleted of enzyme activity, indicating that the two antibodies indeed recognize carboxypeptidase M. Immunoreactivity of both antibodies correlates with the reported tissue distribution of enzyme activity. Expression of carboxypeptidase M on mRNA level and enzymatic activity markedly increase during *in vitro* differentiation of monocytes, according to the described increase in MAX.1 and MAX.11 antigen expression. Moreover, *in vitro* differentiated macrophages show the highest specific activity yet described in any tissue. In addition, carboxypeptidase M expression could be detected in HL-60, U937, and THP-1 myeloid cell lines. Vitamin D_3-induced monocytic differentiation resulted in an increased carboxypeptidase M expression in all three cell lines. Further studies are needed to elucidate the functional role of carboxypeptidase M during monocytic differentiation and activation.

Macrophages (MAC)[1] are believed to be the mature effector cells of the mononuclear phagocyte lineage. They participate in both specific and nonspecific immune responses (1) and play a critical role in extracellular matrix remodeling and wound healing (2). Their differentiation from bone marrow precursors via circulating blood monocytes (MO) is a multistep process that is only partially understood (3, 4).

Peripheral blood MO provide the common source of MAC. Arbitrarily, or in response to so far unknown signals, they infiltrate tissues and body cavities. There, probably depending on the microenvironment and tissue-specific factors, they develop into different types of MAC with functional heterogeneity (4, 5). Under *in vitro* conditions a similar process of maturation from human blood MO to MAC, accompanied by specific changes of morphological, cytochemical, phenotypic, and functional properties can be observed (6, 7). Several cell surface antigens are commonly used as phenotypic markers; for example, the low affinity Fc receptor (CD16), the α-chain of the vitronectin receptor (CD51), the transferrin receptor (CD71), and endoglin (CD105) are preferentially detectable on mature MAC, whereas the B148.4 antigen is mainly expressed on peripheral blood MO (8).

The two monoclonal antibodies MAX.1 and MAX.11 have originally been developed to detect lineage-restricted antigens specific for late differentiation stages of the mononuclear phagocyte lineage (9). During *in vitro* differentiation of human blood MO, surface expression of MAX.1 and MAX.11 antigen is increasing from low or undetectable levels on MO to a high expression level on MAC (after cultivation for 7 days in the presence of serum) (9). *In vivo*, MAC in serous cavities (*e.g.* pleural and peritoneal cavity and alveolar space) express MAX.1 and MAX.11 antigen in a heterogeneous pattern, whereas tissue MAC from various organs express them at a low level (10).

We purified MAX.1 and MAX.11 antigen by immunoaffinity chromatography from the supernatants of phosphatidylinositol-specific phospholipase C (PI-PLC)-treated, *in vitro* differentiated MAC. After NH_2-terminal sequencing we identified carboxypeptidase M (CPM) as the antigen detected by both antibodies MAX.1 and MAX.11. CPM cleaves COOH-terminal arginine or lysine from peptides and proteins (11), and it is known to be anchored to the plasma membrane by glycosylphosphatidylinositol linkage (12). Because of its presence on plasma membranes and an optimal activity at neutral pH, CPM may participate in modulation of peptide hormone activity (*e.g.* kinins and enkephalin hexapeptides), or inactivation of peptides (*e.g.* kinins and anaphylatoxins) at local tissue sites (11, 13). Here we report a detailed study of CPM expression during *in vitro* differentiation of human blood MO. Furthermore, human myeloid leukemia cell lines appear to correspond with different immature stages of myeloid differentiation. The human myeloid leukemia cell lines THP-1, U937, and HL-60 differentiate into MO/MAC-like cells when they are treated with ($1,25(OH)_2D_3$) (14–16), and this effect is mediated through the vitamin D_3 receptor (17). We investigated expres-

* This work was supported by the Deutsche Forschungsgemeinschaft. The costs of publication of this article were defrayed in part by the payment of page charges. This article must therefore be hereby marked "*advertisement*" in accordance with 18 U.S.C. Section 1734 solely to indicate this fact.

‡ To whom correspondence and reprint requests should be addressed: Abt. f. Hämatologie und Internistische Onkologie, Klinikum der Universität Regensburg, 93042 Regensburg, Germany. Tel.: 49-941-944-7110; Fax: 49-941-944-7111; E-mail: Reinhard.Andreesen@klinik.uni-regensburg.de.

[1] The abbreviations used are: MAC, macrophages; MO, monocytes; CD, cluster of differentiation; PI-PLC, phosphatidylinositol-specific phospholipase C; CPM, carboxypeptidase M; $1,25(OH)_2D_3$, 1,25-dihydroxyvitamin D_3; mAb, monoclonal antibody; PAGE, polyacrylamide gel electrophoresis; FACS, fluorescence-activated cell sorting; PBS, phosphate-buffered saline; NHSS-LC-biotin, 6-(+)-biotinylamidohexanoic acid *N*-hydroxysulfosuccinimide ester sodium salt; TSS, Tris/saline solution; NGF, *N*-glycosidase F; ECL, enhanced chemiluminescence; PCR, polymerase chain reaction; dansyl, 5-dimethylaminonaphthalene-1-sulfonyl.

sion of CPM on these myeloid cell lines, and since the induction of MAX.1/11 antigen CPM during monocytic differentiation with $1,25(OH)_2D_3$ has been reported previously (18), we further studied the regulation of the expression of CPM during the process of $1,25(OH)_2D_3$-induced differentiation of THP-1, U937, and HL-60 cell lines.

MATERIALS AND METHODS

Antibodies and Chemicals—The mAbs MAX.1 and MAX.11 were purified from hybridoma supernatants by ammonium sulfate precipitation (55%) followed by protein G-Sepharose chromatography. The purity and immunologic reactivity of both antibodies was documented by SDS-PAGE and immunoperoxidase staining, respectively. Two CD14 mAbs (RMO 52, Dianova-immunotech, Hamburg, Germany, and My4, Coulter Electronics, Krefeld, Germany) and a CD11c mAb (anti-Leu-M5, Becton Dickinson, San Jose, CA) were used as control antibodies for immunoprecipitations and FACS analysis.

All chemical reagents used were purchased from Sigma unless otherwise noted.

Cells—Peripheral blood mononuclear cells were separated by leukapheresis of healthy donors, followed by density gradient centrifugation over Ficoll/Hypaque. MO were isolated from mononuclear cells by countercurrent centrifugal elutriation in a J6M-E centrifuge (Beckman, München, Germany) as described previously (19). MO were >90% pure as determined by morphology and expression of CD14 antigen. Isolated MO were cultured in RPMI 1640 medium (Biochrom KG, Berlin, Germany) supplemented with vitamins, antibiotics, pyruvate, nonessential amino acids (all from Life Technologies, Inc.), 5×10^{-5} M β-mercaptoethanol, and with 2% human pooled AB-group serum on Teflon foils for a period of up to 8 days (19). The human monocytic cell lines THP-1, U937, and HL-60 were grown in culture in RPMI 1640 medium supplemented with 10% fetal calf serum (Life Technologies, Inc.) until used for experiments. $1,25(OH)_2D_3$ was provided by Hoffman-La Roche. Treatment with $1,25(OH)_2D_3$ was performed at a concentration of 1×10^{-7} M for 72 h.

Surface Biotinylation—Cells were surface-labeled using biotin as described (20, 21). Briefly, $1–5 \times 10^7$ cells were labeled in 1 ml of PBS containing 100 μg/ml 6-(+)-biotinylamidohexanoic acid *N*-hydroxysulfosuccinimide ester sodium salt (NHSS-LC-biotin, Serva, Heidelberg, Germany) for 15 min at room temperature. Labeling was stopped by the addition of NH_4Cl to a final concentration of 10 mM, and cells were washed twice with PBS.

Treatment with PI-PLC—1×10^8 cells/ml were suspended in PBS containing 0.2 units/ml PI-PLC (Boehringer Mannheim, Germany) and incubated for 1 h at 37 °C on a rotating mixer. The resulting supernatant was collected by centrifugation and kept at 4 °C until used.

Immunoprecipitation—Biotin-labeled cells were resuspended in 500 μl of Tris-buffered saline containing 20 mM Tris/HCl, pH 8.0, 150 mM NaCl, 1 mM EDTA, 1 mM phenylmethylsulfonyl fluoride, 2 μg/ml aprotinin (Boehringer Mannheim), and 0.5 μg/ml leupeptin (Boehringer Mannheim) and solubilized by the addition of 500 μl of lysis buffer containing 1% Nonidet P-40 (Boehringer Mannheim) and 1% bovine serum albumin in Tris-buffered saline. Lysis was performed for 45 min on ice, and then nuclei and cell debris were removed by centrifugation (12,000 × *g*, 4 °C, 30 min). Supernatants from cell lysis or PI-PLC treatment were precleared with 30 μl of protein G-Sepharose (Pharmacia Biotech Inc.) overnight at 4 °C on a rotating mixer. Immunoprecipitation was done by incubating the precleared supernatant with monoclonal antibodies (10 μg/ml) for 2 h at 4 °C and precipitation with 30 μl of protein G-Sepharose for 45 min on a rotating mixer. Sepharose pellets were washed five times with ice-cold Tris-buffered saline, suspended in SDS sample buffer (22, 23), processed for deglycosylation as described below, or stored at −20 °C.

Immunoaffinity Purification—A 2-ml immunoaffinity column (3 mg/ml mAb linked to 6-(+)-aminohexanoic acid *N*-hydroxysuccinimide ester-Sepharose) was equilibrated with binding buffer (1:1 mixture of PBS and TSS buffer (0.01 M Tris/HCl, pH 8.0, 150 mM NaCl, 0.5% Nonidet P-40, 0.5% sodium desoxycholate)). Supernatant from PI-PLC-treated MAC diluted 1:2 with TSS buffer, was applied to the column. After sample loading the column was washed with 5 column volumes of each of the following buffers: TSS buffer, Tris buffer, pH 8.0 (50 mM Tris/HCl, pH 8.0, 0.5 M NaCl), and Tris buffer, pH 9.0 (50 mM Tris/HCl, pH 9.0, 0.5 M NaCl). Material bound to the column was eluted with 50 mM triethanolamin/NaOH, pH 11.5, 0.1% Nonidet P-40, and 150 mM NaCl, in 1.5-ml fractions, immediately neutralized with 0.2 volumes of 50 mM sodium phosphate, pH 6.3, 0.1% Nonidet P-40, and 150 mM NaCl. Eluates were analyzed by SDS-PAGE to identify fractions containing purified antigen.

Glycosidase Treatment—Deglycosylation of immunoprecipitated proteins still coupled to the protein G-Sepharose involved washing beads with NGF-wash buffer (20 mM sodium phosphate, 10 mM EDTA, pH 7.0) and elution of proteins from the protein G beads by boiling in 50 μl of NGF buffer (20 mM sodium phosphate, 10 mM EDTA, 1% β-mercaptoethanol, 1% SDS, pH 7.0). SDS was neutralized by the addition of 25 μl of 20% *n*-dodecyl maltoside, and supernatant was incubated at 37 °C with 1 unit of *N*-glycosidase F (Boehringer Mannheim) overnight. Alternatively, eluted protein from immunoaffinity purification was dialyzed against NGF-wash buffer, SDS and β-mercaptoethanol were added to a final concentration of 1% each, and the solution was boiled. SDS was neutralized by addition of 50 μl of 20% *n*-dodecyl maltoside (Boehringer Mannheim)/100 μl solution and incubated at 37 °C with *N*-glycosidase F (10 units/ml) overnight. Deglycosylated proteins were precipitated with methanol/chloroform as described (24).

Detection of Biotinylated Protein—Samples from immunoprecipitation were electrophoresed on 12% SDS-polyacrylamide gels under reducing conditions (22, 23) along with biotinylated molecular weight marker proteins (Bio-Rad) and transferred to nitrocellulose membranes (Schleicher & Schuell) for 1 h at 0.8 mA/cm² (25). Membranes were blocked overnight at 4 °C in blocking solution (20 mM Tris/HCl, pH 7.4, 150 mM NaCl) containing 5% bovine serum albumin. After washing with 0.1% Tween-20 in blocking solution the membrane was incubated for 1 h at room temperature with a streptavidin-biotinylated horseradish peroxidase complex (Amersham UK; diluted 1:2,500 in blocking solution containing 5% bovine serum albumin). After extensive washing, biotinylated proteins on the nitrocellulose membrane were visualized by the enhanced chemiluminescence detection system (ECL) of Amersham.

NH_2-terminal Sequence Analysis—Unbiotinylated MAX.11 immunoaffinity-purified protein was subjected to SDS-PAGE (12% polyacrylamide gels, reducing conditions) after deglycosylation and methanol/chloroform precipitation and blotted to polyvinylidene difluoride membrane (Millipore, Eschborn, Germany). After staining with Coomassie Blue, a specific band was cut and subjected to an Applied Biosystems protein sequencer (model 477A) with an online PTH-analyzer (model 120A).

Membrane Fractionation and Enzyme Assay—For determination of enzymatic activity membranes of washed cells or placental microvilli were prepared by Dounce homogenization in ice-cold PBS containing 1 mM phenylmethylsulfonyl fluoride. Cell debris and nuclei were removed by centrifugation (1,500 × *g*, 4 °C, 15 min), and crude membrane preparations were either processed immediately or stored at −20 °C. After centrifugation at 6,000 × *g* for 15 min at 4 °C to remove debris, membrane fragments were further separated by ultracentrifugation at 100,000 × *g* for 1 h at 4 °C. The pellet was washed with 2 M NaCl followed by recentrifugation. The washed pellet was resuspended in PBS containing 0.2% Nonidet P-40, and insoluble material was removed by centrifugation (6,000 × *g*, 4 °C, 15 min). CPM activity was measured with dansyl-Ala-Arg (BioTeZ, Berlin, Germany) as a substrate in a Hitachi F-2000 fluorescence spectrophotometer at 340 nm excitation and 495 nm emission as described (26). In control reactions CPM activity was inhibited by 10 M 2-mercaptomethyl-3-guanidinoethylthiopropanoic acid (Calbiochem).

Protein Assay—The protein concentrations were determined using bicinchoninic acid according to the described procedure (27) with albumin as the standard.

Immunofluorescent Flow Cytometry—Freshly isolated MO or cultured cells were washed twice with cold PBS containing 0.06% immunoglobulin (Sandoz Pharma AG, Basel, Switzerland), and 5×10^6 cells were incubated with saturating amounts of specific mAbs or IgG isotype control (Jackson ImmunoResearch, West Grove, PA) for 30 min at 4 °C. After two further washes, cells were incubated with saturating concentrations of fluorescein isothiocyanate-conjugated goat anti-mouse IgG (Jackson ImmunoResearch) for 30 min at 4 °C. After two more washes, cells were fixed with 1% paraformaldhyde in PBS. Analysis was performed using a FACScan (Becton-Dickinson). Cell populations were gated according to their forward and side scattering.

PCR Amplification of CPM cDNA—Synthetic oligonucleotides designed according to the CPM nucleotide sequence (13) were used for PCR amplification of cDNA prepared from mRNA of *in vitro* differentiated MAC. The sense primer 5′-TTTCAACTACCACCGCCAGGAAGG-3′ corresponded to nucleotides 45–68, and the antisense primer 5′-ATGTGCAAAAGACTCACTAAAAATAA-3′ corresponded to nucleotides 1282–1307. Conditions for PCR amplification were 95 °C for 1 min, 64 °C for 45 s, and 72 °C for 1.5 min repeated for 35 cycles. The amplified PCR product was inserted into a plasmid vector (Ta Cloning

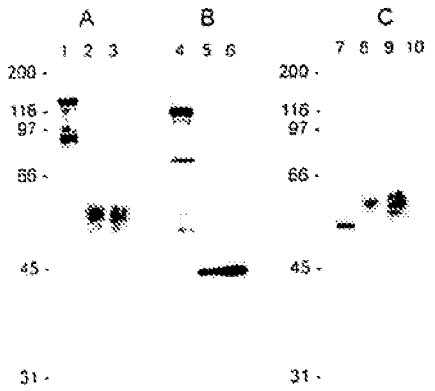

FIG. 1. **Biochemical characterization of MAX.1 and MAX.11 antigen.** SDS-PAGE analysis and ECL detection of immunoprecipitates obtained from lysates (*A* and *B*) or PI-PLC-supernatants of biotin surface-labeled *in vitro* differentiated MAC (*C*) with the following antibodies: CD11c mAb anti-Leu M5 (*lanes 1, 4,* and *10*); mAb MAX.1 (*lanes 2, 5,* and *8*); mAb MAX.11 (*lanes 3, 6,* and *9*); and CD14 mAb RMO 52 (*lane 7*). *B*, immunoprecipitates were treated with *N*-glycosidase F before being subjected to SDS-PAGE.

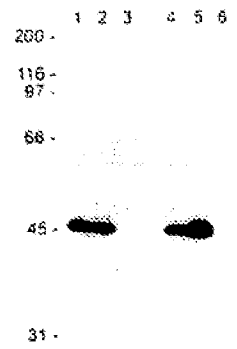

FIG. 2. **Immunological cross-reactivity of mAbs MAX.1 and MAX.11.** MAX.1 (*lanes 1–3*) and MAX.11 (*lanes 4–6*) immunoaffinity purification of lysates of biotin surface-labeled *in vitro* differentiated MAC and subsequent immunoprecipitation from the obtained eluates with the following antibodies: mAb MAX.1 (*lanes 1* and *4*); mAb MAX.11 (*lanes 2* and *5*); and CD11c mAb anti-Leu M5 (*lanes 3* and *6*). All immunoprecipitates were deglycosylated with *N*-glycosidase F before SDS-PAGE and ECL detection.

Kit, Invitrogen, San Diego, CA). Partial DNA sequencing was done by dye deoxy terminator cycle sequencing (Applied Biosystems, Weiterstadt, Germany) according to the manufacturer's instructions, and sequences were analyzed on the Applied Biosystems DNA sequencing system (model 373A).

Northern Analysis—Total RNA was isolated from different cell types by the guanidine thiocyanate/acid phenol method (28). The RNA (10 μg/lane) was separated by electrophoresis on 1% agarose/formaldehyde gels (29) and transferred to nylon membranes (Magna NT, MSI, Westborough, MA). Hybridization (adapted from Refs. 29 and 30) was performed using a ^{32}P-labeled cDNA probe of the *Eco*RI restriction fragments of the cloned CPM PCR fragment (random primed DNA labeling kit, Boehringer Mannheim). To provide an internal control, membranes were reprobed with an oligonucleotide against 18 S rRNA labeled by T4 kinase (5′ end-labeling kit, Amersham). Autoradiography was performed at −70 °C, and bands were scanned with a Molecular Dynamics personal densitometer.

RESULTS

Biochemical Characterization of MAX.1 and MAX.11 Antigens: Immunoprecipitation, Deglycosylation, and PI-PLC Treatment—For a biochemical characterization of antigens detected by monoclonal antibodies MAX.1 and MAX.11, we surface-labeled *in vitro* differentiated MAC with NHSS-LC-biotin and immunoprecipitated antigens from the cell lysates. Both mAbs precipitated a protein with an apparent molecular mass of 58–64 kDa (Fig. 1*A*) Subsequent digestion of the immunoprecipitated material with *N*-glycosidase F resulted in a shift of apparent size to 46 kDa (Fig. 1*B*), indicating a carbohydrate content of about 28% by weight.

Since it was already shown that the antigen detected by MAX.1 can be cleaved from the cell membrane by PI-specific phospholipase C (31), immunoprecipitations were performed using supernatants of surface-labeled MAC after treatment with PI-PLC. The diffuse bands of the antigens precipitated by mAb MAX.1 and MAX.11 after PI-PLC treatment were identical to the bands obtained from cell lysates (Fig. 1*C*).

Immunological Cross-reactivity of MAX.1 and MAX.11—Since the characteristics of antigens detected by mAb MAX.1 and MAX.11 were very similar during the experiments described above, we investigated the possibility that both antibodies detect the same antigen. Cell lysates from surface-labeled *in vitro* differentiated MAC were subjected to chromatography over small immunoaffinity columns (0.5 ml) of MAX.1 or MAX.11 covalently linked to Sepharose. After extensive washing to remove unspecifically bound material, eluates from both columns were reprecipitated with each of the two mAbs and an isotype control antibody. After enzymatical deglycosylation of the precipitated material the characteristic band of 46 kDa was detectable after precipitation with MAX.1 and MAX.11 but not with the isotype control antibody (Fig. 2), confirming that the antigens detected by MAX.1 and MAX.11 are identical.

Purification and Identification of MAX.11 Antigen—*In vitro* differentiated MAC (8×10^8 cells) were exposed to PI-PLC to cause the release of glycosylphosphatidylinositol-anchored proteins into the supernatant. A smaller portion of cells (1×10^8 cells) was surface-labeled with biotin before PI-PLC treatment. Supernatants of labeled and unlabeled cells were combined and subjected to immunoaffinity column chromatography over MAX.11 covalently linked to Sepharose. After washing, the material bound to the column was eluted in small fractions, and a small part of each fraction was analyzed on SDS-PAGE with subsequent immunoblotting and visualization of biotinylated protein by ECL. The fraction containing the immunopurified antigen was used for NH_2-terminal amino acid sequencing, and the following sequence was obtained: Leu-Asp-Phe-Asn-Tyr-*X*-*X*-Gln-Glu-Gly-Met-Glu-Ala. A search of the EMBL nucleic acid data bases revealed identity with the NH_2-terminal sequenced amino acids of CPM (13).

Immunoprecipitation and Enzyme Activity—To further confirm that CPM is identical with MAX.1/11 antigen, we measured CPM activity with dansyl-Ala-Arg as substrate in membrane preparations from *in vitro* differentiated MAC after immunoprecipitation with mAb MAX.1 or MAX.11 or an isotype control antibody. As a positive control with well known CPM activity we used membrane preparations of placental microvilli in a similar experiment. As shown in Table I, in comparison to the isotype control antibody (100%) the majority of enzymatic activity was precipitated by antibodies MAX.1 and MAX.11.

Expression of CPM during Monocytic Differentiation—After it was proven that mAbs MAX.1 and MAX.11 detect CPM, we investigated the correlation of CPM surface expression with membrane-bound enzymatic activity and mRNA-expression during serum-induced *in vitro* differentiation of MO. Cultured MO were harvested at the indicated time points, and preparations of cells for flow cytometry, RNA extraction, and enzyme assay were done in parallel. As shown in Fig. 3, FACS analysis confirmed that the surface expression of CPM markedly increases during monocytic *in vitro* differentiation. A slightly different staining pattern of mAbs MAX.1 and MAX.11 was

TABLE I
Immunoprecipitation of carboxypeptidase activity from membrane fractions of in vitro differentiated macrophages (MAK) or placental microvilli (PM)

Antibodies	Source			
	MAK		PM	
	MSA[a]	%	MSA	%
Isotype control	805 ± 123[b]	100[c]	310 ± 27	100
MAX.1	48 ± 40	6 ± 5	37 ± 34	12 ± 11
MAX.11	73 ± 8	9 ± 1	28 ± 25	9 ± 8

[a] MSA, mean specific activity.
[b] Residual carboxypeptidase activity after immunoprecipitation with isotype control antibody (CD11c mAb), mAb MAX.1, and mAb MAX.11 was measured with dansyl-Ala-Arg as substrate. Data are given as mean specific activity (nmol/h/mg protein) ± S.E. from three independent experiments.
[c] Mean % of control ± SE.

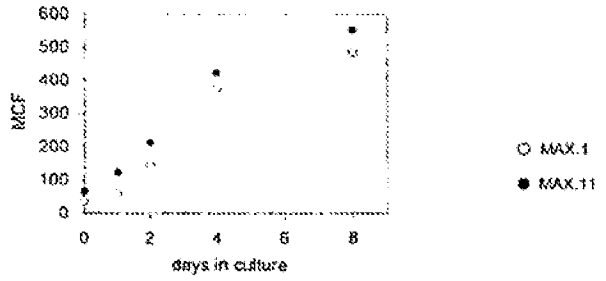

FIG. 3. **Carboxypeptidase M surface expression.** FACS analysis of cell surface expression for CPM during serum-induced differentiation of human MO using mAbs MAX.1 (○) and MAX.11 (●). Freshly isolated MO (day 0), MO after adherence overnight (day 1), and at 1 (day 2), 3 (day 4), and 7 (day 8) days of culture in the presence of serum were used for FACS analysis. Monocytes were gated according to their forward and side scattering; >95% of gated cells were positive for CD14 and CPM expression in all cases. Data are expressed as mean channel fluorescence (*MCF*) of positive cells after subtraction of background obtained with an isotype control antibody from one representative experiment.

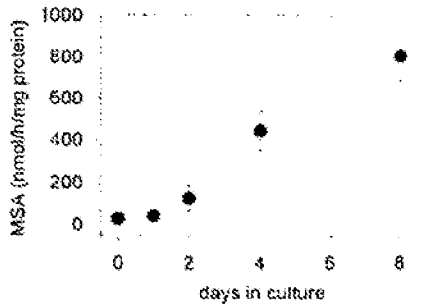

FIG. 4. **Carboxypeptidase M: enzymatic activity during monocyte differentiation *in vitro*.** Membrane fractions were prepared from freshly isolated MO, MO after adherence overnight, and MO at 1, 3, and 7 days of culture in the presence of serum. Carboxypeptidase activity was measured with dansyl-Ala-Arg substrate; data are mean specific activity (*MSA*) S.E. values ($n = 4$).

FIG. 5. **Northern blot analysis of carboxypeptidase M mRNA.** Total RNAs were isolated from freshly isolated MO (*d0*), MO after adherence overnight (*d1*), and MO at 1 (*d2*), 3 (*d4*), and 7 (*d8*) days of culture in the presence of serum, human lymphocytes (*L*), human placental microvilli (*PM*), and human skin fibroblasts (*F*). The blot was sequentially hybridized with a ^{32}P-labeled CPM cDNA (*panel A*) and an 18 S rRNA-specific oligonucleotide probe (*panel B*) to control for equivalent RNA loading.

reproducible in all experiments. For both antibodies, the mean fluorescence, a parameter corresponding to the number of molecules/cell, strongly increased during 7 days of culture in the presence of serum.

In parallel, carboxypeptidase activity of cell membrane preparations was measured with dansyl-Ala-Arg as substrate at the same time points, using a placental membrane preparation as a positive control. The mean specific activity (nmol/h/mg) of CPM increased 30–40-fold during monocytic differentiation (Fig. 4), showing a similar behavior as the surface expression determined by FACS analysis.

To study the regulation of CPM expression at the RNA level, total cellular RNA was prepared at the same time points and hybridized with a CPM-probe. Total RNA prepared from placenta was used as a positive control, and lymphocyte RNA and fibroblast RNA were used as negative controls. As shown in Fig. 5, a strong induction of CPM mRNA expression was detectable during 7 days of culture in the presence of serum.

Expression of CPM on Myeloid Cell Lines HL-60, U937, and THP-1—In addition we studied expression of CPM on myeloid cell lines HL-60, U937, and THP-1, which appear to represent different immature stages of myeloid differentiation.

In promyeloid cell line HL-60 CPM surface expression was almost undetectable. Upon treatment with $1,25(OH)_2D_3$ a weak induction of CPM expression could be demonstrated in FACS analysis (Table II). The histiocytic cell line U937 showed a weak surface expression of CPM that could be slightly enhanced by treatment with $1,25(OH)_2D_3$. In comparison with the other two cell lines the monoblastic cell line THP-1 showed a high surface expression of CPM that markedly increased during the 3 days of $1,25(OH)_2D_3$-treatment.

TABLE II
Carboxypeptidase M surface expression on myeloid cell lines

Myeloid Cell Lines	Treatment with $1,25(OH)_2D_3$	Antibodies		
		CD14	MAX.1	MAX.11
		MCF[a]	*MCF*	*MCF*
THP-1[b]	−	4 ± 6[c]	280 ± 100	310 ± 80
	+	400 ± 130	460 ± 50	510 ± 40
U937	−	0	24 ± 1	28 ± 4
	+	220 ± 190	43 ± 3	47 ± 6
HL-60	−	13 ± 1	14 ± 1	14 ± 2
	+	1600 ± 900	15 ± 1	23 ± 4

[a] MCF, mean channel fluorescence.
[b] Cells (2×10^5/ml) were cultured for 72 h with or without $1,25(OH)_2D_3$ (10^{-7} M); antigen expression was determined by FACS using CD14 mAb My4, mAb MAX.1, and mAb MAX.11.
[c] Data are given as mean channel fluorescence ± S.E. values after subtraction of background obtained with isotype control antibody from at least three independent experiments.

DISCUSSION

The expression and tissue distribution of the glycoproteins detected by mAbs MAX.1 and MAX.11 suggested that they might be of interest for the investigation of MAC differentiation and site-specific activation (9, 10). In this report, we describe the purification, characterization, and identification of the antigen detected by both mAbs. We used PI-PLC cleavage from the plasma membrane to purify the MAX.11 antigen by immunoaffinity chromatography. The quantity and purity of the eluted protein were sufficient for determination of NH_2-terminal amino acid sequence. A comparison of the determined

amino acid sequence with the published amino acid sequence of CPM (13) disclosed that the two molecules are identical. Results from biochemical characterization (58–64-kDa glycoprotein, anchoring to the plasma membrane by glycosylphosphatidylinositol linkage) matched the published data (11–13), and both antibodies were able to almost completely precipitate enzymatic activity from membrane preparations of *in vitro* differentiated MAC and placental microvilli as a control, too. Reactivity of MAX.1 and MAX.11 slightly differs in immunoperoxidase stainings of MAC from different body fluids (9, 10) and immunofluorescent flow cytometry during MO to MAC differentiation. Staining of CPM by mAb MAX.1 seems to be delayed in comparison with mAb MAX.11, suggesting that both antibodies might recognize differentially expressed epitopes on the CPM-molecule. Digestion of precipitated CPM with neuraminidase and β-galactosidase both lead to a marked shift of apparent size to 60 and 56 kDa, respectively (data not shown), indicating that the glycans linked to CPM are, at least in part, of the complex type. It is known that the expression of some glycosyltransferases responsible for glycan structure and composition can be regulated in a maturation-associated manner (32).[2] Therefore, a different glycosylation of CPM during the process of MO to MAC differentiation might be an explanation for the slightly different binding of MAX.1 and MAX.11.

Further evidence for the identity of CPM and MAX.1/11 antigen comes from the described similar tissue distributions of enzymatic activity and antigen expression. In addition to expression on MAC, MAX.1 and MAX.11 antigen could be detected in human kidney (glomerular mesangial cells), in human placenta (cytotrophoblastic and syncytial cells), in the upper gastrointestinal tract (subepithelial structures), and weakly in lymphoid organs (dendritic reticulum cells) (10). This staining pattern correlates with the published distribution of enzymatic activity of CPM. Membrane-bound carboxypeptidase activity is measurable in membrane fractions of various human tissues (placental microvilli, kidney, lung, and brain) (11, 12, 33–35) and in cultured human cells (foreskin fibroblasts, pulmonary arterial endothelial cells, lung fibroblasts, and alveolar type I cells) (33, 34).

Basic carboxypeptidases catalyze the removal of COOH-terminal basic amino acids arginine or lysine from peptides or proteins. The natural substrates appear to be peptide hormones like kinins, enkephalin hexapeptides, and anaphylatoxins or proteins like creatine kinase (36). The removal of COOH-terminal arginine or lysine results in modulation or inactivation of peptide hormone activity and can also change the physical properties of proteins (36).

CPM is a membrane-bound ectopeptidase, present in many organs and tissues. It can participate in control of peptide hormone activity at the cell surface, degradation of extracellular proteins and peptides, and prohormone processing (36), but its regulation and actual functional role in different tissues are still unclear.

The release of L-arginine from peptides or proteins by CPM may increase local concentrations of this amino acid at the MAC cell surface. At sites of a high density of substrates, *e.g.* at inflammatory sites, CPM activity might influence L-arginine metabolism.

In the lung, CPM is present on alveolar type I pneumocytes (33, 34) and on alveolar MAC in yet lower concentrations (9, 10, 34). There is some evidence that CPM is involved in bradykinin metabolism. It may protect the alveolar surface from bradykinin-induced deletious vascular responses (37–39).

In patients with extrinsic allergic bronchiolitis and active pulmonary sarcoidosis, CPM expression on alveolar MAC as detected by mAb MAX.1 is increased in comparison with healthy persons (10). Elevated serum levels of angiotensin-converting enzyme, a predominantly membrane-bound peptidyl dipeptidase that cleaves similar substrates as CPM, is used to diagnose and to assess response to treatment of sarcoidosis (40). CPM expression on alveolar MAC or its activity in the bronchoalveolar fluid could serve as additional markers for this disease. Further investigations should clarify the value of this parameter in diagnosing and monitoring active pulmonary sarcoidosis and other inflammatory lung diseases.

MAC from granulomas of patients with sarcoidosis synthesize the biological active hormonal form of vitamin D_3, $1,25(OH)_2D_3$ (41). $1,25(OH)_2D_3$ may be involved in the stimulation of alveolar MAC to produce CPM. The possibility for a role of vitamin D_3 in regulation of CPM expression is supported by several additional observations; it is shown that, in the absence of serum proteins, MAX.1/CPM is expressed in a maturation-associated manner during $1,25(OH)_2D_3$-induced *in vitro* maturation of MO to MAC (18). As demonstrated in this study, $1,25(OH)_2D_3$-induced differentiation of human promonocytic leukemia cell lines THP-1 and U937 is accompanied by an increased expression of CPM. Also in HL-60 cells, which are thought to represent the earliest differentiation stage of the three cell lines tested, CPM expression slightly increased during $1,25(OH)_2D_3$ treatment.

In renal allograft rejections T-cell activation is required to cause CPM expression in local MAC, since the CPM expression is undetectable in patients treated with Cyclosporin A (10). These results indicate that T-lymphokines may have a possible regulatory role in the expression induction of CPM. Recent observations of our group suggest that tumor cells modulate MAC differentiation and are capable of suppressing CPM expression on MAC associated with solid tumors.[3]

To clarify whether T-cell-derived or tumor-derived factors play an active role in modulation of CPM expression further studies on gene regulation are required.

The functional role of CPM in MAC will depend on its tissue localization and the occurrence of its natural substrates. The present available data on possible substrates are still incomplete. Peptide hormone processing includes complex regulatory mechanisms. Its course and its role in tissue injury and inflammation as well as the effects of peptide hormones and metabolites on cells of the immune system have not yet been characterized.

As described previously (9, 10), CPM expression, detected by mAbs MAX.1 and MAX.11, is restricted to the MO/MAC lineage within hematopoietic cells. Besides other peptidases (neutral endopeptidase (CD10), aminopeptidase N (CD13), and dipeptidyl-peptidase IV (CD26)) carboxypeptidase M should be assigned to a cluster differentiation (CD) group.

Acknowledgments—We thank Dr. Frank Emmerich for providing sufficient amounts of MAX.1 and MAX.11 hybridoma supernatants, Dr. Rainer Deutzman for performing the NH_2-terminal sequencing, Anne Pietryga-Krieger for cDNA sequencing, and Dr. Werner Falk for helpful advice and discussions. The excellent technical assistance of Lucia Schwarzfischer-Pfeilschifter and Ute Ackermann is greatly appreciated.

REFERENCES

1. Van Furth, R. (1982) *Immunobiology* **161**, 175–185
2. Reppoles, D. A., Mark, A., Banda, M. J., and Werb, Z. (1988) *Science* **241**, 708–712
3. Metcalf, D. (1991) *Science* **254**, 529–533
4. Rutherford, M. S., Witsell, A., and Schook, L. B. (1993) *J. Leukocyte Biol.* **53**,

[2] M. Rehli, S. W. Krause, M. Kreutz, and R. Andreesen, unpublished observations.

[3] A. Kunur, M. Kreutz, R. Knüchel, and R. Andreesen, submitted for publication.

602–618
5. Gordon, S., Fraser, I., Nath, D., Hughes, D., and Clarke, S. (1992) *Curr. Opin. Immunol.* **4**, 25–32
6. Musson, R. A. (1983) *Am. J. Physiol.* **111**, 331–340
7. Andreesen, R., Picht, J., and Löhr, G. W. (1983) *J. Immunol. Methods* **56**, 295–304
8. Andreesen, R., and Kreutz, M. (1994) *Ernst Schering Research Foundation Workshop 11: Cell Culture in Pharmaceutical Research* (Fusenig, E., and Graf, H., eds) pp. 9–37, Springer-Verlag Berlin, Heidelberg
9. Andreesen, R., Bross, K. J., Osterholz, J., and Emmerich, F. (1988) *Blood* **67**, 1257–1264
10. Andreesen, R., Gadd, S., Costabel, U., Leser, H. G., Speth, V., Cesnik, B., and Atkins, R. C. (1988) *Cell Tissue Res.* **253**, 271–279
11. Skidgel, R. A., Davis, R. M., and Tan, F. (1989) *J. Biol. Chem.* **264**, 2236–2241
12. Deddish, P. A., Skidgel, R. A., Kriho, V. B., Li, X.-Y., Becker, R. P., and Erdös, E. G. (1990) *J. Biol. Chem.* **265**, 15083–15088
13. Tan, F., Chan, S. J., Steiner, D. F., Schilling, J. W., and Skidgel, R. A. (1989) *J. Biol. Chem.* **264**, 13166–13170
14. Tanaka, H., Abe, E., Miyaura, C., Kuribayashi, T., Konno, K., Nishii, Y., and Suda, T. (1982) *Biochem. J.* **204**, 713–719
15. Bar-Shavit, Z., Teitelbaum, S. L., Reitsma, P., Hall, A., Pegg, L. E., Trial, J., and Kahn, A. J. (1983) *Proc. Natl. Acad. Sci. U. S. A.* **80**, 5907–5911
16. Olsson, I., Gullberg, U., Ivhed, I., and Nilsson, K. (1983) *Cancer Res.* **43**, 5862–5867
17. Mangelsdorf, D. J., Koeffler, H. P., Donaldson, C. A., Pike, J. W., and Haussler, M. R. (1984) *J. Cell Biol.* **98**, 391–398
18. Kreutz, M., and Andreesen, R. (1990) *Blood* **76**, 2457–2461
19. Andreesen, R., Brugger, W., Scheibenbogen, C., Kreutz, M., Leser, H. G., Rehm, A., and Löhr, G. W. (1990) *J. Leukocyte Biol.* **47**, 490–497
20. Cole, S. R., Ashman, L. K., and Ey, P. L. (1987) *Mol. Immunol.* **24**, 699–705
21. Meier, T., Arni, S., Malarkannan, S., Poinctelet, M., and Hoessli, D. (1992) *Anal. Biochem.* **204**, 220–226
22. Shapiro, A. L., Vinuela, E., and Maizel, J. V. (1967) *Biochem. Biophys. Res. Commun.* **128**, 155–164
23. Laemmli, U. K. (1970) *Nature* **227**, 680–685
24. Wessel, D., and Flügge, U. I. (1984) *Anal. Biochem.* **138**, 141–143
25. Towbin, H., Staehelin, T., and Gordon, J. (1979) *Proc. Natl. Acad. Sci. U. S. A.* **76**, 4350–4354
26. Skidgel, R. A. (1991) *Methods Neurosci.* **6**, 373–385
27. Smith, P. K., Krohn, R. I., Hermanson, G. T., Mallia, A. K., Gartner, F. H., Provenzano, M. D., Fujimoto, E. K., Goeke, N. M., Olson, B. J., and Klenk, D. C. (1985) *Anal. Biochem.* **150**, 76–85
28. Chomczynski, P., and Sacchi, N. (1987) *Anal. Biochem.* **162**, 156–159
29. Krause, S. W., Kreutz, M., Zenke, G., and Andreesen, R. (1992) *Ann. Hematol.* **64**, 190–195
30. Church, G. M., and Gilbert, W. (1984) *Proc. Natl. Acad. Sci. U. S. A.* **81**, 1991–1995
31. Van der Schoot, C. E., Huizinga, T. W. J., Gadd, S., Majdic, O., Wijmans, R., Knapp, W., and von dem Borne, A. E. G. K. (1989) in *Leukocyte Typing IV* (Knapp, W., Dörken, B., Gilks, W. R., Rieber, E. P., Schmidt, R. E., Stein, H., and von dem Borne, A. E. G. K., eds), pp. 887–891, Oxford Press, Oxford
32. Mizoguchi, A., Takasaki, S., Maeda, S., and Kobata, A. (1985) *J. Biol. Chem.* **259**, 11949–11957
33. Skidgel, R. A., Johnson, A. R., and Erdös, E. G. (1984) *Biochem. Pharmacol.* **33**, 3471–3478
34. Nagae, A., Abe, M., Becker, R. P., Deddish, P. A., Skidgel, R. A., and Erdös, E. G. (1993) *Am. J. Respir. Cell Mol. Biol.* **9**, 221–229
35. Nagae, A., Deddish, P. A., Becker, R. P., Anderson, C. H., Abe, M., Tan, F., Skidgel, R. A., and Erdös, E. G. (1992) *J. Neurochem.* **59**, 2201–2212
36. Skidgel, R. A. (1988) *Trends Pharmacol. Sci.* **9**, 299–304
37. Chodimella, V., Skidgel, R. A., Krowiak, E. J., and Murias, C. G. (1991) *Am. Rev. Respir. Dis.* **144**, 869–874
38. Desmazes, N., Lockhart, A., Lacroix, H., and Dusser, D. J. (1992) *Am. J. Respir. Cell Mol. Biol.* **7**, 477–484
39. Dragovic, T., Igic, R., Erdös, E. G., and Rabito, S. F. (1993) *Am. Rev. Respir. Dis.* **147**, 1491–1498
40. Lieberman, J. (1989) *Clin. Lab. Med.* **9**, 745–755
41. Adams, J. S., Singer, F. R., Gacad, M. A., Sharma, O. P., Hayes, M. J., Vouros, P., and Holick, M. F. (1985) *J. Clin. Endocrinol. & Metab.* **60**, 960–966

Cell, Vol. 103, 321–330, October 13, 2000, Copyright ©2000 by Cell Press

Opposing Effects of Ras on p53: Transcriptional Activation of *mdm2* and Induction of $p19^{ARF}$

Stefan Ries,*‖ Carola Biederer,*‖ Douglas Woods,* Ohad Shifman,† Senji Shirasawa,‡ Takehiko Sasazuki,‡ Martin McMahon,* Moshe Oren,† and Frank McCormick*§
*University of California, San Francisco Cancer Research Institute
San Francisco, California 94115
†Department of Molecular Cell Biology
Weizmann Institute of Science
Rehovot 76100
Israel
‡Kyushu University
Fukuoka, Japan

Summary

Mdm2 acts as a major regulator of the tumor suppressor p53 by targeting its destruction. Here, we show that the *mdm2* gene is also regulated by the Ras-driven Raf/MEK/MAP kinase pathway, in a p53-independent manner. Mdm2 induced by activated Raf degrades p53 in the absence of the Mdm2 inhibitor $p19^{ARF}$. This regulatory pathway accounts for the observation that cells transformed by oncogenic Ras are more resistant to p53-dependent apoptosis following exposure to DNA damage. Activation of the Ras-induced Raf/MEK/MAP kinase may therefore play a key role in suppressing p53 during tumor development and treatment. In primary cells, Raf also activates the Mdm2 inhibitor $p19^{ARF}$. Levels of p53 are therefore determined by opposing effects of Raf-induced $p19^{ARF}$ and Mdm2.

Introduction

Mdm2 was originally identified as an amplified gene in a spontaneously transformed derivative of BALB/c cell line 3T3 DM, which caused tumors when injected into nude mice (Fakharzadeh et al., 1991). A possible mechanism for the transforming properties of *mdm2* has been provided by reports demonstrating that Mdm2 is a major regulator of the tumor suppressor p53. It binds directly to p53 and inhibits its transcriptional activity (Momand et al., 1992; Oliner et al., 1992, 1993). Mdm2 is a transcriptional target of p53 (Barak et al., 1993; Wu et al., 1993; Leng et al., 1995). p53-responsive elements have been identified in the intronic promoter of the *mdm2* gene, and interaction of p53 with these sites has been well documented (Juven et al., 1993; Barak et al., 1994; Zauberman et al., 1995). Induction of *mdm2* transcription by p53 establishes a negative feedback loop, in which p53 itself initiates its own destruction (Picksley and Lane, 1993).

Mdm2 may have additional functions that are not directly related to p53. It affects cell growth in a p53-independent manner, possibly through interactions with pRb (Xiao et al., 1995) or through interaction with the E2F/DP1 complex (Martin et al., 1995). These functions of Mdm2 are less well characterized than its role in p53 regulation. Indeed, the lethal effects of disrupting *mdm2* genes in vivo are rescued by disrupting p53, suggesting that p53 regulation is the major function of this protein at least during early development (Jones et al., 1995; Montes de Oca Luna et al., 1995).

Mdm2 binds to $p19^{ARF}$ and is inhibited by this interaction (Kamijo et al., 1998; Pomerantz et al., 1998). An attractive model has been presented recently in which $p19^{ARF}$ binds to Mdm2, sequesters Mdm2 in nucleolar structures, and allows accumulation of p53 (Tao and Levine, 1999; Sherr and Weber, 2000). On the other hand, $p19^{ARF}$ directly inhibits Mdm2 ubiquitin ligase activity, suggesting a more direct role in Mdm2 regulation (Honda and Yasuda, 1999). $p14^{ARF}$, the human homolog of $p19^{ARF}$, is induced by E2F, myc and Ras, and thus provides a possible link from mitogenic signaling pathways to p53 induction (Bates et al., 1998; Palmero et al., 1998; Zindy et al., 1998). The Ras-regulated Raf/MEK/ERK kinase pathway has been reported to activate CDK4/cyclin D kinases, thereby phosphorylating pRb, which in turn leads to release of E2F-1 (Albanese et al., 1995; Peeper et al., 1997). The $p14^{ARF}$ promoter contains several E2F-1 binding sites and its activity was shown to be enhanced by overexpression of E2F-1 (Bates et al., 1998). The Ras/Raf/MEK/MAP kinase pathway can therefore lead indirectly to accumulation of $p14^{ARF}$ and inhibition of Mdm2 activity.

Mdm2 expression is often increased following mitogenic activation. Treatment of cells in culture with basic FGF increases levels of Mdm2 protein and cells constitutively exposed to a basic FGF autocrine loop are more refractory to killing by cisplatin, which to a large extent occurs through p53-mediated apoptosis (Shaulian et al., 1997). More recently, a screen for transcripts that accumulate in cells harboring a chimeric M-CSF/PDGF receptor identified *mdm2* as an immediate early gene (Fambrough et al., 1999). In addition, we have observed high levels of Mdm2 protein expression in human tumor cell lines that have little, if any, functional p53 (Ries et al., 2000). These data suggest regulation of *mdm2* expression by p53-independent pathways triggered by growth factors.

A common feature of signaling by diverse growth factors is the activation of the Ras/Raf/MEK/MAP kinase pathway. We therefore explored the possibility that this pathway is responsible for *mdm2* induction. We report that the *mdm2* promoter is indeed a target of the Ras/Raf/MEK/MAP kinase pathway. Hence, activation of Ras during normal cell signaling or through mutation in neoplastic transformation, can suppress p53 and thus facilitate cell proliferation and survival.

Results

Mdm2 Expression Is Regulated by the Ras/Raf Pathway

Mdm2 protein can be induced by exposure of cells to basic FGF (Shaulian et al., 1997) or IGF-1 (Leri et al., 1999). Likewise, *mdm2* mRNA accumulates upon activation of the PDGF receptor (Fambrough et al., 1999).

§To whom correspondence should be addressed (e-mail: mccormick@cc.ucsf.edu).
‖These authors contributed equally to this work.

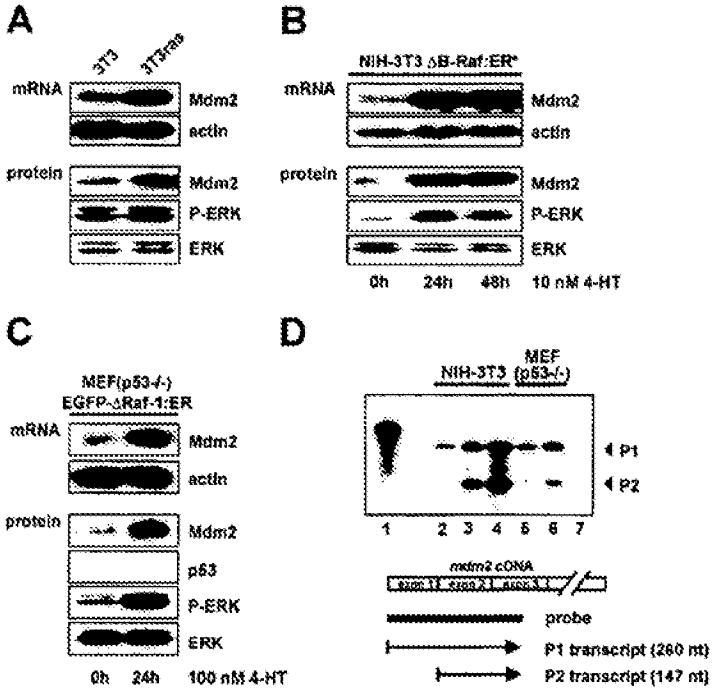

Figure 1. Induction of *mdm2* Transcription by Activated Ras and Raf

(A) *Mdm2* transcriptional induction by constitutively active H-Ras(G12V) in NIH-3T3 cells. NIH-3T3 cells were infected with retroviruses encoding H-Ras(G12V) or empty vector. After selection with G418, total cellular RNA was prepared and subjected to Northern blot analysis using a 1.5 kb fragment spanning the coding region of *mdm2* as a probe. For Western blot analysis, cells were directly lysed with Laemmli buffer, and equal amounts of total protein were subjected to immunoblotting.

(B) Activation of Raf is sufficient to induce *mdm2* transcription in NIH-3T3 cells. NIH-3T3 cells expressing a 4-Hydroxy-Tamoxifen (4-HT) inducible ΔB-Raf:ER* construct were treated with 10 nM 4-HT, total cellular RNA and protein harvested at the times indicated and subjected to Northern blot analysis or Western blot analysis.

(C) Transcriptional induction of *mdm2* by Raf is independent of p53. $p53^{-/-}$ mouse embryonic fibroblasts (MEF) harboring the 4-HT inducible EGFP-ΔRaf1:ER construct were treated with 100 nM 4-HT, and total cellular RNA and protein was harvested after 24 hr.

(D) Transcription by activated Raf initiates mainly from the internal *mdm2* promoter (P2). Total cellular RNA was prepared from the cell lines as indicated (top). Ten micrograms of each RNA was subjected to RNase protection analysis. Lanes 1 and 7 contain the probe alone and the control reaction consisting of 10 μg of yeast tRNA, respectively. Composition and sizes (in nucleotides) of potential RNase-resistant fragments are indicated in the schematic representation.

Since Ras is downstream of all these mitogens, we tested whether the Ras pathway is responsible for *mdm2* induction. NIH-3T3 cells expressing an activated Ras allele, H-Ras (G12V), were analyzed for *mdm2* mRNA and protein expression. Figure 1A shows that expression of constitutively active Ras resulted in increased levels of *mdm2* mRNA and protein.

Ras targets several distinct downstream effectors, of which the best characterized are Raf kinase, PI3-kinase, and RalGDS (Marshall, 1995; Katz and McCormick, 1997; Rodriguez-Viciana et al., 1997). We examined the effects of a conditionally active Raf kinase on cellular Mdm2 levels. This conditional Raf kinase consists of the kinase domain of B-Raf fused to a modified form of the hormone binding domain of the mouse estrogen receptor, which renders the receptor insensitive to estrogen, but still sensitive for the estrogen analog 4-hydroxy-tamoxifen (4-HT) (Samuels et al., 1993; Woods et al., 1997). NIH3T3 cells stably expressing the ΔB-Raf:ER* were treated with 10 nM 4-HT (Woods et al., 1997). Addition of 4-HT resulted in remarkable MAPK activation and accumulation of high levels of *mdm2* mRNA and protein (Figure 1B). To rule out any contribution of p53 to the increased Mdm2 levels after Raf activation, we assessed Mdm2 expression in $p53^{-/-}$ mouse embryo fibroblasts (MEFs) stably expressing EGFP-ΔRaf1:ER (Woods et al., 1997). Figure 1C shows increased transcription and accumulation of Mdm2 protein in response to Raf/MEK/MAPK activation occurred also in $p53^{-/-}$ fibroblasts. In a time course experiment using NIH3T3(ΔB-Raf:ER*) cells, elevated *mdm2* mRNA levels can be detected as early as 4 hr after Raf activation and increase steadily (data not shown). Thus, the Ras/Raf/MEK/MAP kinase pathway induces increased expression of *mdm2* mRNA and Mdm2 protein in a p53-independent manner.

The murine *mdm2* gene has two promoters, an internal promoter (P2), which responds directly to p53 activation, and an upstream constitutive promoter (P1), which is not affected by p53 (Barak et al., 1994). The cDNA riboprobe used for RNase protection assay spans exon 1, exon 2, and part of exon 3 (Figure 1D), allowing discrimination between P1 and P2 transcripts. Transcription from the P2 promoter was dramatically induced in response to activation of the Raf kinase, whereas a more moderate induction occurred with transcription from P1 (Figure 1D, lanes 2, 3, and 4). Induction of P2 transcription occurs in a p53-independent manner as p53-deficient MEFs show similar enhanced transcription arising from P2 (Figure 1D, lanes 5 and 6). Note that only P1 transcripts are detectable in control NIH-3T3 cells.

Analysis of Ras-Responsive Elements within the *mdm2* P2 Promoter

To determine the role of Raf activation on basal *mdm2* transcription, the effect of a constitutively activated form of Raf (Raf-CAAX) on *mdm2* promoter activity was examined in p53-deficient 10(1) cells (Stokoe et al., 1994). Raf-CAAX expression induced *mdm2* P2 promoter activity 5- to 6-fold (Figure 2B). Sequence analysis of the *mdm2* P2 promoter revealed the existence of binding sites for transcription factors of the AP-1 and Ets family (Figure 2A), which have been shown to be responsive to ERK activation in other genes. To determine the region of the *mdm2* P2 promoter required for regulation by Raf, several *mdm2* P2 5′ promoter deletions were generated and transfected in the presence of Raf-CAAX into 10(1) cells. Figure 2B shows that the upstream Ets site within the P2 promoter (designated EtsA in Figure 2B) of the *mdm2* gene is important for the Raf-induced

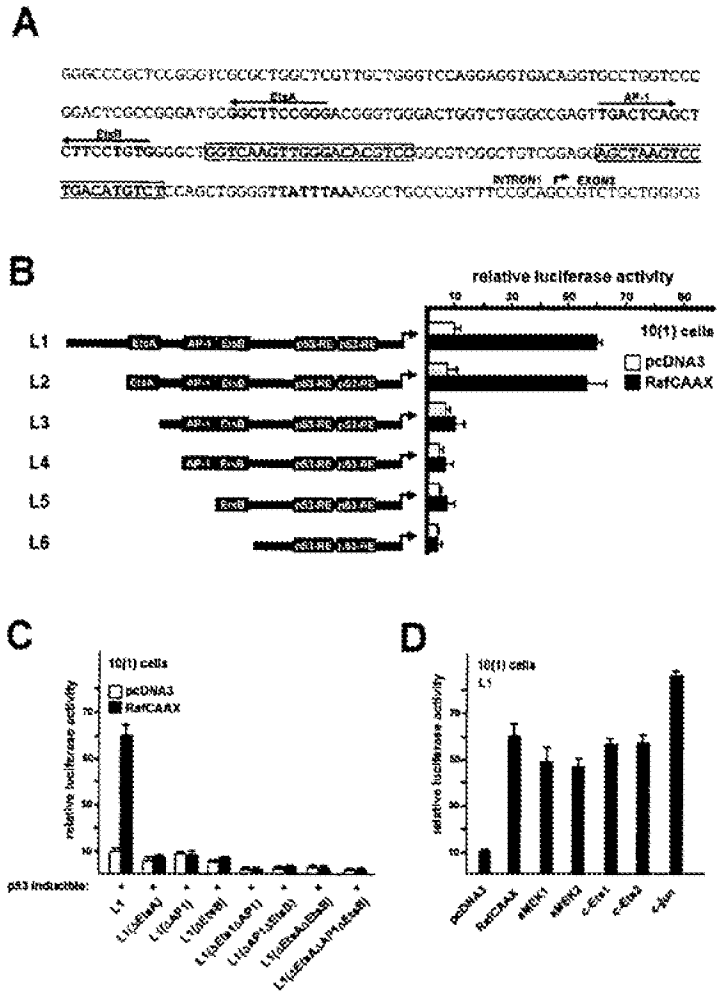

Figure 2. Ets/AP-1 Motifs in the Intronic P2 Promoter Mediate Transcription of the *mdm2* Gene upon Raf Activation

(A) DNA sequence of the intronic *mdm2* promoter (P2). The Ets and AP-1 binding sites are indicated by arrows, the p53-responsive elements are boxed, and the TATA box is marked in bold.

(B) Various 5′ deletions of the *mdm2* promoter were cloned in front of the firefly luciferase gene. 10(1) cells were cotransfected with 1 μg of each luciferase reporter construct and either 100 ng of a vector expressing CAAX-tagged Raf or the parental control vector (pcDNA3). Luciferase activity was determined using a luminometer.

(C) Using in vitro mutagenesis, Ets and AP-1 sites of the *mdm2* promoter luciferase construct L1 as in (B) were selectively mutated. Luciferase activity of the mutated promoter constructs in 10(1) cells was determined. All promoter constructs were responsive to cotransfected p53 (indicated as +).

(D) 10(1) were transiently transfected with 1 μg of the *mdm2* promoter luciferase construct L1 combined with 100 ng of plasmids directing expression of either constitutively active MEK1, c-Ets-1, c-Ets-2, or c-jun. Luciferase activity was determined.

transcriptional activation in a transient assay. To assess the importance of the more downstream Ets (designated EtsB) and AP-1 sites in the *mdm2* P2 promoter in response to activated Raf, single point mutations were introduced into the full-length *mdm2* P2 promoter construct L1 by site-directed mutagenesis. All promoter constructs that contain mutations in one of the Ets sites or the AP-1 site are nonresponsive to activated Raf anymore (Figure 2C). Furthermore, combinations of mutations of the Ets and AP-1 sites led to a significant decrease of basal *mdm2* P2 promoter activity (Figure 2C). To exclude the occurrence of potential nonspecific mutations during the generation of these constructs and to address whether the Raf kinase and p53 responsive elements are distinguishable, p53 was cotransfected with the mutated P2 promoter constructs in parallel experiments. All mutated *mdm2* promoter constructs showed a strong induction by p53 (~10-fold) similar to that of the parental L1 mdm2 promoter construct, demonstrating a clearly distinct regulation of the P2 promoter by either Raf or p53 (data not shown). Overexpression of constitutively activated forms of MEK1 and MEK2, c-Ets-1, c-Ets-2, and c-jun, which are known downstream targets of Ras and Raf, led to an approximately 5- to 8-fold induction of *mdm2* P2 promoter activity, respectively (Figure 2D). To determine whether the *mdm2* AP-1 and Ets sites were capable of binding the respective transcription factors, nuclear extracts were prepared from NIH-3T3 cells expressing ΔB-Raf:ER* at various times after stimulation with 10 nM 4-HT. The *mdm2* AP-1 site in probe GS1 bound a complex in NIH-3T3 nuclear extracts, the formation of which was increased strongly after activation of Raf (Figure 3A). This complex was competed by 50-fold molar excess cold cognate competitor oligonucleotide or unlabeled GS1 probe but not by mutant AP-1 sequences or unlabeled probe GS2 (Figure 3A). When the labeled upstream *mdm2* Ets site (EtsA) was used as probe in electrophoretic mobility shift assays, formation of a complex could be detected, whose intensity remained unchanged after Raf activation. These studies demonstrate that transcription factors bind to the AP-1 and Ets elements in the *mdm2* promoter.

Raf Regulates p53 Levels through Its Effects on Mdm2

Induction of Mdm2 protein expression is expected to decrease levels of p53, since Mdm2 effectively promotes p53 degradation (Haupt et al., 1997; Kubbutat et al., 1997). To test this prediction, Raf kinase was activated in human tumor cells expressing mutant p53, and levels of Mdm2 and p53 proteins were analyzed by Western blotting. DKO4 cells were used, in which mutant

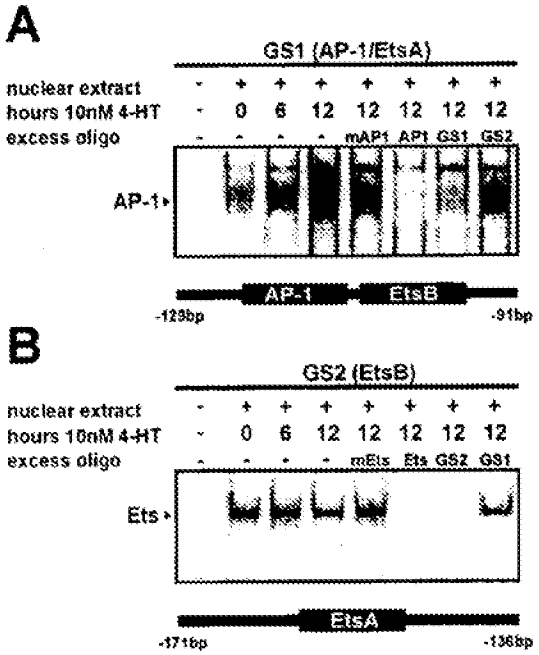

Figure 3. Transcription Factors Bind to the AP-1 and Ets Elements in the *mdm2* Promoter

(A) Nuclear extracts were prepared from NIH-3T3 cells expressing ΔB-Raf:ER* at the indicated time points after stimulation with 4-HT. EMSAs were performed with ^{32}P-labeled GS1-oligonucleotide comprising the AP-1/Ets element. In competition experiments, 50-fold molar excess of cold AP-1 or mutated AP-1 consensus oligonucleotide (AP1 and mAP1, respectively) was added to the binding reaction.
(B) EMSAs were carried out with ^{32}P-labeled GS2-oligonucleotide comprising the Ets site of the *mdm2* promoter.

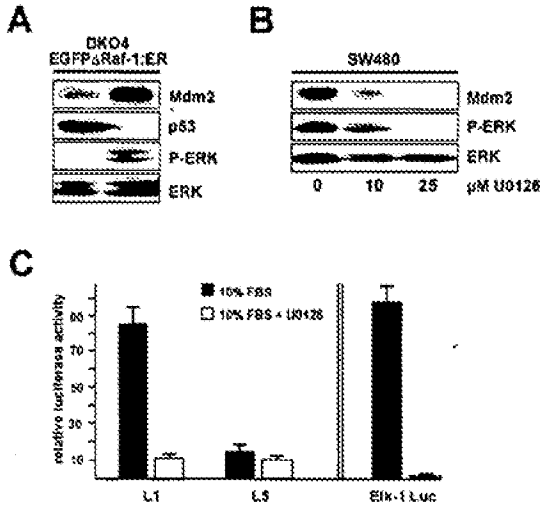

Figure 4. The Ras/Raf/MEK/MAPK Pathway Has an Impact on Mdm2 Expression Levels in Colon Cancer

(A) DKO4 cells expressing a EGFP-ΔRaf-1:ER construct were treated with 100 nM 4-HT. Twenty-four hours later, total cellular lysates were prepared. Equal amounts of proteins were separated by SDS-PAGE followed by immunoblotting with antibodies against Mdm2, p53, phosphorylated ERK1/2, or total ERK.
(B) SW480 cells were cultured 48 hr in the presence or absence of the MEK inhibitor U0126 and 10% fetal bovine serum. Equal amounts of proteins were electrophoretically separated prior to immunoblotting with Mdm2, phosphorylated ERK1/2, or total ERK antisera.
(C) SW480 cells were transfected with either 1 μg of the *mdm2* promoter luciferase construct L1 or the further 5′-deleted promoter construct L5, which lacks the Ras responsive elements. Transfected cells were incubated 48 hr in the presence or absence of 25 μM U0126 prior to measurement of luciferase activity. To monitor efficacy of the MEK inhibitor, U0126 Elk-1 activity was determined using a commercially available Elk-1 luciferase reporter system (right panel).

Ras had been deleted by homologous recombination (Shirasawa et al., 1993), and a conditionally active Raf allele (EGFP-ΔRaf-1:ER) was stably expressed in these cells (Woods et al., 1997). Raf kinase was turned on by addition of 4-HT, and Mdm2 levels accumulated (Figure 4A). p53 is transcriptionally inactive in these cells (Esteller et al., 2000). Hence, these data further confirm that Raf-dependent *mdm2* transcription is independent of p53 transcriptional activity. Importantly, increased Raf activity led to a dramatic decrease of p53 protein levels (Figure 4A). It is important to note that DKO4 cells, despite harboring a mutated p53 gene, do not express $p14^{ARF}$ due to hypermethylation of the $p14^{ARF}$ promoter (Esteller et al., 2000).

SW480 cells express an activated Ras allele and a mutant form of p53 that is transcriptionally inactive (Sharma et al., 1993). Treatment of these cells with the MEK inhibitor U0126 resulted in dose-dependent decrease in Mdm2 protein expression (Figure 4B) consistent with reduced MAPK activation, showing that sustained activity of the Ras/Raf/MEK/MAP kinase pathway is necessary for high levels of Mdm2.

To examine whether decrease of Mdm2 protein expression results from reduced transcriptional activity of the *mdm2* promoter upon MAPK inhibition, we measured *mdm2* P2 promoter activity. SW480 cells were transfected with either the *mdm2* P2 promoter construct L1, containing all the Raf-responsive elements, or the 5′ deleted L5 *mdm2* P2 promoter construct lacking the Ets and AP-1 binding motifs. Immediately after transfection, one fraction of the cells was incubated with 25 μM U0126 for 48 hr, while the other fraction of cells was incubated in medium without the MEK inhibitor. As displayed in figure 4C, an approximately 7-fold decrease of *mdm2* P2 promoter activity was observed upon U0126 treatment only in cells transfected with the Raf responsive *mdm2* promoter construct L1. Luciferase activity of cells containing the *mdm2* promoter construct L5 was significantly lower and did not change upon addition of MEK inhibitor U0126.

Ras Mutations Lead to Attenuation of the p53 Response and Increased Survival Rate upon γ-Irradiation

To investigate whether the increased Mdm2 protein levels due to constitutive activation of Ras can prevent or attenuate p53 induction in response to cellular stress, we γ-irradiated NIH-3T3 cells or NIH-3T3 cells stably expressing a vector encoding H-Ras (G12V). Figure 5A shows the time course of p53 induction in both cell lines. In the parental NIH-3T3 cells, p53 protein was dramatically induced after γ-irradiation. Increased p53 levels are already detectable after 30 min and reach a

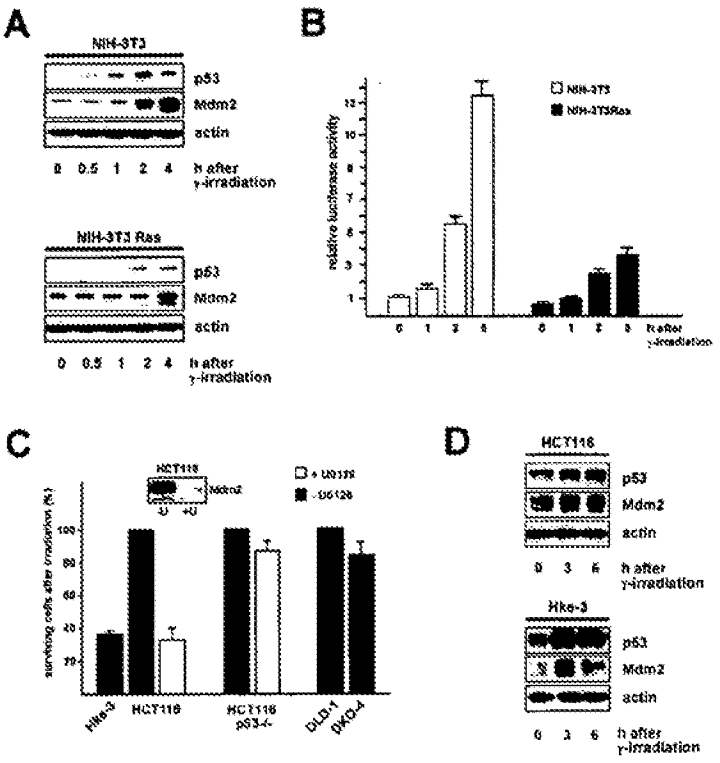

Figure 5. Kinetics of p53 Induction upon γ-Irradiation and Radiation Survival Are Affected by the Ras/Raf/MEK/MAPK Pathway

(A) Logarithmically growing cultures of NIH-3T3 cells stably transfected with oncogenic H-Ras(G12V) or vector alone were subjected to γ-irradiation at a dosage of 3 Gy. Proteins were electrophoretically separated, immobilized, and immunoblotted with antibodies specific to Mdm2, p53, or β-actin. Lysates (NIH-3T3 and NIH-3T3 Ras) were run on the same gel. Exposure time is identical for each protein shown, allowing direct comparison of signal intensity.

(B) 1×10^5 NIH-3T3 cells and Ras-transformed NIH-3T3 cells, respectively, were seeded in 6-well plates. The next day, cells were transfected with 1 μg p53-responsive luciferase reporter and exposed to ionizing radiation at a dosage of 3 Gy. Luciferase activity was determined using a luminometer.

(C) Clonal survival assays were performed using the human colon cancer cell lines HCT116 and DLD-1, and their isogenic derivatives Hke3, HCT116 $p53^{-/-}$, and DKO4, respectively. Cells were irradiated at a dosage of 5 Gy in a ^{137}Cs source. Survival rate for HCT116, HCT116 $p53^{-/-}$, and DLD-1, respectively, was set 100% in each set of comparisons.

(D) Time course of Mdm2 and p53 protein levels in HCT116 cells and its derivative Hke-3 after γ-irradiation (3 Gy). All lysates were run on the same gel. Exposure time is identical for each protein shown, allowing direct comparison of signal intensity.

maximum at 2 hr post irradiation. After 4 hr, p53 protein levels decreased but were still above the basal level in nonirradiated cells. Expression of Mdm2 protein in NIH-3T3 cells was strongly induced beginning 1 hr after irradiation of the cells and peaked at 4 hr. In contrast, γ-irradiation of NIH-3T3 cells harboring an activated Ras led to only a moderate increase of p53 protein. Furthermore, the onset of p53 induction in these cells is delayed compared to the parental NIH-3T3 cell line (1 hr in Ras-transformed NIH-3T3 cells versus 30 min in NIH-3T3 cells). While Ras-transformed NIH-3T3 cells have already higher basal Mdm2 protein levels (originating from the induced transcription of the *mdm2* P2 promoter by activated Ras), there was no significant increase of Mdm2 protein up to 4 hr after γ-irradiation. Thus, NIH-3T3 cells harboring an activated form of Ras are capable of attenuating the p53 response upon γ-irradiation, which is consistent with their increased basal Mdm2 protein expression.

Next, we wished to investigate the activity of the induced p53 in response to irradiation. We examined p53 activity after γ-irradiation in NIH-3T3 Ras cells using a luciferase assay. For this purpose, we transfected a synthetic p53 luciferase reporter construct into NIH-3T3 and Ras-transformed NIH-3T3 cells. Twenty-four hours after transfection, cells were irradiated at a dosage of 3 Gy and luciferase activity was determined at the indicated time points. Figure 5B displays the time course of p53 activation after γ-irradiation. While NIH-3T3 cells reveal a 12-fold induction of p53 transcriptional activity 4 hr after irradiation, their Ras-transformed counterparts show only a modest p53 response (4-fold). Thus, Ras overexpression attenuates not only p53 accumulation but also p53 activation in response to DNA damage.

This attenuation of p53 might explain the higher resistance of transformed NIH-3T3 cells toward γ-irradiation as determined in clonal survival assays (data not shown) (Sklar, 1988). Because Ras activation targets many downstream effectors (Katz and McCormick, 1997), we examined whether increased Mdm2 protein levels could mimick Ras-mediated radioresistance. Therefore, we established a stable NIH-3T3 cell line expressing Mdm2 protein under control of a mifepristone-inducible promoter (NIH-3T3-imdm2). Mifepristone-treated NIH-3T3-imdm2 cells and their parental counterpart, stably expressing the empty vector, were irradiated and subsequently, clonal survival assays were performed. Mdm2 expression partially rescues NIH-3T3 cells from irradiation-induced apoptosis (92% survivors in Mdm2 expressing NIH-3T3 versus 78% at 3 Gy; 49% versus 29% at 5 Gy).

To determine whether oncogenic Ras mutations confer radioresistance in human tumor cells, we performed clonal survival assays with the human colon cancer cell line HCT116 (wild-type p53, mutant Ras) and its derivative Hke-3, in which the mutant Ras has been deleted by homologous recombination (Shirasawa et al., 1993). Figure 5 shows Hke-3 express less Mdm2 protein and more p53 than HCT116 cells, consistent with a role for Ras in this pathway. p53 accumulated to significantly higher levels in Hke3 cells after γ-irradiation, presumably because of lower levels of Mdm2 (Figure 5D), and radiosensitivity of these cells increased dramatically (80% survivors versus 28% survivors at 5 Gy; similar results were obtained at a dosage of 1 Gy). Furthermore, inhibition of MEK in the parental HCT116 cell line through addition of U0126 resulted in a similar radiosensitive phenotype as in Hke-3 cells (Figure 5D). Treatment of

the p53-deficient isogenic cell line HCT116 $p53^{-/-}$ (Bunz et al., 1998) with the MEK inhibitor U0126 revealed no significant difference in radiosensitivity, showing that Ras-mediated radioresistance is dependent on p53. The colon cancer cell line DLD-1 harboring mutant p53 and Ki-Ras genes shows no difference in radioresistance compared to its counterpart DKO4, in which the mutant Ras has been deleted (Figure 5C), suggesting that Ras has no impact in cells lacking p53. However, it is important to note that DLD-1 and HCT116 cells do not share an identical genetic background. Nonetheless, this demonstrates an important role for oncogenic Ras mutations in the presence of wild-type p53 in conferring radioresistance in human tumors.

Taken together, these results provide strong evidence that activated H-Ras leads to increased basal Mdm2 protein expression, which is capable of attenuating p53 induction upon γ-irradiation and renders cells more resistant to the inhibitory effects of irradiation.

Attenuation of p53 Accumulation in Response to DNA-Damaging Reagents by Activated Raf is Dependent on the $p19^{ARF}$ Status

$p19^{ARF}$ physically interacts with Mdm2 and consequently stabilizes p53 (Kamijo et al., 1998; Pomerantz et al., 1998; Stott et al., 1998). To investigate whether the presence of $p19^{ARF}$ can prevent Raf-induced Mdm2 from degrading p53, we established wild-type MEFs and $p19^{ARF}$ null MEFs expressing a conditionally active Raf allele (EGFP-ΔRaf-1:ER) (Kamijo et al., 1997). MEFs and $p19^{ARF}$ null MEFs with induced and noninduced Raf kinase were treated with the DNA damaging reagent adriamycin (0.25 μg/ml). As shown in Figure 6, activation of Raf leads to a significant induction of Mdm2 protein after 24 hr in both cell lines. Concomitantly, $p19^{ARF}$ levels increase in 4-HT-treated wild-type MEFs expressing EGFP-ΔRaf1:ER (Figure 6A). While Raf-induced Mdm2 can attenuate p53 accumulation in response to DNA damage in $p19^{ARF}$ null MEFs, we detect no attenuation of p53 response in wild-type MEFs upon Raf activation (Figures 6A and 6B). These results provide evidence that $p19^{ARF}$ is capable of neutralizing the increased Mdm2 protein in response to activation of the Ras/Raf/MEK/MAP kinase pathway. If $p19^{ARF}$ is not expressed due to a targeted deletion of exon1β of the INK4A gene locus (Kamijo et al., 1997), induced Mdm2 protein is fully functional, can bind to p53, and promote its degradation.

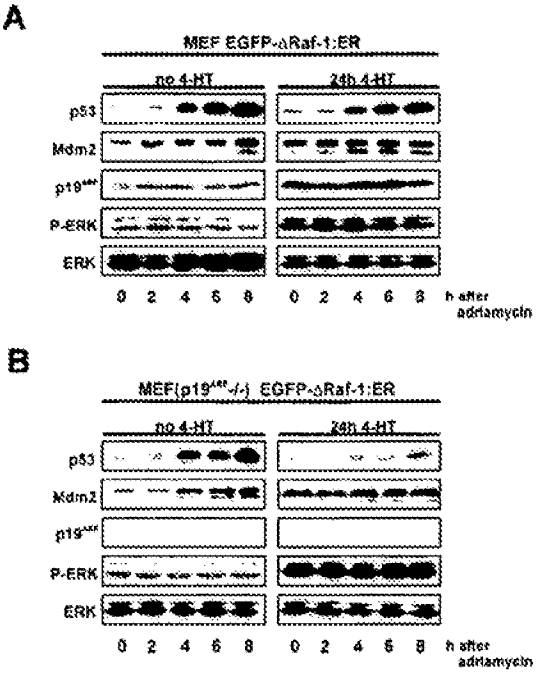

Figure 6. Attenuation of the p53 Accumulation by Raf-induced Mdm2 in Response to DNA Damage Depends on the $p19^{ARF}$ Status

(A) Wild-type MEFs expressing a 4-Hydroxy-Tamoxifen (4-HT) inducible EGFP-ΔRaf1:ER construct were treated with 1 μM 4-HT (right panel), or mock treated (left panel). After 24 hr, adriamycin (0.25 μg/ml) was added to the culture medium. Total protein was harvested at the indicated time points after addition of adriamycin and subjected to Western blot analysis. Lysates (+/− 4-HT) were run on the same gel. Exposure time is identical for each protein shown, allowing direct comparison of signal intensity.

(B) $p19^{ARF}$ null MEFs expressing a 4-Hydroxy-Tamoxifen (4-HT) inducible EGFP-ΔRaf1:ER construct were treated with 1 μM 4-HT (right panel), or mock treated (left panel). Twenty-four hours later, adriamycin (0.25 μg/ml) was added to the medium.

Discussion

p53 is the major known regulator of its own inhibitor, Mdm2 (Barak et al., 1993; Wu et al., 1993). Mdm2-mediated degradation of p53 occurs in the cytoplasm, through a proteasome-dependent pathway (Haupt et al., 1997; Kubbutat et al., 1997). Hence, p53 and Mdm2 have been postulated to form an autoregulatory negative feedback loop. Regulation of *mdm2* expression by p53 is thought to keep p53 function under control, thereby preventing widespread p53-dependent apoptosis (Lane and Hall, 1997; Prives, 1998).

In this study, we demonstrate that Mdm2 expression is also modulated by the Ras/Raf/MEK/MAP kinase pathway through activation of Ets and AP-1 sites in the P2 promoter, upstream from the p53 responsive element and independent of its activity. Furthermore, Mdm2 induced by the Ras/Raf/MEK/MAP kinase pathway is functionally active and leads to degradation of p53. This signaling pathway is intact in tumor cells expressing activated Ras as Mdm2 protein levels decrease dramatically after inhibiting MEK activity in these cells. Importantly, the effects of induced Mdm2 on p53 are regulated by $p19^{ARF}$. Ras therefore acts on p53 through two competing pathways (Figure 7). Activation of the Ras/Raf/MEK/MAP kinase cascade results in elevated levels of Mdm2 protein. However, in normal cells, this pathway also induces the expression of $p19^{ARF}$ (Bates et al., 1998; Palmero et al., 1998), which inhibits Mdm2 activity (Tao and Levine, 1999; Sherr and Weber, 2000). Thus, in normal cells, levels of p53 are determined by a balance between opposing effects of the Ras/Raf/MEK/MAP kinase pathway. In MEFs, these opposing effects are equivalent, and Raf is ineffective at inducing p53, despite its effects in $p19^{ARF}$. In different cell types, or even in MEFs growing under slightly different conditions, the balance of these opposing pathways is likely to be different. For example, in IMR90 human diploid fibroblasts, activated MEK leads to accumulation of p53, presumably because $p14^{ARF}$ exceeds Mdm2 induction (Lin et al., 1998). In Figure 7, DNA damaging agents are shown

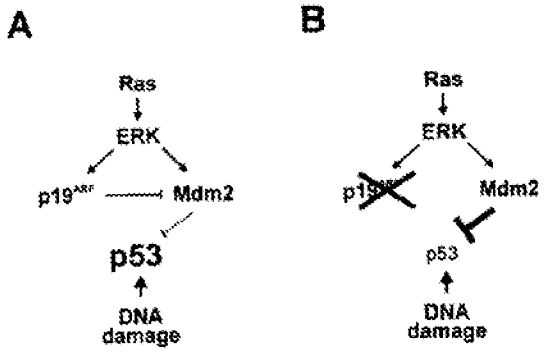

Figure 7. Model for the Regulation of p53 by the Ras/Raf/MEK/MAP Kinase Pathway

(A) Control of p53 levels in wild-type cells. Activation of the Ras/Raf/MEK/MAP kinase leads to transcriptional induction of $p19^{ARF}$ by E2F-1 via the cyclin D/CDK4/Rb pathway. Although Mdm2 protein is also induced, $p19^{ARF}$ is capable of keeping Mdm2 functionally inactive. p53 accumulates rapidly after DNA damage.

(B) Control of p53 levels in cells lacking $p19^{ARF}$. Activated Ras/Raf/ERK kinase induces the transcription of *mdm2*. Because $p19^{ARF}$ is not expressed, the elevated Mdm2 protein is functionally active and attenuates p53 accumulation in response to DNA damage.

regulating p53 in a $p19^{ARF}$-independent manner; however, it is possible that $p19^{ARF}$ affects the magnitude or duration of the p53 response to DNA under some physiological circumstances. In contrast to the Ras/Raf/MEK/MAP kinase pathway, which activates opposing regulators of p53, E1A induces $p19^{ARF}$ but does not directly induce Mdm2 (de Stanchina et al., 1998). E1A is therefore a potent inducer of p53.

p53 function is lost by mutation of the p53 gene in about 60% of all human tumors (Hollstein et al., 1991; Levine et al., 1991). In many of the remaining tumors, p53 function is abrogated by overexpression of Mdm2 (Oliner et al., 1992), expression of HPV E6 (Scheffner et al., 1991), or by loss of $p14^{ARF}$ expression (Kamb et al., 1994; Cordon-Cardo, 1995; Haber, 1997). In about 30% of human tumors, Ras is activated by mutation (Bos, 1989). Although Ras mutation and p53 mutation seem to be independent events (Mitsudomi et al., 1992), Ras-induced Mdm2 might block p53 from inducing apoptosis or growth arrest in the early phase of tumor development allowing coexistence of Ras mutations and wild-type p53. For example, Ras mutations precede p53 mutations in the stepwise development of colon cancer (Kinzler and Vogelstein, 1996). Activation of Ras may suppress p53 during the early stages of tumor development. Moreover, some mutant forms of p53 may retain residual activity (Friedlander et al., 1996). Elevated Mdm2 protein levels induced by Ras activation may bind those mutated forms of p53 and abolish remaining p53 function. Consistent with this, we find that the Ras/Raf/MEK/MAP kinase pathway suppresses expression of mutant p53 in DKO4 colon cancer cells. In addition, p53-independent transformation properties of Mdm2 have been reported. Sarcomas harboring *mdm2* gene amplifications together with p53 mutations show worse prognosis, when compared to tumors with genetic alterations of p53 or *mdm2* alone (Cordon-Cardo et al., 1994). Therefore, Ras-induced Mdm2 might contribute to tumor progression in a p53-independent manner. Mouse models have revealed that tumors in which p53 is lost through mutation or by loss of $p19^{ARF}$ are phenotypically similar, at least in the early stages of tumor development (Donehower et al., 1992; Kamijo et al., 1997). However, tumors that have lost p53 by direct mutation are genetically unstable relative to those that have lost p53 function through mutation of $p19^{ARF}$ (Kamijo et al., 1997). The latter tumors may retain residual p53 function that protects cells from genetic rearrangement. Indeed, p53 transcriptional activity can be measured easily in $p14^{ARF}$-deficient tumor cells that retain low levels of p53 protein. In these tumors, activation of Ras may suppress residual p53 and allow tumor progression.

In addition to a role in tumor development, Ras regulation of *mdm2* and p53 may have important implications in cancer treatment. Tumors carrying constitutively active forms of Ras might be more resistant to treatment with ionizing radiation and chemotherapy. This idea is supported by previous observations that Ras-transformed NIH-3T3 cells are relatively resistant to radiation induced apoptosis (FitzGerald et al., 1985; Sklar, 1988). Chang and coworkers examined the radiation survival of various NIH-3T3 transformants representative of the various classes of oncogenes that may be involved in the pathway. In their study, Ras, Raf, Ets, and jun overexpressed in NIH-3T3 cells conferred a radiation resistant phenotype (Pirollo et al., 1993). Interestingly, chronic Ras transformation leads to an increase in AP-1 activity and upregulation of c-jun (Cook et al., 1999). As overexpression of transcription factors c-jun and Ets mediates radioresistance, a newly transcribed protein that functions as an inhibitor of radiation-induced apoptosis is likely to be involved. We provide evidence that Mdm2, a well characterized inhibitor of p53 activity, mediates the radioresistant phenotype conferred by oncogenic Ras. Our study demonstrates that constitutively active Ras induces *mdm2* transcription via activation of transcription factors binding to the AP-1 and Ets elements within the promoter. In the absence of $p19^{ARF}$, elevated Mdm2 protein levels resulting from constitutively active Ras/Raf/MEK/MAP signaling lead to attenuated and diminished p53 response and increased survival rates upon DNA damage. We propose that higher basal levels of Mdm2 protein in Ras-transformed cells prevents the accumulation of stable p53 protein and the subsequent induction of apoptosis or growth arrest in response to DNA damage.

Recently, we have suggested that high levels of Mdm2 activity explain why the E1B55k-deleted adenovirus dl1520 (ONYX-015) replicates efficiently in many tumor cell lines that retain wild-type p53 (Ries et al., 2000). Oncogenic Ras, or other events that upregulate the MAP kinase pathway, could contribute to replication of dl1520 in these cells by elevating levels of Mdm2 protein.

In vivo studies provide further evidence for the importance of Ras-controlled Mdm2 expression. Inhibition of oncogenic Ras activity in mouse models, through pharmacological intervention or genetic manipulation, leads to death by apoptosis (Lebowitz et al., 1997; Johnson et al., 1997; Heimbrook and Oliff, 1998). This could be due, in part, to activation of p53 through reduced expression of Mdm2. To reevaluate the role of *mdm2* and $p19^{ARF}$ in Ras-induced tumor development in vivo, we are currently investigating the contribution of this pathway in a defined multistage mouse tumor model.

In conclusion, we have shown that Mdm2 is a transcriptional target of the Ras/Raf/MEK/MAP kinase pathway, and that this activation is independent of p53. Ras

therefore regulates p53 through opposing pathways involving Mdm2 and its inhibitor p14^{ARF}. In cancer cells lacking p14^{ARF}, Ras suppresses p53 expression. This may have important implications in cancer development and therapy.

Experimental Procedures

Antibodies and Reagents

Rabbit polyclonal anti-phospho-ERK and anti-ERK antibodies were obtained from NEB, mouse monoclonal anti-β-actin antibody was purchased from Sigma, and sheep polyclonal anti-p53 antibody Ab-7 was obtained from Calbiochem. Mouse monoclonal anti-Mdm2 antibody 2A10 was kindly provided by G. Zambetti (St. Jude Children's Hospital). The Dual Luciferase system and the MEK-inhibitor U0126 were from Promega.

Plasmids

Retroviral vectors (pBabe puro or pWZL3blast) expressing ΔB-Raf:ER*, EGFPΔRaf-1:ER proteins, or H-Ras(G12V) have been described elsewhere (Rodriguez-Viciana et al., 1997; Woods et al., 1997). Antisense riboprobe for RNase protection assay contains the murine *mdm2* cDNA fragment spanning from nt +264 to nt +3 (Barak et al., 1994).

Tissue Culture and Cell Lines

p19^{ARF} null mouse embryo fibroblasts (Kamijo et al., 1997) and wild-type mouse embryo fibroblasts expressing the EGFP-ΔRaf-1:ER construct were used for experiments between passage 5 and 8 (Kamijo et al., 1997).

All cell lines were maintained in phenol-free DMEM H21 medium to prevent basal activation of the Raf:ER fusion protein. Asynchronous cell populations were treated with 10 nM 4-HT (for ΔB-Raf:ER*) or 100 nM (for EGFPΔRaf-1:ER) at 80% confluency for 24 hr or 48 hr, respectively. SW480 cells were maintained in Leibovitz medium supplemented with 10% heat-inactivated fetal bovine serum. To establish an inducible Mdm2 NIH-3T3 cell line, the commercially available pSwitch system (Invitrogen) was used. In radiation survival experiments, NIH-3T3 cells stably transfected with the pSwitch vector only treated with mifepristone (10^{-8} M) served as control.

Transfections and Luciferase Reporter Gene Assay

Reporter assays were performed as described previously using the Dual Luciferase system from Promega (Biederer et al., 2000). p53 activity was monitored using the PathDetect In Vivo Signal Transduction Pathway *Cis*-Reporting System (Stratagene, LaJolla, CA).

Northern Blot Analysis

Total cellular RNA was isolated using the RNeasy kit (Qiagen). Ten micrograms of total RNA per lane was subjected to a 0.9% agarose formaldehyde gel electrophoresis, transferred to Hybond N^{+} membrane, and UV cross-linked (1200 μJ). Prehybridization, hybridization, and washing of blots were performed at 60°C in QuickHyb buffer (Amersham). The blots were stripped by boiling in 0.1% SDS, and then reprobed.

RNase Protection Assay

Ribonuclease protection assays were performed using the RPA II kit (Ambion) and a cDNA riboprobe corresponding to exons 1–3 of the full-length *mdm2* transcript. *Mdm2* mRNA arising from the upstream promoter protects a fragment of 260 nt, whereas mRNA initiated from the internal promoter (P2) yields a fragment of 147 nt (Barak et al., 1994).

Western Blot Analysis

Cells were lysed in 2×Laemmli buffer and equal amounts of protein were separated by SDS-PAGE, transferred onto nitrocellulose membranes, and incubated with various antibodies. All immunoblots were visualized by enhanced chemiluminescence detection system (Amersham).

Site-Directed Mutagenesis

Missense mutations were engineered into the various mdm2 promoter luciferase constructs by primer-mediated mutagenesis using the QuickChange mutagenesis kit (Stratagene). All mutations were verified by sequencing.

Electrophoretic Mobility Shift Assay

Double-stranded oligonucleotides spanning regions −129 bp to −91 bp (GS1), and −171 bp to −136 bp (GS2) of *mdm2* intron 1 (respective to the first nucleotide of exon 2) were labeled with [α-^{32}P]dCTP. Nuclear extracts of NIH-3T3 cells were prepared as described elsewhere (Andrews and Faller, 1991). EMSAs were carried out using 10 μg nuclear extract as previously described (Moser et al., 1995).

Acknowledgments

We are grateful to G. Zambetti for the generous gift of Mdm2 antibody 2A10 and P. Rodriguez-Viciana for H-Ras(G12V) expression vector. The p19^{ARF} null MEFs were generously provided by C. Sherr and M. Roussel. HCT116 p53$^{-/-}$ cells were a kind gift of F. Bunz and B. Vogelstein. We thank J. Ghysdael and M. Karin for expression vectors encoding c-ets-1, c-ets-2, and c-jun, F. Zindy for helpful advice with the mouse p53 antibody Ab-7, and M. Humbert for DKO4 cells expressing ΔRaf:ER. We are indebted to C. Brandts for critically reading the manuscript and to A. Balmain for exciting discussions. We thank P. Sabbatini, H. Jiang, O. Tetsu, C. O'Shea, D. Stokoe, A. Bhat, and A. Mirza for fruitful discussions and all members of the McCormick lab for their support. S. Ries received a DAAD fellowship as part of the "Gemeinsames Hochschulsonderprogramm III von Bund und Laendern". This study was supported by the David A. Wood Foundation.

Received May 30, 2000; revised September 5, 2000.

References

Albanese, C., Johnson, J., Watanabe, G., Eklund, N., Vu, D., Arnold, A., and Pestell, R.G. (1995). Transforming p21ras mutants and c-Ets-2 activate the cyclin D1 promoter through distinguishable regions. J. Biol. Chem. *270*, 23589–23597.

Andrews, N.C., and Faller, D.V. (1991). A rapid micropreparation technique for extraction of DNA-binding proteins from limiting numbers of mammalian cells. Nucleic Acids Res. *19*, 2499.

Barak, Y., Juven, T., Haffner, R., and Oren, M. (1993). mdm2 expression is induced by wild type p53 activity. EMBO J. *12*, 461–468.

Barak, Y., Gottlieb, E., Juven-Gershon, T., and Oren, M. (1994). Regulation of mdm2 expression by p53: alternative promoters produce transcripts with nonidentical translation potential. Genes Dev. *8*, 1739–1749.

Bates, S., Phillips, A.C., Clark, P.A., Stott, F., Peters, G., Ludwig, R.L., and Vousden, K.H. (1998). p14ARF links the tumour suppressors RB and p53. Nature *395*, 124–125.

Biederer, C., Ries, S., Moser, M., Florio, M., Israel, M., McCormick, F., and Buettner, R. (2000). The basic helix-loop-helix transcription factors myogenin and Id2 mediate specific induction of the caveolin-3 gene expression during embryonic development. J. Biol. Chem. *275*, 28245–28251.

Bos, J.L. (1989). ras oncogenes in human cancer: a review. Cancer Res. *49*, 4682–4689.

Bunz, F., Dutriaux, A., Lengauer, C., Waldman, T., Zhou, S., Brown, J.P., Sedivy, J.M., Kinzler, K.W., and Vogelstein, B. (1998). Requirement for p53 and p21 to sustain G2 arrest after DNA damage. Science. *282*, 1497–1501.

Cook, S.J., Aziz, N., and McMahon, M. (1999). The repertoire of fos and jun proteins expressed during the G1 phase of the cell cycle is determined by the duration of mitogen-activated protein kinase activation. Mol. Cell. Biol. *19*, 330–341.

Cordon-Cardo, C., Latres, E., Drobnjak, M., Oliva, M.R., Pollack, D., Woodruff, J.M., Marechal, V., Chen, J., Brennan, M.F., and Levine,

A.J. (1994). Molecular abnormalities of mdm2 and p53 genes in adult soft tissue sarcomas. Cancer Res. *54*, 794–799.

Cordon-Cardo, C. (1995). Mutations of cell cycle regulators. biological and clinical implications for human neoplasia. Am. J. Pathol. *147*, 545–560.

de Stanchina, E., McCurrach, M.E., Zindy, F., Shieh, S.Y., Ferbeyre, G., Samuelson, A.V., Prives, C., Roussel, M.F., Sherr, C.J., and Lowe, S.W. (1998). E1A signaling to p53 involves the p19(ARF) tumor suppressor. Genes Dev. *12*, 2434–2442.

Donehower, L.A., Harvey, M., Slagle, B.L., McArthur, M.J., Montgomery, C.A., Jr., Butel, J.S., and Bradley, A. (1992). Mice deficient for p53 are developmentally normal but susceptible to spontaneous tumours. Nature *356*, 215–221.

Esteller, M., Tortola, S., Toyota, M., Capella, G., Peinado, M.A., Baylin, S.B., and Herman, J.G. (2000). Hypermethylation-associated inactivation of p14(ARF) is independent of p16(INK4a) methylation and p53 mutational status. Cancer Res. *60*, 129–133.

Fakharzadeh, S.S., Trusko, S.P., and George, D.L. (1991). Tumorigenic potential associated with enhanced expression of a gene that is amplified in a mouse tumor cell line. EMBO J. *10*, 1565–1569.

Fambrough, D., McClure, K., Kazlauskas, A., and Lander, E.S. (1999). Diverse signaling pathways activated by growth factor receptors induce broadly overlapping, rather than independent, sets of genes. Cell *97*, 727–741.

FitzGerald, T.J., Daugherty, C., Kase, K., Rothstein, L.A., McKenna, M., and Greenberger, J.S. (1985). Activated human N-ras oncogene enhances x-irradiation repair of mammalian cells in vitro less effectively at low dose rate. Implications for increased therapeutic ratio of low dose rate irradiation. Am. J. Clin. Oncol. *8*, 517–522.

Friedlander, P., Haupt, Y., Prives, C., and Oren, M. (1996). A mutant p53 that discriminates between p53-responsive genes cannot induce apoptosis. Mol. Cell. Biol. *16*, 4961–4971.

Haber, D.A. (1997). Splicing into senescence: the curious case of p16 and p19ARF. Cell *91*, 555–558.

Haupt, Y., Maya, R., Kazaz, A., and Oren, M. (1997). Mdm2 promotes the rapid degradation of p53. Nature *387*, 296–299.

Helmbrook, D.C., and Cliff, A. (1998). Therapeutic intervention and signaling. Curr. Opin. Cell Biol. *10*, 284–288.

Hollstein, M., Sidransky, D., Vogelstein, B., and Harris, C.C. (1991). p53 mutations in human cancers. Science *253*, 49–53.

Honda, R., and Yasuda, H. (1999). Association of p19(ARF) with Mdm2 inhibits ubiquitin ligase activity of Mdm2 for tumor suppressor p53. EMBO J. *18*, 22–27.

Johnson, L., Greenbaum, D., Cichowski, K., Mercer, K., Murphy, E., Schmitt, E., Bronson, R.T., Umanoff, H., Edelmann, W., Kucherlapati, R., and Jacks, T. (1997). K-ras is an essential gene in the mouse with partial functional overlap with N-ras. Genes Dev. *11*, 2468–2481.

Jones, S.N., Roe, A.E., Donehower, L.A., and Bradley, A. (1995). Rescue of embryonic lethality in Mdm2-deficient mice by absence of p53. Nature *378*, 206–208.

Juven, T., Barak, Y., Zauberman, A., George, D.L., and Oren, M. (1993). Wild type p53 can mediate sequence-specific transactivation of an internal promoter within the mdm2 gene. Oncogene *8*, 3411–3416.

Kamb, A., Gruis, N.A., Weaver-Feldhaus, J., Liu, Q., Harshman, K., Tavtigian, S.V., Stockert, E., Day, R.S., 3rd, Johnson, B.E., and Skolnick, M.H. (1994). A cell cycle regulator potentially involved in genesis of many tumor types. Science *264*, 436–440.

Kamijo, T., Zindy, F., Roussel, M.F., Quelle, D.E., Downing, J.R., Ashmun, R.A., Grosveld, G., and Sherr, C.J. (1997). Tumor suppression at the mouse INK4a locus mediated by the alternative reading frame product p19ARF. Cell *91*, 649–659.

Kamijo, T., Weber, J.D., Zambetti, G., Zindy, F., Roussel, M.F., and Sherr, C.J. (1998). Functional and physical interactions of the ARF tumor suppressor with p53 and Mdm2. Proc. Natl. Acad. Sci. USA *95*, 8292–8297.

Katz, M.E., and McCormick, F. (1997). Signal transduction from multiple Ras effectors. Curr. Opin. Genet. Dev. *7*, 75–79.

Kinzler, K.W., and Vogelstein, B. (1996). Lessons from hereditary colorectal cancer. Cell *87*, 159–170.

Kubbutat, M.H., Jones, S.N., and Vousden, K.H. (1997). Regulation of p53 stability by Mdm2. Nature *387*, 299–303.

Lane, D.P., and Hall, P.A. (1997). MDM2 arbiter of p53's destruction. Trends Biochem. Sci. *22*, 372–374.

Lebowitz, P.F., Sakamuro, D., and Prendergast, G.C. (1997). Farnesyl transferase inhibitors induce apoptosis of Ras-transformed cells denied substratum attachment. Cancer Res. *57*, 708–713.

Leng, P., Brown, D.R., Shivakumar, C.V., Deb, S., and Deb, S.P. (1995). N-terminal 130 amino acids of MDM2 are sufficient to inhibit p53-mediated transcriptional activation. Oncogene *10*, 1275–1282.

Leri, A., Liu, Y., Claudio, P.P., Kajstura, J., Wang, X., Wang, S., Kang, P., Malhotra, A., and Anversa, P. (1999). Insulin-like growth factor-1 induces Mdm2 and down-regulates p53, attenuating the myocyte renin-angiotensin system and stretch-mediated apoptosis. Am. J. Pathol. *154*, 567–580.

Levine, A.J., Momand, J., and Finlay, C.A. (1991). The p53 tumour suppressor gene. Nature *351*, 453–456.

Lin, A.W., Barradas, M., Stone, J.C., van Aelst, L., Serrano, M., and Lowe, S.W. (1998). Premature senescence involving p53 and p16 is activated in response to constitutive MEK/MAPK mitogenic signaling. Genes Dev. *12*, 3008–3019.

Marshall, M.S. (1995). Ras target proteins in eukaryotic cells. FASEB J. *9*, 1311–1318.

Martin, K., Trouche, D., Hagemeier, C., Sorensen, T.S., La Thangue, N.B., and Kouzarides, T. (1995). Stimulation of E2F1/DP1 transcriptional activity by MDM2 oncoprotein. Nature *375*, 691–694.

Mitsudomi, T., Steinberg, S.M., Nau, M.M., Carbone, D., D'Amico, D., Bodner, S., Oie, H.K., Linnoila, R.I., Mulshine, J.L., Minna, J.D., et al. (1992). p53 gene mutations in non-small-cell lung cancer cell lines and their correlation with the presence of ras mutations and clinical features. Oncogene *7*, 171–180.

Momand, J., Zambetti, G.P., Olson, D.C., George, D., and Levine, A.J. (1992). The mdm-2 oncogene product forms a complex with the p53 protein and inhibits p53-mediated transactivation. Cell *69*, 1237–1245.

Montes de Oca Luna, R., Wagner, D.S., and Lozano, G. (1995). Rescue of early embryonic lethality in mdm2-deficient mice by deletion of p53. Nature *378*, 203–206.

Moser, M., Imhof, A., Pscherer, A., Bauer, R., Amselgruber, W., Sinowatz, F., Hofstadter, F., Schule, R., and Buettner, R. (1995). Cloning and characterization of a second AP-2 transcription factor: AP-2 beta. Development *121*, 2779–2788.

Oliner, J.D., Kinzler, K.W., Meltzer, P.S., George, D.L., and Vogelstein, B. (1992). Amplification of a gene encoding a p53-associated protein in human sarcomas. Nature *358*, 80–83.

Oliner, J.D., Pietenpol, J.A., Thiagalingam, S., Gyuris, J., Kinzler, K.W., and Vogelstein, B. (1993). Oncoprotein MDM2 conceals the activation domain of tumour suppressor p53. Nature *362*, 857–860.

Palmero, I., Pantoja, C., and Serrano, M. (1998). p19ARF links the tumour suppressor p53 to Ras. Nature *395*, 125–126.

Peeper, D.S., Upton, T.M., Ladha, M.H., Neuman, E., Zalvide, J., Bernards, R., DeCaprio, J.A., and Ewen, M.E. (1997). Ras signalling linked to the cell-cycle machinery by the retinoblastoma protein. Nature *386*, 177–181.

Pickksley, S.M., and Lane, D.P. (1993). The p53-mdm2 autoregulatory feedback loop: a paradigm for the regulation of growth control by p53? Bioessays *15*, 689–690.

Pirollo, K.F., Tong, Y.A., Villegas, Z., Chen, Y., and Chang, E.H. (1993). Oncogene-transformed NIH 3T3 cells display radiation resistance levels indicative of a signal transduction pathway leading to the radiation-resistant phenotype. Radiat Res *135*, 234–243.

Pomerantz, J., Schreiber-Agus, N., Liegeois, N.J., Silverman, A., Alland, L., Chin, L., Potes, J., Chen, K., Orlow, I., Lee, H.W., et al. (1998). The Ink4a tumor suppressor gene product, p19Arf, interacts with MDM2 and neutralizes MDM2's inhibition of p53. Cell *92*, 713–723.

Prives, C. (1998). Signaling to p53: breaking the MDM2-p53 circuit. Cell *95*, 5–8.

Ries, S.J., Brandts, C.H., Chung, A., Biederer, C.H., Hann, B.C., Upner, E.M., McCormick, F., and Korn, W.M. (2000). Loss of p14ARF facilitates replication of the adenovirus mutant dl1520 (ONYX-015) in tumor cells. Nat. Med., in press.

Rodriguez-Viciana, P., Warne, P.H., Khwaja, A., Marte, B.M., Pappin, D., Das, P., Waterfield, M.D., Ridley, A., and Downward, J. (1997). Role of phosphoinositide 3-OH kinase in cell transformation and control of the actin cytoskeleton by Ras. Cell *89*, 457–467.

Samuels, M.L., Weber, M.J., Bishop, J.M., and McMahon, M. (1993). Conditional transformation of cells and rapid activation of the mitogen-activated protein kinase cascade by an estradiol-dependent human raf-1 protein kinase. Mol. Cell. Biol. *13*, 6241–6252.

Scheffner, M., Munger, K., Byrne, J.C., and Howley, P.M. (1991). The state of the p53 and retinoblastoma genes in human cervical carcinoma cell lines. Proc. Natl. Acad. Sci. USA *88*, 5523–5527.

Sharma, S., Schwarte-Waldhoff, I., Obermuber, H., and Schafer, R. (1993). Functional interaction of wild-type and mutant p53 transfected into human tumor cell lines carrying activated ras genes. Cell Growth Differ. *4*, 861–869.

Shaulian, E., Resnitzky, D., Shifman, O., Blandino, G., Amsterdam, A., Yayon, A., and Oren, M. (1997). Induction of Mdm2 and enhancement of cell survival by bFGF. Oncogene *15*, 2717–2725.

Sherr, C.J., and Weber, J.D. (2000). The ARF/p53 pathway. Curr. Opin. Genet. Dev. *10*, 94–99.

Shirasawa, S., Furuse, M., Yokoyama, N., and Sasazuki, T. (1993). Altered growth of human colon cancer cell lines disrupted at activated Ki-ras. Science *260*, 85–88.

Sklar, M.D. (1988). The ras oncogenes increase the intrinsic resistance of NIH 3T3 cells to ionizing radiation. Science *239*, 645–647.

Stokoe, D., Macdonald, S.G., Cadwallader, K., Symons, M., and Hancock, J.F. (1994). Activation of Raf as a result of recruitment to the plasma membrane. Science *264*, 1463–1467.

Stott, F.J., Bates, S., James, M.C., McConnell, B.B., Starborg, M., Brookes, S., Palmero, I., Ryan, K., Hara, E., Vousden, K.H., and Peters, G. (1998). The alternative product from the human CDKN2A locus, p14(ARF), participates in a regulatory feedback loop with p53 and MDM2. EMBO J. *17*, 5001–5014.

Tao, W., and Levine, A.J. (1999). P19(ARF) stabilizes p53 by blocking nucleo-cytoplasmic shuttling of Mdm2. Proc. Natl. Acad. Sci. USA *96*, 6937–6941.

Woods, D., Parry, D., Cherwinski, H., Bosch, E., Lees, E., and McMahon, M. (1997). Raf-induced proliferation or cell cycle arrest is determined by the level of Raf activity with arrest mediated by p21Cip1. Mol. Cell. Biol. *17*, 5598–5611.

Wu, X., Bayle, J.H., Olson, D., and Levine, A.J. (1993). The p53-mdm-2 autoregulatory feedback loop. Genes Dev. *7*, 1126–1132.

Xiao, Z.X., Chen, J., Levine, A.J., Modjtahedi, N., Xing, J., Sellers, W.R., and Livingston, D.M. (1995). Interaction between the retinoblastoma protein and the oncoprotein MDM2. Nature *375*, 694–698.

Zauberman, A., Flusberg, D., Haupt, Y., Barak, Y., and Oren, M. (1995). A functional p53-responsive intronic promoter is contained within the human mdm2 gene. Nucleic Acids Res. *23*, 2584–2592.

Zindy, F., Eischen, C.M., Randle, D.H., Kamijo, T., Cleveland, J.L., Sherr, C.J., and Roussel, M.F. (1998). Myc signaling via the ARF tumor suppressor regulates p53-dependent apoptosis and immortalization. Genes Dev. *12*, 2424–2433.

Amplification of a gene encoding a p53-associated protein in human sarcomas

J. D. Oliner*, K. W. Kinzler*†, P. S. Meltzer‡, D. L. George§ & B. Vogelstein*

* The Johns Hopkins Oncology Center, 424 North Bond Street, Baltimore, Maryland 21231, USA
‡ Departments of Pediatrics and Radiation Oncology, University of Michigan Cancer Center, MSRB 11 C560B, 1150 West Medical Center Drive, Ann Arbor, Michigan 48109, USA
§ Department of Human Genetics, University of Pennsylvania, Clinical Research Building, Philadelphia, Pennsylvania 19104, USA

DESPITE extensive data linking mutations in the p53 gene to human tumorigenesis[1], little is known about the cellular regulators and mediators of p53 function. MDM2 is a strong candidate for one such cellular protein; the *MDM2* gene was originally identified by virtue of its amplification in a spontaneously transformed derivative of mouse BALB/c cells[2] and the MDM2 protein subsequently shown to bind to p53 in rat cells transfected with p53 genes[3,4]. To determine whether MDM2 plays a role in human cancer, we have cloned the human *MDM2* gene. Here we show that recombinant-derived human MDM2 protein binds human p53 *in vitro*, and we use *MDM2* clones to localize the human *MDM2* gene to chromosome 12q13–14. Because this chromosomal position appears to be altered in many sarcomas[5–7], we looked for changes in human *MDM2* in such cancers. The gene was amplified in over a third of 47 sarcomas, including common bone and soft tissue forms. These results are consistent with the hypothesis that MDM2 binds to p53, and that amplification of *MDM2* in sarcomas leads to escape from p53-regulated growth control. This mechanism of tumorigenesis parallels that for virally-induced tumours[8,9], in which viral oncogene products bind to and functionally inactivate p53.

To obtain human complementary DNA clones, a murine *MDM2* cDNA probe was used to initiate cDNA walking in a human library (see legend to Fig. 1). Sequence analysis of 25 clones revealed several cDNA forms indicative of alternative splicing. The predominant human form is compared with its murine counterpart in Fig. 1. There was an open reading frame extending from the 5′ end of the human cDNA sequence to nucleotide 1,784. Although this signal for translation initiation could not be unambiguously defined, the ATG at nucleotide 312 was considered the most likely position for several reasons. First, the sequence similarity between human and mouse *MDM2* declined dramatically upstream of nucleotide 312. Second, an inverse polymerase chain reaction (PCR) was used in an attempt to acquire additional upstream cDNA sequence[10]. The 5′ ends of the PCR-derived clones were very similar (within 12 base pairs) to the 5′ ends of clones obtained from the cDNA library, indicating that the 5′ end of the human *MDM2* sequence shown in Fig. 1 may represent the 5′ end of the transcript. Third, *in vitro* translation of the sequence shown in Fig. 1, beginning with the methionine encoded by the ATG at position 312, generated a protein similar in size to that observed in human cells (see below).

Comparison of the human and mouse *MDM2* coding regions showed that they were 80.3% identical and shared a basic nuclear localization signal at codons 181 to 185 (ref. 11), several casein kinase II serine-phosphorylation sites[12], an acidic activation domain at codons 223 to 274 (ref. 13), and two metal-binding sites at codons 305 to 322 and 481 to 478, neither of which is highly related to known DNA-binding domains[14].

To determine whether the human MDM2 protein could bind to human p53 protein *in vitro*, a human *MDM2* expression vector was constructed from the cDNA clones (see legend to Fig. 2). RNA transcribed from this vector using T7 RNA polymerase was used to program a rabbit reticulocyte lysate. Although the predicted size of the protein generated from the construct was only 55.2K (M_r 55,200, extending from the methionine at nucleotide 312 to nucleotide 1,784), protein translated *in vitro* migrated at ~90 K. The MDM2 protein was not immunoprecipitated with antibodies against either the C-terminal or N-terminal regions of p53 (Fig. 2, lanes 2 and 3). But when *in vitro*-translated human p53 was mixed with the human *MDM2* translation product, the anti-p53 antibodies precipitated MDM2 protein with p53 (Fig. 2, lanes 5 and 6). As a control, a protein of similar electrophoretic mobility (MCC[15]) was mixed with p53 and there was no coprecipitation (Fig. 2, lanes 8 and 9). When an *in vitro*-translated His-175 mutant form of p53 was mixed with human MDM2 protein, a similar coprecipitation of MDM2 and p53 proteins was also observed (data not shown).

Polyclonal rabbit antibodies were raised against an *Escherichia coli*-produced human MDM2–glutathione S-transferase fusion protein. The anti-MDM2 antibodies immunoprecipitated p53 when mixed with MDM2 protein (Fig. 2, lane 15) but failed to precipitate p53 alone (Fig. 2, lane 13).

To establish the chromosomal localization of human *MDM2*, somatic cell hybrids were screened, and a human–hamster hybrid containing only human chromosome 12 hybridized to the human *MDM2* probe. Screening of hybrids containing portions of chromosome 12 (ref. 16) with the same probe narrowed the localization to chromosome 12q13–14. Because this region of chromosome 12 is often aberrant in human sarcomas[5–7], southern blot analysis to evaluate whether *MDM2* was genetically altered in such cancers. We found a striking amplification of *MDM2* sequences in several of these tumours (see examples in Fig. 3, lanes 2, 3 and 5). Of 47 sarcomas analysed, 17 showed a 5–50-fold *MDM2* amplification. These tumours included 7 of 13 liposarcomas, 7 of 22 malignant fibrous histiocytomas, 3 of 11 osteosarcomas, and 0 of 1 rhabdomyosarcoma. Five benign soft tissue tumours (lipomas) and seventy-four carcinomas (colorectal or gastric) were also analysed by Southern blotting and no amplification was seen.

We next determined whether this gene amplification was associated with increased expression. Because of RNA degradation in primary sarcomas, only the cell lines could be productively analysed by northern blotting. In the one available sarcoma cell line with *MDM2* amplification, a single transcript of ~5.5 kilobases (kb) was observed (Fig. 4*a*, lane 1). The amount of this transcript was much higher than in a sarcoma cell line without amplification (Fig. 4*a*, lane 2) or in a carcinoma cell line (Fig. 4*a*, lane 3). When purified messenger RNA (rather than total RNA) from the carcinoma cell line was used for analysis, a human *MDM2* transcript of 5.5 kb could also be observed (Fig. 4*a*, lane 4). Expression of the *MDM2* RNA in the sarcoma with amplification was estimated to be at least 30-fold higher than that in the other lines examined. This was consistent with results from western blot analysis. A protein of M_r ~90K was expressed at high levels in the sarcoma cell line with *MDM2* amplification (Fig. 4*b*, lane 3), whereas no expression was evident in two sarcoma cell lines without amplification or in the carcinoma cell line (Fig. 4*b*, lanes 1, 2 and 4). Five primary sarcomas were also analysed by western blotting. Three primary sarcomas with amplification expressed the same sized protein as that in the sarcoma cell line (Fig. 4*c*, lanes 1–3), but no protein was observed in the two sarcomas without amplification (Fig. 4*c*, lanes 4 and 5).

Our results demonstrate that human MDM2 binds to p53 *in vitro* and is genetically altered in a significant fraction of the most common sarcomas of soft tissue and bone[17,18]. It is important to note, however, that amplifications in human tumours

† To whom correspondence should be addressed.

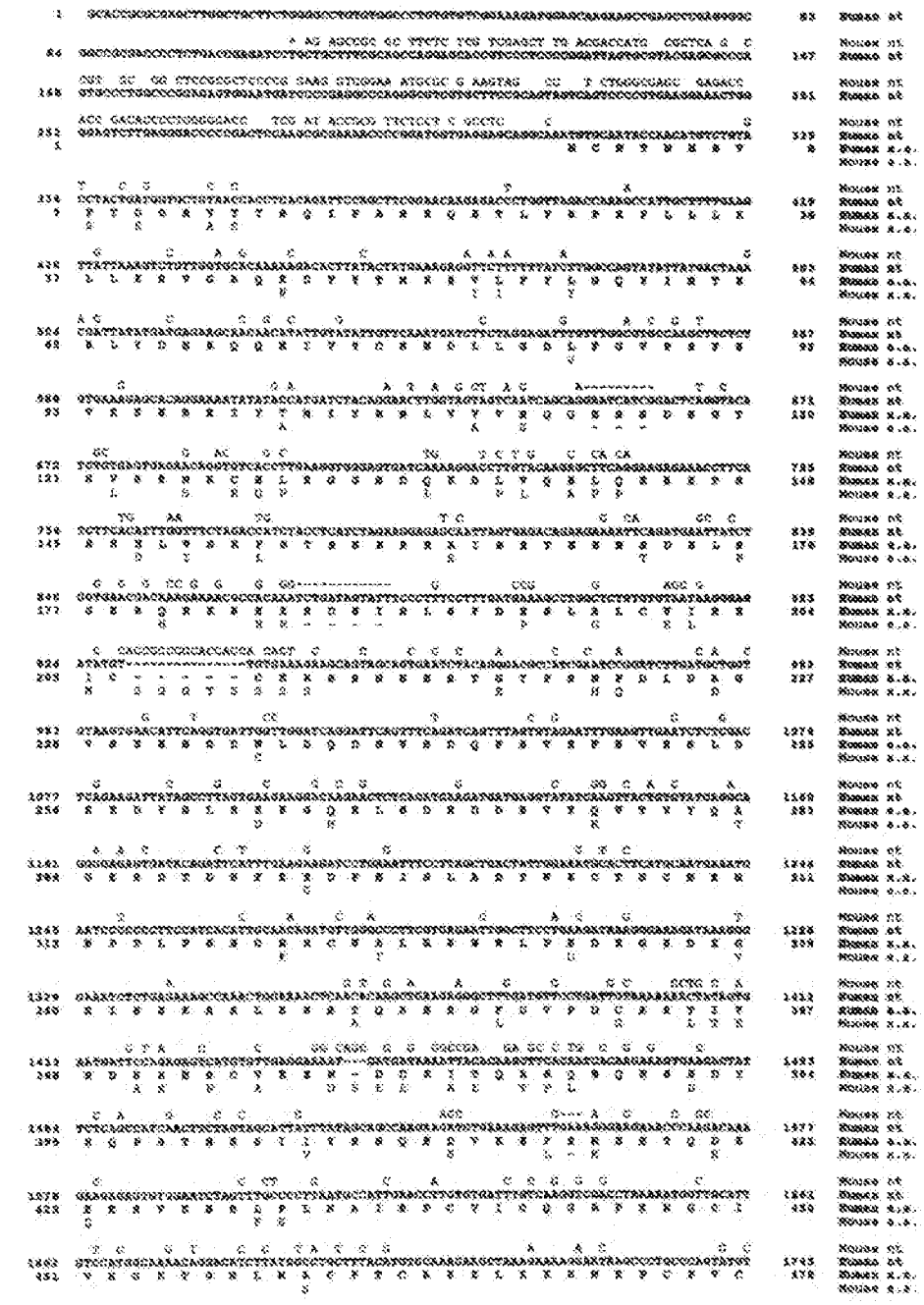

FIG. 1 Human *MDM2* cDNA sequence: human and mouse *MDM2* nucleotide (nt) and amino-acid (a.a.) sequences are compared (single-letter code). The mouse sequence is only shown where it differs from the corresponding human sequence. Asterisks mark the 5′ and 3′ boundaries of the previously published mouse *MDM2* cDNA[3]. Dashes indicate insertions.

METHODS. Polyadenylated RNA isolated from the human colonic carcinoma cell line CaCo-2 was used as a template for the production of random hexamer-primed double-stranded cDNA[22]. The cDNA was ligated to adaptors and then to the lambda YES phage vector, packaged and plated as described[23]. The library was screened initially with a ^{32}P-labelled [24] mouse *MDM2* cDNA probe (nt 259 to 1,508; ref. 2) and then rescreened with a human *MDM2* cDNA clone containing nt 40 to 702. In total, 25 clones were obtained, partially or totally sequenced, and mapped. The sequence shown is representative of the most abundant class and was assembled from three clones: c14–2 (nt 1–549), c89 (nt 467–1,737), and c33 (nt 390–2,372). The 3′ end of the untranslated region has not yet been cloned. The 5′ end is likely to be at or near nt 1 (see text). The mouse and human amino-acid sequences are compared from the putative translation start site at nt 312 to the conserved stop codon at nt 1,784. This nucleotide sequence has been deposited at the EMBL Data Library, accession number Z12020.

often involve large stretches of the genome, encompassing 300 to 1,000 kb[1,18–21]. Other genes in the *MDM2* amplicon could contribute to, or be responsible for, the growth advantage afforded by the amplification event. Nevertheless, MDM2 is a good candidate for the 'target' of amplification for two reasons. First, MDM2 has oncogenic activity after transfection into NIH3T3 cells[2]. Second, it binds to a protein (p53) with known growth suppressive effects on a wide variety of human tumour types. MDM2 may functionally inactivate p53 in ways similar to those employed by virally encoded oncoproteins such as simian virus 40 T antigen, adenovirus E1B and human papilloma virus E6 (refs. 4, 8, 9). Consistent with this hypothesis, no sarcomas with *MDM2* amplification (of five tested) had any of the p53 gene mutations that occur commonly in other tumours

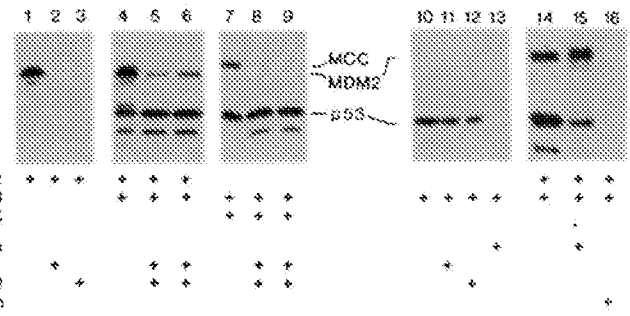

FIG. 2 Coprecipitation of human MDM2 and p53. *In vitro*-translated MDM2, p53 and MCC proteins were mixed as indicated and incubated with p53 Ab1 (monoclonal antibody specific for the C terminus of p53), p53 Ab2 (monoclonal antibody specific for the N terminus of p53), MDM2 Ab (polyclonal rabbit anti-human MDM2 antibodies), or serum (preimmune serum obtained from the rabbit that produced the MDM2 antibody). Lanes 1, 4, 7, 10 and 14 contain aliquots of the protein mixtures used for immunoprecipitation. Bands running slightly faster than p53 are polypeptides produced from internal translation initiation sites.

METHODS. A human *MDM2* expression vector was constructed in pBluescript SK + (Stratagene) from overlapping cDNA clones. The construct contained the sequence shown in Fig. 1 from nt 312 to 2,176. A 42-bp black beetle virus ribosome entry sequence[25] was placed immediately upstream of the *MDM2* sequence in order to obtain high expression. This construct, as well as p53 (ref. 26) and *MCC*[15] constructs in pBluescript SK +, were transcribed with T7 RNA polymerase and translated in a rabbit reticulocyte lysate (Promega) according to the manufacturer's instructions. Lysate (10 μl) containing the three proteins, alone or mixed in pairs, was incubated at 37 °C for 15 min. 1 μg (10 μl) of p53 Ab1 or Ab2 (Oncogene Science) or 5 μl of rabbit serum containing MDM2 antibody or preimmune rabbit serum, were added as indicated. 90 μl RIPA buffer (10 mM Tris, pH 7.5, 1% sodium deoxycholate, 1% NP40, 150 mM NaCl, 0.1% SDS), SNNTE buffer[3], or binding buffer[26] were then added and the mixtures allowed to incubate at 4 °C for 2 h. The three buffers produced similar results, although the coprecipitation was less efficient in SNNTE buffer (containing 0.5 M NaCl; lanes 5 and 8) than in binding buffer (containing 0.1 M NaCl; lanes 6 and 9). Following addition of 2 mg protein A-Sepharose, the tubes were rotated end-over-end at 4 °C for 1 h. After pelleting and washing, immunoprecipitates were electrophoresed on SDS–polyacrylamide gels and the dried gels autoradiographed in the presence of Enhance (New England Nuclear). Rabbits were immunized with a glutathione *S*-transferase (Pharmacia)–MDM2 fusion protein containing human MDM2 from the region corresponding to nt 390–816.

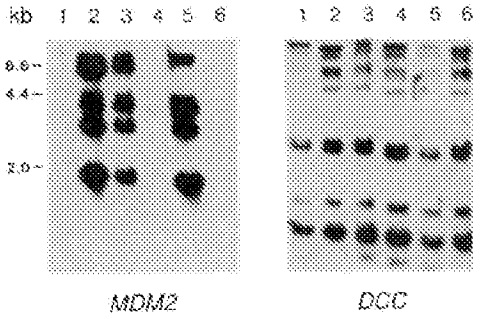

FIG. 3 Amplification of the human *MDM2* gene in sarcomas. DNA (5 μg) was digested with *EcoR*I, separated by agarose gel electrophoresis and transferred to nylon as described[27]. Filters were then hybridized with a human *MDM2* cDNA fragment probe (nt 1–942; Fig. 1) or to a control probe that identifies fragments of similar size (pOCC 1.65; ref. 38). Hybridization was as previously described[28]. DNA was derived from 5 primary sarcomas (lanes 1–4, 6) and one sarcoma cell line (OsA-CL; lane 5). On longer exposure, the same sized *MDM2* fragments were observed in lanes 1, 4 and 6. DNA fragment sizes are shown on the left in kb.

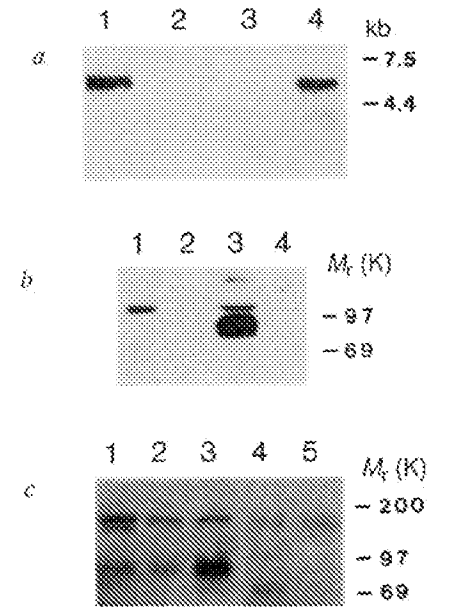

FIG. 4 *MDM2* expression. *a*, Northern blot analysis. RNA was separated by electrophoresis in a MOPS–formaldehyde gel and electrophoretically transferred to nylon filters. Transfer and hybridization were as described[29]. RNA was hybridized to the MDM2 fragment described in Fig. 3 legend. Total RNA (10 μg) was derived, respectively, from two sarcoma cell lines (OsA-CL, lane 1, and RC13, lane 2) and the colorectal cancer cell line (CaCo-2) used to make the cDNA library (lane 3). Lane 4 contains 10 μg polyadenylated CaCo-2 RNA. RNA sizes are shown on the right in kb. *b*, Western blot analysis of the sarcoma cell lines RC13 (lane 1), OsA-CL (lane 3), HOS (lane 4), and the carcinoma cell line CaCo-2 (lane 2). *c*, Western blot analysis of primary sarcomas. Lanes 1 to 3 contain protein from sarcomas with *MDM2* amplification, and lanes 4 and 5 contain protein from sarcomas without *MDM2* amplification. Western blots using affinity-purified MDM2 antibody were performed with 50 μg protein per lane as described[31], except that the membranes were blocked in 10% non-fat dried milk and 10% goat serum, and secondary antibodies were coupled to horseradish peroxidase to allow chemiluminescent detection (Amersham ECL). MDM2 antibody was affinity-purified with a pATH-MDM2 fusion protein using methods described in ref. 31. Nonspecific reactive proteins of 75, 105 and 170K are seen in all lanes, irrespective of *MDM2* amplification. MDM2 proteins, of M_r 90K, were observed only in the MDM2-amplified tumours. Protein marker sizes are shown on the right.

(unpublished results with T. Tokino and D. Sidransky). The amplification of *MDM2* provides another provocative parallel between viral carcinogenesis and the naturally occurring genetic alterations underlying sporadic human cancer. □

Received 28 March; accepted 5 May 1992.

1. Hollstein, M., Sidransky, D., Vogelstein, B. & Harris, C. C. *Science* **253**, 49–53 (1991).
2. Fakharzadeh, S., Trusko, S. P. & George, D. *EMBO J.* **10**, 1565–1569 (1991).
3. Hinds, P. W. *et al. Cell Growth Differ.* **1**, 571–580 (1990).
4. Momand, J., Zambetti, G. P., Olson, D. C., George, D. L. & Levine, A. J. *Cell* (in the press).
5. Mandahl, N. *et al. Genes Chrom. Cancer* **1**, 9–14 (1989).
6. Turc-Carel, C. *et al. Cancer genet. Cytogenet.* **23**, 291–299 (1986).
7. Meltzer, P. S. *et al. Cell Growth Differ.* **2**, 495–501 (1991).
8. Lane, D. P. & Benchimol, S. *Genes Dev.* **4**, 1–8 (1990).
9. Werness, B. A., Levine, A. J. & Howley, P. M. *Science* **248**, 76–79 (1990).
10. Ochman, H., Ajioka, J., Garza, D. & Hartl, D. in *PCR Technology: Principles and Applications for DNA Amplification* (ed. Erlich, H. A.) 105–111 (Stockton, New York, 1989).
11. Tanaka, K. *et al. FEBS Lett.* **271**, 41–46 (1990).
12. Prives, L. A. *Biochim. biophys. Acta* **1054**, 267–284 (1990).
13. Ptashne, M. *Nature* **335**, 683–689 (1988).
14. Harrison, S. C. *Nature* **353**, 715–719 (1991).
15. Kinzler, K. W. *et al. Science* **251**, 1366–1370 (1991).
16. Law, M. L. *et al. Ann. hum. Genet.* **50**, 131–137 (1986).
17. Weiss, S. W. & Enzinger, F. M. *Cancer* **41**, 2250–2266 (1978).
18. Malawer, M.M., Abelson, H. T. & Suit, H. D. in *Cancer: Principles and Practice of Oncology* (eds DeVita, V. T., Hellman, S. & Rosenberg, S. A.) 1293–1342 (Lippincott, Philadelphia, 1985).
19. Kinzler, K. W. *et al. Science* **236**, 70–73 (1987).
20. Kinzler, K. W. *et al. Proc. natn. Acad. Sci. U.S.A.* **83**, 1031–1035 (1986).
21. Brodeur, G.M. & Seeger, R.C. *Cancer genet. Cytogenet.* **19**, 101–111 (1986).
22. Gubler, U. & Hoffmann, B. J. *Gene* **25**, 263–269 (1983).
23. Elledge, S. J., Mulligan, J. T., Ramer, S. W., Spottswood, M. & Davis, R. W. *Proc. natn. Acad. Sci. U.S.A.* **88**, 1731–1735 (1991).
24. Feinberg, A. & Vogelstein, B. *Analyt. Biochem.* **132**, 6–13 (1983).
25. Sakonju, S., ... & Schwartz, J. *Nucleic Acids Res.* **15**, 3933 (1987).
26. El-Deiry, W. S., Kern, S. E., Pietenpol, J. A., Kinzler, K. W. & Vogelstein, B. *Nature Genet.* **1**, 45–49 (1992).
27. Seed, B. C. & Mann, D. A. *Nucleic Acids Res.* **13**, 7207–7215 (1985).
28. Fearon, E. R. *et al. Science* **247**, 49–56 (1990).
29. Vogelstein, B. *et al. Cancer Res.* **47**, 4806–4813 (1987).
30. Kinzler, K. W., Ruppert, J. M., Bigner, S. H. & Vogelstein B. *Nature* **332**, 371–374 (1988).
31. Kinzler, K. W. & Vogelstein, B. *Molec. cell. Biol.* **10**, 634–642 (1990).

ACKNOWLEDGEMENTS. We thank A. J. Levine for the information about MDM2–p53 interaction that stimulated this work, M. L. Law for somatic cell hybrids, S. Elledge for the lambda YES vector, and T. Gwiazda for preparation of the manuscript. This work was supported by the Preuss Foundation, the Clayton Fund, and grants from the National Institutes of Health.

Wild-type p53 activates transcription *in vitro*

George Farmer, Jill Bargonetti, Hua Zhu, Paula Friedman, Ron Prywes & Carol Prives

Department of Biological Sciences, Columbia University, New York 10027, USA

THE p53 protein is an important determinant in human cancer and regulates the growth of cells in culture[1–3]. It is known to be a sequence-specific DNA-binding protein[4,5] with a powerful activation domain[6–8], but it has not been established whether it regulates transcription directly. Here we show that intact purified wild-type human and murine p53 proteins strongly activate transcription *in vitro*. This activation depends on the ability of p53 to bind to a template bearing a p53-binding sequence. By contrast, tumour-derived mutant p53 proteins cannot activate transcription from the template at all, and when complexed to wild-type p53, these mutants block transcriptional activation by the wild-type protein. Moreover, the simian virus 40 large T antigen inhibits wild-type p53 from activating transcription. Our results support a model in which p53 directly activates transcription but this activity can be inhibited by mutant p53 and SV40 large T antigen through interaction with wild-type p53.

A DNA-binding immunoassay has been used to screen human genomic clones and show that p53 binds specifically to a region upstream of the transcription start site for the human ribosomal gene cluster (RGC)[4]. We have confirmed and extended this observation by DNase I footprinting and shown that addition of immunopurified p53 to a DNA fragment containing the RGC site leads to strong and specific protection of only the RGC region (Fig. 1). All tumour-derived mutant p53 proteins tested failed to protect this sequence (J.B. *et al.*, manuscript in preparation).

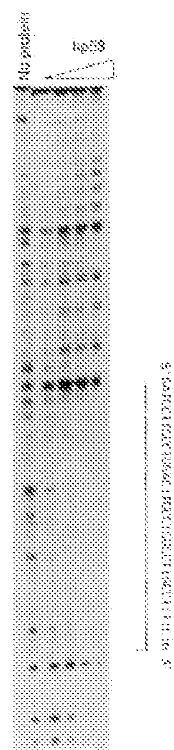

FIG. 1 The p53 protein binds specifically to a site in the human ribosomal gene cluster. DNA binding was assayed in 50-μl volumes containing 40 mM creatine phosphate, pH 7.7, 4 mM ATP, 7 mM $MgCl_2$, bovine serum albumin (0.2 mg ml^{-1}) 0.5 mM dithiothreitol, 10 ng carrier plasmid (pAT153) and 10 fmol of 5' ^{32}P-labelled DNA fragment containing the ribosomal gene cluster (RGC) p53-binding site[4] and either no protein (lane a) or increasing amounts of wild-type human p53 in increments of 15 ng up to 60 ng (lanes b–e). DNase I treatment of mixtures and processing of samples for electrophoresis on 8% polyacrylamide urea gels has been described[9]. Wild-type p53 was immunopurified from Sf27 cells expressing a recombinant baculovirus, pEV55hwt, using the monoclonal antibody Pab421 crosslinked to Sepharose A[14].

To determine whether p53 can activate transcription *in vitro*, we used as templates the plasmids fos1wt and fos1mt, which contain the human RGC p53 DNA-binding fragment or a mutated RGC fragment respectively (Fig. 2*a*). Three partially purified fractions from HeLa cell nuclear extracts were used as a source of transcription factors[9]. RNA products were analysed by S1 nuclease digestion using specific probes for each construct. Increasing amounts of p53 stimulated transcription from fos1wt (compare lanes 1–4 with lanes 5–8). These reaction mixtures also included a construct containing an abridged adenovirus major late promoter (pMLS; ref. 10) whose transcription was not significantly affected by p53.

The p53 protein activated transcription from another promoter as well (Fig. 2*b*). Plasmids containing either one or sixteen copies of the RGC site, or one mutant RGC site, inserted adjacent to the polyoma virus early promoter to create Py1wt, Py16wt and Py1mt, respectively, were used as templates in transcription reactions. We found that p53 activated transcription of constructs containing the wild-type RGC (lanes 1–9) but not the mutant RGC (lanes 10–12). Diagrams of the templates and the test probe used in these experiments are shown in Fig. 2*c* with the expected S1 nuclease products.

The high incidence of p53 gene mutations in cancer patients suggests that alteration of the normal function of p53 is an important part of the oncogenic process. Therefore it was of interest to examine whether tumour-derived mutant p53 proteins activate transcription. The mutant p53 proteins we chose are defective in both nonspecific and specific DNA binding[4,5,11], so providing an opportunity to confirm that p53 must bind DNA to activate transcription. We compared the ability of wild-type and two tumour-derived mutant p53 proteins with mutations at either amino acid 175 (His 175) or at amino acid 273 (His 273)

Available online at www.sciencedirect.com
SCIENCE DIRECT
Gene 338 (2004) 217–223
GENE
AN INTERNATIONAL JOURNAL ON GENES AND GENOMES
www.elsevier.com/locate/gene

Genomic organisation of the human *MDM2* oncogene and relationship to its alternatively spliced mRNAs☆

Huiling Liang[a,1], Helen Atkins[a], Rana Abdel-Fattah[a], Stephen N. Jones[b], John Lunec[a,*]

[a] *Cancer Research Unit, Medical School, University of Newcastle upon Tyne, Newcastle upon Tyne NE2 4HH, UK*
[b] *University of Massachusetts Medical School, 55 Lake Avenue North, Worcester, MA 01655, USA*

Received 26 January 2004; received in revised form 26 April 2004; accepted 17 May 2004
Available online 21 July 2004
Received by A.J. van Wijnen

Abstract

The *MDM2* proto-oncogene, which encodes a protein that binds to the p53 tumour suppressor, has been found amplified and overexpressed in a range of human tumours. Although the human *MDM2* cDNA sequence has been reported, the genomic organisation of the human gene has not been documented. We have previously reported the detection of five alternative internally deleted *MDM2* transcripts in human tumours and suggested these may represent alternatively spliced forms. Here we demonstrate two novel *MDM2* transcripts with internal deletions, using RT-PCR followed by sequencing. To definitively ascribe these variant transcript forms to alternative splicing, and to explore associated mechanisms, we have determined the intron–exon organisation of the human genomic sequence. The human *MDM2* gene spans approximately 33 kb and is divided into 12 exons. Exon sizes range from 50 to ≥ 1161 bp and intron sizes vary from 121 to ~ 7000 bp. The positions of intron–exon boundaries are compared with the deletion junctions of the multiple-sized transcripts and discussed in relation to alternative splicing mechanism.

Keywords: p53; genomic mapping; long range PCR

1. Introduction

The *mdm2* proto-oncogene was initially identified as an amplified gene from a mouse double minute chromosome present in a spontaneously transformed Balb/C 3T3 cell line, 3T3DM (Haines et al., 1994; Sigalas et al., 1996; Steinman et al., 2004). The causal role of this gene in tumorigenesis was originally established by transfection studies using genomic DNA sequences. In these studies, experimental overexpression of *mdm2* resulted in the immortalisation of primary rat embryo fibroblasts and induced a fully transformed phenotype in the cells when cotransfected with an activated *ras* gene (Finlay, 1993). The human homologue of the *MDM2* gene has been found to be amplified in over 30% of human sarcomas (Oliner et al., 1992; Leach et al., 1993), which consequently results in high levels of the *MDM2* gene product. In addition, *MDM2* overexpression can also occur through enhanced transcription and translation (Bueso-Ramos et al., 1993; Landers et al., 1997; Momand et al., 1998).

The human *MDM2* gene has been localised to chromosome 12q13–14. Although the human *MDM2* cDNA sequence has been previously reported (Oliner et al., 1992), little is known about its genomic organisation. The MDM2 protein is composed of 491 amino acids and contains a p53 binding domain (codons 19–102), a putative nuclear localisation signal (codons 181–185), an acidic domain (codons 223–274), a central zinc-finger motif (codons 305–332) and a ring-finger motif towards the C-terminal end of the protein (codons 438–478) (Boddy et al., 1994).

Abbreviations: *MDM2*, mouse double minute 2 gene; RT-PCR, reverse transcription polymerase chain reaction; cDNA, complementary DNA; kb, kilobase; bp, base pair; TE, tris(hydroxymethyl)aminomethane ethylene diamine tetra acetate.

☆ Database accession numbers: AF144014-AF144033 and AF201370-AF201371.

* Corresponding author. Northern Institute for Cancer Research Medical School, University of Newcastle upon Tyne, Newcastle upon Tyne NE2 4HH, UK. Tel.: +44-191-246-4420; fax: +44-191-246-4301.
E-mail address: john.lunec@newcastle.ac.uk (J. Lunec).
[1] Present address: University of Massachusetts Medical School, 55 Lake Avenue North, Worcester, MA 01655, USA.

0378-1119/$ - see front matter © 2004 Elsevier B.V. All rights reserved.
doi:10.1016/j.gene.2004.05.015

MDM2 appears to be a pluripotential oncoprotein, exerting its transforming properties through several alternative mechanisms, of which the most extensively studied has been the negative regulation of p53 function. MDM2 blocks p53 transcriptional function by binding to p53 (Momand et al., 1992; Oliner et al., 1993). The binding of MDM2 to p53 also results in the rapid degradation of p53 (Haupt et al., 1997; Kubbutat et al., 1997). In addition, MDM2 has been reported to have p53-independent tumorigenic properties. This includes the ability to interact with and inactivate the pRb tumour suppressor protein (Xiao et al., 1995) and to bind to and activate the E2F1 transcription factor (Martin et al., 1995). Furthermore, two independent transgenic studies have shown *MDM2* to have tumourigenic properties in p53 null mice (Lundgren et al., 1997; Jones et al., 1998).

One of the distinctive properties of *MDM2* is the possession of an extremely complex expression pattern. Its multiple-sized transcripts and proteins have been found in tumour samples and cell lines by a number of groups (Haines et al., 1994; Sigalas et al., 1996; Bartel et al., 2002). In our previous studies, five alternatively sized transcripts of the human *MDM2* were found in human ovarian tumour, bladder tumour and leukaemic cell samples (Sigalas et al., 1996). The expression of the alternatively sized forms was found to be more frequent in tumours of advanced stage and high histological grade, and they also retained their ability to transform NIH3T3 cells. Here, we present data demonstrating two further *MDM2* transcript forms with internal sequence deletions in human tumour tissue. We hypothesised that these transcripts are generated by alternative splicing. To test this hypothesis and to explore the associated mechanisms, we have investigated the genomic structure and organisation of the human *MDM2* gene. This gene is ~ 33 kb in length and comprises at least 12 exons. The sizes of exons vary from 50 to ≥ 1161 bp, and introns range in size from 121 to ~ 7000 bp. The position of intron–exon boundaries is compared with the sequences of the *MDM2* variant transcripts and discussed in relation to alternative splicing mechanisms.

2. Materials and methods

2.1. Nested RT-PCR

Total RNA was extracted from human bladder tumour and normal bladder tissues. Nested RT-PCR was carried out as previously described (Sigalas et al., 1996).

2.2. Genomic DNA extraction

Genomic DNA was prepared from frozen normal human placental tissue by digestion with proteinase K and phenol–chloroform extraction. The DNA was precipitated with a half volume of 7.5M ammonium acetate and one volume of isopropanol, washed in 70% ethanol and resuspended in 1 × TE buffer (10 mM Tris, 0.1 mM EDTA pH 7.5).

2.3. Long-range PCR

Primers (Table 1) were designed from the published *MDM2* cDNA sequence (Oliner et al., 1992). Each primer pair was designed to cross the deletion junctions of multiple-sized transcripts (Sigalas et al., 1996) or according to the predicted exon/intron boundaries by referring to the mouse *mdm2* gene structure (Jones et al., 1996; Montes de Oca luna et al., 1996). A long-range PCR protocol was carried out, with the above human genomic DNA as a template, using an XL PCR Kit (Perkin Elmer, Part No. N808-192). For comparison, PCR was also carried out on normal human placental cDNA. The reaction contained 1 × reaction buffer, 0.8 mM dNTP, 1.1 mM $Mg(OAc)_2$ and 4 units of *rTth* DNA polymerase, 40 pmol of each primer and 100 ng of genomic DNA or 20 μl cDNA in a total volume of 100 μl. The long-range PCR was performed using a thermal cycler (Perkin-Elmer Model 480) as follows: 94 °C for 2 min; cycles 1–16 at 94 °C for 30 s, 58–62 °C for 10 min; cycles 17–28 at 94 °C for 30 s, 58–62 °C for 10 min and 15 s of increment

Table 1
The sequences of primer pairs for amplification of genomic nucleotides of the human *MDM2* gene

Primer name	Forward primer (5′→3′)	cDNA position (nt)[a]	Reverse primer (5′→3′)	Position at cDNA (nt)[a]	Annealing temperature (°C)
Pri1	cctgtgtggcctgtgtgtc	30–49	tgttccgaagctggaatctgtg	382–361	60
Pri2	gtgcaaatacccaacatgtctg	314–333	caacagactttaataactttcaaaagc	435–410	60
Pri3	gcttttgaagttattaaagtctgttg	410–435	tacaaatgttgttgcttctcatc	536–513	57
Pri4	ttttatcttggccagtatattatg	474–497	attcctgctgattgactactacc	654–632	57
Pri5	catgatctacaggaaacttggtag	614–636	ttgatcactcccacctttcaagg	716–695	60
Pri6	actcaggtacatctgtgagtgag	661–683	tgtctcactaattgctctttcttc	815–793	60
Pri7	ttgtacaagagcttcaggaagag	724–746	atggcgtccctgtagattcac	969–949	60
Pri8	tgaaagcctggctctgtgtg	893–912	caaatttctacactaaactgatctg	1059–1036	57
Pri9	tcttgatgctggtgtaagtgaac	980–1002	agctaaggaaatttcaggatcttc	1211–1188	57
Pri10	gtgatacagattcattgaaggaag	1168–1191	catctgttgcaatgtgatggaag	1277–1254	60
Pri11	ctattggaaatgcacttcatgc	1213–1235	cggtggctcatgcctgtaatc	2372–2351	57

[a] Sequence of *MDM2* cDNA clones (Oliner et al., 1992).

per cycle, with a final extension of 72 °C for 10 min after the last cycle.

PCR products were separated by electrophoresis on a 1% low melting temperature agarose gel (NuSieve GTG, Flowgen) and visualised by ethidium bromide staining with UV transillumination. DNA bands amplified from genomic DNA were excised and purified with a QIAquick Gel Extraction kit (Qiagen), by following the procedure recommended by the company.

2.4. Cloning PCR products

Purified PCR products were subcloned directly into the pGEM-T Easy vector (Promega) following the protocol recommended by the company. Ligation products were transformed into *Escherichia coli* JM109 and clones containing the desired inserts were identified by PCR screening. Plasmids were prepared by using the Wizard Plus SV Miniprep system (Promega).

2.5. Sequencing

Sequencing was carried out manually by using PCR product directly as a template or automatically by using plasmid PCR product clone as a template. Manual sequencing was performed using the Sequenase Version 2.0 DNA sequencing system (Amersham, Product No.70770). The automated sequencing was carried out in the central core facility at the University of Newcastle upon Tyne Medical Faculty. The sequences were aligned with the published *MDM2* cDNA sequence, using the DNASTAR sequence analysis software package.

3. Results

3.1. The detection of multiple-sized MDM2 transcripts in human tumours

In our previous studies, we have found five alternative-sized *MDM2* transcripts (*MDM2-a*, *-b*, *-c*, *-d* and *-e*) (Sigalas et al., 1996). Our present investigation of the *MDM2* transcriptional pattern in human bladder tumour samples, but not in normal bladder tissue (data not shown), using RT-PCR has revealed two further transcripts, sized 813 and 707 bp, which we have designated *MDM2-a1* and *-g* (Fig. 1). Sequencing shows that these two transcripts have internal sequence deletions: *MDM2-a1* lacks nucleotides from codons 28 to 222 and codons 275 to 300; *MDM2-g* misses nucleotide codons from 28 to $97^2/_3$ and $114^2/_3$ to 300. Fig. 2 shows the structure of these transcripts in relation to the full-length *MDM2* cDNA sequence and previously described variant transcripts (see GenBank accession numbers AF201370 and AF201371 for details of the sequences).

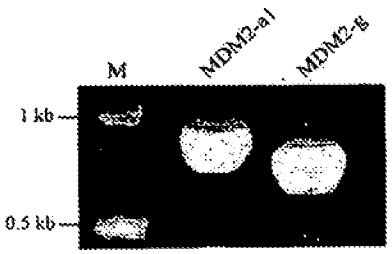

Fig. 1. *MDM2* transcripts were amplified by RT-PCR with nested primers that flank the *MDM2* coding region, as previously described (Sigalas et al., 1996; Matsumoto et al., 1998). M: molecular weight maker.

3.2. MDM2 genomic structure and organisation

We have used long-range PCR amplification, followed by cloning and sequencing to investigate the organisation of the human *MDM2* gene and in particular to define intron–exon boundaries and flanking intronic sequences. Eleven DNA fragments were amplified from genomic DNA with the primer pairs shown in Table 1, which match to the known *MDM2* cDNA sequences. Comparison of the sequences of these PCR products with the published sequences of *MDM2* cDNA clones reveals that the Pri1 primer pair spans introns 1 and 2; while primer pairs Pri2–10 cover one intron per primer pair. However, the region flanked by primer pair Pri11, covering from the 1235th to 2351st nucleotide of the *MDM2* cDNA clone sequence (Oliner et al., 1992), was found not to contain any intronic sequence. Sequence analysis indicates that *MDM2* spans approximately 33 kb of genomic DNA and is separated by 11 introns. Exons range in size from 50 to ≥ 1161 bp. The size of the introns varies from 121 to ~ 7000 bp (Table 2). Exon-intron boundary sequences of the 5′ and 3′ splice sites follow the "GT and AG" rule (Table 3; see GenBank accession numbers AF144014 AF144033 for additional intronic sequence data). Table 4 shows the 3′ ends of the intronic sequences adjacent to the intron–exon boundaries, including branch sites and polypyrimidine tracts. The sequences of branch sites have a good match with the consensus sequence YURA*Y (Y: pyrimidine; R: purine; A*: branch point residue). The distances between the branch points and the 3′ splice sites vary from 18 to 111 bp. The C/T content in the polypyrimidine tracts ranges from 53% to 90%.

Comparison of the structure and organisation of the human *MDM2* gene described here with that published for the mouse gene (Jones et al., 1996) indicates that the number of the exons and introns is the same. The size of the coding exons is similar (Table 2). However, the sizes of the noncoding transcribed regions, including exons 1, 2 and 12 and the introns, differ substantially, with the exception of introns 1 and 3.

3.3. Analysis of alternatively spliced variants of MDM2 mRNA

We have detected seven *MDM2* transcript variants (*MDM2-a*, *-a1*, *-b*, *-c*, *-d*, *-e* and *-g*) previously and

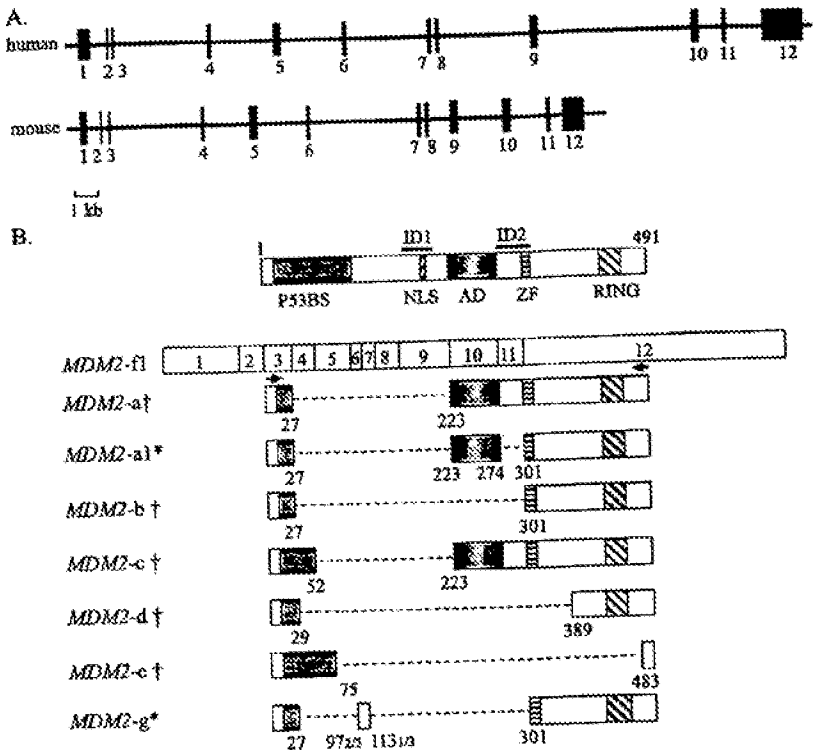

Fig. 2. (A) Genomic organisation of the *MDM2* locus. The top panel presents schematically the human *MDM2* gene structure. For comparison, the mouse *mdm2* gene is illustrated in the bottom panel (Jones et al., 1996). Exons are depicted as vertical bars and numbered underneath. Introns are indicated by horizontal line. (B) The relationship between the various *MDM2* transcripts and the exon–intron boundaries. The second top strip shows the exon organisation of the human *MDM2* gene with its encoded protein above the corresponding exons (top strip). Nucleotide sequence coding for the p53 binding site (p53 BS), nuclear localisation signal (NLS), acidic domain (AD), zinc-finger (ZF), ring-finger (RING) and growth-inhibitory domains 1 and 2 (ID1 and ID2) are depicted with filled boxes. The multiple-sized transcripts that were amplified by RT-PCR with a primer pair (denoted by arrows) are shown with boxes. Dashed lines represent deleted nucleotide sequences. The deletion junctions are numbered by amino acid codons. *detected in this report. †reported by Sigalas et al., 1996.

presently (Sigalas et al., 1996). Some of these variant transcripts have also been demonstrated in astrocytic neoplasms by another group (Matsumoto et al., 1998).

Table 2
Comparison of the human *MDM2* structure with the mouse gene

Exon no.	Exon size (bp)		Intron no.	Intron size (bp)		
	Mouse[a]	Human		Mouse[a]	Human	Difference in size[b] (%)
Exon 1	115	307	Intron 1	~ 500	~ 540	7.4
Exon 2	82	71	Intron 2	160	121	24.4
Exon 3	85	85	Intron 3	~ 4000	~ 4200	5
Exon 4	75	75	Intron 4	~ 2000	~ 3200	37.5
Exon 5	134	134	Intron 5	~ 1750	~ 3500	50
Exon 6	50	50	Intron 6	~ 5100	~ 4000	20
Exon 7	59	68	Intron 7	331	124	62.5
Exon 8	97	97	Intron 8	~ 950	~ 4200	77
Exon 9	164	161	Intron 9	~ 1800	~ 7000	74.3
Exon 10	156	156	Intron 10	~ 1300	~ 900	30.8
Exon 11	78	78	Intron 11	~ 450	~ 2800	83
Exon 12	≥ 615	≥ 1161				

[a] Reference: (Jones et al., 1996).
[b] = bp of difference between mouse and human/bp of the larger corresponding intron.

The alignment of the genomic sequence with the sequences of these seven transcripts discloses that the multiple-sized transcripts resulted from the deletion of multiple entire exons or part of exon sequences (Fig. 2). *MDM2-a* skips exons 4 to 9; *MDM2-a1*, exons 4 to 9 and exon 11; *MDM2-b*, exons 4 to 11; *MDM2-c*, exons 5 to 9; *MDM2-d*, exons 5 to 11, most of exon 4 and the 5′ end of exon 12; *MDM2-e*, exons 6 to 11, the 3′ end of exon 5 and the 5′ end of exon 12. *MDM2-g* splices out exons 4 to 5, and exons 7 to 11 (Fig. 2) Among the skipped exons, exons 4 to 9 and exon 11 were most frequently missed. These commonly excluded exons (with the exception of exon 7) have either less than 60% of C/T content at their upstream polypyrimidine tracts and/or more than 40 bp between their upstream branch points and 3′ sites. Whereas, exons 3, 10 and 12, which are most frequently included in the transcripts, have higher than 60% C/T content within their upstream polypyrimidine tracts and less than 40 bp between their upstream branch points and 3′ splice sites. Since exon 6 contains interrupted codons at both ends, the *MDM2-g* variant, which splices out several exons up- and downstream of

Table 3
Sequence of the human *MDM2* exon/intron boundaries

Exon no.	Sequence of boundary	Exon no.
1	GGAGCAGgtgctggc--intron 1--tttcccagCTGTGTT	2
2	GATCCAGgtaagcac--intron 2--ccttgtagGCAAATG 1	3
3	GACCCTGGgttagtat--intron 3--tcttatagGTTTAGAC 27 28	4
4	GAAAGAGgtaagctg--intron 4--tatttcagGTTCTTT 52 53	5
5	AGCACAGgtaattct--intron 5--tctacaagGAAAATA 96 98	6
6	CAGCAGGgtaagtta--intron 6--tctctcagAATCATC 113 115	7
7	TCAAAAGgtaatcta--intron 7--atgcttagGACCTTG 136 137	8
8	GAGACAGgtatatat--intron 8--statccagAAGAAAA 167 169	9
9	GAATCCGgtaatgtt--intron 9--tgttttagGATCTTG 222 223	10
10	TGATGAGgtatatat--intron 10-tttattagGTATATc 274 275	11
11	CTTACCTgtaagtat--intron 11-cattgaagGACTATT 300 301	12

Exon sequences are shown as uppercase letters. Intron sequences are denoted by lowercase letters. Underlined nucleotides encode amino acids (numbered underneath).

exon 6, has a shifted reading frame after codon 28. The *MDM2-e* variant, which also involves a deletion junction with an interrupted codon sequence, has a shift in the reading frame after codon 484.

4. Discussion

In our previous studies and the results presented here, we detected multiple-sized *MDM2* transcripts in human

Table 4
Branch sites and polypyrimidine tracts of the human *MDM2* gene

Intron no.	Sequences of branch site and polypyrimidine tract (5′ → 3′)	Distance from branch point to 3′ site (nt)	T and C %[a]
1	ctgacttgtctccagctgggctatttaaaccatgcattttcccag/exon 2	>40	59
2	atgattccagttttcatcgtgtcttttttttccttgtag/exon 3	<40	78
3	ttgatggatatgttgctgcagggcctatagttctgggataatttggaagtataatagcagttcttttctcttttag/exon 4	>40	53
4	ctaacatttagttatctttaatgctcagaatcatattgtattttcag/exon 5	>40	60.5
5	ttaatacaaatttttattctaaaatgtacatcttgttatttttttttttctgtctacaag/exon 6	>40	68
6	ctgatccttttctttttctctcag/exon 7	<40	90
7	ctaatgtaatattatttgcaaattggaaaggttatttcaacaagttggcttactggttatgttaagttttgttgtattaattttttcctaaatgctag/exon 8	>40	56.3
8	ttaacttttagaactatttttattgaaactaagttttctgtacaaatcggtactcaaaacagctcaatttttctaaatcacagtacagcaattattttttttccttacatatccag/exon 9	>40	57
9	gtgatgtttatcaaattatatatttttttttctgttttag/exon 10	<40	69
10	ctaatgaatgtgttttattag/exon 11	<40	53
11	ctgactgtgtgtcttattttcattgaag/exon 12	<40	61

Branch site sequences are indicated with underlined letters. /: boundary between intron and exon.
[a] The percentage of T and C content in polypyrimidine tracts.

tumour tissues, but not in normal tissues. Detection of alternative spliced forms of *MDM2* mRNAs varied, and appeared to be relatively abundant in most samples. These variants encoded protein products in vitro and were found to transform NIH3T3 cells and to be associated with high-grade and late-stage human cancer (Sigalas et al., 1996 and unpublished data). Our data were supported by the observations of other groups, who reported that alternatively spliced *mdm2* transcripts promoted tumour formation in mouse model (Fridman et al., 2003; Steinman et al., 2004). These collective observations suggest that alternatively spliced forms of *MDM2*, encoding alternative proteins with differing functional capabilities, may play an important role in tumour development. The human *MDM2* genomic map presented here enable us to relate the genomic structure and organisation of *MDM2* to the appearance of variant transcript forms and provide a basis for considering alternative splicing mechanisms.

Pre-mRNA splicing involves precise excision of intron sequences and the ligation of exon sequences. In cases of alternative splicing, the excision may occur at cryptic splice sites; exons may be skipped and introns may be retained. The organisation of the exon–intron boundaries of the human *MDM2* gene indicates that the *MDM2-a*, *-a1*, *-b*, *-c* and *-g* variant transcript forms (Fig. 2) result from multiple entire exon skipping, because the internal deletion junctions correspond exactly to the location of exon–intron boundaries. However, the deletion junctions of *MDM2-d* and *-e* forms do not correspond to the boundaries between exons and introns, and there are no consensus splicing sequences surrounding them to indicate the possible use of cryptic splice sites. This suggests that they may have resulted from an unusual and possibly aberrant splicing mechanism.

The regulation of alternative splicing involves both *cis* elements and *trans*-acting factors. The *cis* elements include the 5′ and 3′ splice sites, a branch site and a polypyrimidine tract between the branch point and the 3′ splice site. It has been demonstrated that a short distance between the branch point and the 3′ splice site and high C/T content at polypyrimidine tracts give rise to high efficiency of splicing in mammals (Helfman et al., 1988; Libri et al., 1989). Our data show that all the 5′ and 3′ splice sites of the human *MDM2* gene obey the "GT" and "AG" rule. The branch sites also have a good match with the consensus sequence. However, the distances between branch points and 3′ sites, and the percentage C/T content vary between introns. The exons most frequently retained in the splice variants have shorter distances between their upstream branch points and 3′ splice sites and/or a higher percentage C/T content in their upstream polypyrimidine tracts, compared with those exons commonly excluded (Table 2). It suggests that the short distance between the branch point to the 3′ site and the polypyrimidine tract with high C/T content confer high splicing efficiency to their adjacent splicing sites, which is consistent with the observation reported by Smith et al. (1989), Goux-Pelletan et al. (1990), Mueller et al. (1997). However, exon 7 was spliced out with a high frequency although there is only a short distance between its branch point and 3′ splice site and there is also a high C/T content in its upstream polypyrimidine tract. The explanation may be that it is spliced out along with upstream exons. The order of intron removal is governed by preferential binding of splice factors rather than in a sequential numerical order (Lewin, 1994). It may be possible that exon 7 processes splicing before exon 6 does, and the 5′ end of exon 7 may in some circumstances be ligated preferentially to the 3′ end of exon 6. If exon 6 has low splice strength, then in the process of ligation with its upstream exon, it may be outcompeted and skipped out together with exon 7.

Currently, we are not clear why the alternative spliced transcripts appear preferentially in tumour samples, especially in advanced stage and high grade, but not in normal tissues (Sigalas et al., 1996; Bartel et al., 2002). Although variant *MDM2* spliced transcripts have been reported in normal tissues in one study (Bartel et al., 2004), we failed to detect these isoforms in noncancerous tissues. It has been proposed that a mRNA surveillance system exists in cells, which protects them from errors of transcription, mRNA processing, or mRNA transport (Pulak and Anderson, 1993). Mistakes are not uncommon in splicing of RNA from complex genes. Exons can occasionally be skipped (Nigro et al., 1991). In the normal situation, the surveillance system would probably degrade most mRNA with splicing errors as they are transported to the cytoplasm. We speculate that in cancer cells, this system may not function correctly and, consequently, the splice variants may escape degradation. It is also possible that there are mutations in the intron region that cause alternative splicing and the presence of the variants contribute to the cancer. It would be of interest to test this hypothesis by investigating intron nucleotide sequences in tumour samples that show expression of alternatively spliced forms. However, other models can be envisaged; for instance, we cannot rule out the possibility that *trans*-acting factors are involved in the alternative RNA processing by blocking some splice sites and/or enhancing other splice sites.

In conclusion, we have detected two novel *MDM2* alternatively spliced transcripts and have also defined the structure and organisation of the human *MDM2* gene. In addition we have related this information to potential mechanisms by which alternatively sized *MDM2* transcripts are generated. As the alternatively spliced *MDM2* mRNAs have been shown to possess oncogenic potential and to correlate with advanced malignancies to tumour progress (Haines et al., 1994; Sigalas et al., 1996; Steinman et al., in press), our data may assist in clinical diagnosis of sarcomas displaying *MDM2* amplification and alternative splicing of *MDM2* transcripts.

Acknowledgements

We thank Ratchada Suaeyun for her assistance with the work presented in this paper.

References

Bartel, F., Tauber, H., Harris, L., 2002. Alternative and aberrant splicing of MDM2 mRNA in human cancer. Cancer Cell 2, 9–15.

Bartel, F., Pinkert, D., Fiedler, W., Kappler, M., Wurl, P., Schmidt, H., Taubert, H., 2004. Expression of alternatively and aberrantly spliced transcripts of the MDM2 mRNA is not tumor-specific. Int. J. Oncol. 24, 143–151.

Boddy, M.N., Freemont, P.S., Borden, K.L., 1994. The p53-associated protein MDM2 contains a newly characterized zinc-binding domain called the RING finger. Trends Biochem. Sci. 19, 198–199.

Bueso-Ramos, C., Yang, Y., Deleon, E., McCown, P., Stass, S., Albitar, M., 1993. The human MDM-2 oncogene is overexpressed in leukemias. Blood 82, 2617–2623.

Finlay, C.A., 1993. The mdm-2 oncogene can overcome wild-type p53 suppression of transformed cell growth. Mol. Cell. Biol. 13, 301–306.

Fridman, J., Hernando, E., Hemann, M., Stanchina, E., Cordon-Dardo, S., Lowe, S., 2003. Tumor promotion by Mdm2 splice variants unable to bind p53. Cancer Res. 63, 5703–5706.

Goux-Pelletan, M., Libri, D., d'Aubenton-Carafa, Y., Fiszman, M., Brody, E., Marie, J., 1990. In vitro splicing of mutually exclusive exons from the chicken B-tropomyosin gene: role of the branch point location and very long pyrimidine stretch. EMBO J. 9, 241–249.

Haines, D.S., Landers, J.E., Engle, L.J., George, D.L., 1994. Physical and functional interaction between wild-type p53 and mdm2 proteins. Mol. Cell. Biol. 14, 1171–1178.

Haupt, Y., Maya, R., Kazaz, A., Oren, M., 1997. Mdm2 promotes the rapid degradation of p53. Nature 387, 296–299.

Helfman, D.M., Ricci, W.M., Finn, L.A., 1988. Alternative splicing of tropomyosin pre-mRNAs in vitro and in vivo. Genes Dev. 2 (12A), 1627–1638.

Jones, S.N., Ansari-Lari, M.A., Hancock, A.R., Jones, W.J., Gibbs, R.A., Donehower, L.A., Bradley, A., 1996. Genomic organization of the mouse double minute 2 gene. Gene 175, 209–213.

Jones, S.N., Hancock, A.R., Vogel, H., Donehower, L.A., Bradley, A., 1998. Overexpression of mdm2 in mice reveals a p53-independent role for mdm2 in tumorigenesis. Proc. Natl. Acad. Sci. U. S. A. 95, 15608–15612.

Kubbutat, M.H., Jones, S.N., Vousden, K.H., 1997. Regulation of p53 stability by Mdm2. Nature 387, 299–303.

Landers, J.E., Cassel, S.L., George, D.L., 1997. Translational enhancement of mdm2 oncogene expression in human tumor cells containing a stabilized wild-type p53 protein. Cancer Res. 57, 3562–3568.

Leach, F.S., Tokino, T., Meltzer, P., Burrell, M., Oliner, J.D., Smith, S., Hill, D.E., Sidransky, D., Kinzler, K.W., Volgelstein, B., 1993. p53 Mutation and MDM2 amplification in human soft tissue sarcomas. Cancer Res. 53, 2231–2234.

Lewin, B., 1994. The apparatus for nuclear splicing. In: Lwein, B. (Ed.), Genes V. Oxford Univ. Press, Oxford, pp. 914–940.

Libri, D., Marie, J., Brody, E., Fiszman, M.Y., 1989. A subfragment of the beta tropomyosin gene is alternatively spliced when transfected into differentiating muscle cells. Nucleic Acids Res. 17, 6449–6462.

Lundgren, K., Montes de Oca Luna, R., McNeill, Y.B., Emerick, E.P., Spencer, B., Barfield, C.R., Lozano, G., Rosenberg, M.P., Finlay, C.A., 1997. Targeted expression of MDM2 uncouples S phase from mitosis and inhibits mammary gland development independent of p53. Genes Dev. 11, 714–725.

Martin, K., Trouche, D., Hagemeier, C., Sorensen, T.S., La Thangue, N.B., Kouzarides, T., 1995. Stimulation of E2F1/DP1 transcriptional activity by MDM2 oncoprotein. Nature 375, 691–694.

Matsumoto, R., Tada, M., Nozaki, M., Zhang, C.L., Sawamura, Y., Abe, H., 1998. Short alternative splice transcripts of the mdm2 oncogene correlate to malignancy in human astrocytic neoplasms. Cancer Res. 58, 609–613.

Momand, J., Jung, D., Wilczynski, S., Niland, J., 1998. The MDM2 gene amplification database. Nucleic Acids Res. 26, 3453–3459.

Momand, J., Zambetti, G.P., Olson, D.C., George, D., Levine, A.J., 1992. The mdm-2 oncogene product forms a complex with the p53 protein and inhibits p53-mediated transactivation. Cell 69, 1237–1245.

Montes de Oca Luna, R., Tabor, A.D., Eberspaecher, H., Hulbor, D.L., Worth, L.L., Colman, M.S., Finlay, C.A., Lozano, G., 1996. The organization and expression of the mdm2 gene. Genomics 33, 352–357.

Mueller, A., Odze, R., Jenkins, T.D., Shahsesfaei, A., Nakagawa, H., Inomoto, T., Rustgi, A.K., 1997. A transgenic mouse model with cyclin D1 overexpression results in cell cycle, epidermal growth factor receptor, and p53 abnormalities. Cancer Res. 57, 5542–5549.

Nigro, J.M., Cho, K.R., Fearson, E.R., Kern, S.E., Ruppert, J.M., Oliver, J.D., Kinzler, D.W., Vogelstein, B., 1991. Scrambled exons. Cell 64, 607–613.

Oliner, J.D., Kinzler, K.W., Meltzer, P.S., George, D.L., Vogelstein, B., 1992. Amplification of a gene encoding a p53-associated protein in human sarcomas [see comments]. Nature 358, 80–83.

Oliner, J.D., Pietenpol, J.A., Thiagalingam, S., Gyuris, J., Kinzler, K.W., Vogelstein, B., 1993. Oncoprotein MDM2 conceals the activation domain of tumour suppressor p53. Nature 362, 857–860.

Pulak, R., Anderson, P., 1993. mRNA surveillance by the *Caenorhabditis elegans smg* genes. Genes Dev. 7, 1885–1897.

Sigalas, I., Calvert, A.H., Anderson, J.J., Neal, D.E., Lunec, J., 1996. Alternatively spliced mdm2 transcripts with loss of p53 binding domain sequences: transforming ability and frequent detection in human cancer. Nat. Med. 2, 912–917.

Smith, C.W.J., Porro, E.B., Patton, J.G., Nadal-Ginard, B., 1989. Scanning from an independently specified branch point defines the 3′ splice site of mammalian introns. Nature 342, 243–247.

Steinman, H., Burstein, E., Lengner, C., Gosselin, J., Pihan, G., Duckett, C., Jones, S., 2004. An alternative splice form of Mdm2 induces p53-independent cell growth and tumorigenesis. J. Biol. Chem. 279, 4877–4886.

Xiao, Z.X., Chen, J., Levine, A.J., Modjtahedi, N., Xing, J., Sellers, W.R., Livingston, D.M., 1995. Interaction between the retinoblastoma protein and the oncoprotein MDM2. Nature 375, 694–698.

Is "Junk" DNA Mostly Intron DNA?

Gane Ka-Shu Wong,[1,3] Douglas A. Passey,[1] Ying-zong Huang,[1] Zhiyong Yang,[1] and Jun Yu[1,2]

[1]*Human Genome Center, Department of Medicine, University of Washington, Seattle, Washington 98195, USA;* [2]*Human Genome Center, Institute of Genetics, Chinese Academy of Sciences, Beijing, China*

Among higher eukaryotes, very little of the genome codes for protein. What is in the rest of the genome, or the "junk" DNA, that, in *Homo sapiens*, is estimated to be almost 97% of the genome? Is it possible that much of this "junk" is intron DNA? This is not a question that can be answered just by looking at the published data, even from the finished genomes. One cannot assume that there are no genes in a sequenced region, just because no genes were annotated. We introduce another approach to this problem, based on an analysis of the cDNA-to-genomic alignments, in all of the complete or nearly-complete genomes from the multicellular organisms. Our conclusion is that, in animals but not in plants, most of the "junk" is intron DNA.

Among higher eukaryotes, very little of the genome codes for protein. What is in the rest of the genome, or the "junk" DNA, that, in *Homo sapiens*, is estimated to be almost 97% of the genome? If a region is gene-poor, is that because there are vast deserts of intergenic DNA between adjacent genes, or is that because the few genes that are there are large, with enormous introns?

First, a few definitions are needed. We consider only the euchromatic portion of the genome. The heterochromatic portion (e.g., centromeres and telomeres) is highly repetitive and largely devoid of genes. It is extremely difficult to clone, extremely polymorphic, and unlikely to be sequenced correctly anytime soon. We define the exons and introns as "intragenic" and everything else as "intergenic." This is not to imply that intergenic DNA is nonfunctional, especially as we have incorporated the promoters into our definition. However, promoters are difficult to identify, whereas exons and introns are reliably identified by cDNA-to-genomic alignments. Lastly, we will use the term "genomic length" to indicate the sum of the exons and introns in a given gene and "cDNA length" to indicate the sum of only the exons.

Even after a genome is completely sequenced, it is not a straightforward matter to determine the intergenic fraction. Indeed, any assessment that is based only on the fraction of the genome that has not been identified by the gene annotations is likely to be an overestimate of the underlying reality. Consider how the genes are annotated. Most current procedures (The *Caenorhabditis elegans* Sequencing Consortium 1998; Dunham et al. 1999; Lin et al. 1999; Mayer et al. 1999; Adams et al. 2000; Hattori et al. 2000) employ a combination of EST/cDNA/protein alignments and ab initio exon-prediction programs. Given the incomplete state of the EST/cDNA/protein data, most of the annotated exons are in fact based on the exon-prediction programs, even if parts of certain genes are confirmed by the experimental data. There are two problems (Burset and Guigo 1996; Reese et al. 2000). One is that the exon-prediction programs cannot identify untranslated non-coding exons (i.e., the UTRs). The second, more important, issue is that these programs are not particularly proficient at identifying large genes. There are three reasons: (1) The signal-to-noise ratio can be as low as 1/1000, for the extreme case of a 100-bp exon juxtaposed next to a 100-kb intron; (2) the data sets used to train these programs tend to under-represent the large difficult-to-sequence genes; and (3) the codon-usage statistics, by which the exons are initially identified, are not as informative for the large genes of certain organisms (Wright 1990).

The extent of the large-genes problem is organism dependent. The determinant is the distribution of genomic lengths. If the genomic lengths are distributed over many orders of magnitude, then failure to annotate even a small fraction of the largest genes will leave a much larger fraction of the genome unannotated. In this scenario, there is a critical difference between the following two seemingly similar quantities: the fraction of the genes in the genome that is correctly identified and the fraction of the genome sequence that is labeled as intragenic. The first quantity is far more likely to be correct than the second. It is possible that the total gene count is essentially correct, while, at the same time, the intragenic fraction is significantly underestimated and the intergenic fraction is significantly overestimated. Indeed, this is precisely the problem for the animal genomes.

Our solution is to determine the distribution of genomic lengths entirely from cDNA-to-genomic alignments (i.e., independent of the exon-prediction

[3]Corresponding author.
E-MAIL gksw@u.washington.edu; FAX (206) 685-7344.
Article and publication are at www.genome.org/cgi/doi/10.1101/gr.148900.

10:1672–1678 ©2000 by Cold Spring Harbor Laboratory Press ISSN 1088-9051/00 $5.00; www.genome.org

programs). Then, compare the mean genomic length to the mean gene-to-gene distance. The former is taken from the cDNA alignments, but the latter is computed as the ratio of the euchromatic genome size, divided by the gene count, taken from the annotations. Reliable results are expected for *Drosophila melanogaster* and *Caenorhabditis elegans*, because genome sequencing for these organisms is complete and estimates of the gene-to-gene distance are available. For *Arabidopsis thaliana*, the published chromosomes (Lin et al. 1999; Mayer et al. 1999) agree to 4.5%, so we can safely extrapolate to the entire genome. In contrast, for *H. sapiens*, the published chromosomes (Dunham et al. 1999; Hattori et al. 2000) differ by 243%, reflecting the heterogeneity in the gene densities of warm-blooded vertebrates (Bernardi 2000). Coupled with the difficulties of determining the mean genomic length, a result of the lack of large genomic contigs, we refer extensively to the model organism results to guide our interpretations of the *H. sapiens* data.

RESULTS

Figure 1 depicts the distribution of genomic lengths for *H. sapiens*, *D. melanogaster*, *C. elegans*, and *A. thaliana*. Table 1 is a numerical summary. The animal distributions span 2–3 orders of magnitude, but the plant distribution spans only one order of magnitude. The implication for the large-genes problem can be estimated by considering how many of the largest genes would have to be unidentified for half of the intragenic space to be missing. The figures range from 11% and 10% at one extreme, in *H. sapiens* and *D. melanogaster*, to 30% at the other extreme, in *A. thaliana*. Furthermore, the only organism in which the intergenic fraction is

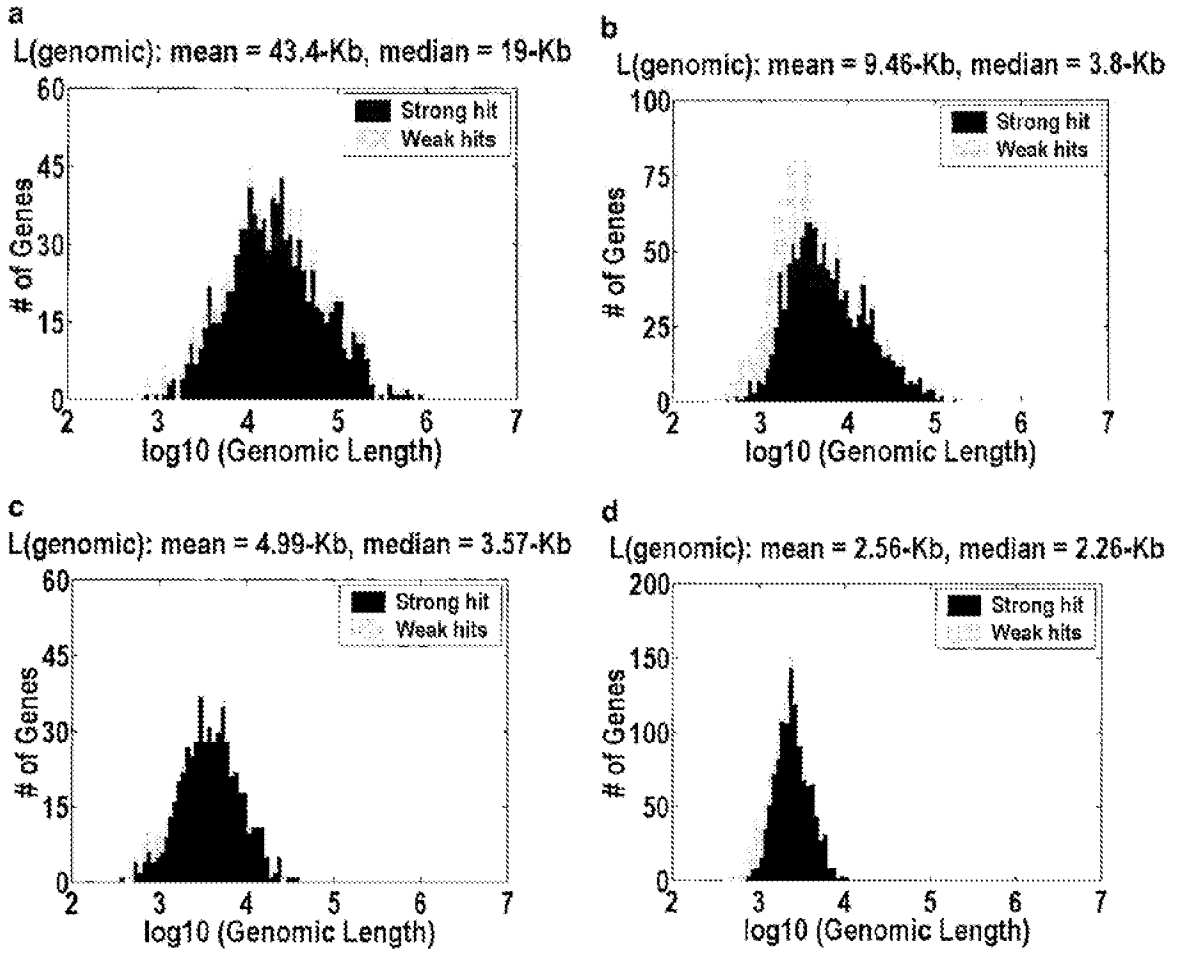

Figure 1 Distribution of genomic lengths for (*a*) *Homo sapiens*, (*b*) *Drosophila melanogaster*, (*c*) *Caenorhabditis elegans*, and (*d*) *Arabidopsis thaliana*. Dark shading indicates strong hits. Weak hits (lightly shaded) represent cDNA-to-genomic alignments with <3 exons or <50% of the cDNA length aligned. An overwhelming majority of these weak hits are actually complete alignments with only one or two exons. Instances in which <50% of the cDNA is aligned represent 7.3%, 3.3%, 1.2%, and 0.9% of the genes in the four organisms, respectively.

Table 1. Estimated Intergenic Fractions

	Homo sapiens	*Drosophila melanogaster*	*Caenorhabditis elegans*	*Arabidopsis thaliana*
Euchromatin	3180000	123000	97800	130000
Sequenced DNA	369000	123000	91000	119000
Gene-to-gene	45.4	9.0	5.3	4.7
cDNA aligned	1061	1628	583	1401
Genomic quality	1.2	23.3	2.4	15.7
Nested genes	6%	8%	4%	1%
05 Percentile	2.5	0.9	0.8	0.9
Genomic length	43.4	9.5	5.0	2.6
95 Percentile	165.5	36.3	14.2	5.4
%, missing half	11%	10%	21%	30%
Intergenic DNA	Discussed in text of article	3%	10%	46%

The first three rows list the euchromatic genome size, the amount of genomic sequence that was analyzed, and the annotation-based estimate of the gene-to-gene distance. The next three rows describe the cDNA alignments. These rows list the number of aligned cDNAs, our quality assessment for the genomic contigs (i.e., the median of the genomic contig size divided by the genomic length for the 95th-percentile gene), and our estimate of the frequency of nested genes (i.e., genes on the reverse strand or inside an intron). The genomic length is given in the next three rows by its arithmetic mean, and its 5th or 95th percentile values. Next, we indicate what fraction of the largest genes would have to be unidentified for half of the intragenic space to be missing. The last row lists the intergenic fraction, computed by correcting the mean genomic length for nested genes, dividing that by the mean gene-to-gene distance, and subtracting the result from one. Note: In *Drosophila melanogaster*, we do not count scaffold joins longer than 1 kb as contiguous when computing the genomic quality. All lengths are reported in kb.

greater than 10% is *A. thaliana*, even though we have included the minor correction for nested genes (genes on the reverse strand or inside an intron). This correction is computed by counting the occurrences of nested genes in our cDNA alignments, and adjusting for the fact that we do not detect every such occurrence because we do not have all of the cDNAs.

The main uncertainty in our method is that we must extrapolate from a subset of the genes to the entire genome to determine the mean genomic length. There will be sampling biases, but they can be categorized and subcategorized as follows: (1) the extent to which cDNA data are enriched for large or small genes, (2) the extent to which genomic data are biased for large or small genes, and then, are the gene-rich regions done first by sequencing projects? Are the contigs large enough for us to align the large genes?

We will argue that the problem is primarily in the genomic data, not the cDNA data. Furthermore, to the extent that there are sampling biases, the tendencies are always to underestimate the mean genomic length and to overestimate the intergenic fraction.

There are two reasons to suspect that biases in the cDNA data will cause us to underestimate the mean genomic length. Keep in mind that large genes are highly correlated with large cDNAs (this paper; data not shown). The first explanation is that full-length cDNAs are extremely difficult to clone, given the ease with which RNA molecules are degraded and the intrinsic bias in the cloning system for smaller inserts. The second reason is that large RNA molecules require more time to transcribe, so large genes might be less highly expressed and more difficult to isolate. However, this expectation is incorrect, because the transcription machinery operates in parallel. As a measure of the expression levels, in *H. sapiens*, we aligned the 1,856,102 ESTs in GenBank against our cDNA data. Multiple reads from the same clone were counted only once. Figure 2 shows that there is no significant variation in EST coverage as a function of genomic length. Notice that the normalization procedures (Hillier et al. 1996) applied to the EST libraries do not affect the rare transcripts, in which we were looking for an effect. The conclusion is that cDNA data, extracted from GenBank, can be representative of all genomic lengths.

Genomic data are biased in two ways. First, there is a sociologic bias toward sequencing gene-rich regions first. Second, even when a genome is complete, lack of long-range contiguity, on the scale of the largest genes, will reduce the estimate of the mean genomic length, because any breaks in the alignment are most likely to occur across the largest introns. Both issues are relevant in the *H. sapiens* data. In Figure 3, we demonstrate that the aligned data are biased toward GC-rich genes, which are of smaller genomic lengths (Bernardi 2000). As for contiguity, we estimate the extent of the problem by computing the ratio of the median genomic contig size to the genomic length of the 95th percentile gene. Ideally, this ratio would be much greater than one. Table 1 shows that it is much greater

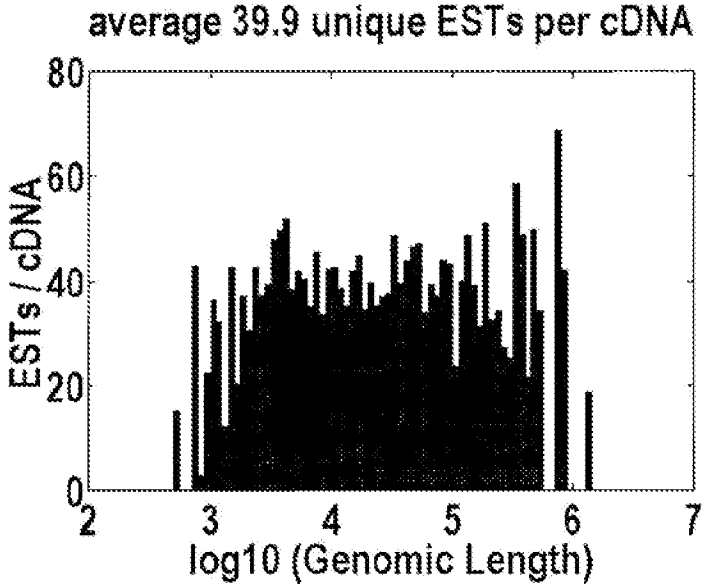

Figure 2 Is the collection of *Homo sapiens* cDNA sequence biased? We aligned the 1,856,102 ESTs in GenBank to our cDNA sequences and plotted the number of aligned ESTs as a function of the genomic length. Multiple reads from the same clone are counted only once. There is no obvious bias, indicating that cDNAs for genes of every genomic length are equally easy to isolate.

than one in *D. melanogaster* and *A. thaliana*. It is only moderately greater than one in *C. elegans*, but that is less important for this organism, because the genomic lengths are not as broadly distributed. However, in *H. sapiens*, the ratio is 1.2, and it would have been even smaller had we not used genomic data from a new division of GenBank in which all of the overlapping clones have been joined together (Jang et al. 1999).

We can estimate the severity of these biases with the different versions of the *D. melanogaster* genomic data. Specifically, we repeated the alignments with the same cDNA data but switched to the 34.9 Mb of finished clone-by-clone genomic data that was available prior to the completion of the whole-genome shotgun (Adams et al. 2000). The contig quality measure is then 2.8, and the resultant mean genomic length of 7.1 kb is off the mark by 34%. By comparing those cDNAs aligned in both data sets, we find that 16% of this effect is attributable to the contiguity problem. The other 18% is attributable to the bias toward sequencing gene-rich regions first. An even more dramatic example of these biases is *Mus musculus*, which has a contig quality measure of 0.3 and a mean genomic length of 9.7 kb. If we assume that there is no difference between *M. musculus* and *H. sapiens*, this estimate is off the mark by 447%. Parenthetically, another unreliable way to estimate the mean genomic length is to extract GenBank annotations. The annotated genes in that 34.9 Mb of genomic data for *D. melanogaster* have a mean genomic length of 3.0 kb, which is off the mark by 317%.

The essential conclusion is that our 43.4 kb figure for the mean genomic length in *H. sapiens* is a substantial underestimate, even if it is already 10 times larger than the training sets used for these exon-prediction programs. However, the gene count itself is also uncertain. The traditional estimate of 70,000 (Antequera and Bird 1993; Fields et al. 1994) has recently been challenged by substantially lower estimates, from 35,000 to 45,000 (Ewing and Green 2000; Hattori et al. 2000; Roest Crollius et al. 2000). How can we interpret the *H. sapiens* data? If we accept the traditional gene count of 70,000, our mean genomic length of 43.4 kb predicts an intergenic fraction of 10%. Suppose we inflate our estimate by the same 34% discrepancy that was observed between the two *D. melanogaster* data sets. The gene count that would be consistent with the same 10% intergenic fraction is

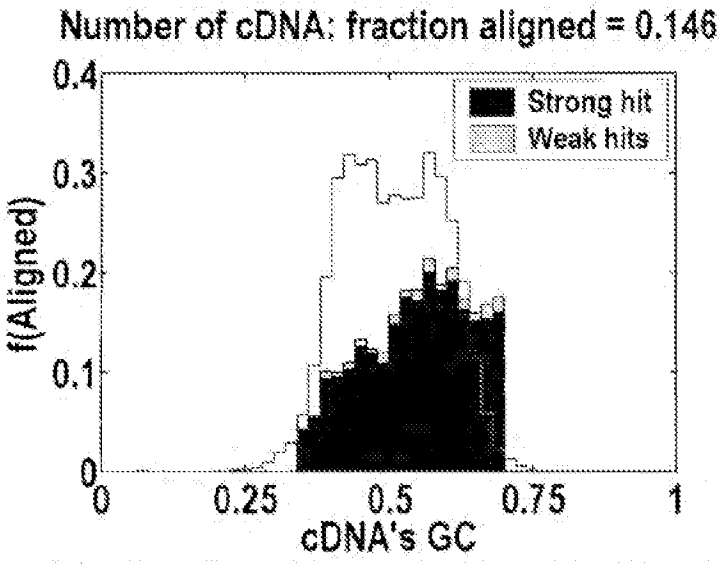

Figure 3 Is the collection of *Homo sapiens* genomic sequence biased? We computed the probability that cDNAs of a particular GC content aligned to genomic sequence, given that only 369 Mb of nonredundant finished genomic sequence were available. The solid line (on an arbitrary scale) indicates the initial collection of cDNAs. The obvious bias toward GC-rich cDNAs is important because these are known to correspond to smaller genes (Bernardi 2000). Dark shading shows strong hits; light shading shows weak hits.

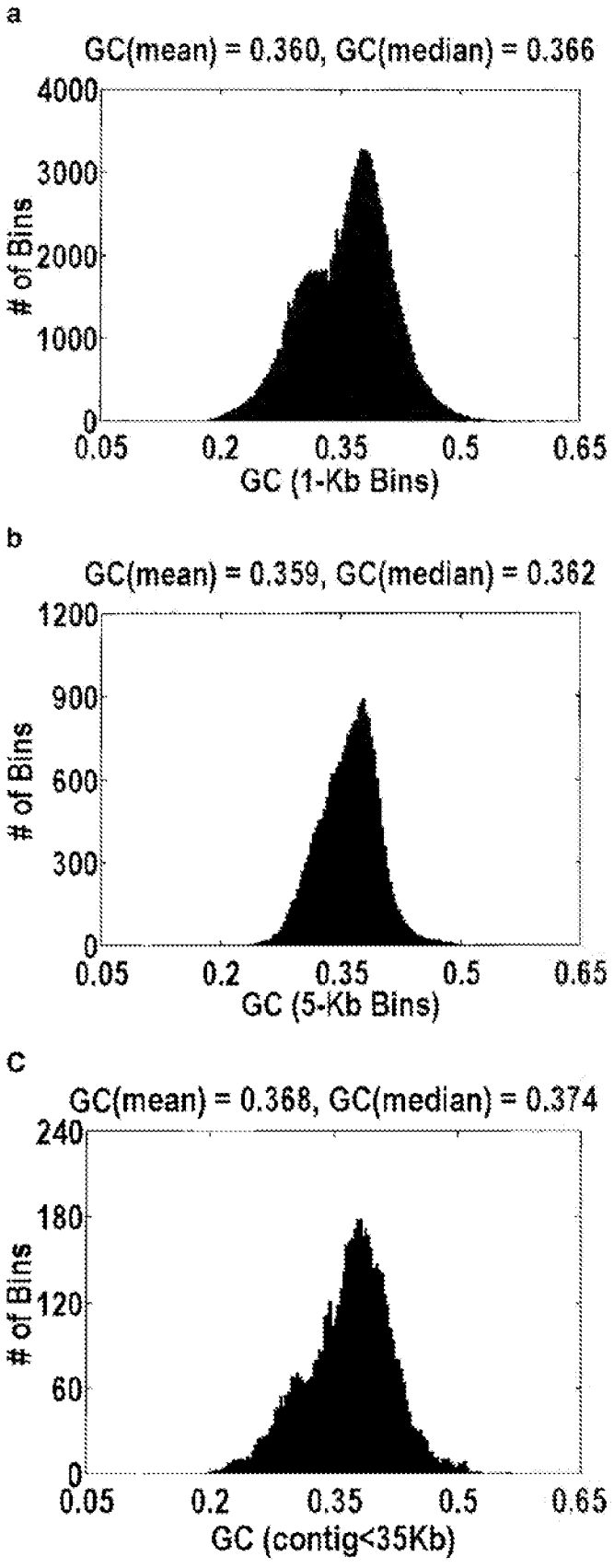

then 51,400. Considering that the contig quality is much worse in *H. sapiens* than in the clone-by-clone *D. melanogaster* data, it is likely that the mean genomic length is underestimated by >34%. Thus, the gene count would have to be substantially less than the current low estimates of 35,000 to 45,000 for our arguments to allow much intergenic DNA.

Given the uncertainty in our method, we cannot give a precise estimate for the intergenic fraction in *H. sapiens*. However, we are prepared to argue that the intergenic fraction in *H. sapiens* cannot be as large as it is for *A. thaliana*, because, at such a high intergenic fraction, the distribution of GC content for genomic DNA is bimodal, as in Figure 4. Fitting the data to a sum of Gaussians reveals that the main mode is centered at 0.382, which is almost identical to the 0.390 GC content of the aligned *A. thaliana* genes. The relative ratio of the two modes implies an intergenic fraction of 30%, which is smaller than the 46% estimate derived from genomic length arguments but not unexpectedly so, because some of the intergenic DNA could have a GC content that is similar to the intragenic DNA. The reason why this bimodality has not been reported previously is that it is extremely sensitive to how the data are plotted. Specifically, the histogram bins must be smaller than the mean genomic length, and smaller genomic contigs (i.e., those sequenced because they contain a likely gene) cannot be used. That said, no such bimodality is observed in *H. sapiens*, *D. melanogaster*, or *C. elegans*, regardless of how the data are plotted.

DISCUSSION

So why do most genome annotation efforts continue to report so much intergenic DNA? One of the most conspicuous features of the recent annotations for *H. sapiens* chromosomes 21 and 22 is the small handful of megabase-sized regions

Figure 4 Distribution of GC content for anonymous genomic sequence in *Arabidopsis thaliana*. The idea that a significant fraction of the genome is intergenic, coupled with the fact that intergenic DNA has a lower GC content than intragenic DNA, suggests that this distribution will be bimodal. However, the bimodality is easily obscured by how the data are plotted. *a* and *b* differ in the size of the bins over which the GC content is computed, 1 kb and 5 kb, respectively. Bin sizes larger than the average gene size of 2.6 kb obscure the effect because every bin is likely to contain a mixture of intragenic and intergenic DNA. *a* and *c* differ in the genomic contigs that are plotted (every contig or only contigs <35 kb, respectively). By removing the large-insert clones favored by the genome centers, what is left behind are those sequences that were analyzed only because they contain a likely gene. Hence, the bimodality disappears.

with absolutely no annotated genes. In all likelihood, each of these regions has one or more large genes, with no counterpart in the EST/cDNA/protein data and which are not being detected by the exon-prediction programs. After accounting for large genes, the remainder of the presently unannotated regions will likely be attributed to untranslated non-coding exons and flanking introns. We must reiterate that the fraction of the genes that is missing does not have to be large to explain away most of the unannotated regions.

What is important is not the precise intergenic fraction or the precise gene count but, at the risk of extrapolating from a limited number of genomes, the differences between plants and animals. There is evidence that plant and animal genomes are organized in different ways. In *H. sapiens*, large genes are caused by a combination of large introns and more introns per gene (this paper; data not shown). At least 35.4% of the total length of the introns in our *H. sapiens* data is due to interspersed repeats (e.g., *Alu* and *L1*). The true fraction is undoubtedly greater, as older repeats, whose sequences are >50% diverged from the ancestral consensus, cannot be identified by existing methods (Smit 1996). Analysis of orthologous genes in *Fugu rubripes* and *H. sapiens* reveals that much of the 10-fold difference in the sizes of these two genomes can be explained by differences in intron sizes (Elgar et al. 1996). In contrast, analysis of syntenic loci among grasses reveals that much of the 40-fold difference in the size of these genomes can be explained by their extensive repeat-filled intergenic regions (SanMiguel et al. 1996; Bennetzen et al. 1998).

The conclusion is that, in animals, most repeats integrate into intron DNA, but, in plants, most repeats integrate into intergenic DNA. Is there something different about the nature of the repeats that insert into animals and plants? Does this dichotomy reflect differences in the operation of the introns and promoters? The answers to these questions will be critical for our understanding of the evolution of large-scale genome features.

METHODS

In *H. sapiens*, cDNA data were extracted from GenBank release 112, but genomic data were downloaded, at the same time, from the new division for nonredundant joined-contigs (Jang et al. 1999). In *D. melanogaster*, cDNA data were taken from release 115 (Dec/15/1999), but genomic data were taken from the whole-genome shotgun (Adams et al. 2000). In *C. elegans* and *A. thaliana*, both cDNA and genomic data were extracted from release 115.

For the cDNA-to-genomic alignments, we required a 98% base pair agreement. We scanned the intron sequences for the consensus splice sites, GT-AG, but we also accepted as a substitute GC-AG, albeit, in <1% of the data. Weak hits, defined as those with <3 exons or <50% of the cDNA length aligned, were plotted separately to verify that they were not anomalous. Immune system-related cDNAs (i.e., with the descriptors immunoglobin, Ig, HLA, MHC, V-region, etc.) were removed. Other redundancies were eliminated, up front by removing all cDNAs that are 90% contained in some other cDNA and post-alignment by comparing the genomic coordinates of the aligned exons. Raw genomic lengths were extrapolated to compensate for incomplete alignments—a small correction even for *H. sapiens*, where a total of 86% of the cDNA lengths was aligned. As another quality control, we required that the exact coordinates of the coding region (i.e., the open reading frame) be known, even though it reduced the number of genes in our final data set.

The partial alignment correction is done by computing an adjusted number of exons, N_{exons}, with a linear extrapolation. The adjusted genomic length, $l_{genomic} = N_{exons}\langle l_{exons}\rangle + (N_{exons} - 1)\langle l_{introns}\rangle$, is extrapolated in a similarly linear manner, with the averages $\langle l_{exons}\rangle$ and $\langle l_{introns}\rangle$ being defined on a per gene basis. Because noncoding terminal exons are generally larger than coding interior exons, both extrapolations are only performed across the coding portion of the cDNA sequence. The intention is to ensure that, if anything, we underestimate the mean genomic length.

ACKNOWLEDGMENTS

We thank Phil Green, Maynard Olson, Carl Ton, and Lee Rowen for many useful discussions and suggestions. This work was partly supported by a grant from the National Institutes of Health (1 RO1 ES09909).

The publication costs of this article were defrayed in part by payment of page charges. This article must therefore be hereby marked "advertisement" in accordance with 18 USC section 1734 solely to indicate this fact.

REFERENCES

Adams, M.D., Celniker, S.E., Holt, R.A., Evans, C.A., Gocayne, J.D., et al. 2000. The genome sequence of *Drosophila melanogaster*. *Science* **287:** 2185–2195.

Antequera, F. and Bird, A.P. 1993. Number of CpG islands and genes in human and mouse. *Proc. Natl. Acad. Sci.* **90:** 11995–11999.

Bennetzen, J.L., SanMiguel, P., Chen, M., Tikhonov, A., Francki, M., et al. 1998. Grass genomes. *Proc. Natl. Acad. Sci.* **95:** 1975–1978.

Bernardi, G. 2000. Isochores and the evolutionary genomics of vertebrates. *Gene* **241:** 3–17.

Burset, M. and Guigo, R. 1996. Evaluation of gene structure prediction programs. *Genomics* **34:** 353–367.

The *C. elegans* Sequencing Consortium. 1998. Genome sequence of the nematode *C. elegans*: A platform for investigating biology. *Science* **282:** 2012–2018.

Dunham, I., Shimizu, N., Roe, B.A., Chissoe, S., Hunt, A.R., et al. 1999. The DNA sequence of human chromosome 22. *Nature* **402:** 489–495.

Elgar, G., Sandford, R., Aparicio, S., Macrae, A., Venkatesh, B., et al. 1996. Small is beautiful: Comparative genomics with the pufferfish (Fugu rubripes). *Trends Genet.* **12:** 145–150.

Ewing, B. and Green, P. 2000. Analysis of expressed sequence tags indicates 35,000 human genes. *Nat. Genet.* **25:** 232–234.

Fields, C., Adams, M.D., White, O., and Venter, J.C. 1994. How many genes in the human genome? *Nat. Genet.* **7:** 345–346.

Hattori, M., Fujiyama, A., Taylor, T.D., Watanabe, H., Yada, T., et al. 2000. The DNA sequence of human chromosome 21. *Nature* **405:** 311–319.

Hillier, L.D., Lennon, G., Becker, M., Bonaldo, M.F., Chiapelli, B., et al. 1996. Generation and analysis of 280,000 human expressed sequence tags. *Genome Res.* **6:** 807–828.

Jang, W., Chen, H.C., Sicotte, H., and Schuler, G.D. 1999. Making

effective use of human genomic sequence data. *Trends Genet.* **15:** 284–286.

Lin, X., Kaul, S., Rounsley, S., Shea, T.P., Benito, M.I., et al. 1999. Sequence and analysis of chromosome 2 of the plant *Arabidopsis thaliana*. *Nature* **402:** 761–768.

Mayer, K., Schüller, C., Wambutt, R., Murphy, G., Volckaert, G., et al. 1999. Sequence and analysis of chromosome 4 of the plant *Arabidopsis thaliana*. *Nature* **402:** 769–777.

Reese, M.G., Hartzell, G., Harris, N.L., Ohler, U., Abril, J.F., and Lewis, S.E. 2000. Genome annotation assessment in *Drosophila melanogaster*. *Genome Res.* **10:** 483–501.

Roest Crollius, H., Jaillon, O., Bernot, A., Dasilva, C., Bouneau, L., et al. 2000. Estimate of human gene number provided by genome-wide analysis using *Tetraodon nigroviridis* DNA sequence. *Nat. Genet.* **25:** 235–238.

SanMiguel, P., Tikhonov, A., Jin, Y.K., Motchoulskaia, N., Zakharov, D., et al. 1996. Nested retrotransposons in the intergenic regions of the maize genome. *Science* **274:** 765–768.

Smit, A.F. 1996. The origin of interspersed repeats in the human genome. *Curr. Opin. Genet. Dev.* **6:** 743–748.

Wright, F. 1990. The 'effective number of codons' used in a gene. *Gene* **87:** 23–29.

Received May 23, 2000; accepted in revised form August 29, 2000.

RELATED PROCEEDINGS APPENDIX

None